Evaluation of a Vibrating Plate Extraction Column by Application of Steady State and Unsteady State Backflow Models

by

Bridget Margaret Hutton

Thesis submitted in fulfilment of the requirements for the degree of

Master of Science in Engineering (Chemical Engineering)

in the Department of Chemical Engineering

at the

University of Stellenbosch

Supervisors:

Prof. L. Lorenzen

Dr A. Heyberger

Stellenbosch

December 2001

Declaration

I, the undersigned, hereby declare that the work contained in this thesis is my own original work and has not previously in its entirety or in part been submitted at any university for a degree.

Signature Date

SUMMARY

Liquid-liquid extraction is a branch of solvent extraction that employs addition of an immiscible solvent, as a separating agent, to a liquid feed. Various types of equipment can be used, however if the process requires more than three stages, typically an extraction column, operated in a countercurrent manner would be employed. In order to scale-up and design a commercial extraction column, it is necessary to quantify the extraction system hydrodynamics and mass transfer characteristics. The principal objectives of countercurrently operated extraction columns concern the mass transfer rate and permissible throughput. The performance of a countercurrent extraction column can be adversely affected by axial mixing, which disturbs countercurrent plug flow.

Various methods have been devised whereby it is possible to evaluate the performance of a column extraction and scale it up to ensure that the commercial operation achieves the same separation achieved on a pilot scale. Classical axial dispersion models allow quantification of axial mixing and mass transfer rates. Two Backflow models were derived to describe the performance of a Vibrating Plate Extraction (VPE) Column, one for steady state and one for unsteady state operation. The steady state model consisted of a series of simultaneous equations, which were solved using the Excel solver function. The unsteady state model consisted of 54 ordinary differential equations, which were solved stagewise using a fourth order Runge Kutta procedure.

The steady state model was based on a dissociation extraction process, whereby *meta*-cresol (*m*-cresol) was separated from *para*-hydroxy-benzaldehyde (*p*HB). The process used the differing de-protonation constants of the two components and the fact that the solubility of the ionic species of each was low in the organic solvent. The extraction system was quantified using a combination of acid-base and extraction theory. Experimentally determined concentration profiles, measured along the length of the column, were force fitted to the model, thereby allowing determination of the model parameters. The mass transfer coefficients ranged between 0.0098 and 0.189 /min, and it was found that backmixing of the dispersed phase was negligible, while that of the continuous phase was low (varying between 0 and 0.3).

The unsteady state model, used to describe the dynamic response of a VPE, was based on a system whereby *tert*-butyl hydroquinone (TBHQ) was recovered from a purge stream.

Conductivity measurements of the raffinate were used to determine the residence time distribution in the column, and hence allowed determination of the extent of axial mixing. It was preferable that the column be operated with minimum settler volumes, otherwise buffering in the settlers occurred, thereby masking axial mixing effects. This method did not facilitate accurate determination of backmixing, at least two other conductivity measurements in the column needed to be measured.

OPSOMMING

Vloeistof-vloeistofekstraksie is 'n vertakking van oplosmiddelekstraksie wat gebruik maak van die toevoeging van 'n onmengbare oplosmiddel as 'n skeidingagent tot die vloeistofvoer. Verskeie tipes apparaat kan gebruik word, maar as die proses meer as drie stadia vereis, sal 'n ekstraksiekolom, in teenstroom bedryf, tipies gebruik word. Om dit moontlik te maak om 'n kommersiële ekstraksiekolom te skalleer en te bedryf, moet die ekstraksiesisteem se hidrodinamika en massa-oordragkarakteristieke gekwantifiseer word. Die hoof doelwitte van ekstraksiekolomme wat teenstroom bedryf word, gaan om die massa-oordrag en toelaatbare deurset. Die skeidingsdoeltreffendheid van 'n teenstroom ekstraksiekolom kan nadelig beïnvloed word deur aksiale vermenging, wat teenstroom propvloei versteur.

Verskeie metodes is voorgestel wat dit moontlik maak om die doeltreffendheid van 'n ekstraksiekolom te evalueer en te verseker dat dieselfde skeiding verkry word vir 'n kommersiële aanleg as vir 'n loodsaanleg. Klassieke aksiale dispersiemodelle laat kwantitatiewe berekening van aksiale vermenging en massa-oordragtempos toe. Twee terugvloeimodelle is afgelei om die werksverrigting van 'n Vibrerende Plaat Ekstraksiekolom (VPE) te beskryf. Die gestadidge toestand model bestaan uit 'n stelsel gelyktydige vergelykings wat opgelos is d.m.v. Excel. Die ongestadige toestand model bestaan uit 54 gewone differensiaalvergelykings, wat stapsgewys opgelos is d.m.v. die vierde orde Runge-Kutta metode.

Die gestadigde teostand model is gebaseer op 'n dissosiasie ekstraksieproses, waardeur m-kresol geskei is van p-hidroksiebensaldehied (pHB). Die proses maak gebruik van die verskillende protoneringskonstantes van die twee verbindings en die feit dat die oplosbaarheid van beide die ioniese spesies laag is in die organiese oplosmiddel. Die ekstraksiestelsel is gekwantifiseer deur gebruik te maak van 'n kombinasie van suur-basis- en ekstraksieteorie. Die model is gepas op eksperimenteel bepaalde konsentrasieprofiele, gemeet langs die lengte van die kolom. Die massa-oordragkoëffisiënte het waardes aangeneem tussen 0.0098 en 0.189 /min en daar is gevind dat die terugvermenging van die verspreide fase weglaatbaar was, terwyl dié van die kontinue fase laag was (tussen 0 en 0.3).

Die ongestadige toestand model wat gebruik is om die dinamiese respons van die VPE te beskryf, is gebaseer op 'n stelsel waar tert-butielhidrokinoon (TBHQ) herwin is vanuit 'n bloeistroom. Geleidingsmetings van die raffinaat is gebruik om die residensietydverspreiding in

die kolom te bepaal en het derhalwe toegelaat dat die mate van aksiale vermenging bepaal kon word. Die kolom moet by voorkeur met minimale skeiervolumes bedryf word, anders is daar 'n buffereffek in die skeiers, wat die aksiale vermenging verskuil. Hierdie metode laat nie die akkurate bepaling van terugvermenging toe nie en minstens twee ander geleidingsmetings in die kolom was benodig.

ACKNOWLEDGEMENTS

I would like to thank and acknowledge the following people:

Dr Ales Heyberger for teaching me the practical aspects of liquid-liquid extraction during the past four years.

Peter Myburgh for proof reading my thesis, and for his support, encouragement and invaluable advice.

Professor Leon Lorenzen for his help with the writing up of my thesis.

My family, Madrie Portwig, Fanie Marais, Paul Statham and Jozef Dudas for their support.

Daniel Menu, Ilse Godwin, Duncan Sibiya, Shadrack Shabangu, Godlieb Lethwane, Dinah Tsebe, Petrus Harmse and CSIR Biochemtek Probe analytical teams for their work during the extraction piloting.

Christa Marais for locating the required literature, and Tabs Mogoru for his assistance with graphics in this thesis.

The CSIR for sponsoring my MSc and AECI for allowing publication of the experimental work.

DEDICATION

I would like to dedicate this thesis to Peter.

TABLE OF CONTENTS

LIST OF FIGURES

LIST OF TABLES

CHAPTER 1. INTRODUCTION

Separation and purification are an integral part of every chemical process, and as such encompass a broad range of unit operations including technologies such as distillation, solvent extraction and crystallisation. Each of these areas is a recognised discipline that requires practical experience, as well as a sound understanding of chemical engineering fundamentals.

Liquid-liquid extraction is a mass transfer operation in which a liquid feed is contacted with a second immiscible or nearly immiscible solvent that has been carefully chosen to preferentially extract a desired component. Two streams result from this contact; the extract, which is the solvent rich solution containing the desired extracted solute, and the raffinate, the residual feed containing little solute. The components are not separated directly and hence extraction is considered an indirect separation technique. Whereas distillation employs differences in boiling point to affect a separation, extraction relies on differences in solubility, which is mostly affected by chemical structure. Extraction is generally applied in order to achieve a separation that is not possible using distillation, such as the separation of close-boiling components, isomers or heat sensitive materials. Typically a process employing extraction would entail three operations; liquid-liquid extraction, solvent recovery and raffinate clean-up.

Since extraction is a diffusional process, extraction equipment is designed to create a uniform distribution of drops of the one phase in the other, to ensure sufficient interfacial area for mass transfer. An array of equipment is available, single stage or multistage, such as mixer-settlers, centrifugal extractors and extraction columns. The equipment may be operated in a batch, differential or continuous manner. Extraction theory is used to establish quantitative relationships between system properties, equipment characteristics and the relevant physical properties (Lo et. al., 1983). This enables extractor performance to be predicted over a wide range of operating conditions. The theory is applied in two areas - the design of new equipment to meet required performance specifications, and the performance evaluation of existing equipment, for purposes of scale-up or to satisfy changed operational requirements (Lo et. al., 1983).

Two extraction processes were investigated, each employing a countercurrent extraction column. The first entailed dissociation extraction to separate *meta*-cresol and *para*-hydroxybenzaldehyde, while the second entailed extraction of *tert*-butyl hydroquinone (TBHQ) from a purge stream.

The column used for the piloting work was a reciprocating plate extraction column, specifically a Vibrating Plate Extraction (VPE) column. The performance of extraction columns can be adversely affected by axial mixing, by disturbing countercurrent plug flow. Axial dispersion models can be used to quantify the extent of axial mixing and predict the performance of an extraction column.

The purpose and specific objectives of this study were as follows:

- to test the feasibility of using a VPE for a dissociation extraction,
- to pilot the dissociation extraction in order to generate scale-up data and produce material for downstream processing,
- to quantify the dissociation extraction system using acid-base and extraction theory,
- to review existing literature on evaluation of extraction column performance by application of axial dispersion models, thereby allowing selection of the most appropriate model for application to the VPE,
- to set-up a steady state and an unsteady state axial dispersion model, and to modify each to be suited to the experimental extraction systems,
- to interpret experimental data, thereby determining the axial mixing properties of the Vibrating Plate Extraction column.

CHAPTER 2. LITERATURE REVIEW

2.1 Liquid-Liquid Extraction Background

2.1.1 Definitions and Extraction Configurations

Liquid-liquid extraction is a mass transfer operation in which a liquid solution, the *feed* is contacted with a second immiscible or nearly immiscible liquid, the *solvent*, that has been carefully chosen to preferentially extract a desired component. Two streams result from this contact (as depicted in **Figure 2-1**) - the *extract*, which is the solvent rich solution containing the desired extracted solute, and the *raffinate*, the residual feed depleted in solute.

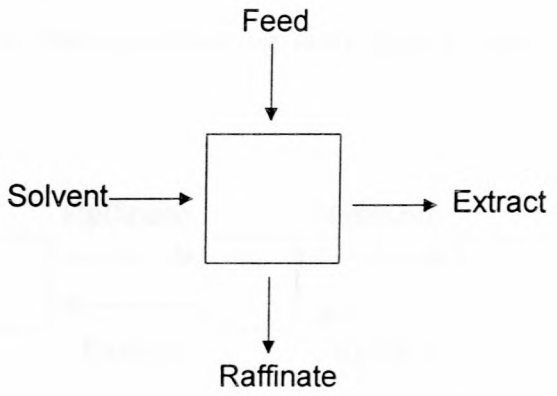

Figure 2-1: Liquid-liquid extraction

A *theoretical stage* is a device or combination of devices that accomplishes the effect of intimately mixing two immiscible liquids until equilibrium concentrations are reached, then physically separating the two phases into distinct phases.

Crosscurrent extraction is a series of stages, as depicted in **Figure 2-2,** in which the raffinate from one extraction stage is contacted with additional fresh solvent in subsequent stages (Robbins, 1984).

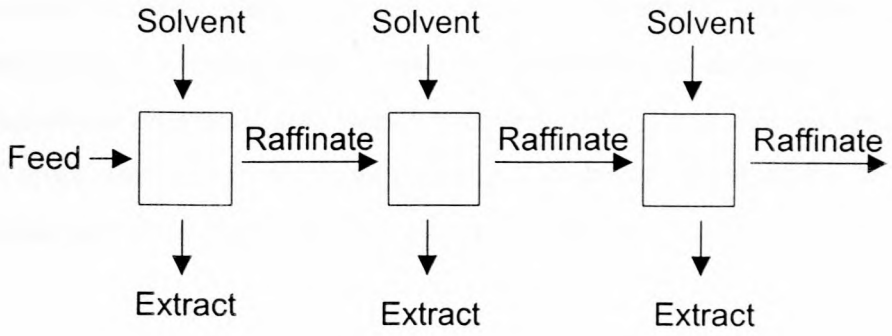

Figure 2-2 : Crosscurrent extraction

Countercurrent extraction is an extraction configuration, as shown in **Figure 2-3**, in which the extraction solvent enters the stage (or end of the extraction) farthest from where the feed enters and the two phases pass countercurrently to each other. This makes maximum use of the concentration driving force, thereby achieving more than a single stage extraction (Robbins, 1984).

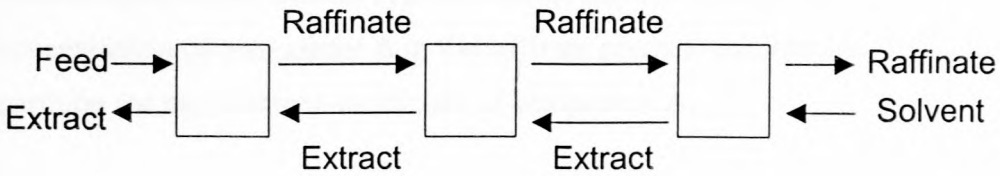

Figure 2-3 : Countercurrent extraction

Dissociation extraction is a process that relies on differing solubilities between protonated and de-protonated states of the same component. The extent of re-protonation depends on the amount of acid added and the de-protonation constant (*pKa*) of the component. The step of adding acid to an aqueous solution to release phenolic derivatives is also referred to as *springing*.

As mentioned, extraction is a mass transfer operation, in which two streams that are not in equilibrium with each other are brought into contact. In an attempt to reach a state of equilibrium, the solute will diffuse from the one phase to the other through the films adjacent to the interface. The driving force is provided by the deviation from equilibrium, while the rate at which this is achieved, is controlled by resistance to inter-phase mass transfer. Rates of mass transfer are influenced by a number of variables, amongst others; temperature, viscosity, turbulence, interfacial tension, interfacial area and rate of renewal.

Each phase exhibits its own resistance during the transfer of solute, while the resistance at the interface is negligible. Consequently extraction equipment is designed to minimise film thickness and maximise interfacial area (which is determined by drop size) by creating a uniform distribution of drops that are as small as possible. However this must be balanced against emulsion formation and throughput capacity (Lo, et al., 1983).

2.1.2 General Extraction Theory

Since liquid-liquid extraction is a mass transfer operation, it is strongly affected by equilibrium considerations. The fundamental equilibrium parameter in extraction is the *partition coefficient*:

$$m_A = \frac{C_{A,E}^*}{C_{A,R}^*} \qquad \textbf{(2-1)}$$

where:

$C_{A,E}^*$: concentration of component A in the extract phase at equilibrium,

$C_{A,R}^*$: concentration of component A in the raffinate phase at equilibrium.

m_A : partition (or distribution) coefficient of component A,

Partition coefficient values (equilibrium data) can be obtained by performing "shake tests", whereby the feed is extracted in a separating funnel, by employing multiple cross extractions. Although high partition coefficients are desirable, even if the value is 1 or below, it can be acceptable, depending on the economic value of the solute to be extracted.

When considering the use of a particular solvent to separate the components of a two component liquid system, it is useful to employ the concept of *selectivity*. *Selectivity* is defined as the ratio of the partition coefficient of the component to be extracted relative to the component that is to remain in the raffinate:

$$Sel_{A/B} = \frac{m_A}{m_B} \qquad \textbf{(2-2)}$$

where:

m_B : partition (or distribution) coefficient of component B,

$Sel_{A/B}$: selectivity of the solvent for component A relative to component B.

For separating two components, the selectivity must be greater than 1, and the higher the value of the selectivity, the more effectively the operation will perform.

At equilibrium, the activities of each phase are equal:

$$a_A^* = \gamma_{A,R}^* . C_{A,R}^* = \gamma_{A,E}^* . C_{A,E}^* \qquad \textbf{(2-3)}$$

where:

a_A* : activity of component A

$\gamma_{A,E}^*$: activity coefficient of component A in extract phase,

$\gamma_{A,R}^*$: activity coefficient of component A in raffinate phase.

Solvents, which lower the activity of the solute relative to that of the feed solution, are preferential in that they yield a high partition coefficient (Cusack, Fremeaux and Glatz, 1991).

Extraction efficiency may be calculated based either on the extract[1], or the raffinate[2], although conventionally, it is based on the latter. However, in the case of limited extraction of a component, the change in concentration in the feed is likely to be of a similar magnitude as that of analytical error, and consequently in this case it is preferable to calculate the efficiency based on the extract.

In many organic systems, association of simple molecules into complex molecules can occur in the organic phase (Glasstone, 1955). Consequently the partition coefficient is not constant, but dependent on the concentration of protonated species in the organic phase.

Consider that component A forms a dimer in the organic phase.

$$2A_\xi \xleftrightarrow{k_{ass}} A_\delta \qquad \textbf{(2-4)}$$

where:

A_δ : associated (dimer) form of component A in extract phase,

A_ξ : non-associated form of component A in extract phase,

k_{ass} : association equilibrium constant.

---

[1] Appendix B, Equation B-4

[2] Appendix B, Equation B-5

The association of any particular acid will have an equilibrium constant,[3] (k_{ass}) which is a measure of the extent of association at equilibrium. By incorporating this with the definitions of the *partition coefficient* of the component (excluding associated molecules), it is possible to derive[4] the following equation:

$$C_{A,E} = \tfrac{1}{2} k_{ass} m_A{}^2 C_{A,R}{}^2 + m_A C_{A,R} \qquad \textbf{(2-5)}$$

Equation 2-5 allows theoretical correlation of equilibrium data (concentration of component A in extract versus concentration in raffinate), relative to the partition coefficient of non-associated component A and the association equilibrium constant.

2.1.3 Combining Acid-Base and Extraction Theory

Generally polar compounds have low solubility in organic solvents, particularly ionic species, which are practically insoluble. This implies that the solubility of compounds such as weak acids can be altered, depending on whether or not they are de-protonated. This can be particularly advantageous if separation of two weak acids is desired. If the de-protonation constant (*pKa*) values of the two acids differ sufficiently, it is possible to selectively protonate and extract one of the compounds, achieving separation. Similarly the reverse is possible, where de-protonated species can be extracted, or selectively extracted from an organic solvent to an aqueous base medium.

Consider the de-protonation of an acid in an aqueous solution:

$$HA \xleftrightarrow{Ka_A} A^- + H^+ \qquad \textbf{(2-6)}$$

where:

A^- : de-protonated species of component A,

H^+ : protons,

HA : protonated species of component A,

Ka : de-protonation equilibrium constant,

---

[3] Appendix B, Equation B-7

[4] Appendix C.2

The de-protonation of any particular acid will have an equilibrium constant *Ka*, which is a measure of the extent of de-protonation at equilibrium. By incorporating this with the definitions of the extent of de-protonation, *pH* and *pKa*, it is possible to derive[5] **Equation 2-7** which relates the extent of de-protonation to the *pKa* of the component and the pH of the system (Atkins, 1978).

$$D_A = \frac{1}{10^{pKa_A - pH} + 1} \qquad \textbf{(2-7)}$$

where:

D_A : extent of de-protonation,

pH = $-log\ (C_{H+})$

pKa = $-log\ (Ka)$,

Consider the separation of *meta*-cresol (*m*-cresol) and *para*-hydroxybenzaldehyde (*p*HB), which exhibit an appreciable difference in their strengths as acids. Knowing the respective *pKa* values, as tabulated in **Table 2-1** and applying **Equation 2-7**, the theoretical extent of de-protonation versus pH can be plotted, as depicted below in **Figure 2-4**.

Table 2-1: *pKa* values at 50°C (Lide, 1992/3)

	***m*-cresol**	**pHB**
***pKa* at 50 °C**	9.83	7.72

[5] Appendix C.1

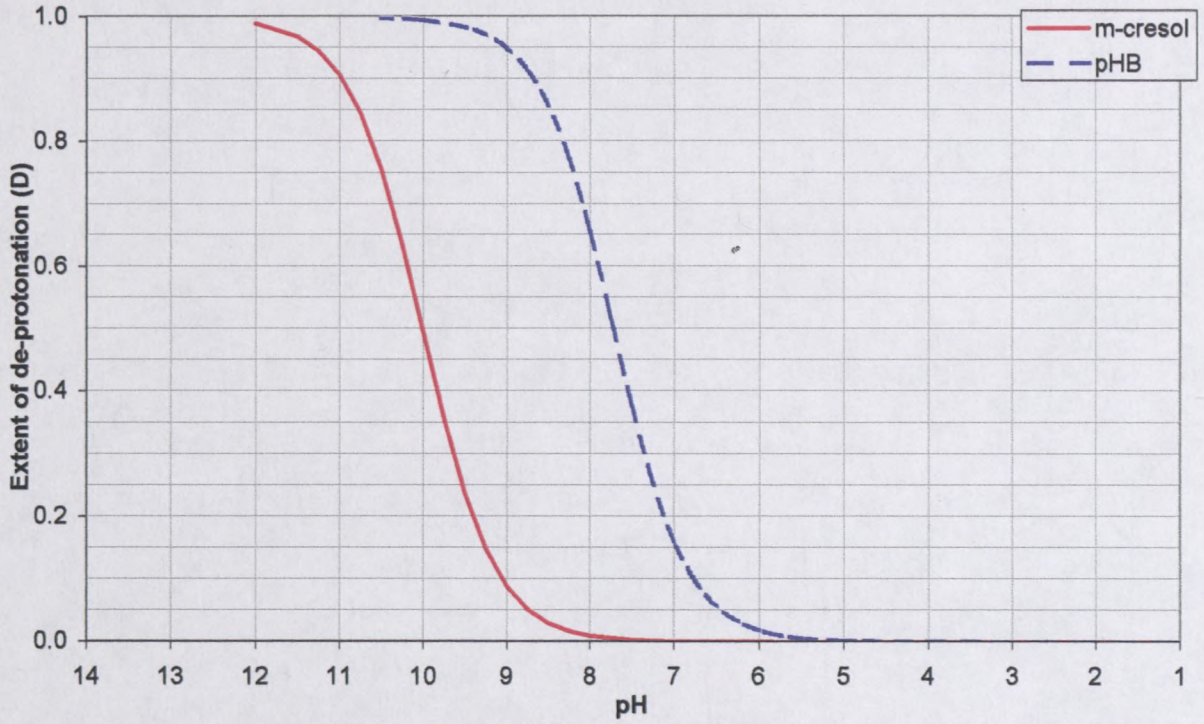

Figure 2-4: Extent of de-protonation *versus* pH

In general, analytical methods employed for determining the concentration of a component do not differentiate between the protonated and de-protonated species. However, a partition coefficient is strictly only applied to one particular species. The protonated and de-protonated forms of a component will each have their own partition coefficient between the two phases. Not differentiating between the two species results in an average partition coefficient (m_A') which is strongly pH dependent (referred to as the *overall* partition coefficient), and which can be defined as:

$$m_A' = \frac{C_{HA,E} + C_{A^-,E}}{C_{HA,R} + C_{A^-,R}} \qquad \textbf{(2-8)}$$

where:

$C_{A^-,E}$: de-protonated species of component A in extract phase,

$C_{A^-,R}$: de-protonated species of component A in raffinate phase

$C_{HA,E}$: protonated species of component A in extract phase,

$C_{HA,R}$: protonated species of component A in raffinate phase,

m_A' : overall partition (or distribution) coefficient of component A,

The solubility of the de-protonated species of component A (*m*-cresol) in a non-polar organic can be expected to be very low, and is usually considered negligible. (*i.e.* $C_{A^-,E} = 0$).

When considering the true *partition coefficient,* m_A of the protonated component between the aqueous and organic phases only the concentration of the protonated species in each phase should be considered. This results in a partition coefficient that is independent of pH. Using **Equation 2-7**, the measured *pH*, the *pKa* and the total concentration of component A (determined analytically), it is possible to quantify the ratio of protonated to de-protonated forms of component A in the aqueous phase. It is then possible to calculate the *partition coefficient of the protonated species* (m_{HA}) of component A, as follows:

$$m_{HA} = \frac{C_{HA,E}}{C_{HA,R}} \qquad \textbf{(2-9)}$$

m_{HA} : partition (or distribution) coefficient of protonated species of component A,

For dissociation extraction, the *extraction efficiency of the protonated species*[6] is calculated (*via* pH) considering only the available protonated species. This allows evaluation of equipment efficiency for a dissociation extraction.

The equilibrium data of the protonated species of *m*-cresol can be determined using the theory mentioned above. However, as mentioned previously, association of simple molecules into complex molecules can occur in the organic phase, resulting in a non-constant partition coefficient, which is dependent on the concentration of protonated species in the organic phase. By modifying **Equation 2-5** slightly, it is possible to theoretically correlate the equilibrium data of the protonated species of the component, relative to the partition coefficient of protonated (un-dimerised) component and the association equilibrium constant.

[6] Appendix B, Equation B-6

2.2 Liquid-Liquid Extraction Equipment

2.2.1 Classification of Equipment

To achieve separation using solvent extraction, use is made of differing chemical, rather than physical characteristics, which are employed in distillation. This unique feature has facilitated the use of solvent extraction to a large variety of applications. Probably more types of equipment have been developed for solvent extraction than for any other chemical engineering unit operation (Lo, 1979).

The differing types of contactors can be divided according to the method applied for inter-dispersion of the phases, and to produce a countercurrent flow pattern. These can both be achieved, either by the force of gravity acting on the density difference between the phases or by application of a centrifugal force. For the former type, further distinction can be made according to the type of mechanical energy input applied. All continuous multistage contactors can be further divided into two broad categories according to the nature of their operation, namely (Lo, 1979):

- discrete stagewise contact,
- differential contact.

In discrete stagewise extractors, (such as mixer-settlers), two phases are brought into contact, equilibrated in one compartment and then separated, before being passed into another stage or unit for another extraction. Equilibrium is completely achieved or an approach to it is reached in each stage. Differential contactors (such as packed or spray extraction columns) provide continuous contact and mass transfer along the full length of the device. The phases are only separated at the ends, and equilibrium is not established at any point along the way (Lo, 1979, Cusack and Fremeaux, 1991).

Equipment of industrial importance can be classified into four major types; mixer-settlers (stagewise), centrifugal extractors (differential), unagitated columns (stagewise or differential) and agitated columns (stagewise or differential) (Blass, et al., 1994):

- ***Mixer-settlers*** – one or more impellers are used to mix the two phases, and then the phases are allowed to settle (Godfrey, et al., 1994; Cusack and Fremeaux, 1991)

  - *Mix-decant tanks* – a simple agitated vessel (used for both mixing and settling) operated in batch mode; multiple tanks can be operated using a cross flow approach to achieve multiple stages.
  - *Countercurrent mixer*-setters – an alternating series of agitated tanks and settling tanks, operated using a countercurrent approach.
  - *Continuous mixer-settlers* - separate mixer and settler compartments, may be single or multi-staged, various configurations include horizontal cylinder or box-type.
  - *Other types,* such as vertical types of mixer-settler.

- ***Centrifugal extractors*** – application of a centrifugal force to contact the two phases and then separate them (Blass, 1994)

  - *Centrifugal extractors with concentric perforated cylinders* – e.g. Podbielniak extractor.
  - *Centrifugal extractors with axial countercurent flow of liquid phases.*
  - *Centrifugal classifiers.*

- ***Unagitated extraction columns*** – the two phases are distributed in a column, which may be equipped with or without internals; the density difference between the two phases is used as the driving force for flow and final separation (Refer to **Figure 2-5** below).

  - *Spray columns* – are the simplest extraction columns, consisting merely of an empty shell, with the dispersed phase being fed through a distributor, they operate as differential contactors (Cusack and Fremeaux, 1991).
  - *Packed columns* – generally employ random packing, although structured packings are used occasionally, the packing aids in the formation of drops, which helps mass transfer and packing also lessens axial mixing; they operate as differential contactors (Stevens, 1994).

- *Sieve-plate columns* - contain a series of perforated plates plus downcomers or upcomers, they operate on the principle of successive coalescence and regeneration of the dispersed phase, and are thus stagewise contactors (Cusack and Fremeaux, 1991).

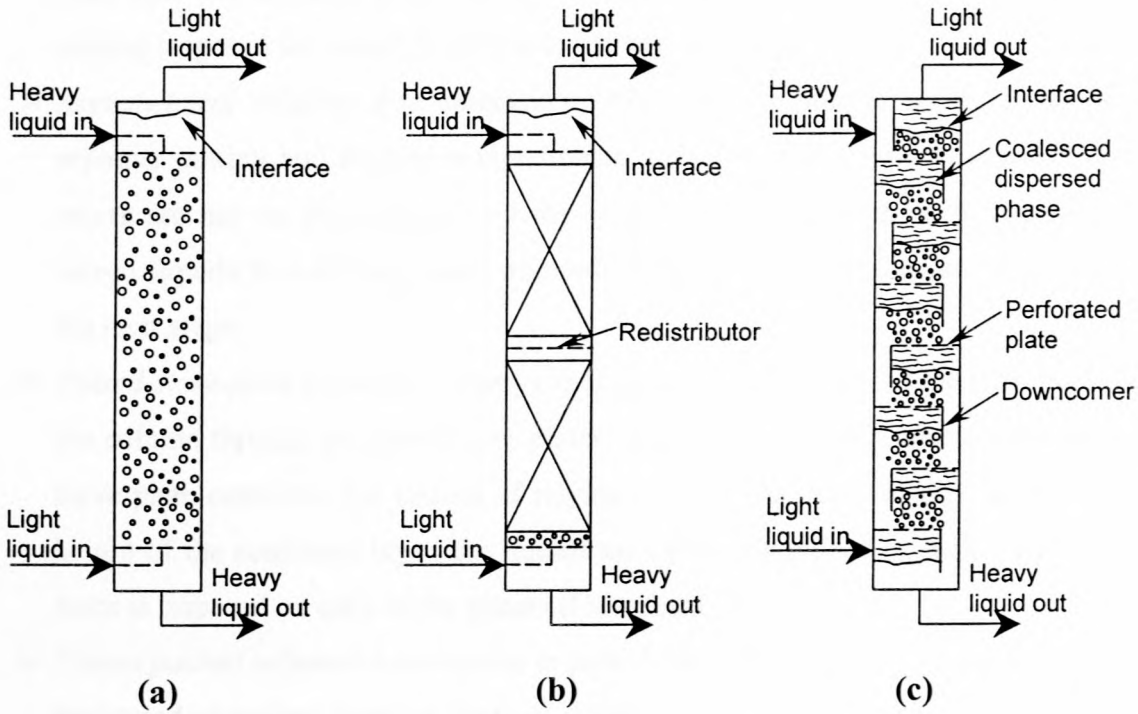

Figure 2-5: Unagitated Column Extractors, (a) Spray column, (b) Packed column, (c) Sieve- plate column (Lo, 1979)

- ***Mechanically agitated extraction columns*** – receive mechanical energy *via* either rotating or reciprocating elements or pulsation, the density difference between the two phases is used as driving force for flow and final separation (Refer to **Figure 2-6** below).

  - *Scheibel columns* – comprise sets of mixing stages on top of each other, each consisting of a turbine impeller between a set of inner baffles, that direct flow to the outer column shell, where stator baffles separate the settling zones of the column (Cusack and Fremeaux, 1991).
  - *Oldshue-Rushton columns* – comprise a series of baffled mixing tanks on top of one another, and equipped with vertical baffles to enhance mixing characteristic and horizontal baffles to define mixing stages and minimise axial mixing (Cusack and Fremeaux, 1991).

- *Khuni columns* - similar to Scheibel columns, consisting of a series of mixing compartments, each of which has a shrouded turbine impeller located between two perforated plates (Cusack and Fremeaux, 1991).
- *Rotating disc contactors (RDC)* – consists of a series of rotors mounted on a central shaft that sits within a series of stator rings, which limit axial mixing and define the mixing stages in the vessel (Korchinsky, 1994).
- *Asymmetrical rotating disc contactors (ARDC)* – are similar to the RDC but have separate mixing and settling compartments, they are asymmetric in that the shaft and rotors are not on the centreline of the vessel; baffles between each stages direct the mixed liquids to a settling zone, from which they either pass upward or downward to the next stage.
- *Pulsed sieve-plate columns* – energy is imparted by pulsation of the liquid contents of the column through stationary sieve plates, they operate as stagewise contactors like the sieve plate extractor, but instead of relying only on the hole velocity generated by the height of the coalesced layer, the liquids are cyclically pulsed in such a way that axial force is imposed on each of the phases (Haverland, 1994).
- *Pulsed packed columns* – are similar to pulsed sieve plate column, however they contain structured or random packing (Stevens, 1994)
- *Karr reciprocating plate columns* – employ a series of perforated plates (having large diameter holes, with considerable open area of 55 to 60%), which are reciprocated by a drive; baffle plates along the platestack length limit axial mixing (Baird, et al., 1994; Cusack and Fremeaux, 1991).
- *Vibrating Plate Extraction (VPE) columns* – are similar to the Karr column, however plates have smaller holes (less free area of about 25%) and employs downcomers or upcomers for the continuous phase (Baird, et al., 1994; Cusack and Fremeaux, 1991)).

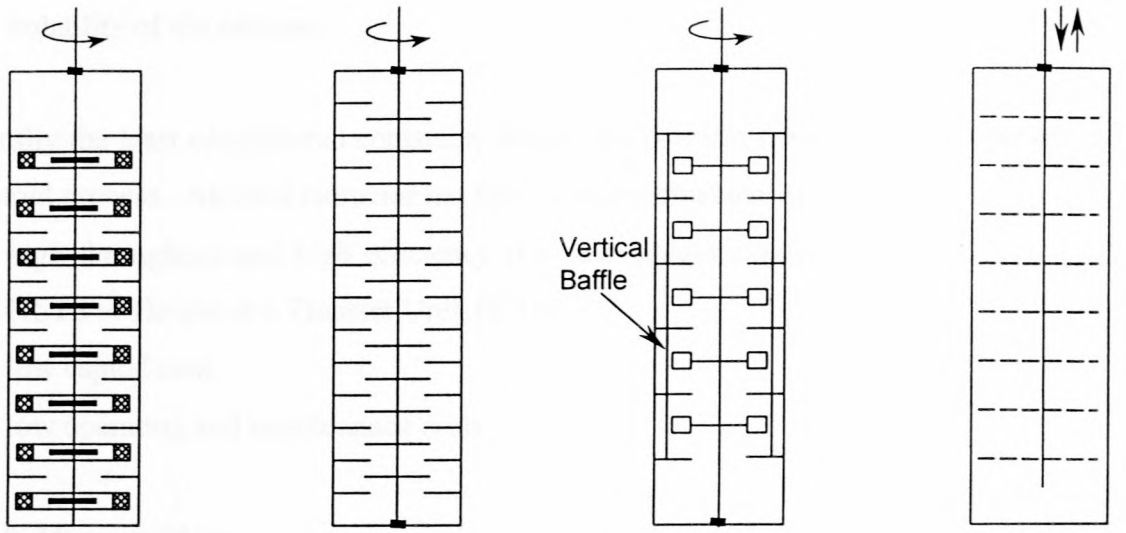

Figure 2-6: Mechanically agitated column extractors, (a) Scheibel, (b) RDC (c) Oldshue-Rushton, (d) Reciprocating plate (Lo, 1979)

2.2.2 Selection and Application of Extraction Equipment

Frequently liquid-liquid extraction equipment has been developed for specific processes, with which they then tend to become associated. Consequently, for a new process application, selection of an extractor can be quite complex. The choice of extractor can involve many factors, including the following (Lo, 1979):

- reliability of scale-up,
- number of stages required,
- required flowrates of each phase,
- capital costs,
- maintenance requirements,
- materials of construction,
- floor space available,
- headroom available,
- turn-down flexibility,
- liquid residence time,
- emulsification tendencies,

- volatility of the solvent.

Generally the least complicated contactor, which will perform the extraction, is preferred for an industrial process. An ideal extractor has the following characteristics (Lo, 1979):

- high throughput and high efficiency (i.e. low Height Equivalent to a Theoretical Stage, HETS or Height of a Transfer Unit, HTU),
- low capital cost,
- low operating and maintenance costs.

2.2.2.1. Mixer-settlers

Mixer-settlers are widely used in the chemical process industry, and also extensively in the mining industry, where high flowrates up to 22,7 m^3/min are encountered. They are particularly practical and economical for operations (such as washing, two phase reactions and neutralisations) that require a residence time of 0.5 to 2 minutes or longer to reach equilibrium as well as processes requiring intense mixing and small droplets to promote mass transfer. They have high stage efficiency and capacity, and can handle a wide range of solvent ratios. In addition, mixer-settlers have good flexibility, are reliable on scale-up and can handle liquids with high viscosity. However, this type of equipment tends to be bulky, has large space requirements and has a high inventory of material held up. This type of equipment should be used only when a few stages are required, typically less than three, and generally is not suitable for systems that tend to emulsify easily (Godfrey, et al., 1994; Cusack and Fremeaux, 1991; Lo, 1979)

2.2.2.2. Centrifugal Extractors

Centrifugal extractors are typically used for extracting heat sensitive antibiotics from fermentation broth's using a very short residence time and low working volume. Centrifugal extractors are also commonly used for systems exhibiting a small density difference (<0.05 kg/*l*), a strong tendency to emulsify or requiring short contact times. However, since centrifugal extractors operate at high speed, maintenance tends to be high. In addition, these extractors are only suitable when three or fewer stages are required (up to 7 stages have however been reported) and if solids are present, plugging can be problem due to the small clearances involved (Blass, 1994; Cusack and Fremeaux, 1991).

2.2.2.3. Unagitated Columns

Gravity columns without mechanical agitation require no moving parts and are utilised extensively in petroleum refining applications, which require only a few theoretical stages. But the height of the column required can become excessive when a large number of theoretical stages is required. Mechanically agitated columns can generally attain a shorter height equivalent to a theoretical stage than an unagitated column (Lo, 1979)

Spray columns are simple, however they incur much axial mixing, so that they seldom represent more than a single stage. The lack of internals in these columns does however render them suitable for streams containing large amounts of suspended solids (Cusack and Fremeaux, 1991).

Sieve plate extractors have reasonably high throughput capacity since they can be built in large diameters, and are simple to scale-up since they have limited axial mixing. They are however very susceptible to solids plugging, and a specific column has a relatively narrow operating range with regard to throughput (Cusack and Fremeaux, 1991)

The packing in packed columns lessens axial mixing and aids in the formation of drops, which aid mass transfer. However the packing also restricts the free area available for flow of the liquids fluids, and thus hinders throughput. Packed columns have no moving internals requiring maintenance, but offer advantages only when few stages (up to three) are required. They are difficult to scale up, subject to plugging when solids are present, and effective initial distribution of the dispersed phase is critical for performance of the extractor (Cusack and Fremeaux, 1991).

2.2.2.4. Columns with Rotating Internals

Columns such as the Scheibel, Oldshue-Rushton, Khuni columns, Rotating disc contactors and Asymmetrical rotating disc contactors generally have a high number of theoretical stages per unit height. However due to the shear forces involved, the drops size distribution produced in these extractors is not very uniform, resulting in low throughputs, as compared to other columns. The shear action also renders application of these columns unsuitable for systems that tend to emulsify easily. The scale-up of these columns is not simple, due to the fact that shear forces increase with increasing diameter (Cusack and Fremeaux, 1991).

2.2.2.5. Pulsed Sieve Plate and Packed columns

Pulsed columns are very suitable for the nuclear industry, since the pulsing mechanism can be placed in a remote location and because there are no seals to leak. Significant energy is however required for pulsing the entire liquid column contents, particularly on a large scale commercial extractor. Design of the pulsing mechanism is critical for effective operation (Cusack and Fremeaux, 1991; Haverland, 1994).

2.2.2.6. Reciprocating/Vibrating Plate Extraction Columns

Reciprocating/Vibrating plate extraction columns operate at very low agitation intensities, apply uniform shear across the column cross section, and achieve uniform dispersion. They are particularly suitable for systems, which exhibit emulsifying tendencies. In addition they have very high throughput and relatively low Height Equivalent to a Theoretical Stage (HETS) (which results in high volumetric efficiencies) as compared to other agitated extractors. This can be attributed to the uniform shear mixing characteristics of the equipment, which tends to generate a narrower and more uniform drop size distribution. These columns have enormous versatility and flexibility and can be operated over a very wide range of agitation intensities. They have relative simplicity in construction, low maintenance requirements and can handle liquids containing suspended solids (as long as size of solids is less than the size of the plate perforations). The reciprocating or vibrating agitation can usually reduce the height required for extraction, especially if the interfacial tension is high. While pulsed columns require considerable energy to pulse the entire liquid content of the column (particularly on a large scale commercial extractor) reciprocating the plates is an alternative solution to achieving uniform dispersion and similar mixing patterns using relatively much less energy. (Baird, et al., 1994; Cusack and Fremeaux, 1991, Lo, 1979)

2.2.3 Countercurrent Column Extraction

A typical countercurrent Vibrating Plate Extraction (VPE) column (equipped with a plate stack and drive) is depicted in **Figure 2-7**, below. In this case it is assumed that the feed has a greater density than the solvent and that the aqueous phase is the continuous phase while the organic phase is dispersed as droplets.

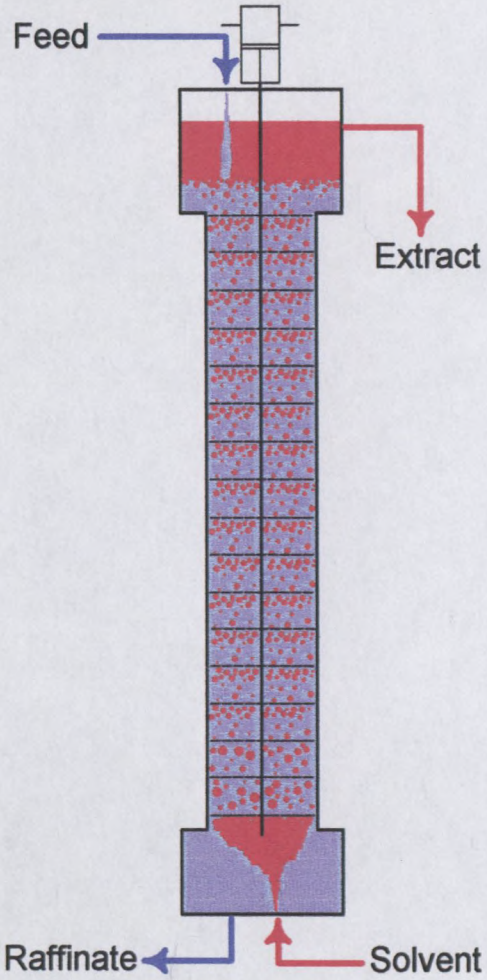

Figure 2-7: Typical countercurrent extraction column

The feed enters at the top of the column while the solvent is fed at the bottom of the column, and the two streams pass each other counter-currently. The solvent rich phase (extract) containing the extracted solute overflows at the top of the column, while the residual feed (raffinate) leaves at the bottom of the column. The advantage of countercurrent extraction is that it is far more efficient than cocurrent extraction, because a concentration profile exists along the length of the column, and it is possible to achieve more than a single stage extraction.

The continuous aqueous phase fills the volume of the column. The organic phase is dispersed as droplets in the active section of the column (by the internals), thereby contacting the two immiscible phases, and enabling mass transfer. The top settler, which may have an enlarged diameter to assist in phase distribution or disengagement, has no internals. In the settler the droplets re-coalesce, allowing the two phases to settle and separate, thus forming an interface. The difference in density between the two phases provides the driving force for movement of the

dispersed phase through the continuous phase and separation of the phases in the settler. The position of the interface can be controlled, by manipulating the flowrate of whichever phase is pumped out of the bottom of the column (typically organic solvents are less dense than aqueous feeds and hence the aqueous raffinate would be removed from the bottom) (Lo and Prochazka, 1983).

Various terms typically used to describe column extraction are defined as follows:

Dispersed phase: the phase dispersed as droplets in a column.

Continuous phase: the phase that remains coalesced and does not disperse in a column.

Hold-up: is the fraction of the column volume occupied by the dispersed phase. In practical design of VPE's, the hold-up is kept to within 15 to 20%, which corresponds to 70 to 80% of the flooding throughput (Lo and Prochazka, 1983, Souhrada et al., 1970)

Flooding: occurs when the hold-up increases unstably so that countercurrent flow of the phases cannot be maintained. It is caused by the terminal velocity of the dispersed phase being less than the average velocity of the continuous phase. Since the amount of agitation affects the drop size and the drop size effects the throughput, when operating at fixed flowrate, increasing the agitation will increase the hold-up until the column floods. In VPE and Karr extraction columns the degree of agitation is dependent on the plate frequency, spacing and amplitude of reciprocation. Similarly, at a particular column frequency, it is possible to increase the flowrate until the flooding point is reached. Flooding is visually apparent since it creates what could be described as a "blockage" in the column, and the phases begin to leave the column at the ends that they are introduced. In a rapidly coalescing system, flooding is associated with a phase inversion, where the dispersed phase becomes the continuous one and *vice versa*. This results in the formation of a second interface near the end of the column, opposite to that at which the interface is normally being controlled. Effectively, when the column floods, this is the maximum performance that the column can achieve; however, it is not a stable, operable state. Consequently, the column is usually operated at a flowrate of about 10 to 15% lower than that used when flooding occurred, or by reducing the agitation by 5 to 10%. This ensures stable operation, while still maintaining sufficient specific throughput and extraction efficiency. It is possible to predict flooding using various correlations. The concept of flooding is further

quantified in **Section 2.2.4**, in terms of the various flow regimes (Cusack and Karr, 1991; Baird et al. 1994; Lo and Prochazka, 1983).

Axial mixing: is the undesired forward and back mixing of the continuous and dispersed phases. Ideally, pure plug flow of each phase is preferred, since this maximises the concentration driving force over the length of the column.

Emulsion: is a stable mixture of two immiscible liquids that do not separate into two phases, or take impractically long to separate.

Specific throughput[7]: is the flowrate of a particular phase per column cross sectional area.

It is essential that column internals are preferentially wetted by the continuous phase. If the dispersed phase wets the internals, the droplets tend to coalesce on the surface, which in turn leads to further coalescence and localised flooding. The collapse of the droplets result in a loss of interfacial area and a decrease in mass transfer efficiency. The choice of the continuous phase is based on visual inspection of the settling characteristics of a "shake test". The phase that coalesces more easily and rapidly is generally selected as the dispersed phase. In addition it is theoretically better to extract the solute from droplets into a continuous medium (in terms of extraction efficiency) as this minimises the average distance between the solute and the mass transfer interface. It also promotes coalescence, termed the *Marangoni effect* (Slater, 1994; Gourdon et al., 1994).

When the aqueous phase is continuous, and the organic phased dispersed, the internals are usually metal, and the interface is positioned in the top settler. Conversely, when the continuous phase is organic, and the dispersed phase aqueous, the internals are usually a non-metallic material, such as Teflon. In this case the interface would usually be positioned in the bottom settler (since the organic phase is usually less dense than the aqueous phase). In most cases the natural wetting properties of the liquids can be used, however in other cases the surface of the metal plates could be treated (by polishing, electroplating etc.). Teflon coated internals are generally more expensive than stainless steel internals.

---

[7] Appendix B, Equation B-20

The rate at which the dispersed phase passes through a column, and consequently the hold-up, is related to the terminal settling velocity of a droplet, and is determined by various factors including:

- the size of the droplets,
- the viscosity of the continuous phase,
- the difference in density between the dispersed and continuous phases.

Bond and Newton studied the velocity of isolated liquid drops immersed in another liquid and determined the relationship between the terminal settling velocity[8] (U_∞), viscosity, drop radius, density and interfacial tension (Treybal, 1951). The equation comprises Stoke's law for rigid spheres and a correction factor. For small drops, the correction factor approaches unity, and Stoke's law becomes directly applicable. The equation cannot be applied directly to settling of emulsions or families of droplets, since coalescence will vary the radius of the drops, and because the close crowding drops interact, resulting in different behaviour to simple drops. It does indicate, however, that settling will be slower the greater the viscosity of the continuous phase, the smaller the density difference, and the smaller the drop size (Treybal, 1951).

In agitated extraction columns, the rate of break-up of drops is affected by the amount of agitation. The greater the agitation, the smaller the drop size, which results in a greater hold-up and hence slower the terminal settling velocity of the dispersed phase. Similarly, the smaller the relative density difference between the phases, the slower the settling rate. In the VPE, coalescence on or under the plates (depending on which phase is continuous) of the drops occurs, followed by re-breaking up by the action of the reciprocating plate. The major factor promoting coalescence is interfacial tension, whereas several factors oppose it, and in general, the greater the interfacial tension, the greater the tendency to coalesce. Interfacial tension is low for liquids of high mutual solubility and is lowered by the presence of emulsifying agents. High viscosity of the continuous phase hinders coalescence by decreasing the rate at which the thin film between drops is depleted. The formation of tough interfacial films by emulsifying agents may prevent coalescence, while the presence of minute dust particles, (which generally accumulate at the interface when dispersed in two-liquid-phase systems), can also prevent coalescence (Treybal, 1951).

[8] Appendix B, Equation B-13

2.2.4 Reciprocating Plate Extraction Columns

Typically reciprocating plate extraction columns are furnished with internals in the form of a plate stack, positioned in the active section of the column. The plate stack consists of a number of perforated plates mounted on a central shaft, the upper end of which is connected to an adjustable eccentric contrivance (for changing rotary into backward-and-forward motion), which is attached to the shaft of a drive motor. The spacing between plates is typically between 25 to 150 mm, and may be varied with position in the column if the system properties are known to change due to mass transfer (Baird et al., 1994).

The reciprocation of the plates breaks the dispersed phase into droplets at each plate, thus providing interfacial surface area for mass transfer. For reciprocating plate extraction columns (and pulsed columns) terms have been defined to describe the various flow regimes observed. The regimes are depicted in **Figure 2-8**, below, assuming the aqueous phase is continuous (with organic phase continuous, the droplets would be positioned on top of the plates).

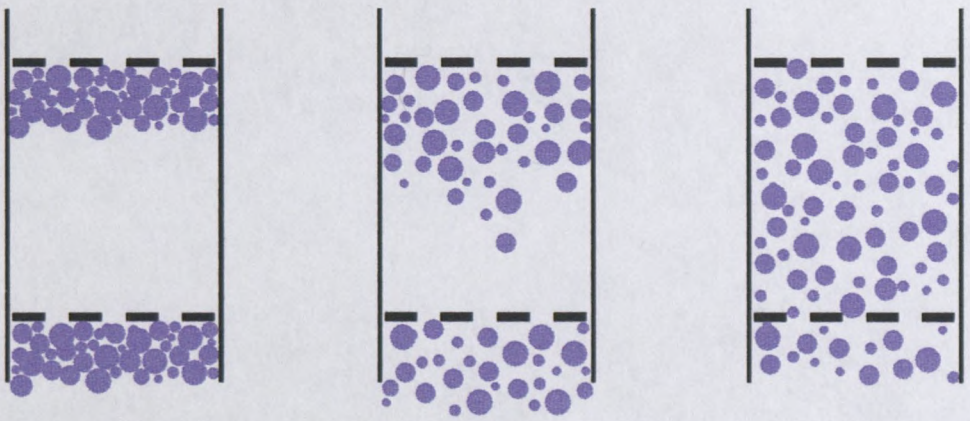

Figure 2-8: Flow regimes: (a) mixer-settler regime, (b) dispersion regime, (c) emulsion regime

The various regimes are defined as follows (Baird, et al., 1994; Lo and Prochazka, 1983, Nemecek and Prochazka, 1974):

- *Mixer-settler* regime is characterised by a layer consisting of a clear dispersed phase or a densely packed (cellular) aggregation under the plates, the boundary between the layer and

the continuous phase being clearly observable, and the thickness of the layer changing periodically. This regime can occur at zero or low agitation rates in plates with open area fraction less than about 0.4, and is more likely to occur for higher interfacial tensions and lower inter-phase density differences. Hold-up is largely determined by the depth of the layer of dispersed phase formed under each plate, since hold-up in the remaining volume is negligible. The vertical component of the velocity of the drops prevails and no back flow of the dispersion through the plate occurs.

- *Dispersion (or transitional) regime* – the dense layer of drops on the plates expands over the height of the stage, however at very low agitation there is a tendency for drops to cluster closely near the plates. The dispersion regime differs from the mixer-settler regime in that a discrete layer of the dispersed phase is not visible. A region of low local hold-up near the dispersed phase inlet and a region of higher local hold-up near the outlet end are still clearly visible. The drops move predominantly in a vertical direction and no back flow of the dispersion through the plate occurs.

- *Emulsion regime* - well-agitated, two phase mixture with uniform hold-up over the height of the stage. The drops move erratically resulting in backflow through the plate. In the emulsion regime the importance of the enlarged settling zones increases. Since in this case no coalescence and re-dispersion occurs on individual plates, the flow through the column is not limited by these processes, but the area of the main interface must be sufficient to provide an adequate coalescence rate. The continuous phase velocity must be reduced in the settling zone to prevent entrainment of drops (Baird et al., 1994)

In the mixer-settler regime, flooding is observed as a continuous increase in the depth of the dispersed phase layer at each plate. In the emulsion regime, two types of flooding can be distinguished, depending on the tendency of the system to coalesce and the phase velocity ratio. In a poorly coalescing system a massive entrainment of the dispersed phase by the continuous phase starts 'flooding by excessive reciprocation' in the column region with highest hold-up, which ultimately spreads to the dispersed phase inlet. In a rapidly coalescing system that is close to flooding, the increase in hold-up usually leads to a phase inversion. In the case of low ratios of dispersed to continuous phase, the hold-up at flooding may be rather low (Baird, et al., 1994; Lo and Prochazka, 1983).

The emulsion regime need not always be the optimum regime to reach the most effective operation of the extractor, since in a number of practical situations, it calls for a substantial cut in total throughput (Nemecek and Prochazka, 1974).

2.2.5 Classification of Reciprocating Plate Extraction Columns

Two main types of reciprocating plate column, the "open" type (Karr) and the "segmental passages" type (VPE) are widely used in industry. The two types of column have been developed independently, with the Karr column in use mainly in North America and the VPE mainly in Eastern Europe and the Soviet Union (Lo and Prochazka, 1983). The Karr and VPE columns are both classified as reciprocating plate columns, however the main difference between the two types lies in the design and function of the plates (Lo and Prochazka, 1983). Typical Karr and VPE column plates are depicted in **Figure 2-9**.

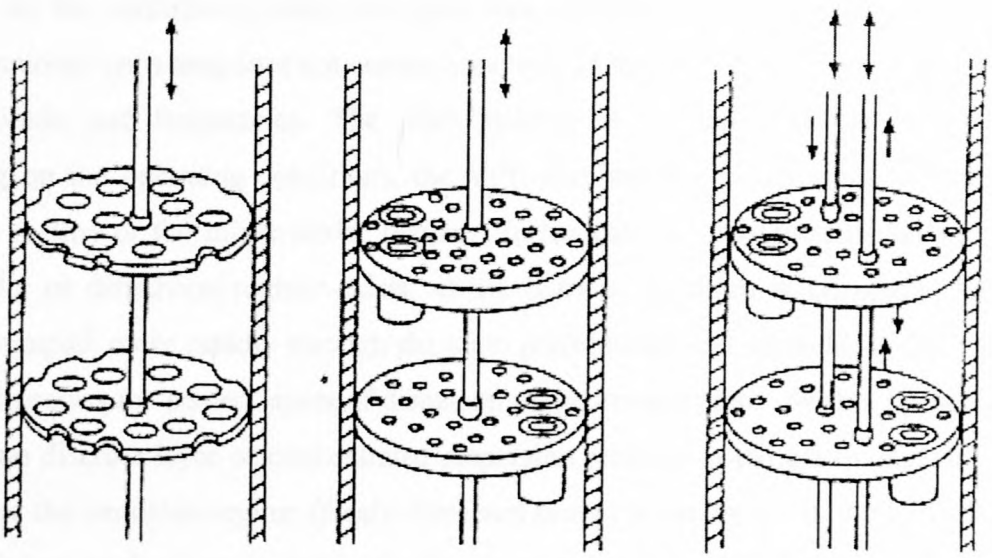

Figure 2-9: Karr and VPE reciprocating plate extraction columns, (a) Karr column, (b) VPE column, (c) VPE column (counterphase) (Baird, et al., 1994)

There are two variations of the VPE, columns with uniform motion of the plates, and those with countermotion of plates.

The Karr column plates (Refer to **Figure 2-9(a)**) have a large fractional open area (50 to 60%) and hole diameter (10 to 16 mm), significantly larger than the average dispersed drop size. No downcomers are provided since the open structure of the plate is sufficient for countercurrent flow. Because of the open plate structure, the columns usually only operate in the emulsion regime of two-phase flow, although a slight clustering of drops around the plates may occur. As agitation is increased, initially, the effect on the hold-up is negligible, but as the agitation is increased further, due to the corresponding decrease in drop size, the hold-up increases in a non-linear manner. In industrial sized Karr columns, doughnut-shaped baffles are inserted at intervals in the platestack to reduce non-uniformities in the flow, thereby minimise axial mixing. The amplitude can normally range from 3 to 23 mm, but is typically 19 mm and the reciprocating frequency is adjustable up to 1000 strokes/min (of from 1 to 5 Hz). The plate spacing can vary between 25 to 100 mm (Baird, et al., 1994; Lo and Prochazka, 1983).

The VPE column plates (refer to **Figure 2-9(b)**) have perforations of 2 to 5mm diameter, and small fractional open area, in the 4 to 30% range. The plates can be equipped with downcomer segments for the continuous phase, the open area of which ranges between 10 to 25%. The overall fractional open area does not normally exceed 25 to 30%. The VPE operates at relatively low amplitude and frequencies. The plate spacing is typically between 60 to 150 mm. Depending on the operating conditions, the VPE may operate in the emulsion regime or the dispersion regime or the mixer-settler regime. In the case of low levels of agitation, where a mixer-settler or dispersion regime exists, as the level of agitation is increased, the dispersed phase is 'pumped' more rapidly through the plate perforations and the hold-up decreases, as the agitation disperses the settled layers of dispersed phase at each plate. With a further increase in agitation, no discrete layer or concentrated dispersion remains at the plates, and the hold-up is increased as the emulsion regime (freely dispersed drops) is achieved. In the VPE the breakage of drops occurs predominantly during their passage through the holes. Under these conditions the breakage mechanism favours a narrow drop size distribution around an optimum mean drop size (a pre-condition for high extractor efficiency). By reducing the hindering effect of the continuous phase on the dispersed phase, the plate downcomers have the effect of increasing the throughput and reducing the hold-up at low levels of agitation. For smaller VPE columns, the downcomers of successive plates are placed on opposite sides of the column axis so that a crossflow of phases between the plates can be achieved. On large plates the distribution of passages is such that several parallel sections with a cross flow of phases are created. In conclusion, the VPE plate design and the action of droplet coalescence and re-dispersion,

facilitates very high throughputs compared to other agitated extractors. A variation of the VPE design (for column diameters exceeding 400 mm) uses two separate sets of plates, each set being supported by its own shaft, as depicted in **Figure 2-9(c)**. The motion of the two shafts is such that each plate reciprocates 180° out of phase with its two adjacent plates. Thus the instantaneous velocities of plates are neighbouring plates are of equal magnitude and in opposite directions. This countermotion increases capacity and efficiency (Baird, et al., 1994; Cusack and Fremeaux, 1991; Lo and Prochazka, 1983).

2.3 Evaluating the Performance of VPE Columns

In order to scale-up and design a commercial extraction column, it is necessary to quantify the system hydrodynamics and mass transfer characteristics, based on fundamental studies (Lo and Prochazka, 1983). The principal performance objectives of countercurrently operated extraction columns concerns the following aspects (Novotny, et al., 1970, Baird et al., 1994):

- mass transfer rate per unit volume and unit concentration driving force,
- permissible throughput for each phase, per cross sectional area,
- axial mixing, which disturbs countercurrent plug flow.

The limit on throughput of a column is determined by the flooding rate, above which countercurrent flow of the phases cannot be maintained. The mass transfer performance of a column is indicated by the length of column required to produce a given degree of separation. The factors affecting throughput are hydrodynamic in nature, while those controlling mass transfer performance are the system properties, such as the rates of inter-phase mass transfer, equilibrium relationships and the extent of backmixing. The controlling factors are independent in nature, however they can interact. Frequently those factors which enhance the mass transfer rate by increasing the magnitude of the mass transfer coefficient and the interfacial area, also tend to diminish it by increasing the extent of longitudinal mixing, thereby reducing the mean driving force. This is particularly true in pulsed and reciprocating plate extraction columns (Novotny, et al., 1970). Also improvement in mass transfer performance (by for instance increasing agitation) can simultaneously reduces the permissible column throughput (Lo et al., 1983).

The extent of agitation in the column is defined by the agitation intensity and takes into account rotational speed, amplitude and plate spacing (Lo, 1979):

$$I_a = \frac{am.rpm}{Ps} \qquad \textbf{(2-10)}$$

where:

am : amplitude, distance between the extreme positions of the stack, i.e. twice the stroke (m),

I_a : agitation intensity (/min),

Ps : plate spacing (m),

rpm : rotational speed (rpm).

The *specific throughput* (or superficial velocity) is defined as flowrate per column cross sectional area:

$$\psi = \frac{F}{CSA} \qquad \textbf{(2-11)}$$

where:

CSA : cross sectional area of column (m^2),

F : flowrate (m^3/hr),

ψ : specific throughput (m^3/m^2h).

The effectiveness of an extractor can be measured by volumetric efficiency - the greater this number, the smaller the column volume required to perform a given extraction (Godfrey, et al., 1994). This parameter requires determination of the Height Equivalent to a Theoretical Stage (HETS), which is discussed in **Section 2.6.1**:

$$\eta_v = \frac{\psi}{HETS} \qquad \textbf{(2-12)}$$

where:

$HETS$: Height Equivalent to a Theoretical Stage (m),

η_v : volumetric efficiency (/h).

In well designed VPE columns, a total specific throughput of between 30 and 80 m/h, and HETS of 0.4 to 1.5 m can be achieved depending on the nature of the liquid system (Baird, et al., 1994). This implies that the volumetric efficiency of the VPE can vary between 20 to 200 /h.

Various methods have been devised whereby it is possible to evaluate the performance of a column extraction system, and scale it up to ensure that the commercial operation achieves the same separation achieved on a pilot scale. Extractor theory combines: the equilibrium relationship, the material balance, which yields an operating line, and the mass transfer rate expression. Either graphical or analytical methods can be used for determining the system; each having associated advantages and disadvantages (Lo, et al., 1983). The most common method is similar to the graphical McCabe Thiele approach used for distillation. The system can also be defined mathematically by using transfer units, and solved analytically. A major assumption in these methods is that each phase moves as plug flow. However in practice it is necessary to consider axial mixing within each phase, because of the tendency to lower performance of the columns.

Models, which account for axial dispersion can be derived to predict the behaviour of a column. The Diffusion model involves performing a mass balance over a differential element of the column, and then integrating axially to obtain entry and exit concentrations. For the Backflow or Tanks-in-series model, it is assumed that the column consists of a series of continuously-stirred-tank-reactors (CSTR's), and a mass balance is performed, resulting in a number of equations that must be solved simultaneously. These methods are all derived for steady state operation, however unsteady state models can also be used to evaluate the performance of an extraction. For the application of these models to the design of an extractor, it is necessary to determine both the extent of axial mixing and to quantify the rate of mass transfer. (Souhrada et al., 1966a)

Theoretical evaluation of an extraction system must be combined with experimentally determined results. Piloting tests provide the following qualitative and quantitative information for scale-up and design of the column extractor (Lo and Prochazka, 1983):

- total throughput and agitation speed,
- height equivalent to a theoretical stage (HETS), or Height of a Transfer Unit (HTU)
- column efficiency,
- hydrodynamic conditions – droplet dispersion, phase separation, flooding, emulsive layer formation, etc.,
- selection of dispersed phase or direction of mass transfer,
- material of construction and plate wetting characteristics,
- solvent to feed ratio,

- stage efficiency,
- confirmation of desired separation.

2.4 Kinetics of Extraction

In a countercurrent extraction column it is unlikely that complete equilibrium is attained, even at low flow rates because of the nature of the countercurrent flow (Lo et al., 1983). Consequently in order to design a commercial extraction column using piloting data, the kinetics of the process must first be quantified. The kinetics of diffusion processes are usually characterised either directly, by means of the mass transfer coefficient, or indirectly, by means of efficiency. For stagewise processes, conventionally the latter characteristic is employed (Prochazka and Landau 1966)

2.4.1 Mass Transfer

2.4.1.1. Rate of Mass Transfer

The classical two-film theory is used to describe the mechanism of mass transfer of a solute between two liquid phases. The theory is described with reference to **Figure 2-10**, which depicts the concentration profiles that exist between phases A and B.

The theory postulates that there is no resistance to transfer across the interface, and consequently at the interface, the two phases are at equilibrium. The resistance to mass transfer occurs in the films on either side of the interface. In the bulk phases, the concentrations are assumed to be uniform, as a consequence of a combination of eddy and molecular diffusion.

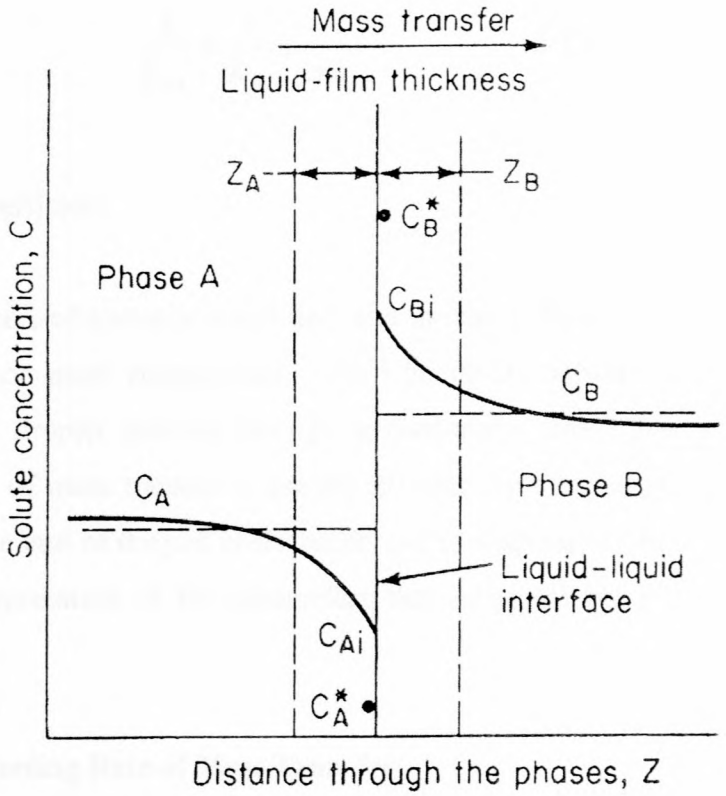

Figure 2-10: Concentration profiles in inter-phase mass transfer (Lo, 1979)

By considering the rate of mass transfer from a bulk solution of A to the bulk of B, the following equations may be derived (Pratt, 1983a; Treybal, 1951):

$$N_f = k_A A\left(c_A - c_{Ai}\right) = k_B A\left(c_{Bi} - c_B\right) \qquad \textbf{(2-13)}$$

$$N_f = k_{oA} A\left(c_A - c_A^*\right) = k_{oB} A\left(c_B^* - c_B\right) \qquad \textbf{(2-14)}$$

where:

A : interfacial surface area (m^2),

c_{ij} : solute concentration in phase j, adjacent to the interface (mol/*l*),

c_j : solute concentration in the bulk of phase j (mol/*l*),

c_j^* : solute concentration in phase j in equilibrium with the other phase in the system (mol/*l*),

k_j : film mass transfer coefficient for phase j (m/s),

k_{oj} : overall mass transfer coefficient based on phase j (m/s),

N_f : flux of mass transfer (mol/h).

The overall mass transfer coefficient is related to the individual film mass transfer coefficients by the following relationship (Lo, 1979):

$$\frac{1}{k_{oA}} = \frac{1}{k_A} + \frac{1}{mk_B} \qquad \textbf{(2-15)}$$

where:

m : partition coefficient.

The approach summarised above is simplified, and in reality the exact mechanism of inter-phase mass transfer is much more complicated. The film theory assumes an unchanging interface, where in reality, a droplet moving through a continuous phase has a constantly changing interface. The rate of mass transfer is greatly affected by the complicated hydrodynamics of interfacial turbulence and of droplet coalescence and re-dispersion. However the film theory is convenient for interpretation of the parameters that influence the rate of mass transfer (Lo, 1979).

2.4.1.2. Factors Affecting Rate of Mass Transfer

The rate of mass transfer can be affected by influencing the mass transfer coefficients, the interfacial area or the concentration driving force. The factors that can affect each of these are summarised below (Lo, 1979):

Mass transfer coefficient:

- *phase composition* by promoting interfacial turbulence and governing diffusivity,
- *temperature* by affecting the rates of diffusion,
- *type and degree of agitation* by governing film thickness and interfacial turbulence,
- *direction of mass transfer*, determined by selecting which phase is dispersed,
- *physical properties*, such as density, viscosity and interfacial tension.

Interfacial area:

- *phase composition* by affecting the interfacial tension and the phase densities,
- *temperature* by affecting the interfacial tension,
- *type and degree of agitation* by creating a more intimate type of dispersion of the two phases,
- *phase ratio*,
- *physical properties*, such as interfacial tension.

Concentration driving force:

- *solute bulk concentration* of the two phases,
- *partition coefficient* which governs C_{Ai} and C_{Bi},
- *temperature*, which affects the partition coefficient.

The mass transfer coefficients for each phase can be estimated approximately from the drop size and system properties, having particular regard to surface behaviour. For small drops (less than 1 mm), in systems containing surface active agents, it is likely that the drop surface will be immobile and the mass transfer coefficients will typically be in the order of 10 μm/s. In interfacially "clean" systems, with no trace of surfactant, the drop surface may be mobile and the overall mass transfer coefficient can be in the order of 100 μm/s (Baird et al., 1994).

2.4.2 Efficiency

In continuous countercurrent extraction columns the departure from equilibrium is appreciable and thus it is important to define efficiency. In terms of extraction, efficiency has two interpretations (Pratt, 1983b):

- measure of performance of a real extractor as compared to an ideal one,
- measure in terms of actual mass transfer mechanisms.

The three efficiencies defined below are primarily only for the case of one solute. In the case of more than one solute, coupling between the motions of the diffusing species greatly complicates the theory.

2.4.2.1. Overall Efficiency

The overall efficiency η_o is the ratio of the number of ideal to real stages required to achieve the same concentration change with the given flows. This efficiency is useful only for linear equilibrium relationships (Pratt, 1983b).

$$\eta_o = \frac{N_{S,ideal}}{N_{S,real}} \qquad \textbf{(2-16)}$$

where:

η_o : overall efficiency

N_S : number of stages

2.4.2.2. Murphree Efficiency

The Murphree efficiency is defined as the ratio of the actual concentration change of that phase within the stage to the change that would have occurred if equilibrium had been reached, as depicted in **Figure 2-11** (Pratt, 1983b).

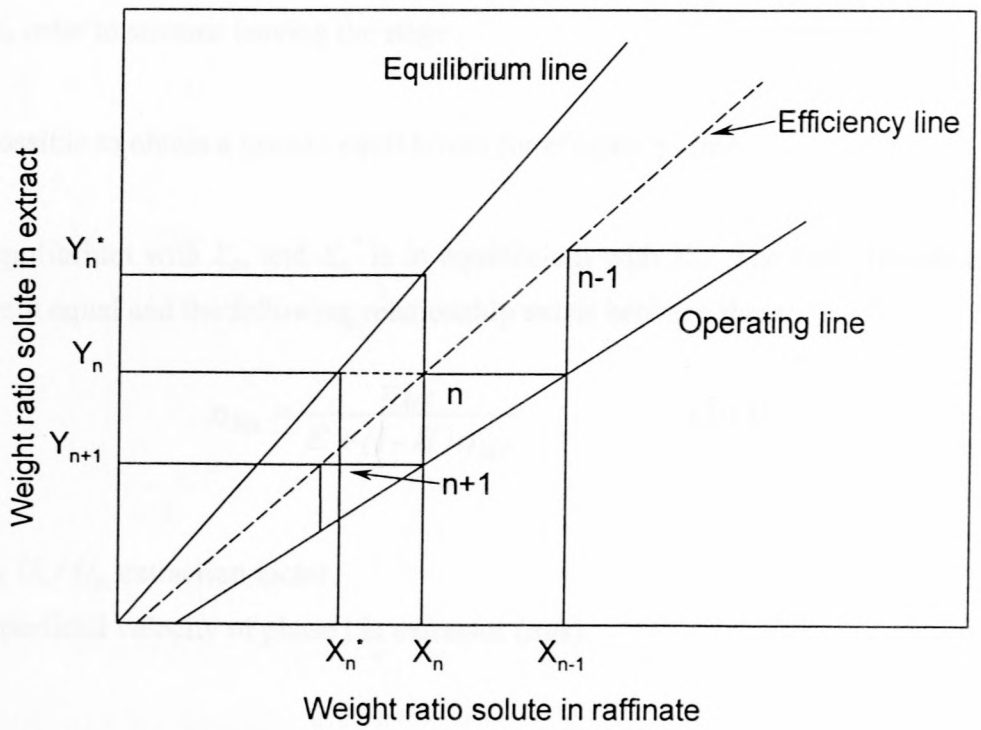

Figure 2-11: Murphree Efficiency (Pratt, 1983)

The Murphree efficiency is defined as follows:

$$\eta_{Mx} = \frac{X_{n-1} - X_n}{X_{n-1} - X_n^*} \qquad \textbf{(2-17)}$$

$$\eta_{My} = \frac{Y_n - Y_{n+1}}{Y_n^* - Y_{n+1}} \qquad \textbf{(2-18)}$$

where:

η_{Mj} : Murphree efficiency based on phase j,

n : stage number counted from feed inlet

X : weight or mole ratio of component in x phase,

Y : weight or mole ratio of component in y phase,

superscript:

* : equilibrium value.

These efficiencies relate to overall stage efficiencies:

- X_{n-1} and Y_{n+1} refer to streams entering the stage,
- X_n, Y_n refer to streams leaving the stage

It is thus possible to obtain a pseudo equilibrium (or efficiency) line.

Y_n^* is in equilibrium with X_n, and X_n^* is in equilibrium with Y_n. The two efficiencies (of each phase) are not equal and the following relationship exists between them:

$$\eta_{Mx} = \frac{\eta_{MY}}{\boldsymbol{E} + (1 - \boldsymbol{E})\eta_{MY}} \qquad \textbf{(2-19)}$$

where:

$\boldsymbol{E}$ $= m\, U_x / U_y$, extraction factor,

U_j : superficial velocity of phase j in extractor (m/s)

2.4.2.3. Stage Efficiency

The stage efficiency is defined as follows, as depicted in **Figure 2-12** (Prochazka and Landau, 1966):

$$\eta_Y = \frac{(Y_n - Y_{n+1})}{(Y_n^{\bullet} - Y_{n+1})} \qquad \textbf{(2-20)}$$

$$\eta_X = \frac{(X_{n-1} - X_n)}{(X_{n-1} - X_n^{\bullet})} \qquad \textbf{(2-21)}$$

where the equilibrium concentrations $X_n^\bullet$ and $Y_n^\bullet$ are given by means of the following relation:

$$\frac{F_x}{F_y} X_{n-1} + Y_{n+1} = \frac{F_x}{F_y} X_n + Y_n = \frac{F_x}{F_y} X_n^\bullet + Y_n^\bullet \qquad \textbf{(2-22)}$$

where:

Fj : rate of flow in phase j, (m^3/s),

η_j : stage efficiency of phase j.

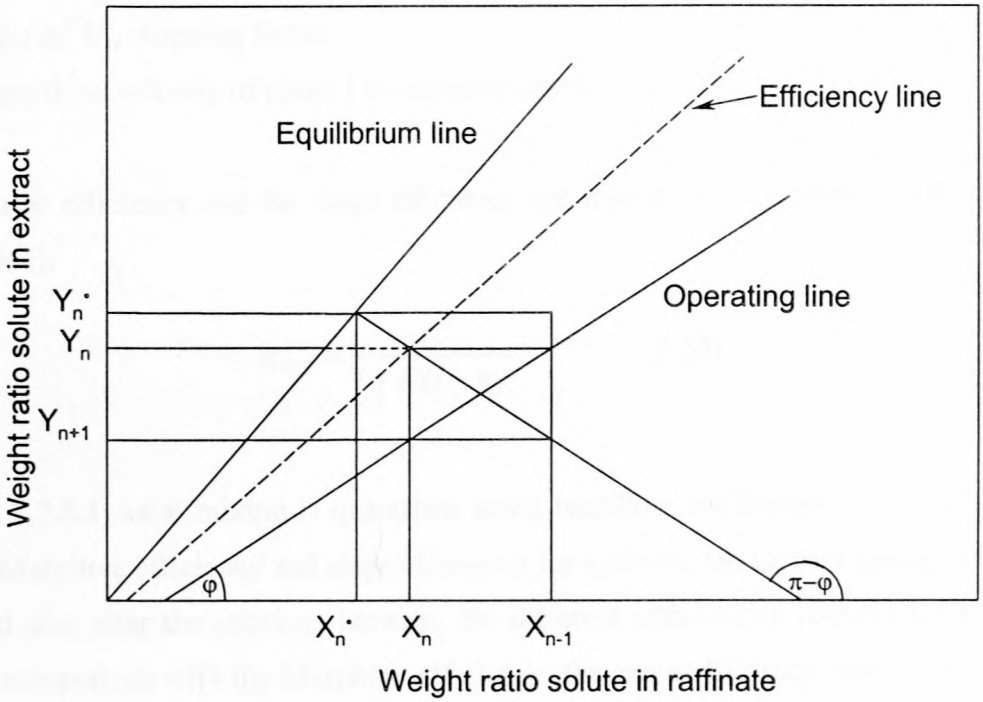

Figure 2-12: Stage efficiency (Prochazka and Landau, 1966):

The numerical value for the stage efficiency is the same for both phases (i.e. $\eta_X = \eta_Y = \eta$)

2.4.2.4. Relationships Between the Various Efficiencies

Various relationships have been derived, between the stage efficiency and the coefficient of mass transfer and between the stage efficiency and the Murphree efficiency (Prochazka and Landau, 1966).

The overall and Murphree efficiencies for countercurrent extractors are related by the following (Pratt, 1983b):

$$\eta_o = \frac{log\left[1 + \eta_{Mx}(E - 1)\right]}{log\, E} \qquad \textbf{(2-23)}$$

$$\eta_o = \frac{log\left[1 + \eta_{My}(S - 1)\right]}{log S} \qquad \textbf{(2-24)}$$

where:

E $= m^{\bullet} U_x / U_y$, extraction factor,

$m^{\bullet}$: reciprocal slope of equilibrium line

S $= U_y / m^{\bullet} U_x$, stripping factor,

U_j : superficial velocity of phase j in extractor (m/s),

The Murphree efficiency and the stage efficiency are related by the following (Prochazka and Landau, 1966):

$$\eta_{MX} = \frac{\eta}{1 + E(1 - \eta)} \qquad \textbf{(2-25)}$$

In **Section 2.7.5.1**, axial mixing is quantified using backflow coefficients, and it is possible to derive the Murphree efficiency and stage efficiency for systems, taking backmixing into account. This would also alter the relations between the different efficiencies (Prochazka and Landau, 1966). In comparison with the Murphree efficiency, the stage efficiency has the advantage that its numerical value is the same for both phases.

2.4.3 Relationships Between the Coefficient of Mass Transfer and Efficiency

The form of the relationships between the stage efficiency and the mass transfer coefficient depends on the arrangement of the flow of phases in the stage. The relationship for countercurrent flow can be derived (assuming a linear equilibrium relationship) and is as follows (Prochazka and Landau, 1966):

$$\eta = (1+E)\frac{1-exp[-(1-E)N_{OX}]}{1-E\,exp[-(1-E)N_{OX}]} \qquad (2\text{-}26)$$

$$= (1+E)\frac{1-exp\left[\frac{-(1-E)N_{OY}}{E}\right]}{1-E\,exp\left[\frac{-(1-E)N_{OY}}{E}\right]}$$

where:

a : specific interfacial or superficial area of contact of the phases (m^2/m^3),

E $= m^{\bullet} U_x / U_y$, extraction factor,

k_{oj} : mass transfer coefficient of phase j (m/s),

L : length or height of differential extractor (m)

$m^{\bullet}$: reciprocal slope of equilibrium line,

N_{ox} $= k_{ox}\, a\, L / U_x$, number of transfer units based on X phase,

N_{oy} $= k_{oy}\, a\, L / U_y = E\, N_{ox}$, number of transfer units based on Y phase,

U_j : superficial velocity of phase j in extractor (m/s),

η : stage efficiency

It is possible to derive the relations between the stage efficiency and the mass transfer coefficient, taking backmixing into account (Prochazka and Landau, 1966).

2.5 Calculation Basis

2.5.1 Use of Dimensionless Concentrations

Results can be expressed more concisely in terms of dimensionless concentrations X (feed phase) and Y (solvent phase) by means of a change of co-ordinates. This is depicted in **Figure 2-13**, which represents a typical operating diagram on c_x-c_y co-ordinates.

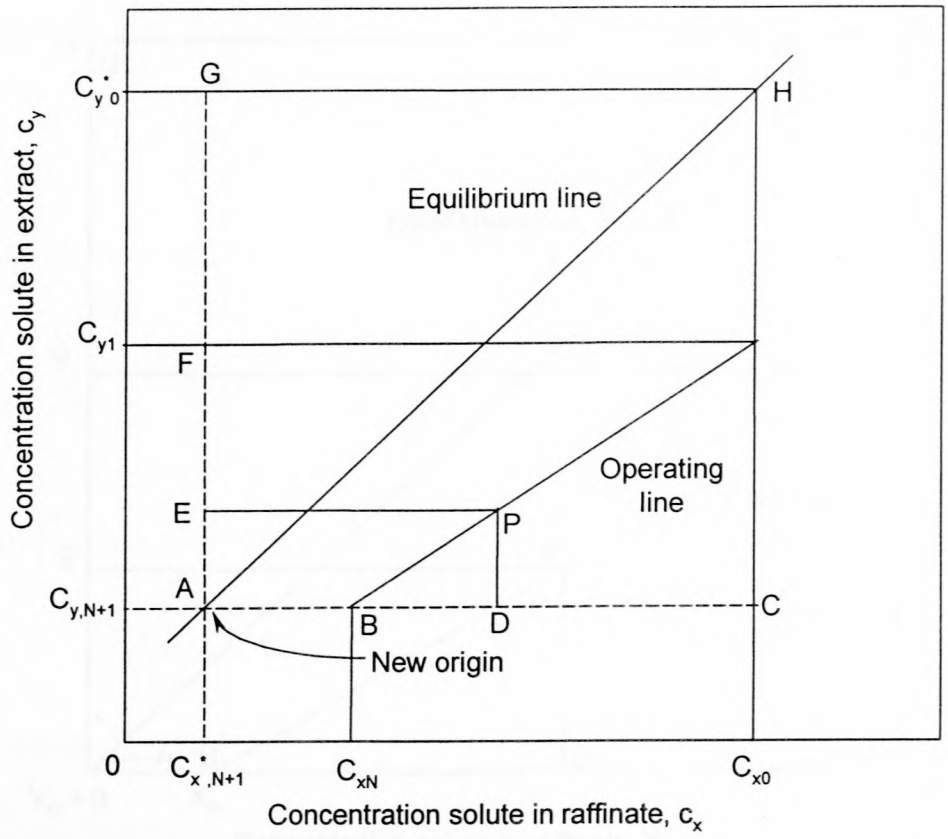

Figure 2-13: Typical operating diagram on c_x-c_y coordinates (Pratt, 1983b)

The procedure (with reference to **Figure 2-14**, which depicts the operating diagram using dimensionless concentrations) is as follows:

- the concentration $c_{x,N+1}^{*}$ in equilibrium with the inlet Y-phase composition $c_{y,N+1}$ is located and the co-ordinate origin is moved to point A,
- the co-ordinate scales are expanded or contracted such that the inlet concentration $c_{x,o}$ and the equilibrium Y-phase composition $c_{y,o}^{*}$ both have values of 1. By this means the new co-ordinate of any point, say P, are defined by:

$$X = \frac{AD}{AC}$$
$$Y = \frac{AE}{AG} \qquad \textbf{(2-27)}$$

The resulting modified operating diagram is shown in **Figure 2-14**, in which the equilibrium line is represented by $Y^* = X$.

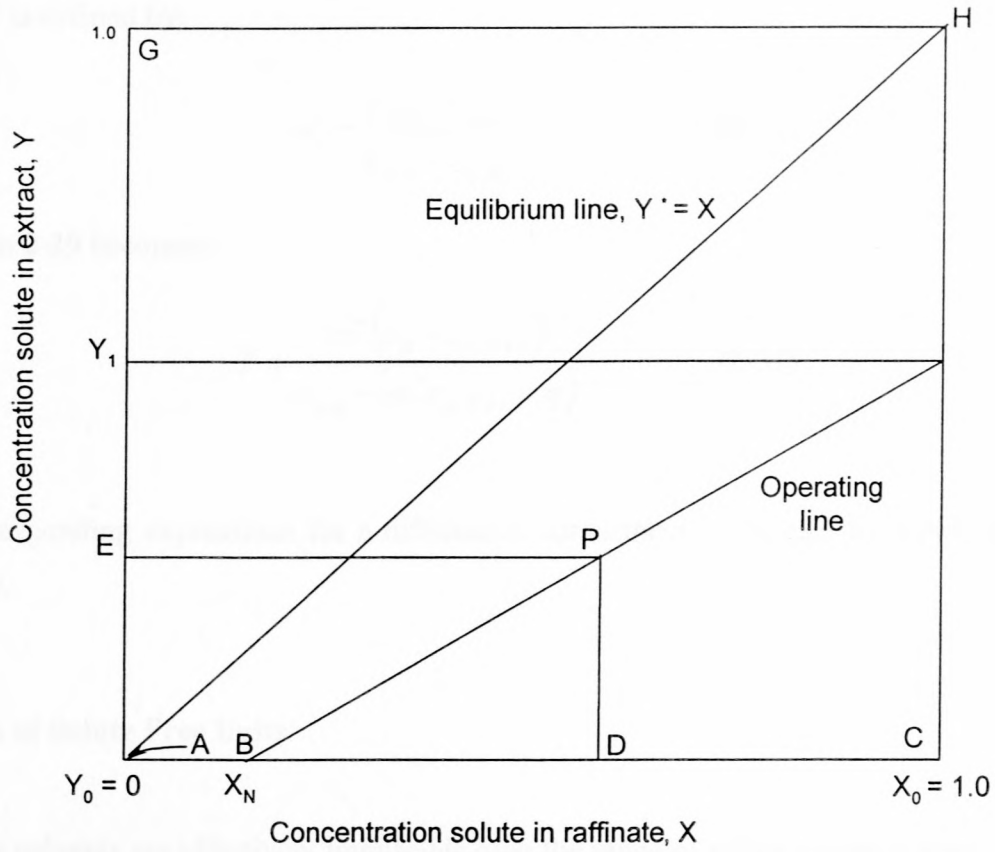

Figure 2-14: Operating diagram using dimensionless co-ordinates (Pratt, 1983b)

The dimensionless concentrations are expressed algebraically as follows in terms of the measured concentrations c_x and c_y, using units of mass or moles per unit volume:

$$X = \frac{c_x - c_{x,N+1}^{*}}{c_{x,o} - c_{x,N+1}^{*}} = \frac{c_x - (m^{\bullet} c_{y,N+1} + q)}{c_{x,o} - (m^{\bullet} c_{y,N+1} + q)} \qquad \textbf{(2-28)}$$

$$Y = \frac{c_y - c_{y,N+1}}{c_{y,o}^{*} - c_{y,N+1}} \qquad \textbf{(2-29)}$$

where:

q : intercept of equilibrium line,

$m^{\bullet}$: reciprocal slope of equilibrium line

X : dimensionless concentration of solute in X phase,

Y : dimensionless concentration of solute in Y phase,

Since $m^{\bullet}$ is defined by:

$$m^{\bullet} = \frac{c_{x,o} - c^{*}_{x,N+1}}{c_{y,o} - c^{*}_{y,N+1}} \qquad \textbf{(2-30)}$$

Equation 2-29 becomes:

$$Y = \frac{m^{\bullet}\left(c_{y} - c_{y,N+1}\right)}{c_{x,o} - \left(m^{\bullet} c_{y,N+1} + q\right)} \qquad \textbf{(2-31)}$$

The corresponding expressions for a differential contactor are obtained by replacing subscript $N+1$ by I.

2.5.2 Use of Solute Free Units

When the solvents are effectively immiscible over the range of solute concentrations involved, it is possible to express the flow rates in terms of pure solvents, with concentrations in the corresponding mass ratio units. This method is used for the convenience of the straight operating lines produced (where the slope is equivalent to the mass ratio of pure feed to pure solvent)

2.6 Plug Flow Computation

2.6.1 Graphical Method of Height Equivalent to a Theoretical Stage (HETS)

In order to calculate the height of column required to perform a particular extraction, a method similar to the McCabe Thiele method commonly associated with distillation can be used. In this method the height required for an equivalent theoretical stage can be calculated. Experimental data is required, to perform this calculation, namely:

- equilibrium data (by performing multiple cross extraction shake tests),
- samples of raffinate and extract taken during steady-state operation of the column.

The assumption is made that the mutual solubilities of the feed and solvent are negligible.

By performing a component mass balance over the entire column an operating line is generated. It is assumed that the column is comprised of N stages, however in reality the column is a continuous operation. The balance is performed on a solute free basis (i.e. the solute free mass rate of solvent and feed do not change through the length of the column due to extraction). A sketch depicting the column mass balance is shown in **Figure 2-15**.

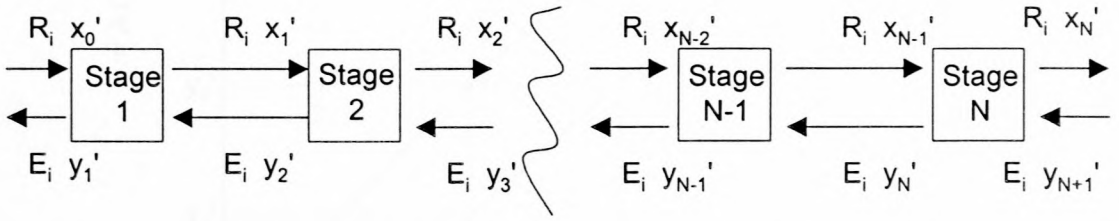

Figure 2-15: Mass balance over the extraction column

The extractor operating line, which relates the composition between stages is as follows (Pratt, 1983b):

$$y'_{n+1} = \frac{R_i}{E_i} x'_n + \left[y'_{N+1} - \frac{R_i}{E_i} x'_N \right] \qquad \textbf{(2-32)}$$

where:

E_i : extract mass rate, on solute-free basis (kg/s),

R_i : raffinate mass rate, on solute-free basis (kg/s),

x' : weight or mole ratio of solute to solvent in x phase,

y' : weight or mole ratio of solute to solvent in y phase

Equilibrium data collected by performing shake tests is plotted on an equilibrium distribution diagram with **Equation 2-32**, which represents a straight line of slope R_i/E_i, is shown with the equilibrium data in **Figure 2-16**.

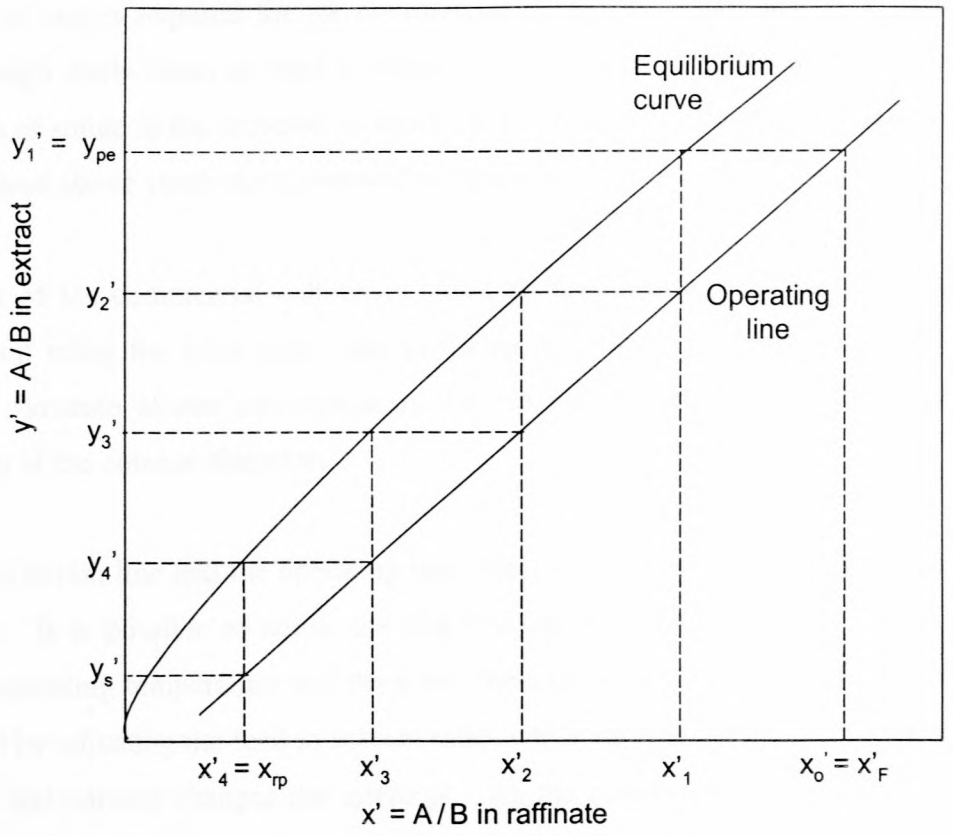

Figure 2-16: Method of HETS (Pratt, 1983b)

The starting point of the operating line is the feed composition (x'_F) and the extract composition (y'_1). If fresh solvent is used ($y'_s = 0$), the intercept is equal to the composition of the raffinate (x'_N). At low concentrations, the equilibrium line is often linear. However this is not always the case since the partitioning coefficient may vary with concentration, yielding a curved equilibrium line.

The method allows determination of the number of theoretical stages in an extraction column by stepping off the stages from the feed point to the raffinate point. The height of an equivalent theoretical stage (HETS) is determined from the active height of the pilot column as follows:

$$HETS = \frac{H_A}{N_S} \qquad \textbf{(2-33)}$$

where:

H_A : column active height (m)

$HETS$: Height Equivalent to a Theoretical Stage (m)

N_S : number of stages

The number of stages required for the commercial system is determined in a similar manner using the design basis (such as feed concentration, required raffinate concentration, and the concentration of solute in the recycled solvent). Multiplication of this number of stages with the HETS calculated above yields the theoretical height of the commercial column required.

The diameter of the commercial column is based on the specific throughput of the dispersed phase achieved using the pilot scale column. This, together with knowledge of the required design basis flowrate allows calculation of the cross sectional area required, which allows determination of the column diameter.

Both the equilibrium line and the operating line affect the number of theoretical stages required for a system. It is possible to adjust the slope of the equilibrium line by choice of solvent, varying the operating temperature and the ionic concentration. The slope of the operating line can be varied by adjusting the feed to solvent ratio, while varying the concentrations of solute in the raffinate and solvent changes the intercept. As the concentration of solute in the solvent (possibly recycled) increases, the bottom section of the operating line approaches the equilibrium line, resulting in a pinch. In an extreme case, when the operating line intersects with the equilibrium line, and the desired concentrations fall beyond the pinch, then the extraction is not possible.

Generally the graphical method of determining the Height Equivalent to a Theoretical Stage (HETS) is recommended particularly for systems with non-linear partition coefficients (since analytical solution could prove impossible, necessitating the use of a numerical method). When the partition coefficient can be adequately described mathematically, the McCabe-Thiele type of method is also suitable for computer calculations. Graphical solutions can be used advantageously when the solvents exhibit appreciable miscibility (Pratt, 1983b). In all cases the use of solute free co-ordinates is recommended for liquid-liquid extraction calculations (Godfrey et al., 1994)

The HETS method is used extensively in practice, and can be successfully applied, although previous experience in the case of gas absorption and distillation has proven that fundamentally the HETS method is unsound. The method is not the most appropriate one, since it applies a procedure involving stepwise changes in concentration to an operation where the concentration actually changes differentially with height. Consequently the HETS is found to vary widely with

operating conditions such as rates of flow, concentration and type of extractor used. This makes it necessary to have at hand very specific HETS data for the contemplated design (Treybal, 1951). In addition, considerable backmixing of both phases can occur, in which case the HETS method is based on fictive concentrations, as given by the supposed operating line.

2.6.2 Analytical Methods

Methods whereby the mathematical expressions used to describe the system are solved analytically are more accurate and convenient than graphical solutions. However use of this approach is limited by solvent-feed miscibility and complex equilibrium relations, and hence modified methods have been derived for systems exhibiting some curvature in the equilibrium relationship. One such method, for stage wise contactors divides the extractor into sections, in each of which the equilibrium and operating lines are approximated by straight line segments (Pratt, 1983b).

2.6.2.1. Transfer Units

In true differential contactors the phase concentrations change continuously through the extractor, not in steps. A simplified representation (the phases are shown as separate flow channels) of a typical contactor and a mass balance is depicted in **Figure 2-17**, below (Pratt, 1983b):

The following derivation considers the transfer of solute from the bulk of the phase to the interface. As discussed below, it is difficult to determine reliable values for the parameters of the equation derived, and consequently the approach is later modified.

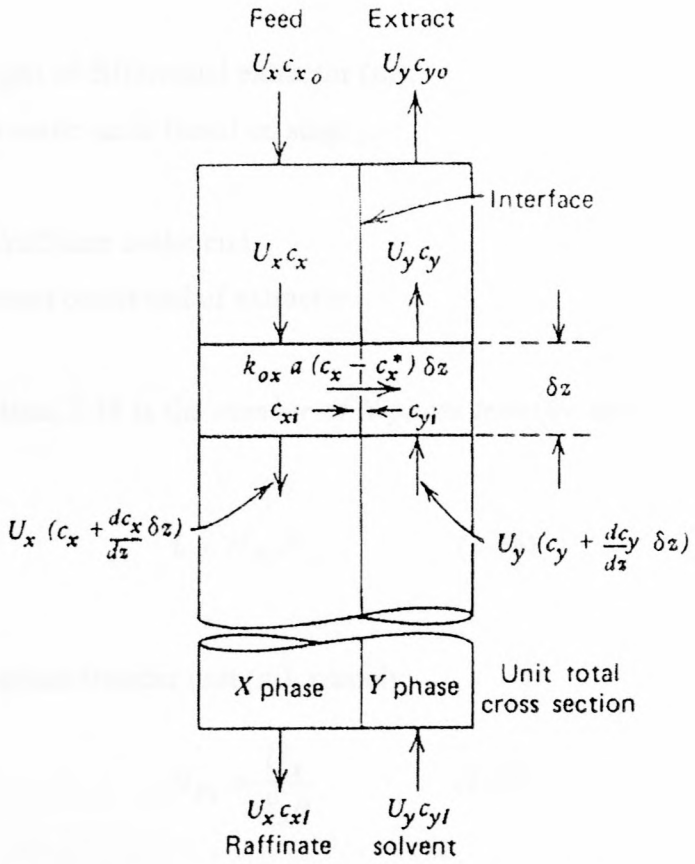

Figure 2-17: Balance on differential extractor over height δz (Pratt, 1983b)

By considering the flux of solute A in phase X in the section of height *dz* (Pratt, 1983b):

$$dN_A = -U_x dc_x = k_x a\left(c_x - c_{xi}\right)dz \qquad \textbf{(2-34)}$$

where:

a : specific interfacial area of contact of the phases (/m),

c_j : bulk-phase concentration of phase j (kg/m^3),

c_{ji} : interfacial concentration of phase j (kg/m^3),

k_j : mass transfer coefficient for phase j (m/s),

N_A : flux of solute A (kg/m^{2}s),

U_j : superficial velocity of phase j (m/s),

z : height or length within the extractor (m).

By rearranging and integrating **Equation 2-34** between $z = 0$ and L; $c_x = c_{x0}$ and c_{xl}, the following is derived:

$$\frac{k_x aL}{U_x} = \int_{c_{xl}}^{c_{x0}} \frac{dc_x}{\left(c_x - c_{xi}\right)} = N_{Tx} \qquad \textbf{(2-35)}$$

where:

L : length or height of differential extractor (m),

N_{Tj} : Number of transfer units based on stage j,

subscripts:

I : solvent inlet/raffinate outlet end,

o : feed inlet/extract outlet end of extractor.

The integral in **Equation 2-35** is the *number of X-phase transfer units*, and can be expressed in the following form:

$$L = H_{Tx} N_{Tx} \qquad \textbf{(2-36)}$$

where:

H_{Tj} : height of a j-phase transfer unit (m), namely:

$$H_{Tx} = \frac{U_x}{k_x a} \qquad \textbf{(2-37)}$$

H_{Tx} is the height of column that produces a change in concentration Δc_x numerically equal to the mean driving force over the interval. N_{Tx} can be considered a dimensionless measure of the difficulty of a given separation.

Similarly the Y phase can be considered (Pratt, 1983b):

$$\frac{k_y a L}{U_y} = \int_{c_{yI}}^{c_{yo}} \frac{dc_y}{\left(c_{yi} - c_y\right)} = N_{Ty} \qquad \textbf{(2-38)}$$

$$L = H_{Ty} N_{Ty} \qquad \textbf{(2-39)}$$

$$H_{Ty} = \frac{U_y}{k_y a} \qquad \textbf{(2-40)}$$

In practice it is difficult to determine reliable values of the individual mass transfer coefficients k_x and k_y, and thus overall coefficients k_{ox} and k_{oy} are used. **Equation 2-34** then becomes:

$$dN_A = -U_x dc_x = k_{ox} a\left(c_x - c_x^*\right)dz \qquad \textbf{(2-41)}$$

where:

c_j^* : solute concentration in phase j, in equilibrium with the other phase in the system (kg/m^3),

k_{oj} : overall mass transfer coefficient, based on phase j (m/s).

Integration of **Equation 2-41** yields the following:

$$N_{Tox} = \int_{c_{xl}}^{c_{x0}} \frac{dc_x}{\left(c_x - c_x^*\right)} \qquad \textbf{(2-42)}$$

$$H_{Tox} = \frac{U_x}{k_{ox} a} \qquad \textbf{(2-43)}$$

where:

N_{Toj} : number of overall transfer units based on stage *j*,

H_{Toj} : height of an overall transfer unit based on phase *j* (m).

Similarly the Y-phase is as follows:

$$N_{Toy} = \int_{c_{xl}}^{c_{x0}} \frac{dc_y}{\left(c_y^* - c_y\right)} \qquad \textbf{(2-44)}$$

$$H_{Toy} = \frac{U_y}{k_{oy} a} \qquad \textbf{(2-45)}$$

The values of c_x^* and c_y^* are the equilibrium values corresponding to c_x and c_y respectively, and the integrals can be evaluated.

The individual and overall values of H_T are related by the summation of the resistances given in **Equation 2-15** and thus:

$$H_{Tox} = H_{Tx} + \boldsymbol{E} H_{Ty} \qquad \textbf{(2-46)}$$

where $\boldsymbol{E}$, the extraction factor is defined as follows:

$$E = \frac{U_x}{m_y^* U_y} \qquad \textbf{(2-47)}$$

where:

m^* : slope of equilibrium line

Similarly for the Y phase:

$$H_{Toy} = H_{Ty} + SH_{Tx} \qquad \textbf{(2-48)}$$

where S, the stripping factor is defined as follows:

$$S = \frac{m_x^* U_y}{U_x} \qquad \textbf{(2-49)}$$

An important restriction applies to the above equations; m_x^* and m_y^* are not constant when the equilibrium line is curved and hence the overall transfer coefficients and H_T vary, even if the individual film values are constant. The approach does not provide a sound basis for obtaining individual H_{Tj} values (Pratt, 1983b).

The transfer units can be expressed in various other forms. If both the operating lines and equilibrium lines are straight then **Equation 2-41** can be integrated directly allowing calculation of contactor length. The transfer units can be also be calculated by solving the derived mathematical expressions analytically (Pratt, 1983b).

2.7 Axial Dispersion

2.7.1 Axial Mixing

In early extraction work, all counter-current extraction columns were designed on the assumption that the flow pattern was countercurrent with perfect plug flow of each phase. However in practice, for the majority types of equipment, this assumption is not fulfilled, even approximately. Perfect plug flow is limited to extractors in which phase separation between stages is virtually complete, such as in discreet stage mixer-settlers and perforated plate columns. The performance of extractors is adversely affected by deviations from plug flow and

consequently a more advanced treatment is necessary (Lo, 1979; Pratt, and Baird, 1983; Rod, 1965). Considerable backmixing of either or of both phases is likely and since axial mixing within each phase lowers the performance of an extraction column, it must be taken into account. In order to ensure accurate design of a commercial extractor, pilot scale experiments should be completed and the experimental results should be evaluated using a mathematical model that takes into consideration axial mixing (Slavickova, et al., 1978). When axial dispersion is accounted for however, the theory is considerably more complex than plug flow.

The methodology for designing extraction columns allowing for axial mixing is limited in practice by (Pratt, and Baird, 1983; Baird et al., 1994):

- the assumptions that hold-up, drop size and axial mixing remain constant along the column axis,
- the need for accurate values of the mass transfer coefficients and the hydrodynamic parameters.

However, data and refined models to be found in the literature have helped to broaden the criteria for scale-up of reciprocating plate extractors from pilot scale results, and have facilitated the prediction of column performance for different systems. The difficulty in applying the models lies not so much in the calculations, but in the choice of accurate values of the parameters, such as the axial dispersion coefficient, the backflow ratio and mass transfer coefficient. Because the factors relating to mass transfer and hydrodynamics are extremely complex, it is inevitably necessary to combine pilot test results with scale-up procedures (Lo and Prochazka, 1983). Data on axial mixing in the dispersed phase is limited. Much of the data on axial mixing in reciprocating plate columns is for columns with a diameter of 150 mm or less, however it is known that hydraulic non-uniformity effects increase with column diameter (Baird et al., 1994).

Various factors that contribute to reduced performance include the following (Lo, 1979; Pratt and Baird, 1983):

1. circulatory flow of the continuous phase as a result of the energy dissipation of the dispersed phase droplets or films,
2. transport and shedding of the continuous phase in wakes (only if the droplet Reynold's number (Re_d) is greater than 150) attached to the rear of dispersed phase droplets,

3. molecular and turbulent diffusion of the continuous phase in both axial and radial directions along concentration gradients,
4. for mechanically agitated contactors, circulation of the continuous phase results in entrainment of the dispersed phase,
5. channelling, which causes maldistribution, as a result of the contactor geometry characteristics, the packing or internal fittings,
6. non-uniform velocity profiles of phases as a result of frictional drag of stationary surfaces, resulting in a distribution of residence times of the fluid elements, which affect the performance of the extractor negatively,
7. range of droplet diameters causes dispersion of droplet velocities ("forward mixing")

Factors 1 and 2 cause pure backmixing of the continuous phase, while the next two lead indirectly to a degree of backmixing. The fourth factor also causes backmixing of the dispersed phase, while the seventh influences the residence time distribution of the dispersed phase. The combined result of the various effects is more accurately termed *axial dispersion*.

When two liquid phases are passed through an open structure type of column (such as the Karr column) large scale circulation currents are induced by the dispersed phase (Aravamudan and Baird, 1996).

2.7.2 Effect of Axial Mixing on Extraction Efficiency

Deviations in concentration profiles due to axial mixing, reduce the concentration driving force for inter-phase mass transfer below that assumed for plug flow. This results in loss of extractor efficiency, and consequently an increase in the height of column required to achieve a given separation. The effect of axial mixing on concentration profiles in a countercurrent extraction column is depicted in **Figure 2-18**.

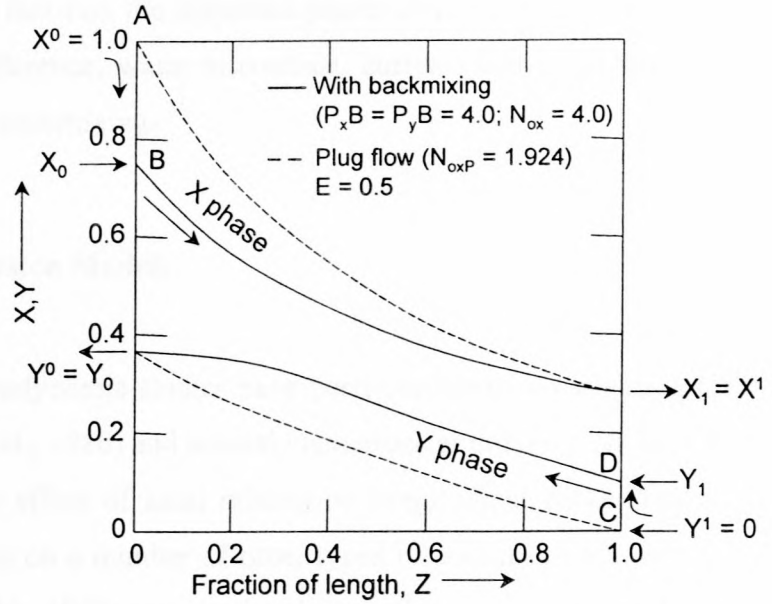

Figure 2-18: Effect of axial mixing on concentration profiles (Pratt and Baird, 1983)

The inlet concentration jumps are depicted in **Figure 2-19**, below.

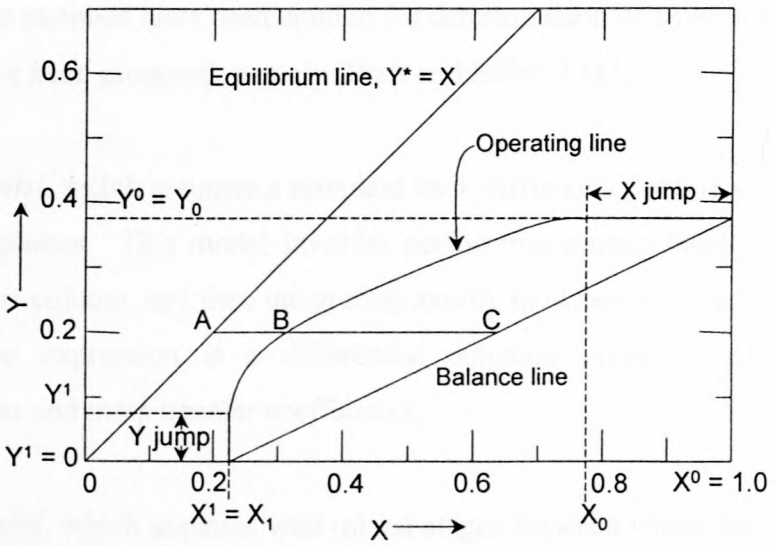

Figure 2-19: Operating diagram on X-Y co-ordinates (Pratt and Baird, 1983)

The actual operating line is significantly displaced from the plug flow operating line (which represents the overall mass balance on the extractor), and which is referred to as the *balance line*. Some extractors exhibit only backmixing in the continuous phase, and consequently in these cases the dispersed phase profile does not show the inlet jump or the zero gradient at the exit. Backmixing in the continuous phase is typically more severe than that in the dispersed phase.

This is due to the fact that the dispersed phase droplets are independent and have a net motion due to density difference, while in contrast, currents can be induced in the continuous phase, which can lead to backmixing.

2.7.3 Axial Dispersion Models

A number of hydrodynamic studies have been performed on vibrating plate extraction columns (such as Jiricny et al., 1980) and several mathematical models have been formulated with the aim of quantifying the effect of axial mixing on longitudinal concentration profiles and extractor efficiency. Studies on a number of other types of columns, such as pulse plate (Defives et al., 1961; Bell and Babb, 1969) and rotational extraction columns (Strand et al.1962, Westerterp and Meyberg, 1962) have also been completed.

Contactor performance is adversely influenced by departures from the plug flow pattern. This has necessitated the application of more advanced theory to facilitate prediction of systems. Various calculation methods have been applied for determination of axial mixing. Two different types of model have been proposed, namely (Pratt and Baird, 1983):

- *Diffusion model*, which assumes a turbulent back diffusion of solute superimposed on plug flow of the phases. This model involves performing a mass balance over a differential element of the column, and then integrating axially to obtain entry and exit concentrations. The resultant expression is a differential equation involving partition coefficients, concentrations and mass transfer coefficients.

- *Backflow model*, which assumes well-mixed stages between which backflow occurs. This model assumes that the column consists of a series of continuously-stirred-tank-reactors (CSTRs), and a mass balance is performed, resulting in a number of equations that must be solved simultaneously.

These two models represent limiting cases. In practice the former is used for differential contactors such as packed and baffle plate columns, while the latter is applied to stagewise equipment such as mixer-settlers in series (cocurrent settling) with heavy entrainment in the separated phases. Between the extremes a variety of extractors exist, which do not conform

closely to either model. These are either of the non-coalescing type (such as multi impeller and pulsed plate columns) or the countercurrent mixer-settler type (such as the Scheibel column). However as the number of compartments used in each model is increased, the two models become closer. This allows contactor performance to be expressed in terms of either model with reasonable accuracy (Pratt and Baird, 1983; Rod, 1965). Application of these models facilitates correlation of experimental data, scale-up and interpretation of behaviour of various types of columns (Miyauchi and Vermeulen, 1963a)

2.7.4 Diffusion Model

2.7.4.1. Derivation

The assumptions inherent in the model, as derived below are as follows (Pratt and Baird, 1983):

- backmixing of each phase can be characterised by a constant turbulent diffusion coefficient E_j,
- the mean velocity and concentration of each phase is constant through the column cross section,
- the volume mass transfer coefficient is constant or can be averaged over the column,
- the solute concentration gradients are continuous (except at the phase inlets),
- the solvent and raffinate phases are effectively immiscible or have constant miscibility irrespective of solute concentration,
- the volumetric flowrates of feed and solvent (i.e. X and Y) phases are constant throughout the extractor,
- the equilibrium relationship is linear or can be approximated by a straight line.

The defining equation for the axial dispersion coefficient is analogous to Fick's Law for molecular diffusion. The flux due to axial dispersion is given by the following (Baird et al., 1992):

$$N_f = E\frac{\partial c}{\partial z_a} \qquad \textbf{(2-50)}$$

where:

c : concentration (kg/m^3),

E : axial dispersion coefficient (m^2/s),

N_f : flux (kg/s),

z_a : axial distance (m)

The values of E are several order of magnitudes larger than the molecular diffusion coefficients, since axial dispersion is caused by hydrodynamic rather than molecular behaviour (Baird et al., 1992).

Material balances for one-dimensional countercurrent flow, over a differential length of contactor are shown in **Figure 2-20**.

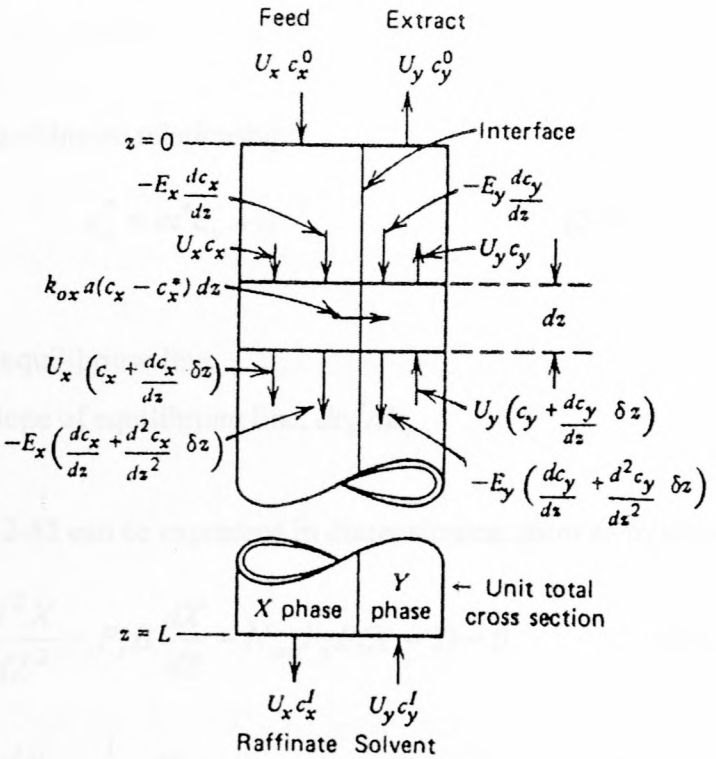

Figure 2-20: Diffusion model – material balance over differential section (Pratt and Baird, 1983)

By mass balance, the following are derived (Pratt and Baird, 1983):

$$E_x \frac{d^2 c_x}{dz^2} - U_x \frac{dc_x}{dz} - k_{ox} a\left(c_x - c_x^*\right) = 0 \qquad \textbf{(2-51)}$$

$$E_y \frac{d^2 c_y}{dz^2} + U_y \frac{dc_y}{dz} + k_{ox} a\left(c_x - c_x^*\right) = 0 \qquad \textbf{(2-52)}$$

where:

a : superficial area of contact of the phases (m^3/m^2),

c_j : concentration in phase j (kg/m^3),

c_j^* : equilibrium concentration in phase j (kg/m^3),

E_j : effective longitudinal diffusion coefficient in the jth phase (m^2/s),

k_{ox} : overall mass transfer coefficient based on X phase (m/s),

U_j : superficial velocity of phase j (m/s),

z : length measured from X (feed) = phase inlet (m).

If backmixing is absent and $E_j = 0$, then the expressions describe plug flow (refer to **section 2.6.2.1**).

Assuming a linear equilibrium relationship:

$$c_x^* = m^\bullet c_y + q \qquad \textbf{(2-53)}$$

where:

q : intercept of equilibrium line,

$m^\bullet$: reciprocal slope of equilibrium line, dc_x^*/dc_y

Equations 2-51 and **2-52** can be expressed in dimensionless form as follows:

$$\frac{d^2X}{dZ^2} - P_x B\frac{dX}{dZ} - N_{ox}P_x B(X-Y) = 0 \qquad \textbf{(2-54)}$$

$$\frac{d^2Y}{dZ^2} - P_y B\frac{dY}{dZ} + \boldsymbol{E}N_{ox}P_y B(X-Y) = 0 \qquad \textbf{(2-55)}$$

$$X = \frac{c_x - \left(m^\bullet c_y^I + q\right)}{c_x^O + \left(m^\bullet c_y^I + q\right)} \qquad \textbf{(2-56)}$$

$$Y = \frac{m^\bullet\left(c_y - c_y^I\right)}{c_x^O + \left(m^\bullet c_y^I + q\right)} \qquad \textbf{(2-57)}$$

where:

B = L/d_c (m),

d_c : characteristic dimension (m),

$\boldsymbol{E}$ $= m^{\bullet} U_x / U_y$, extraction factor,

L : length or height of differential contactor (m),

$m^{\bullet}$ $= dc_x^*/dc_y$, reciprocal slope of equilibrium line,

N_{ox} $= k_{ox}aL/U_x$, number of "true" overall transfer units based on X phase,

P_j $= U_j d_c/E_j$, turbulent Peclet number of jth phase,

X : dimensionless concentration of X phase,

Y : dimensionless concentration of Y phase,

Z $= z/L$, fractional length within contactor,

subscripts:

I : Y-phase inlet end, within contactor,

O : Y-phase outlet end, within contactor,

superscripts:

I : Y-phase inlet end, external to contactor,

O : Y-phase outlet end, external to contactor.

Elimination of Y between **Equation 2-54** and **Equation 2-55,** gives the following:

$$\frac{d^4X}{dZ^4} - \alpha\frac{d^3X}{dZ^3} - \beta\frac{d^2X}{dZ^2} - \gamma\frac{dX}{dZ} = 0 \qquad \textbf{(2-58)}$$

where:

$$\alpha = B\left(P_x - P_y\right)$$

$$\beta = N_{ox}B\left(P_x + \boldsymbol{E}P_y\right) + P_xP_yB^2 \qquad \textbf{(2-59) a, b, c}$$

$$\gamma = N_{ox}P_xP_yB^2(1-\boldsymbol{E})$$

These equations can be fitted to existing experimental data, and the parameters obtained.

The parameters *Pj* and *B* always appear in combination, and are termed the *column Peclet numbers* (*Pe*):

$$P_jB = \frac{U_jL}{E_j} \qquad \textbf{(2-60)}$$

where:

E_j : effective longitudinal diffusion coefficient in the *j*th phase (m^2/s),

L : length or height of differential contactor (m),

U_j : superficial velocity of phase j (m/s),

Dispersion in columns is characterised by the continuous-phase axial Peclet number. If this number is low, the continuous phase can be considered as being "well mixed", and for countercurrent flow, results in a reduction in the equivalent number of transfer units.

2.7.4.2. Variations and Application of the Diffusion Model

To quantify longitudinal dispersion, various investigators (amongst others Sleicher, 1959; Rod, 1965; Miyauchi and Vermeulen, 1963b) derived Diffusion models, with simplifying assumptions, such as:

- mean longitudinal dispersion coefficient E_j,
- mean velocity for each phase,
- linear distribution,
- perfectly mixed phases,
- constant mass transfer coefficient-interfacial area product.

Rod (1965) employed a graphical integration method for the calculation of the coefficients of a diffusional model. Souhrada et al. (1966b) derived a diffusion model for a tracer experiment, for single phase flow and with no transfer between the phases. Axial mixing measurements under single phase flow conditions can be done with more accuracy and in more detail then under two phase conditions. Although the presence of a second phase affects E_c strongly at low levels of agitation, the difference becomes negligible at high agitation levels (Kim and Baird, 1976a; Hafez et al., 1979; Baird et al., 1994)

Miyauchi and Vermeulen (1963a) showed that concentrations in the equipment and at the outlet depend on four dimensionless parameters, which are functions of:

- the dispersion rates and velocities,
- the equilibrium partition coefficient,
- the "true" overall mass transfer coefficient.

Rama Rao and Baird, (1998) stated that it is preferable that the continuous phase moves in a "plug flow" manner, with a Peclet number greater than 20 (or as close as possible to that condition). Vermeulen et al. (1966) indicated that if the axial Peclet number for either phase is less than approximately 50, a significant reduction in column performance is observed. For a 15 cm Karr column, Hafez et al. (1979) determined a Peclet number in the order of 25, and indicated that the Peclet number would decrease further with increase in the column diameter, unless circulation effects were reduced. This could be achieved by various plate and baffle arrangements, however the permissible throughput also requires consideration. Ultimately, economic analysis of the costs of changes in column height and diameter is required to determine the most suitable arrangement (Hafez et al., 1979).

Since the continuous phase superficial velocity (U_c) and the length of differential contactor are fixed, it is preferable that the axial dispersion coefficient (E) be reduced as much as possible (Rama Rao and Baird, 1998). The value of E is typically in the order of 1 to 10 cm^2/s.

Rama Rao and Baird, (1998) and Baird and Rama Rao (1991) found that the principal factors in determining the value of the axial dispersion coefficient under given conditions, include:

- flowrates of each phase,
- column design (including internals),
- level of mechanical agitation,
- physical properties of the system (density differences, interfacial tension)
- "hydraulic non-uniformity" (axial density gradients),

Typically mass transfer results in variation of the density of the continuous phase in a countercurrent extraction column. If the density increases with vertical height, the potential exists for increased axial mixing due to natural convection (Baird et al., 1992).

Modelling of the effects of unstable density gradients has been on the basis of a turbulent mechanism involving the mixing length (Kostanyan, et al., 1979), as originally proposed by Kolmogoroff (1941):

$$E = l^{4/3}\,\varepsilon_t^{1/3} \qquad \textbf{(2-61)}$$

where:

E : axial dispersion coefficient,

l : mixing length,

ε_t : total specific energy dissipation rate (W/kg).

The mixing length (l) is characteristic of the effective eddy size, and is about 0.45 times the column diameter in the absence of fixed internals, and about 70% in the presence of stationary plates (Baird and Rama Rao, 1991). The total specific energy dissipation rate comprises dissipation due to mechanical agitation, agitation due to the dispersed phase drops, and energy dissipation due to the unstable density gradient in the continuous phase. The last term is much smaller than the other two, however it can have a significant effect on the mixing length (Rama Rao and Baird, 1998).

As a result of studies of these phenomena, several investigators (Holmes, et al., 1991, Baird and Rama Rao, 1991, Baird et al., 1992, Aravamudan and Baird, 1996) confirmed that extremely small unstable density gradients can significantly increase axial dispersion coefficients. Details of the work completed are shown in **Table 2-2**.

Table 2-2: Experimental work of various investigators on the effects of unstable density gradient on axial mixing in the continuous phase

Reference	Type of column (D_c)	System
Holmes, et al. (1991)	Karr column (7.62 cm)	Single phase, calcium chloride-water system, steady state measurements
Baird and Rama Rao (1991)	Karr column (5.08 cm)	Single phase, sodium chloride-water system, hot/cold water, steady state measurements
Baird et al. (1992)	Open column (1.48, 1.91, 2.63 cm)	Single phase, sodium chloride-water system, unsteady state measurements
Aravamudan and Baird (1996)	Karr column (5.08 cm)	Single and two phase, sodium chloride-water, kerosene system

Several observations were made as a result of the work:

- backmixing is reduced when more plates are included in the stack (Holmes, et al. 1991),
- with agitation, the axial dispersion coefficients were reduced to approximately 30% of the non agitated column *E* values for concentration gradient induced axial mixing, probably due to the fact that supply of mechanical energy reduces the eddy size (mixing length) (Holmes, et al. 1991),
- under intense agitation, the axial variation of E is reduced considerably, since the sensitivity of E to the density gradient is decreased (Baird and Rama Rao, 1991)

It is expected that convective mixing increases with column diameter, which suggests that the effect of unstable density gradient will be greater at larger scales. It is expected that convective mixing would be reduced (from that of a single phase system) by the presence of a counter flowing liquid, and in columns with plates having smaller open areas, such as the VPE (Holmes, et al. 1991, Aravamudan and Baird, 1996). It was recommended that to prevent increases in axial dispersion, designers of extraction columns should avoid conditions where an unstable density gradient exists, and that the effect of a stable density gradient should be quantified

Further work, to study the effect of a stable density gradient (whereby the continuous phase density decreases with height) was completed by Rama Rao and Baird, (1998). Axial dispersion coefficients were measured in a 5.08 cm diameter Karr-type reciprocating plate column for single and two phase flow. A steady state tracer injection method was used whereby the concentration profile was measured upstream of the tracer injection. The tracer solution was a strong sodium chloride solution, and a significant stable density gradient (decreasing with height) was created. Control experiments were performed using a neutrally buoyant tracer solution. In contrast to the initial studies, it was concluded that a stable density gradient did not have any effect in reducing the axial dispersion coefficient from that in a system with an absence of any density gradient. However the authors were in agreement that unstable density gradients should be avoided in Karr extraction columns, as they can lead to increased axial mixing.

Baird (1974) quantified axial dispersion data for a pulsed column (with geometry similar to that of a Karr column) for single phase flow. It was concluded that the axial dispersion coefficient:

- increases linearly with frequency and the square of the amplitude,
- is little affected by the continuous phase velocity,

- is significantly decreased by doubling the plate spacing.

Kim and Baird (1976a) measured axial dispersion coefficients using a 5 cm diameter Karr reciprocating plate column, by observing the course of an instantaneous chemical reaction between acid and base in the continuous phase. Kerosene was used as the organic phase, the feed consisted of a hydrochloric acid solution containing phenolphthalein as an indicator, and a caustic solution was added to the column as a tracer. Kim and Baird (1976b) performed experiments using a Karr column and a similar system as to that of Kim and Baird (1976a). It was found that by halving the hole size from 13.6 to 6.35 mm (and keeping the plate free area constant), the amount of axial dispersion could be reduced by approximately 75%. The following relation for the axial dispersion coefficient was derived for single phase flow:

$$E \propto am^{1.8} f_c^{1.0} d_h^{1.8} d_t^{-0.3} h_c^{-1.3} \qquad \textbf{(2-62)}$$

where:

am : amplitude (half stroke) (m),

d_h : diameter of holes in plate (m),

d_t : thickness of plate (m),

E : overall dispersion coefficient (m^2/s),

f_c : frequency of reciprocating motion (Hz),

h_c : height of a stage (m)

In contrast, Hafez et al. (1979) concluded that the dispersion coefficient, E is proportional to the amplitude, and also significantly dependent on the continuous phase velocity. The test work was performed on a 15 cm diameter Karr column, with a variety of plate types and arrangements using a kerosene–water system. Single phase mixing data was correlated to yield the following:

$$E = 5.56.am^{1.77} f_c^{1.00} h_c^{-1.32} \qquad \textbf{(2-63)}$$

where:

am : amplitude (cm),

E : overall dispersion coefficient (cm^2/s),

f_c : frequency of reciprocating motion (Hz),

h_c : height of a stage (cm)

Hafez et al., (1979) found that for single phase flow, the axial dispersion coefficients increased at low values of the amplitude-frequency product ($am.f_c$), and were affected by phase velocity in the larger diameter column, unlike the results of work performed using smaller columns. It was found that the axial dispersion coefficients in a Karr reciprocating plate column tend to increase with column diameter, as a result of circulation effects.

Baird and Rama Rao (1988) performed single-phase experiments using a 5 cm diameter Karr column and unsteady state techniques to determine axial dispersion coefficients. It was concluded that the dispersion coefficient, E:

- varies with the amplitude-frequency product,
- decreases substantially with increases in plate spacing,
- is not significantly affected by flowrate.

Karr et al. (1987) performed experimental work on a single-phase system using Karr columns of 2.54 and 50.8 cm (industrial scale) in diameter, with an n-heptane-water system, using a tracer solution of ammonium chloride. Steady state operation of the column was established (water-solvent), and then a pulse of tracer solution was injected near the top of the column. The tracer responses in the aqueous phase were measured lower down the column at two points, using electrical conductivity. Electrical conductivity was found to be a linear function of tracer concentration. The authors determined that the dispersion coefficient, E is proportional to the amplitude-frequency product. It was also concluded that the axial dispersion coefficients went through a minimum as the agitation level was increased from 0, and that for single phase flow, the coefficients were almost an order of magnitude higher in the larger diameter column.

Parthasarathy et al. (1984) studied air-water and water-kerosene systems using a reciprocating plate extraction column (without varying hole size), and determined the following correlation for two-phase axial dispersion:

$$\frac{E}{u_c L} = 4.22x10^{-2}(2am)^{0.457} t^{0.344} u_c^{-0.3} d_h^{0.27} S^{-0.68} h_c^{-0.687} \qquad \textbf{(2-64)}$$

where:

am : amplitude (half stroke) (cm),

d_h : diameter of hole (cm),

E : overall dispersion coefficient (m^2/s),

h_c : height of a stage (cm),

L : length of column (cm),

S : fractional open area (m),

t : time (s),

u_c : continuous phase velocity (m/s),

Rama Rao et al. (1983) determined the following axial dispersion coefficient correlation, for a water-kerosene system (without varying hole size):

$$E = 4(2am)^{0.5} f_c^{0.33} u_c^{0.6} d_h^{0.2} S^{-0.6} h_c^{-0.69} \qquad \textbf{(2-65)}$$

where:

am : amplitude (half stroke) (cm),

d_h : diameter of hole (cm),

E : overall dispersion coefficient (m^2/s),

f_c : frequency (Hz),

h_c : height of a stage (cm),

S : fractional open area (m),

u_c : continuous phase velocity (m/s),

For the correlation in **Equations 2-64** and **2-65**, above, the axial dispersion coefficient is shown to vary in a similar manner with fractional free area, hole diameter and plate spacing, however they differ significantly from those obtained by Kim and Baird (1976a) in **Equation 2-62**. The effects of amplitude and frequency are also significantly different, however this could be due to the fact that **Equation 2-62** describes single-phase flow, whereas the other two equations were derived using two phase flow. In addition the fractional open area used by the latter two authors ranged from 0.09 to 0.3, which is significantly less than the value of 0.55 used by Kim and Baird (1976a).

The discrepancy of results between workers may be attributed to the different ranges of frequencies used, varying plate geometries and the difference in column size (Stevens and Baird, 1990). Because of the number of mechanisms affecting axial dispersion, and the complexity of these interactions, no reliable equation has been formulated to predict axial dispersion. However many equations for axial dispersion coefficients (E) have been derived that are specific to particular types and sizes of equipment (Rama Rao and Baird, 1998).

2.7.5 Backflow Model

2.7.5.1. Derivation

This model assumes a series of stages interconnected as shown in **Figure 2-21**, below. Each stage contains a mixing device and may or may not include a settler in which partial or complete coalescence occurs.

The assumptions inherent in this model are as follows (Pratt and Baird, 1983):

- each stage is well mixed, both phases are completely mixed before separation so that the driving force is constant throughout the stage as the exit value of (c_{x2}-c_{x2}^*) and that the dispersed phase behaves as a second continuous phase (i.e. coalescence and re-dispersion are very rapid)[9]
- backmixing occurs by mutual entrainment of the phases between stages, after coalescence, if appropriate,
- the backmixing is expressed in terms of the ratios α_j of backmixed to net forward interstage flow and is constant for all stages,
- all mass transfer occurs in the mixer,
- the value of $k_{ox}aV$, the product of volume mass transfer coefficient and stage volume is constant for each stage,
- the solvent and raffinate phases are effectively immiscible or have constant miscibility irrespective of solute concentration,
- the volumetric flowrates of feed and solvent (i.e. X and Y) phases are constant throughout,
- the equilibrium relationship is linear or can be approximated by a straight line.

The material balance for the two phases around stage n are depicted in **Figure 2-21**, where α_j represents the backmixing ratio, the ratio of backflow to volumetric flow of the *j*th phase, *Fj* (Pratt and Baird, 1983).

[9] Miyauchi et al., 1963b, showed that this assumption is permissible as long as the partition coefficient is constant and droplet size, hold-up and overall mass transfer coefficient are all constant

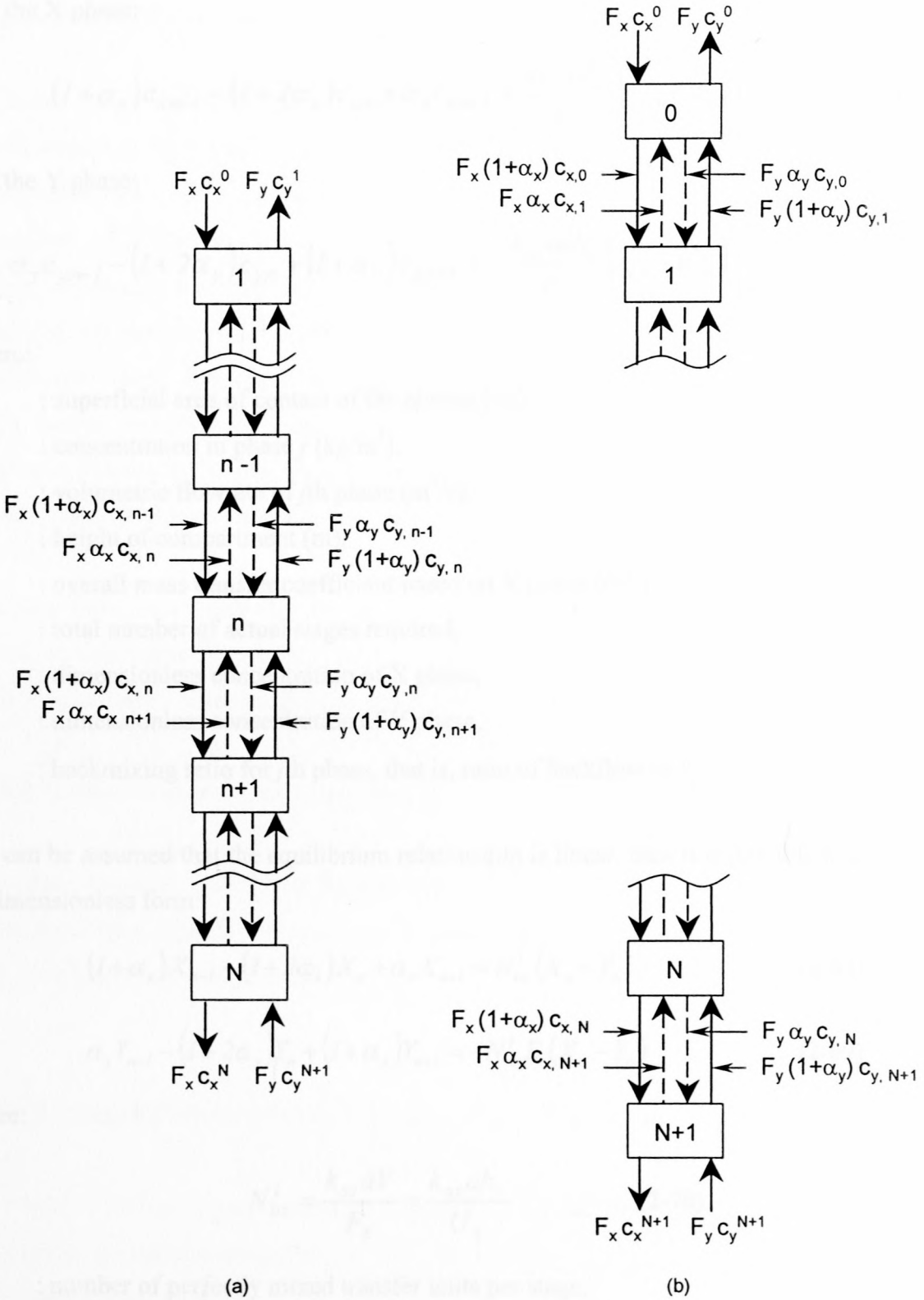

Figure 2-21: Backflow model: material balance over stage (a) normal arrangement; (b) with fictitious end stages (Pratt and Baird, 1983)

For the X phase:

$$(1+\alpha_x)c_{x,n-1} - (1+2\alpha_x)c_{x,n} + \alpha_x c_{x,n+1} = \frac{k_{ox} a s h_c}{F_x}\left(c_{x,n} - c^*_{x,n}\right) \qquad \textbf{(2-66)}$$

For the Y phase:

$$\alpha_y c_{y,n-1} - (1+2\alpha_y)c_{y,n} + (1+\alpha_y)c_{y,n+1} = -\frac{k_{ox} a s h_c}{F_y}\left(c_{x,n} - c^*_{x,n}\right) \qquad \textbf{(2-67)}$$

where:

a : superficial area of contact of the phases (/m),

c_j : concentration in phase j (kg/m^3),

F_j : volumetric flowrate of jth phase (m^3/s),

h_c : height of compartment (m),

k_{ox} : overall mass transfer coefficient based on X phase (m/s),

N : total number of actual stages required,

X : dimensionless concentration of X phase,

Y : dimensionless concentration of Y phase,

α_j : backmixing ratio for jth phase, that is, ratio of backflow to F_j

If it can be assumed that the equilibrium relationship is linear, then it is possible to convert these to dimensionless form:

$$(1+\alpha_x)X_{n-1} - (1+2\alpha_x)X_n + \alpha_x X_{n+1} = N^1_{ox}\left(X_n - Y_n\right) \qquad \textbf{(2-68)}$$

$$\alpha_y Y_{n-1} - (1+2\alpha_y)Y_n + (1+\alpha_y)Y_{n+1} = -N^1_{ox} E\left(X_n - Y_n\right) \qquad \textbf{(2-69)}$$

where:

$$N^1_{ox} = \frac{k_{ox} a V}{F_x} = \frac{k_{ox} a h_c}{U_x} \qquad \textbf{(2-70)}$$

N^1_{ox} : number of perfectly mixed transfer units per stage,

U_j : superficial velocity of phase j (m/s),

V : volume of extract compartment (m^3).

2.7.5.2. Further Complexities

Extensive work has been done to quantify the effect of axial mixing on longitudinal concentration profiles and extractor efficiency, and several mathematical Backflow models have been formulated. Of particular interest are two forms of the Backflow model that have been developed. The first approach (**Section 2.7.5.2.1**) will be referred to as the *Mass Transfer Coefficient model*, whereby the kinetics of the extraction process is characterised directly by means of the mass transfer coefficient. The second approach, derived in **Section 2.7.5.2.2**, is termed the *Stage Efficiency model*, whereby the kinetics of the extraction process are characterised indirectly by means of the efficiency. This model is typically employed for stagewise processes. It has been shown that the two models are equivalent (Prochazka, and Landau, 1963; Prochazka and Landau, 1966).

The Backflow model can also be used with tracer experiments, where no transfer of solute occurs, as detailed in **Section 2.7.5.2.3**. The behaviour of the dispersed phase is an important consideration, as discussed in **Section 2.7.5.2.4**.

2.7.5.2.1. Mass Transfer Coefficient Model

The Mass Transfer Coefficient Model was derived by Miyauchi and Vermeulen (1963b), assuming a linear equilibrium relationship, and is shown in **Section 2.7.5.1**, **Equations 2-66** to **2-70**, with reference to **Figure 2-21**.

2.7.5.2.2. Stage Efficiency Model

The model is derived with reference to **Figure 2-22** below (Prochazka and Landau, 1963). The assumptions for the derivation include:

- immiscible solvents,
- a constant partition coefficient,
- perfectly mixed phases
- constant backmixing ratios of the phases.

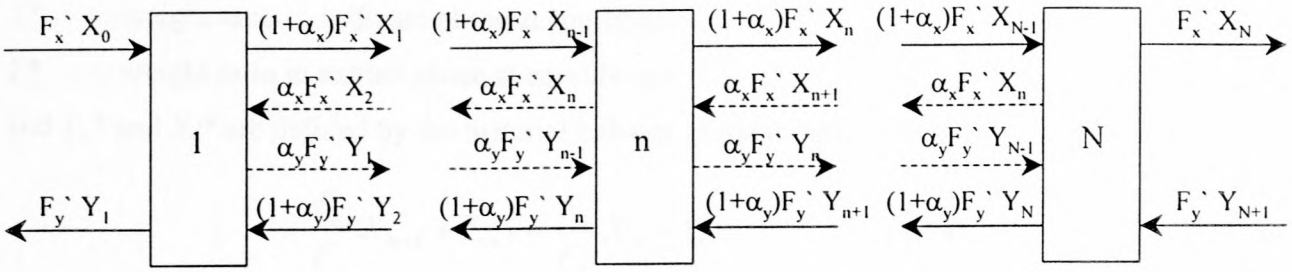

Figure 2-22: Stagewise countercurrent process with backmixing between stages (Prochazka and Landau, 1963)

The mass balance for solute for stages 1 to n inclusive, on a solute free basis is (Prochazka and Landau, 1963):

$$F_x' X_0 + \alpha_x F_x' X_{n+1} + (1+\alpha_y) F_y' X_{n+1} = (1+\alpha_x) F_x' X_n + F_y' Y_1 + \alpha_y F_y' Y_n \qquad \textbf{(2-71)}$$

where:

F_j' : mass rate of flow of phase j,

X : weight ratio of solute in raffinate phase,

Y : weight ratio of solute in extract phase,

n : general stage,

N : number of stages,

αj : coefficient of backmixing in phase j,

subscripts:

x : raffinate phase,

y : extract phase,

For the case where the streams leaving the individual streams are not in equilibrium, the efficiency of the n^{th} stage can be defined as:

$$\eta_y \equiv \frac{(Y_n - Y_{n+1})}{(Y_n^* - Y_{n+1})} \qquad \textbf{(2-72)}$$

$$\eta_x \equiv \frac{(X_{n-1} - X_n)}{(X_{n-1} - X_n^*)} \qquad \textbf{(2-73)}$$

where:

η_j : stage efficiency of phase j,

X^* : weight ratio in raffinate phase at equilibrium,

Y^* : weight ratio in extract phase at equilibrium.

and Y_n^* and X_n^* are defined by the material balance of the n^{th} stage:

$$\frac{F_x}{F_y} X_{n-1} + Y_{n+1} = \frac{F_x}{F_y} X_n + Y_n \qquad \textbf{(2-74)}$$

$$\frac{F_x}{F_y} X_n + Y_n = \frac{F_x}{F_y} X_n^* + Y_n^* \qquad \textbf{(2-75)}$$

Various case studies can be considered for differing stage efficiencies.

Case 1: Stage Efficiency Equal to Unity

For a constant partition coefficient:

$$Y^* = m X^* \qquad \textbf{(2-76)}$$

With a stage efficiency is equal to 1, and using the equilibrium relationship, it is possible to eliminate X_{n+1} and Y_n, resulting in an operating line representing backmixing between stages:

$$Y_{n+1} = \varpi X_n + \gamma_1 \qquad \textbf{(2-77)}$$

where:

$$\gamma \equiv Y_1 - \kappa X_0 = Y_{N+1} - \kappa X_N$$

$$\gamma_1 = \frac{\gamma}{\left(1 + \alpha_y + \alpha_x \frac{\kappa}{m}\right)}$$

$$\kappa \equiv \frac{F_x}{F_y} = \frac{(Y_1 - Y_{N+1})}{(X_0 - X_N)}$$

$$\varpi = \frac{\left[\alpha_y m + (1 + \alpha_x)\kappa\right]}{\left(1 + \alpha_y + \alpha_x \frac{\kappa}{m}\right)}$$, slope of the inner operating line,

A graphical calculation is possible, as depicted in **Figure 2-23**. Two operating lines can be distinguished; an outer operating line represents plug flow (line 2) and an inner operating line (line 3) represents backmixing between stages (in stepping off the stages it is necessary to pass

from the outer operating line to the inner operating line and visa versa). The equilibrium line is represented by line 1.

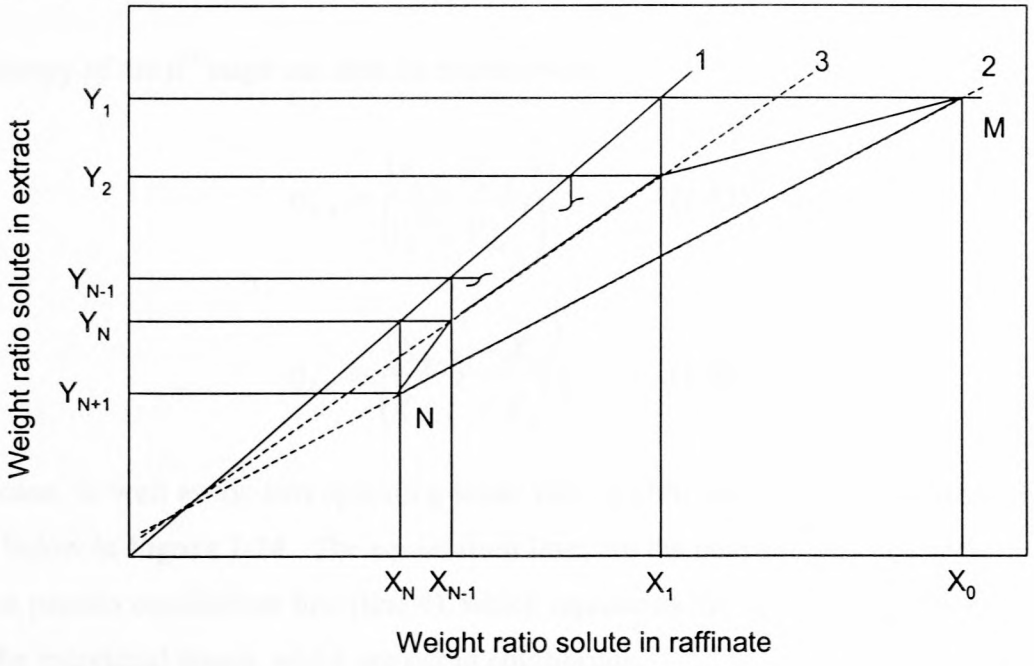

Figure 2-23: Graphical determination of number of stages for extraction with backmixing of phases and stage efficiency equal to 1, (1) equilibrium line, (2) outer operating line, (3) inner operating line (Prochazka and Landau, 1963)

Case 2: Stage Efficiency not Equal to Unity

When the stage efficiency is not equal to 1, the quantities Y_{n+1}, X_{n+1} and Y_n, X_n in the mass balance do not represent equilibrium conditions and therefore cannot be eliminated by means of the partition coefficient relation. However a further independent equation can be written. The balance of solute over the n^{th} stage can be written:

$$(1+\alpha_x)\kappa X_{n-1}{}' + \alpha_x \kappa X_{n+1} + (1+\alpha_y)Y_{n+1}{}' + \alpha_y Y_{n-1} = (1+2\alpha_x)\kappa X_n + (1+2\alpha_y)Y_n \qquad \textbf{(2-78)}$$

For the raffinate phase the initial composition is:

$$X_{n-1}{}' = \frac{[(1+\alpha_x)X_{n-1} + \alpha_x X_{n+1}]}{(1+2\alpha_x)} \qquad \textbf{(2-79)}$$

and for the extract phase it is:

$$Y_{n+1}{}' = \frac{\left[\left(1+\alpha_y\right)Y_{n+1} + \alpha_y Y_{n-1}\right]}{\left(1+2\alpha_y\right)} \qquad \textbf{(2-80)}$$

The efficiency of the n^{th} stage can then be expressed as:

$$\eta_{y,n} \equiv \frac{\left(Y_n - Y_{n+1}{}'\right)}{\left(Y_n{}^* - Y_{n+1}{}'\right)} \qquad \textbf{(2-81)}$$

$$\eta_{x,n} \equiv \frac{\left(X_{n-1}{}' - X_n\right)}{\left(X_{n-1}{}' - X_n{}^*\right)} \qquad \textbf{(2-82)}$$

For this case, as well as the two operating lines, two equilibrium lines are also distinguished as depicted below in **Figure 2-24**. The equilibrium lines are the conventional equilibrium line (line 1) and the pseudo equilibrium line (line 4), which represents the actual compositions of streams leaving the individual stages, which are not in equilibrium.

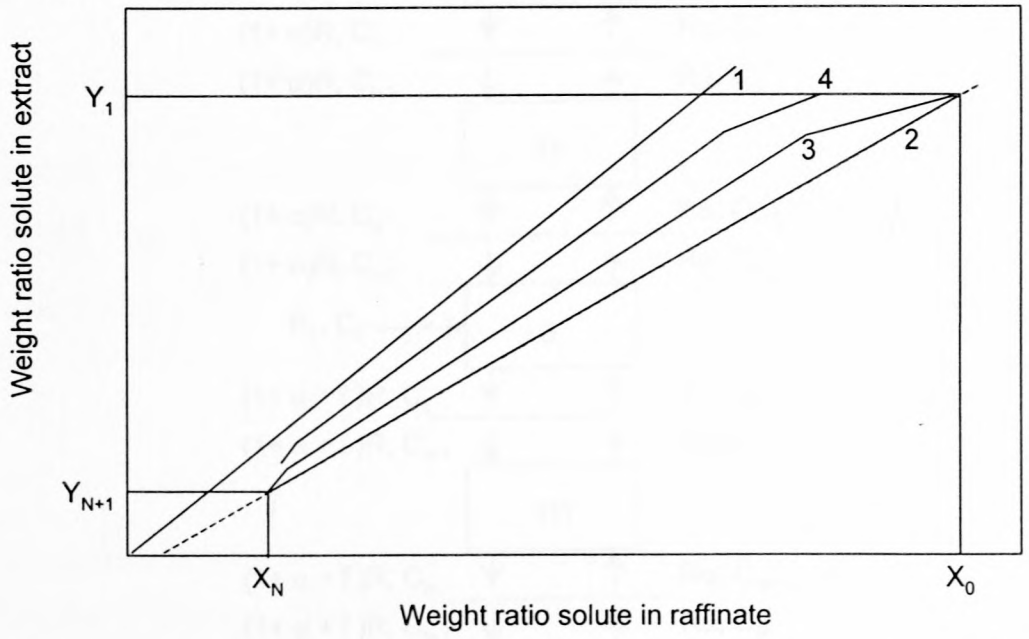

Figure 2-24: Backmixing of phases and stage efficiency not equal to 1, (1) equilibrium line, (2) outer operating line, (3) inner operating line, (4) pseudo equilibrium line (Prochazka and Landau, 1963)

Since the number of unknown parameters exceeds the number of independent equations, the equations of the inner operating line or of the pseudo equilibrium line cannot be obtained, and thus simple graphical calculations are not possible. The system of equations must be solved simultaneously and two types of problems are distinguished; either two of the terminal

compositions and the number of stages are given, or all the terminal compositions are given and the number of stages is to be determined (Prochazka and Landau, 1963). Rod, (1965) differentiated between the operating lines of the plug flow and backmixing cases using the terms "balance line" and "operating line" respectively.

2.7.5.2.3. Tracer Experiments

The backflow model derived in **Section 2.7.5.1** can also be used with tracer experiments, where no transfer of solute between the phases occurs. The assumption that the composition of the back-mixed stream is the same as the composition of the main stream leaving the given stage must hold. The process for single-phase flow experiments is represented in **Figure 2-25** below (Souhrada et al., 1966b).

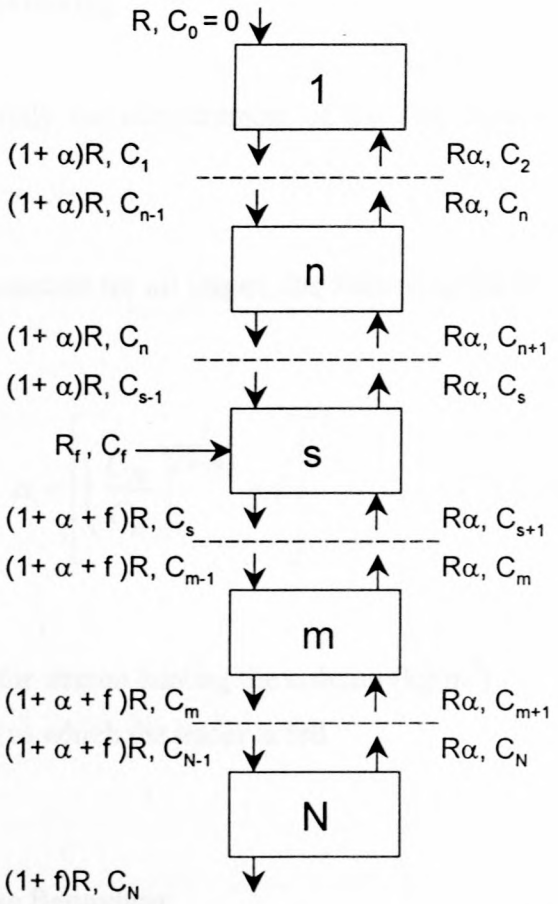

Figure 2-25: Schematic representation of a static stagewise model using a tracer (Souhrada et al., 1966b)

The given phase, not containing tracer is introduced to stage 1 at a constant rate R (Souhrada et al., 1966b). The tracer is introduced at stage s with a concentration of C_f and a constant flow rate of R_f. The back-mixed stream R_r flows in the opposite direction to that of the main flow. The assumption is made that the back-mixed stream has the same composition as the final composition of the main stream from the same stage. By performing a balance on the tracer from the 1st to the n^{th} stage (and assuming that the backmixing coefficient α_n, varies between stages), the following can be derived (Souhrada et al., 1966a,b):

$$\alpha_n = \frac{c_n}{(c_{n+1} - c_n)} \qquad \textbf{(2-83)}$$

where:

C_n : concentration leaving stage n (kg/m^3),

α : coefficient of backmixing

Equation 2-83 requires only the measurement of the end concentrations for two consecutive stages.

For the case where α is constant for all stages, the following relationship can be used (Souhrada et al., 1966a,b):

$$\alpha = \left[\left(\frac{C_N}{C_n} \right)^{\frac{1}{(s-n)}} - 1 \right]^{-1} \qquad \textbf{(2-84)}$$

where:

C_N : concentration in the stream leaving the column (kg/m^3)

s : number of stages to which the tracer is fed

2.7.5.2.4. Dispersed Phase Behaviour

For two-phase flow in an extractor, the one phase is typically dispersed in the other in the form of droplets. The basic equations expressing the behaviour of the continuous phase have been shown to explain experimental results. However, there is a question as to how the models fit the

dispersed phase, since the basic equation requires that all of the dispersed phase at a given level in a column have the same concentration (Miyauchi and Vermeulen, 1963a).

Two scenarios can exist (Miyauchi and Vermeulen, 1963b):

- if sufficient coalescence and re-dispersion occurs, then the concentration of each droplet of the dispersed phase is the same and the phase can be considered as a second continuous phase,
- if this is not the case, then the overall rate process must be quantified by considering the residence time distribution of droplets and the respective concentration distribution as the droplets enter.

For the case consistent with the assumption that the dispersed phase behaves as a second continuous phase, models can be derived, assuming that the value of the dispersed phase concentration leaving stage n is the mean value (calculated on a volume basis), and $k_{ox}a$ is constant through the length of the column. For the case where in any stage, the concentration of each droplet is different, (depending on the residence time in the stage, the droplet size and entering concentration) Miyauchi and Vermeulen, (1963b) developed an approach, and showed that if the following conditions are satisfied, that it is possible to treat the dispersed phase as if it were a second continuous phase:

- drop size is uniform,
- over-all coefficient of mass transfer is constant,
- volume fraction (hold-up) of the dispersed phase is constant throughout the column,
- linear equilibrium holds.

These restrictions may be relaxed depending on how fast coalescence and re-dispersion of the dispersed phase takes place in the system. There is a positive indication of coalescence and re-dispersion of liquid droplets for agitated liquid-liquid systems, which renders the restrictions less necessary in such cases. The dispersed phase in mixer-settler extractors can be treated as a second continuous phase, and in addition it is not necessary that the dispersed droplets be separated into a homogenous phase before entering the next phase (Miyauchi and Vermeulen, 1963b).

2.7.5.3. Application of the Backflow Model

Several investigators have derived Backflow models, and initially investigators assumed that the parameters were constant along the extractor (Prochazka, et al. 1963; Rod, 1965). However, investigation of extraction concentration profiles showed a variability of the parameter values with position in the column (Slavickova et al., 1978). It has been concluded that when columns are operated in intense regimes, the dispersed phase hold-up profiles vary in an axial direction. As a consequence of this in homogeneity, as well as changes in physical properties and non-linear equilibrium, (Slavickova et al., 1978), parameters such as the stage efficiency, height of a transfer unit (HTU), the volumetric mass transfer coefficient, and the coefficients of axial dispersion or of backmixing can vary in an axial direction. This parameter variation is likely to exert an unfavourable effect on the overall efficiency of the equipment and impede the process of scale-up (Heyberger et al., 1982). In order to confirm this hypothesis, Heyberger et al., (1982), suggested that simultaneous measurements of hold-up profiles, drop size distribution and mass transfer should be taken when performing experiments to determine backmixing parameters.

Several authors have quantified axial distribution of the respective parameters in a vibrating plate extraction column by combining experimentally determined longitudinal solute concentration profiles with a Backflow model. Slavickova et al., (1978) investigated extraction of uranyl nitrate in a VPE, whereby solute concentration profiles in both phases were used to calculate the stage efficiency and backmixing coefficients. Two algorithms were used, the first assuming constant value parameters, while the second used smooth analytical approximations of axial distributions of the parameters. In this study, the parameters were evaluated using mostly artificially constructed concentration profiles. The general case of non-linear equilibrium was also considered. It was found that for this system, considerable variation of the parameter values occurred.

Heyberger at al. (1982) evaluated parameters in a VPE (85 mm in diameter, with 2 m active height) with backmixing, for a water-acetone-toluene system using a stage efficiency model. Samples were taken in the middle of each stage height, and in a perfectly mixed stage k, Xk, Yk, would represent samples taken from the central part of the stage respectively. However in real stagewise equipment the assumption of perfect mixers is not usually fulfilled (Slavickova et al., 1978). Thus the stages were not considered to be perfectly mixed, and at the point that the sample was taken, it was assumed that the extract (continuous phase) concentration approached

that flowing out of the downcomer. Therefore the stages were defined by the horizontal planes bisecting the distance between neighbouring plates (not the plane of the plates), so that the concentrations of samples between the k^{th} and the $k+1^{st}$ plate were designated as X_k, Y_{k+1} respectively. The parameters (stage efficiency and back mixing coefficients of the extract and raffinate phases) in the model were not considered constant, but were represented by polynomials of the stage number. The coefficients of the polynomials were determined using Marquardt's optimisation procedure (Marquardt, 1963), whereby the mean square deviation of measured and calculated concentrations were determined. It was found that the backmixing coefficients of the dispersed aqueous phase were low (a property typical for the VPE extractor which was also supported by Slavickova et al., 1978) and could be approximated by a constant. For the backmixing coefficient of the continuous organic phase, and the stage efficiency, good agreement between the calculated and experimental concentration profiles was obtained with polynomials of 4^{th} degree. In most cases, the model assuming constant values for all parameters failed to adequately describe the profiles and the exit concentrations, and it was found that the deviations increased with increased intensity of hydrodynamic regime. It is likely that the deviations were due to an in homogenous distribution of dispersed phase through the column (Heyberger et al., 1982).

Another consideration was the meaning of the measured concentrations with respect to the model. The concentration field may change its shape with variations in the intensity of mechanical agitation. To minimise the ambiguity of the real stage concept, Heyberger et al. (1982) suggested that further study to quantify flow patterns between plates should be completed. The strongest variability in parameters was observed near the column ends. For a commercial scale column, these parts of the parameter profiles will be less representative than the values in the central part of the extraction column. The authors contend however that application of a variable parameter model is impractical for design purposes, and the use of arithmetic mean values may be the best choice. This approach is preferable to that using values obtained using a constant parameter model, since the former takes into account the end effects of the experimental equipment. The local values of the continuous organic phase backmixing coefficient and the stage efficiency were found to be sensitive to the shape of the concentration profiles, and thus can be used to identify local in homogeneities (caused by uneven distribution of the dispersed phase) in the column (Heyberger et al. 1982).

Miyauchi and Vermeulen (1963b) derived a mass transfer coefficient backflow model and took into account the fact that constructional stages do not behave as ideal mixers, by representing each stage of the cascade by several ideal mixers and assuming that the extent of backmixing between them is the same as between the constructional stages.

Although the theory of extraction with backmixing has been developed, application of this in extractor design is limited by the lack of data, which would facilitate proper selection of parameter values of the mathematical models. This appears to be as a result of the complexity of the parameters, which are functions of a number of variables, such as the geometrical and mechanical characteristics of various extractors, as well as physiochemical properties of the liquid phases. Various empirical relations have been proposed (Ingham, 1971) but these do not satisfactorily take into account equipment size or geometry, phase interaction, the influence of mass transfer on axial mixing, or the effect of interfacial phenomena (Slavickova et al., 1978).

Souhrada, et al., (1966a,b) investigated the influence in variations in the flow rate on back-mixing by performing tracer experiments and using a stage efficiency model (**Section 2.7.5.2.3**). The authors found that at constant amplitude and frequency, the continuous phase backmixing coefficient did not alter much with the rate of flow. It was concluded that the influence of variations in the flow of the dispersed phase on backmixing in a vibrating plate extractor is better than that in a pulsed extractor. Whereas in the latter case with increasing rates of flow of the dispersed phase, back-mixing of the continuous phase increases or at least it does not decrease, in the former case it decreases. This can be explained by the fact that in the vibrating plate column at higher rates of flow of the dispersed phase a higher layer of this phase forms on the plates, and this prevents the continuous phase from passing through the plate openings. At sufficiently high rates of flow of the dispersed phase, back-mixing apparently occurs predominantly through the free cross section between the plate and wall, through the continuous phase flows. It was also concluded that by increasing the height of a stage (distance between plates) by reducing the number of plates per unit length of column, backmixing in the continuous phase was reduced.

2.7.6 Comparison of Diffusion and Backflow Models

A number of relationships have been derived between the stagewise and differential models to enable comparison of results obtained using the two models (Prochazka and Landau, 1966; Souhrada et al., 1966b). Miyauchi and Vermeulen, (1963b) showed that the Diffusion Model, can be derived as an extreme case of the backflow model.

The following relationship between the backmixing coefficient and the coefficient of axial dispersion was derived (Miyauchi and Vermeulen, 1963b):

$$\frac{HU_c}{E_c} = \frac{1}{2} + \alpha \qquad \textbf{(2-85)}$$

where:

E_c : coefficient of axial dispersion (m^2/s)

H : height of stage (m),

U_c : superficial velocity of continuous phase in extractor (m/s),

α : backmixing coefficient

The relationship between the stage efficiency and the Murphree efficiency and between the stage efficiency and the coefficient of mass transfer, as shown in **Sections 2.4.2.4** and **2.4.3,** as well as the relationship between the backmixing coefficient and the coefficient of axial dispersion defined above, enable comparison of the results obtained on the basis of different formulations of stagewise and the differential model (Prochazka and Landau, 1966).

The backflow model is more suitable for sieve plate columns, with or without pulsation (Nemecek and Prochazka, 1974) and for rotating disc contactors, while the diffusion model is more appropriate for packed or spray columns (Vermeulen et al., 1966). It has been concluded that either model should apply with reasonable accuracy to extractors of intermediate type, such as the rotary disk and pulsed plate columns, provided the number of stages is large. The Backflow model is however favoured when the open area fraction of the plates is small, such as the VPE, while the Diffusion model is more appropriate in open columns, such as the Karr column (Pratt and Baird, 1983, Aravamudan and Baird, 1996). The Backflow model is more

versatile and is more suitable for difficult situations such as side streams, partially miscible solvents and the simultaneous transfer of several solutes (Pratt and Baird, 1983).

2.7.7 Combination of the Backflow and Diffusion Model Theories

Various authors, including Prochazka and Landau (1963) and Souhrada et al., (1966a,b) concluded that the concept of ideal mixers is an oversimplification. It is apparent that the assumption of perfect mixing within the stage implies that longitudinal mixing does not depend on plate geometry, which contradicts experimental evidence (Nemecek and Prochazka, 1974). In addition for much of the work concerned with axial mixing, the data was examined using dimensional analysis, assuming a power-law dependence of the axial dispersion coefficient upon the operating and geometric variables of the column. Use of this type of analysis is limited to the range of data upon which it is based and the assumption was made that axial dispersion varied in a continuous and regular manner with these variables (Stevens and Baird, 1990). Thus a different type of model was developed, based on local axial mixing.

The two-phase model was derived by taking into account the existence of two separate hydrodynamic regions, for which there are two mechanisms for axial dispersion. A stage is described as two ideal mixers (in the volume swept out by the reciprocating plate) separated by a region of axial dispersion (between the plates) as depicted in **Figure 2-26** below (Nemecek and Prochazka, 1974).

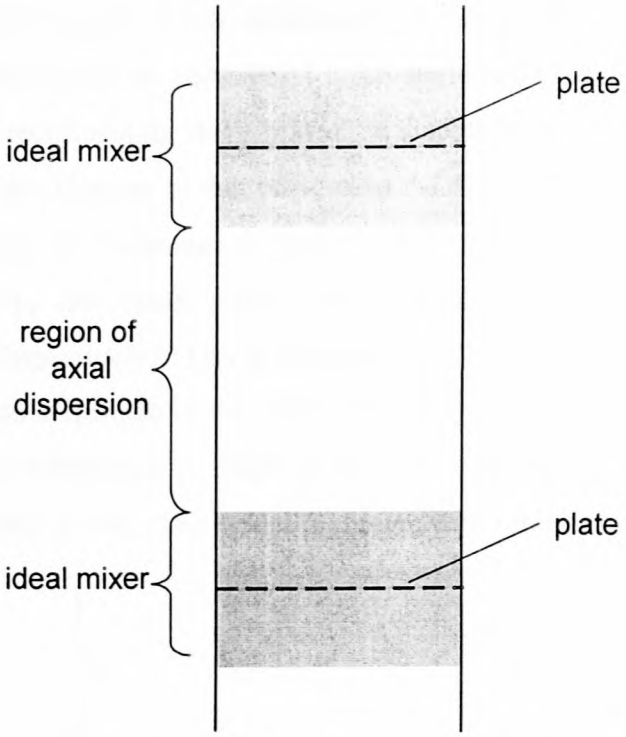

Figure 2-26: A stage consisting of two ideal mixers separated by a region of axial dispersion

Longitudinal mixing of the continuous phase in the VPE can be described as a process consisting of backflow through the plates, and longitudinal mixing within the stage, the intensity of which depends strongly on the distance from the plate. In the proximity of the plates, the regions can be regarded as perfectly mixed, and these two regions are separated by a low intensity mixing region. The width of this region and the intensity of mixing are functions of plate geometry and spacing, the intensity of vibrations and the character of the flow of the dispersed phase (which affects longitudinal mixing of the continuous phase most markedly, though differently for each hydrodynamic flow regime). The region of vigorous mixing near the plate (and high axial mixing) originates as a consequence of the circulating flows at individual openings, which reach deeper into the stage the greater the velocity from the opening. The distance that can be penetrated by the circulation is limited by the height of the stage. A full contact of the two circulating layers seems unlikely, and ultimately this results in a layer of constant thickness encompassing approximately homogenous turbulent field, as a consequence of the breakdown of the circulating flows (Stevens and Baird, 1990) .

Novotny et al., (1970), derived a stagewise model which expressed the effect of the plate geometry, (specifically amplitude, frequency, flowrates, distance between plates, plate fractional free area and hole size) on longitudinal mixing, for single phase flow, in a VPE. The model takes into account both backmixing between stages and axial mixing within stages. The work

concerned operation in the region of low amplitude and correspondingly higher frequencies, for which the flow in the stage may be considered quasi-stationary. The relations developed were valid for columns with reciprocating sieve plates. A backflow model was derived for a single phase system using a tracer (similar to that of **Section 2.7.5.2.3** and **Figure 2-25**). Experimental validation was performed on a column 51 mm in diameter and 1 m long, equipped with a reciprocating plate stack, and using water and glycerol solutions (with tracers potassium chromate and fuchsine respectively). Use was made of a VPE with open area ranging from 0.02 to 0.146, with a pulsation amplitude in the order of 1 mm and frequencies in the range of 3.3 to 16.6 Hz. The data was interpreted in terms of the two-zone model. The derived model was shown to fit the data within ±12%. The model is shown, with reference to **Figure 2-27**

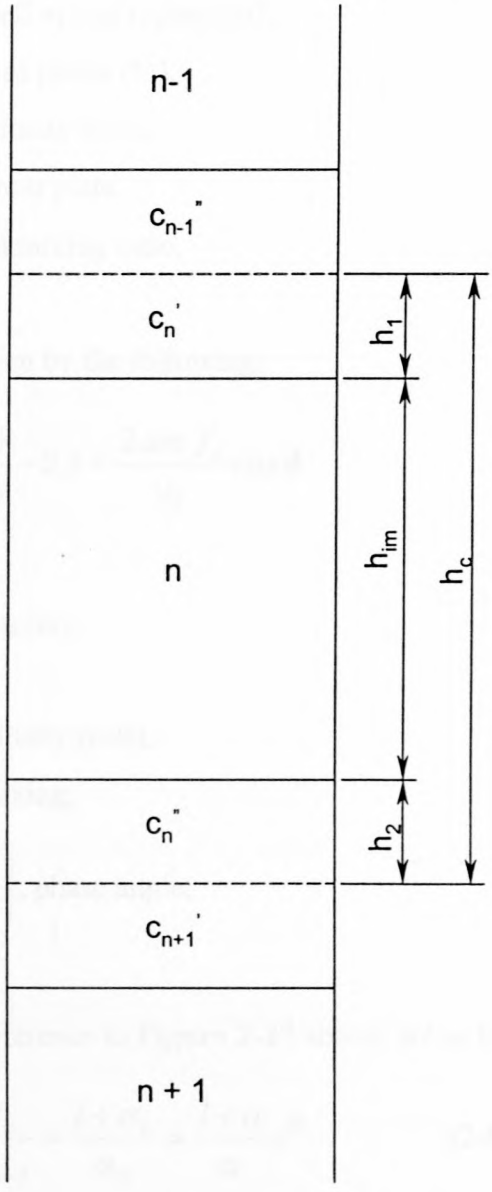

Figure 2-27: Model of a stage (Novotny et al., 1970)

The effective back ratio was given by:

$$\alpha_e = \left\{ \left(1 + 1/\alpha\right) exp\left[6.6\left(h_c - h^{\bullet}\right) \frac{S^{1.5} u_c}{d_h am\, f_c} \right] \right\}^{-1} \qquad \textbf{(2-86)}$$

where:

am : amplitude (half stroke) (m),

d_h : diameter of holes in plate (m),

f_c : frequency of reciprocating motion (Hz),

h_c : height of a stage (m),

$h^{\bullet}$ = $h_1 + h_2$, height of well mixed region (m),

S : fractional open area of plates (%),

u_c : continuous phase velocity (m/s),

α : backmixing ratio across plate,

α_e : overall effective backmixing ratio.

The backflow ratio α was given by the following:

$$\alpha = \frac{\phi}{\pi} - 0.5 + \frac{2.am.f_c}{u_c} cos\,\phi \qquad \textbf{(2-87)}$$

where:

am : amplitude, half stroke (m),

f_c : frequency (Hz),

u_c : continuous phase velocity (m/s),

α : coefficient of backmixing,

ϕ = $arcsin\left(\frac{u_c}{2.\pi.am.f_c} \right)$, phase angle,

The derived relations, with reference to **Figure 2-27** above, are as follows:

$$\frac{c_n}{c_{n-1}} = \frac{1+\alpha_e}{\alpha_e} = \frac{1+\alpha}{\alpha} e^P \qquad \textbf{(2-88)}$$

$$P = K' \frac{(H - h^{\bullet}) u \varepsilon^{3/2}}{am f_c d_h} \qquad \textbf{(2-89)}$$

where:

am : amplitude (m),

d_h : diameter of holes in plate

f_c : frequency of reciprocating motion,

h_{im} : height of imperfectly mixed region,

$h^{\bullet}$ $= h_1 + h_2$, overall height of ideal mixers,

h_c : stage height,

K' : empirical parameter,

P : Peclet number,

u : mean flow velocity referred to cross sectional area of extractor,

ε : fractional free area of plate

α : coefficient of backmixing,

α_e : effective coefficient of backmixing.

Values of $h^{\bullet}$ and K' were determined, and it was found that the overall height ($h^{\bullet}$) in one stage behaving as ideal mixers is 4.5 cm. It was found that the value of the backmixing coefficient, α, very strongly depends on the arrangement of holes on the plate. The backmixing coefficient, α increases rapidly with decreasing plate hole pitch, which can be attributed to the larger continuous full area on the plate, resulting from the closer spacing of the given number of holes. The periodic flow through the holes then tends to create circulating flows above and below the plate, which penetrate further into the respective stages and tend to increase longitudinal mixing. The extent of longitudinal mixing rapidly increases when the holes are less uniformly spaced over the plate, while longitudinal mixing decreases rather rapidly with increasing distance between plates (Novotny et al., 1970).

The intensity of longitudinal mixing of the continuous phase is typically very different from that under single phase flow, however the work to derive a model by Novotny et al., (1970), was extended by Nemecek and Prochazka, (1974) to two phase flow.

Nemecek and Prochazka, (1974) examined longitudinal mixing in the continuous phase of a water-tri-chloroethylene system (with the organic phase dispersed and potassium chromate as a tracer) using a 50 mm diameter, 240 mm long VPE, and operating at 23°C. Since the hydrodynamic regimes differ in various parts of the column, the measurement of longitudinal mixing should be localised. The data of Novotny et al. (1970) was reanalysed and the value of $h^{\bullet}$ changed to the following: (Nemecek and Prochazka, 1974).

$$h^{\bullet} = 0.5025\left(\frac{2.am.f_c}{S^2}\right)^{0.29} \quad for\ h^{\bullet} < 0.3255(h_c + 2.35)$$
$$= 0.3255(h_c + 2.35) \quad elsewhere \qquad \textbf{(2-90)}$$

where:

am : amplitude (m),

f_c : frequency of reciprocating motion,

h_c : height of a stage (m),

$h^{\bullet}$ = $h_1 + h_2$, overall height of ideal mixers,

S : fractional open area of plates.

The equation was developed empirically by observing small tracer particles in the column and measuring the maximum movement of particles around the reciprocating plates. This was interpreted as the height of well-mixed region.

The two-zone concept was refined by Stevens and Baird (1990), using a 5 cm diameter reciprocating plate extraction column, however only for single phase conditions. The system consisted of distilled water, with the addition of a sodium chloride tracer solution to the column just above the column outlet. Various samples were taken throughout the length of the column and the samples analysed using an electrical conductivity meter, which was pre-calibrated with salt solutions to facilitate measurements of concentration profiles. The amplitude, plate frequency, plate spacing, hole size and free area fraction were varied. The following hydrodynamic model with two adjustable parameters, based on the observed concentration profiles was proposed and used to predict a range of experimental data available in the literature:

$$E = \left(\frac{ln\left(\frac{1+\alpha}{\alpha}\right)}{h_c.u_c} + \frac{2.S\left(1 - \frac{K_2.am}{h_c}\right)}{K_1.d_h\left\{\left(u_c + 2.\pi.am.f_c\right)\left[\left(\frac{\pi}{2.\sqrt{3}S}\right)^{0.5} - 1\right]\right\}} \right)^{-1} \quad \textbf{(2-91)}$$

where:

am : amplitude (m),

E : axial dispersion coefficient (m^2/s),

E_1 : axial dispersion coefficient in the poorly mixed region (m^2/s),

d_h : diameter of hole,

f_c : frequency of reciprocating motion,

h_c : height of a stage (m),

K_1 $= \frac{E_1}{v.l_v}$, constant,

l_v : characteristic size of vortices in the poorly mixed region (m),

S : fractional open area of plates,

u_c : continuous phase velocity (m/s),

v : characteristic velocities of vortices in the poorly mixed region (m/s),

α : coefficient of backmixing.

This equation is only applicable when the two well-mixed regions do not overlap.

For cases where amplitude is large in relation to plate spacing, a third parameter is necessary to allow for a minimum width of the poorly mixed zone (Stevens and Baird, 1990).

An example of the concentration profiles determined by Stevens and Baird (1990) is depicted in **Figure 2-28** below:

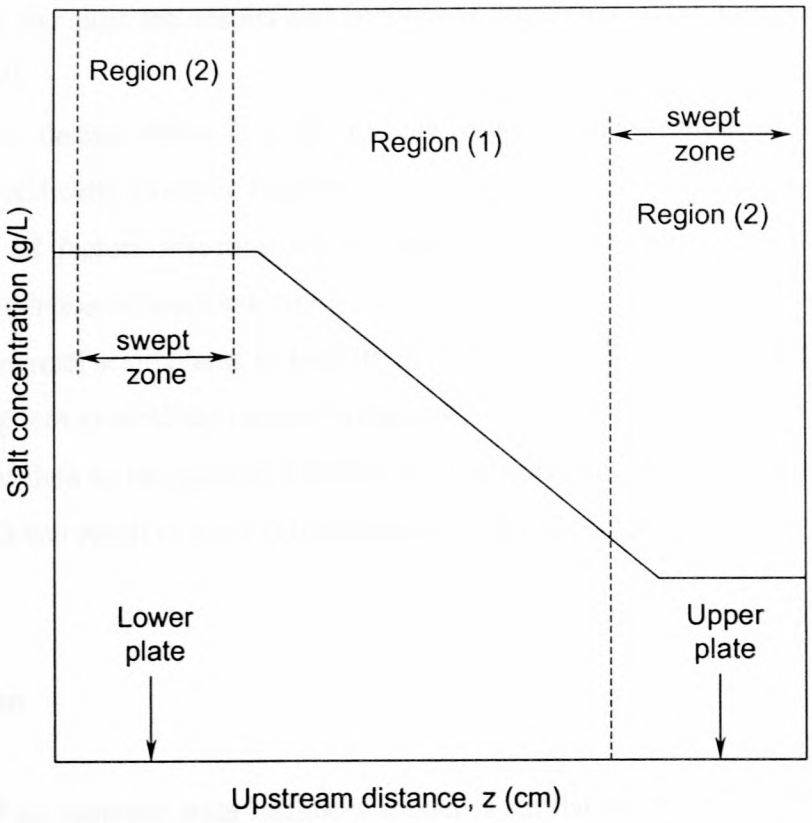

Figure 2-28:Concentration profiles between two plates: region (2) – well mixed zone, region (1) – poorly mixed zone

2.8 Unsteady State Extraction

2.8.1 Stagewise Backflow Model

Extraction columns are normally designed to operate at steady state for extended operating times without varying operating parameters. However the study of unsteady state operation can be useful and it is possible to obtain parameters such as backmixing, hold-up, and mass transfer coefficients experimentally by application of unsteady state techniques. In order to quantify an unsteady state process, a model must be derived to predict the column behaviour and unsteady state experimental results used to determine the model parameters. The model can then be used as a tool to predict the response of the column to external changes, for dealing with problems associated with control (Souhrada, et al. 1970) and for the scale–up and design of commercial equipment from pilot plant data (Steiner and Hartland, 1983).

The importance of dynamic test results and analysis is illustrated by the following uses (Pollock and Johnson, 1969):

- control system design relies heavily on the dynamic description of the process and controllers, specifically dynamic response,
- determination of factors affecting the extraction operation, which are not obvious from theory, and validation of assumptions,
- study of commercial scale plants to identify disturbances and indicate changes that should be made in the system to yield the required response,
- contribution of data to the general knowledge of process phenomena (such as mass transfer studies), which can result in more reliable design and scale-up methods.

2.8.1.1. Derivation

The derivation of an unsteady state backflow model is similar to that of the steady state model derived in **Section 2.7.5.1**. The extractor is divided into a large number of stages, which in the VPE would represent the spaces between plates. The assumption is made that in each stage, both phases are perfectly mixed, that the stages are not at equilibrium and that there are step changes in concentration between the stages. Backmixing in the column is expressed by the use of backflow ratios (in the opposite direction to the main flow), which indicate the ratio of the backflow inside the column, to the feed flow of the same phase outside the column. The model is described by an ordinary set of ordinary differential equations, the number of which is equal to the number of stages (Steiner and Hartland, 1983).

The notation used for a column divided into N perfectly mixed stages with backmixing in both phases is shown in **Figure 2-29** below. In this case, the solvents are considered immiscible. The flows will not be constant along the column, but will be dependent only on the solute concentration and thus the mass rates and concentrations of the dispersed and continuous phases are on a solute free basis (Steiner and Hartland, 1983).

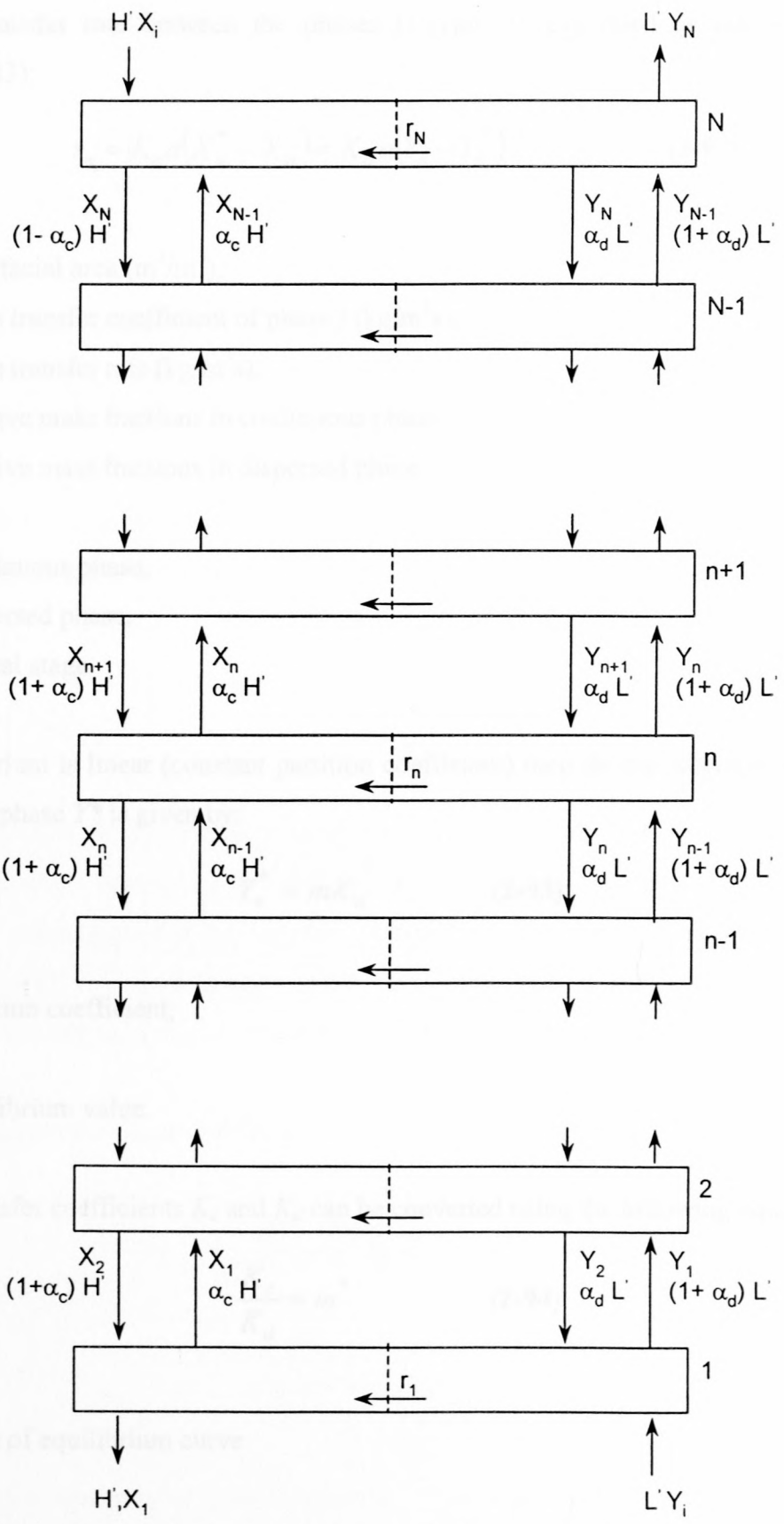

Figure 2-29: Notation for stagewise backflow model (Steiner and Hartland, 1983)

The mass transfer rate between the phases is typically expressed as follows (Steiner and Hartland, 1983):

$$r_n = K_c a\left(X_n^* - X_n\right) = K_d a\left(Y_n - Y_n^*\right) \qquad \textbf{(2-92)}$$

where:

a : interfacial area (m^2/m^3),

K_j : mass transfer coefficient of phase j (kg/m^2s),

r_n : mass transfer rate (kg/m^3s),

X : relative mass fractions in continuous phase,

Y : relative mass fractions in dispersed phase.

subscripts:

c : continuous phase,

d : dispersed phase,

n : typical stage.

If the equilibrium is linear (constant partition coefficient) then the equilibrium concentration in the dispersed phase Y^* is given by:

$$Y_n^* = mX_n \qquad \textbf{(2-93)}$$

where:

m : partition coefficient,

superscript:

$*$: equilibrium value.

The mass transfer coefficients K_c and K_d can be converted using the following equation:

$$\frac{K_c}{K_d} = m^* \qquad \textbf{(2-94)}$$

where:

m^* : slope of equilibrium curve

This is based on the assumption that the equilibrium curve is sufficiently straight to be represented by its slope for concentration changes between X_{n-1} and X_{n+1}. The balance equations for a typical stage are as follows:

$$\frac{dX_n}{dt} = \frac{u_c}{h}\{(1+\alpha_c)(X_{n+1} - X_n) - \alpha_c(X_n - X_{n-1})\} - \frac{r_n}{\rho_c(1-\varphi)} \qquad \textbf{(2-95)}$$

$$\frac{dY_n}{dt} = \frac{u_d}{h}\{(1+\alpha_d)(Y_{n-1} - Y_n) - \alpha_d(Y_n - Y_{n+1})\} + \frac{r_n}{\rho_d\varphi} \qquad \textbf{(2-96)}$$

h : height of hypothetical stage (m),

H' : flowrate of the continuous phase (kg/s),

L' : flowrate of the dispersed phase (kg/s),

t : time (s),

u_c : continuous phase velocity (m/s),

u_d : dispersed phase velocity (m/s),

α_j : backflow coefficient of phase j,

φ : volumetric ratio of the dispersed phase in each stage (hold-up),

ρ : density (kg/m^3).

The forward flow of the continuous phase in the column is $(1+\alpha_c)H'$, while $\alpha_c H'$ is the backflow. The magnitude of the backflow coefficients is dependent on the number of stages used. There is mixing in the column even if the backflow coefficients are zero since each stage has a finite volume that is well mixed. The mass transfer coefficients can be evaluated from concentration profiles along the length of the column (Steiner and Hartland, 1983).

Solvent velocities are defined as follows:

$$u_s = \frac{H'}{(1-\varphi)\rho_c CSA} \qquad \textbf{(2-97)}$$

$$v_s = \frac{L'}{\varphi\,\rho_d CSA} \qquad \textbf{(2-98)}$$

where:

CSA : cross sectional area of the column (m^2)

Since the backflows do not leave the column, the first stage equations are:

$$\frac{dX_1}{dt} = \frac{u_s}{h}(1+\alpha_c)(X_2 - X_1) - \frac{r_1}{\rho_c(1-\varphi)} \qquad \textbf{(2-99)}$$

$$\frac{dY_1}{dt} = \frac{v_s}{h}\{Y_i + \alpha_d Y_2 - (1+\alpha_d)Y_1\} + \frac{r_n}{\rho_d \varphi} \qquad \textbf{(2-100)}$$

and for the last stage:

$$\frac{dX_N}{dt} = \frac{u_s}{h}\{X_i + \alpha_c X_{N-1} - (1+\alpha_c)X_N\} - \frac{r_N}{\rho_c(1-\varphi)} \qquad \textbf{(2-101)}$$

$$\frac{dY_N}{dt} = \frac{v_s}{h}\{(1+\alpha_d)(Y_{N-1} - Y_N)\} + \frac{r_N}{\rho_d \varphi} \qquad \textbf{(2-102)}$$

Only simple cases, which incorporate immiscible solvents and constant partition coefficients (linear equilibrium data) can be solved analytically. For other cases the ODE's can be solved using a method such as a Runga-Kutta procedure, on a computer. Complicated problems with side streams entering and leaving the columns and partially miscible solvents with complicated equilibrium conditions can be simulated using this method (Steiner and Hartland, 1983).

2.8.1.2. Further Complexities

In order to determine information about the dynamic response of a system, a disturbance is required, to excite the dynamic characteristics of the process. The common methods can be classified as follows (Pollock and Johnson, 1969):

- steady state forcing,
- pulse input forcing,
- initial condition or step forcing.

As with the steady state backflow model, tracer experiments can be performed with the dynamic model.

2.8.1.2.1. Tracer Experiments

Backmixing coefficients of the unsteady state (dynamic) backflow model can be determined by measuring the concentrations of a component that is only soluble in one of the phases (a tracer), whereby no transfer of solute between the phases occurs. This may be achieved experimentally by introducing an instantaneous pulse of tracer to the first stage. The output concentration of tracer can either be indicated by a probe placed at the exit from the last stage, or by taking samples at this place at regular intervals. For this model, the assumption of perfect mixing in the phases must hold. A schematic representation of the model is depicted in **Figure 2-30**.

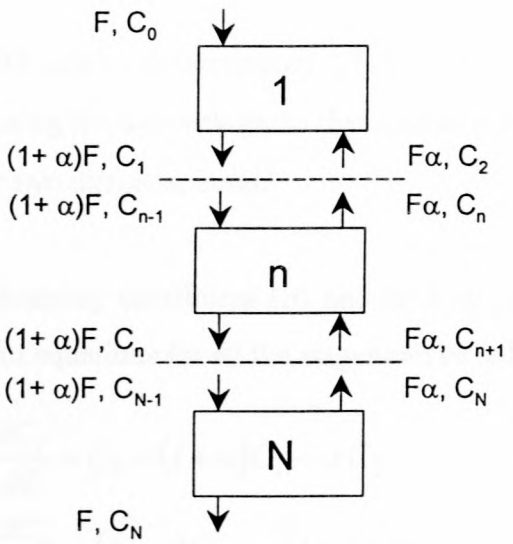

Figure 2-30: Schematic representation of stagewise model (Souhrada et al., 1966)

By performing a mass balance for the tracer over the *n*th stage, the following can be written (Souhrada et al., 1966):

$$(1+\alpha_{n-1})FC_{n-1}+\alpha_n FC_{n+1}=(1+\alpha_n)FC_n+\alpha_{n-1}FC_n+\frac{d}{dt}\int_{M_n}C_n dM_n \qquad \textbf{(2-103)}$$

where:

C : concentration of tracer (kg/m^3),

F : volumetric flowrate (m^3/s),

t : time (s),

In order to determine the tracer accumulation in the *n*th stage, it is necessary to know the distribution of its concentration in the stage. If ideal mixing conditions can be assumed, and using dimensionless time (θ_n), the following can be derived:

$$\frac{dC_n}{d\theta_n} = (1+\alpha_{n-1})C_{n-1} + \alpha_n C_{n+1} - (1+\alpha_n)C_n - \alpha_{n-1}C_n \qquad \textbf{(2-104)}$$

where:

φ : hold-up,

θ_n = $t\,F/\varphi$, dimensionless time,

In principle, **Equation 2-104**, allows determination of the value of the backmixing coefficient (α) for each stage, by measuring the concentrations that appear in **Equation 2-104** and the value of the derivative $dC_n/d\theta_n$ for two different times.

When the value of the backmixing coefficient (α) and hold-up (φ) do not vary from stage to stage, the following system of equations for all the stages can be solved:

$$\begin{aligned}
&\textit{for the first stage} && \frac{dC_1}{d\theta} = C_0 - (1+\alpha)C_1 + \alpha C_2 \\
&\textit{for } 1 < n < N && \frac{dC_n}{d\theta} = (1+\alpha)C_{n-1} - (1+2\alpha)C_n + \alpha C_{n+1} \qquad \textbf{(2-105)} \\
&\textit{for the } N-th \textit{ stage} && \frac{dC_N}{d\theta} = (1+\alpha)C_{N-1} - (1+\alpha)C_N
\end{aligned}$$

The following applies for tracer experiments: (Souhrada et al., 1966)

- when the value of the backmixing coefficient (α) varies from stage to stage, the concentrations for three consecutive stages have to be measured, as well as the derivative with time,
- when the value of the backmixing coefficient (α) is constant in all stages, the system of equations in **Equation 2-105** must be solved for a number of selected values of α, and only the time dependence of the terminal concentration need be measured,
- measurements can be influenced by the different behaviour of the column end sections,

- the hold-up in the column must be measured,
- the system of equations in **Equation 2-105** can only be used if the hold-up is the same in all the stages, otherwise **Equation 2-104** must be employed, even if the back-mixing coefficient is the same in all stages.

It is crucial when performing tracer experiments to quantify axial mixing, that precautions are taken to ensure that the density of the tracer solution is close to that of the continuous phase, however test work has shown that even a small unstable density difference (in the order 0.001 g/m*l* can increase axial dispersion (Aravamudan and Baird, 1996).

2.8.1.3. Application of the Unsteady State Backflow Model

Souhrada et al., (1966) carried out static and dynamic tracer tests, using a VPE (with a square cross section of 70 mm x 35 mm), on a water-acetone-toluene system, and using potassium chromate as the tracer. Concentration profiles were also measured to compare results. The temperature was maintained within 0.1°C, and no significant variation in hold-up through the length of the column was observed. Samples were taken from the centre of the respective stages, and the assumption of perfect mixers was tested by also measuring the tracer in five positions, in each stage. It was concluded that the concentration profile in the extractor was clearly stagewise, however at lower frequency, the differences in the local concentrations were considerable. The static test results indicated that the backmixing coefficient did not vary from stage to stage, and that backmixing in the dispersed phase was insignificant (Souhrada et al., 1966).

Souhrada et al., 1970 also derived a dynamic stagewise model. The assumptions were made that variations in hold-up, efficiency and backmixing coefficients over the transient period were negligible. In addition, it was assumed that the coefficients of backmixing did not vary from stage to stage. For the case of non-linear equilibrium data, two procedures were proposed. Either the equilibrium data was approximated by a linear relation for the concentration range of interest (termed Model 1), or for each stage a linear relation was written (termed Model 2). The mathematical system derived using the model was integrated using the Runga-Kutta-Merson method. The method was validated on a toluene-acetone-water system using a 50 mm diameter reciprocating plate extractor, 1 m in length, and fitted with wide calming sections at each end. Eight plates were attached to the central shaft and spaced 125 mm apart, and each stage was

equipped with an organic phase sampler and an aqueous phase sampler. Two types of measurement were made; steady state concentration profiles in each phase, and the time dependence of the exit concentrations. The results of the two methods were compared. Different values for the efficiencies were found for the two models, however the calculated and experimentally determined concentration profiles agreed, which indicated that the values of the coefficients of backmixing and the stage efficiency were determined with sufficient accuracy. The Model 1 method of approximating non-linear equilibrium was in good agreement with the experimental results, while Model 2 only gave satisfying results for the raffinate phase.

2.9 Comparison of Unsteady and Steady State Backflow Models

It is also possible to also derive an unsteady state (dynamic) diffusional model. This is slight variation of the steady state (static) model derived in **Section 2.7.4**, whereby accumulation is taken into account. Baird et al. (1992) quantified unsteady axial mixing using a diffusion model and unsteady state measurements. Some authors (Westerterp, et al. 1962, Stemerding et al. 1963) have found that static and dynamic methods for the diffusional model for the rotating disc contactor, yield significantly different results.

For the backflow model the assumptions required for a dynamic model to hold are perfect mixing in the phases, whereas for the static model the assumption is less strict; that the composition of the back-mixed stream is the same as the composition of the main stream leaving the given stage. Both methods will give the same and correct results for a cascade of perfect mixers. However if this criterion is not met, the two methods may not give the same results and it is necessary to investigate, using experimental tests, which of the results is more appropriate. Souhrada et al., (1966) performed experiments (water-acetone-toluene system, with potassium chromate as the tracer) using three methods of measurement; static and dynamic tracer methods and a concentration profile method. It was concluded that the results obtained using the three methods agreed well, which indicated that the assumptions required for tracer experiments were fulfilled, even though the measured concentrations in different parts of the stages showed that perfect mixing was not achieved. Consequently, tracer methods are applicable over a wider range of conditions than those given by the assumptions detailed in **Section 2.8.1.2.1** (Souhrada et al., 1966).

When the required assumptions are fulfilled, the static and dynamic tracer methods can be compared. The following applies for tracer experiments: (Souhrada et al., 1966)

- when the value of the backmixing coefficient (α) varies from stage to stage; for the static method, only the measurement of the end concentrations for two consecutive stages are required; while for the dynamic method, the concentrations for three consecutive stages have to be measured, as well as the derivative with time,
- for the static method at least one measurement inside the column must be made, whereas for the dynamic method, it is sufficient to measure the time dependence of the terminal concentration,
- dynamic method measurements can be influenced by the different behaviour of the column end sections,
- for the dynamic method, the hold-up in the column must be measured.

Souhrada et al., 1966 claim that the determination of backmixing coefficients by means of a tracer has several advantages over its determination from the concentrations of the transferred substance. However the authors do state that the assumption of perfect mixing in the stages must be met. Since it is difficult to determine to what degree the required assumption is fulfilled, it is advantageous to check the tracer test results using the results of direct determination from the concentration profiles of the transferred component.

Steady state values of the Backflow model parameters, which are required for the design of the plant, can provide sufficient information for simulation of the transient behaviour of a given process (Souhrada et al., 1970). Pollock and Johnson (1969) reviewed and compared the published work in the field of extraction dynamics. It was concluded that pulse testing and frequency response analysis are important tools for the determination of extraction dynamics, and that staged models as opposed differential contact models offer the most help for realistic control and simulation studies.

2.10 Measurement of Axial Mixing

Two methods can be used for the measurement of axial dispersion, and determination of the axial mixing parameters:

- by measuring the concentrations of a component which is soluble in only one of the phases (tracer injection methods),
- from direct measurement of concentration profiles of a transferring solute in a column.

The tracer experiments take two main forms according to whether steady state or dynamic tracer injection is employed (Souhrada, et al., 1966). The axial dispersion determined by using steady injection of a tracer near the phase outlet gives a measure of true backmixing but does not include the effect of residence time distribution caused by non-uniform forward flow. However the dynamic tracer injection method in which a pulse or step change is introduced near the phase inlet, gives a mean residence time distribution, and hence total axial dispersion (Kumar and Hartland, 1994). It is essential to ensure that the tracer does not pass into the other phase, and does not influence the hydrodynamic conditions and the structure of the dispersion (Souhrada et al., 1966).

The second method involving measurement of concentration profiles along the length of the column gives a measure of total axial mixing. The experimental results are normally interpreted by "force fitting" to the plug flow-backmix model and it is evident that the model is being used to describe all the factors affecting performance (Lo, et., al., 1983). However the experimental difficulty in carrying out the profile studies (the evaluation of parameters is generally laborious since a large number of samples have to be taken from each stage of the extractor), together with the insensitivity of the profiles to axial dispersion (Pratt and Baird, 1983) make it difficult to determine axial mixing data in this manner. Slavickova et al. (1978) developed an evaluation method which used only a limited number of concentration measurements.

Pratt and Baird (1983) state that it is acceptable to use data from tracer experiments unless there are known mass transfer induced hydrodynamic effects. In contrast, Slavickova et al., (1978) state that it is preferable to evaluate all parameters characterising longitudinal mixing from mass transfer experiments and not to use tracer experiments because of the uncertainty in the relevance of tracer methods.

CHAPTER 3. EXPERIMENTAL DESCRIPTION

3.1 Process Descriptions

3.1.1 Extraction Systems

Liquid-liquid extraction is frequently applied in the development of processes for speciality and fine chemicals. This is due in part to the fact that these materials may be non volatile or display heat sensitivity, which renders the application of distillation infeasible. In addition, it is sometimes required to separate components that have similar physical properties, and hence chemical properties must be used to affect the separation. The processes are developed for industrial purposes, and the focus of work is not extensive research, but an economical trade-off between developing a process that is sufficiently risk free and process development that is cost effective. The implication is that the experimental work has only a limited period during which time parameters can be varied, before fixed operating conditions are required, both for producing reproducible material for downstream processing and to test the robustness of the process, particularly in terms of recycles.

The procedure for developing a column extraction process typically involves four experimental phases:

- Labscale work to determine physical and chemical properties of the system (such as equilibrium data, solubility, settling and coalescing characteristics). This allows appropriate selection of the operating conditions of the system (such as choice of solvent, feed to solvent ratio, operating temperature, concentrations).
- Benchscale tests (using a 25 mm diameter column) to determine the feasibility of the process and to quantify the performance (such as approximate specific throughput, extraction efficiency) and operating conditions of the system (such as choice of continuous phase, operating temperature, feed to solvent ratio). This facilitates planning for the piloting phase and allows an initial estimation of the commercial mass balance, as well as the commercial column design and costing.
- Pilotscale tests (using a 50 or 75 mm diameter column) to generate scale up data (for design of the commercial column), to test the robustness of the system, to quantify the effect of recycle streams and produce representative material for downstream processing.

- Toll manufacture, whereby the entire process is operated continuously, in order to produce market samples and to demonstrate the stability of the process during extended operation.

It is important that the actual process feed and solvent are used for the test work because the process streams usually contain impurities. The presence of surfactants, even in trace amounts substantially reduces the mass transfer rate by reducing the mass-transfer coefficients (Godfrey and Slater, 1994).

Two processes were investigated, each involving liquid-liquid extraction as part of the downstream processing. The first entailed production of *para*-hydroxy benzaldehyde (*p*HB), an intermediate produced for the synthesis of various chemicals, such as anisaldehyde, a sunscreen additive. The extraction formed part of the purification process, whereby *meta*-cresol (*m*-cresol) was separated from the *p*HB. The second process entailed extraction of *tert*-butyl hydroquinone (TBHQ), an anti-oxidant that is added to edible oils.

Both processes were tested on a benchscale extraction column (25 mm diameter VPE column) and subsequently pilotscale extraction tests were performed (using a 50 mm diameter VPE column) to generate scale-up data for the commercial column design. All pilotscale extraction test work was conducted using representative material produced by upstream process operations.

3.1.2 Extraction of *m*-cresol

The process to produce *p*HB involves oxidation of a cresolic mixture of isomers *para* and *meta*-cresol. The *para*-cresol (*p*-cresol) is oxidised to form *p*HB, while the *meta*-cresol (*m*-cresol) remains unreacted. The post oxidation material consisting of *p*HB, residual unreacted *p*-cresol and significant quantities of *m*-cresol, is subjected to various downstream processes operations to isolate *p*HB as depicted in **Figure 3-1**. The *p*HB is then methylated and processed further to produce anisaldehyde. The *p*HB purification operations include partial acidification, filtration (to remove the oxidation catalyst and also resinous material produced during the reaction), distillation (to remove the solvent used in the oxidation), and solvent extraction (to separate the *m*-cresol from the *p*HB).

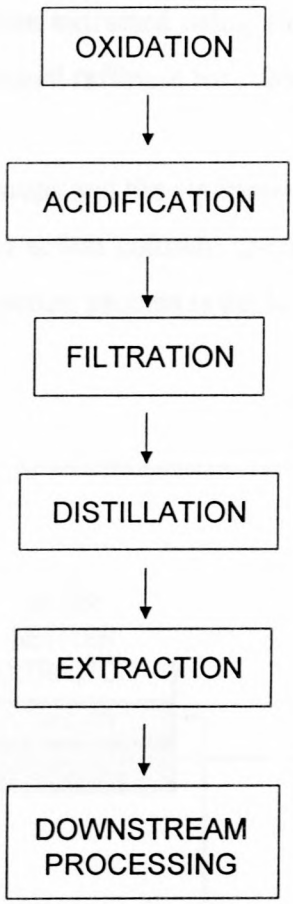

Figure 3-1: Purification of *p*HB

It was found that separation of *p*HB and *m*-cresol by employing distillation or simple solvent extraction was not feasible. However the *p*HB and cresols exhibit appreciable differences in their component strengths as acids (as evident by considering the respective de-protonation constants, *Ka*). Hence it was possible to effect the separation using dissociation extraction, whereby the difference in the *pKa* values of *p*HB and *m*-cresol (refer to **Table 3-1**) and the fact that the ionic forms of neither are soluble in the solvent, were exploited.

Table 3-1: *pKa* values at 50°C (Lide, 1992/1993)

	***m*-cresol**	***p*HB**
***pKa* at 50 °C**	9.83	7.72

The pH was adjusted to the required level by adding a stoichiometric deficiency of a mineral acid to the mixture, thereby allowing selective protonation of *m*-cresol and not *p*HB. The re-

protonated species of *m*-cresol was then extracted using an organic solvent, toluene, while the ionic form of *p*HB remained in the residual raffinate for subsequent processing.

The extraction was performed in two steps and the equipment configuration consisted of a single stage mixer-settler followed by an extraction column, specifically a Vibrating Plate Extraction (VPE) column. The layout of the extraction process is depicted in **Figure 3-2** below.

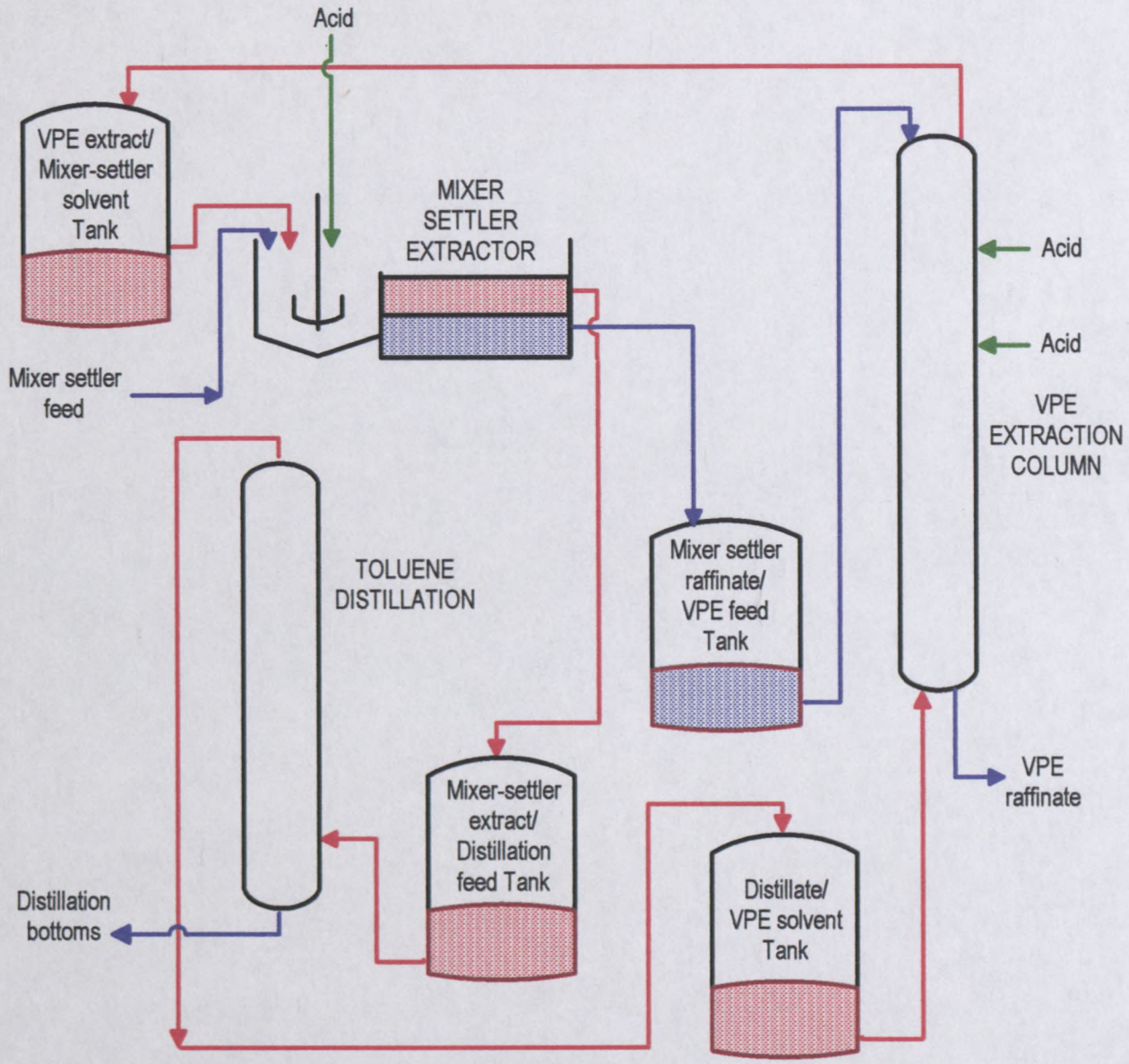

Figure 3-2: *m*-cresol extraction process

The first step entailed extraction of a major portion of the *m*-cresol in the mixer-settler. The feed pH was maintained at 9.8 by the addition of acid in the mixer. The raffinate from the mixer-settler was then extracted in the column in order to achieve the required level of *m*-cresol in the

final raffinate. Acid was added to the column at two points along the active section of the column and the raffinate maintained at a pH of 9. The extract from the mixer-settler was subjected to distillation to recover the toluene, for recycle and the *m*-cresol, for resale. The two extraction processes were further coupled by the fact that toluene recovered from the toluene distillation (containing very low levels of component *m*-cresol) was used as solvent for the column, while the toluene extract from the column was used as solvent for the mixer-settler. In this manner the solvent was enriched with *m*-cresol. The feed to solvent ratio was maintained at 5:1 (volume basis) and the temperature between 50°C to 60°C. Prior to each run, an acid titration was performed on the feed in order to ascertain the required acid flowrates.

All extraction test work was conducted using representative feed material produced by upstream process operations, a batch being typically 300ℓ in volume. In total, 16 pilot scale batches were performed, as detailed in **Table 3-2**.

Table 3-2: Column extraction tests performed

BATCH NUMBER		**SX - 1 to 6B**	**SX – 6C to 8**	**SX - 9 to 16**
Continuous phase		organic	aqueous	aqueous
Agitation intensity	**/min**	4.45 - 6.26	3.23 - 4.05	3.65
Feed flowrate	**ℓ/h**	36.2 - 67.3	35.9 - 55.1	54.2 - 56.6
Total specific throughput	**m^3/m^2h**	23.9 - 44.0	23.9 - 36.8	36.3 - 37.6
Feed to solvent volume ratio		3.2 - 5.6 : 1	4.8 - 6.5 : 1	4.8 - 5.1 : 1
Feed pH		9.09 - 10.16	9.04 - 9.66	9.76 - 10.04
Raffinate pH		8.86 - 11.04	8.81 - 9.35	8.82 - 9.29
Acid concentration	**%m/m**	29	29	50
Temperature	**°C**	50 – 60	50 - 60	50 - 60

For the first 8 batches, operating conditions were varied in order to ascertain the effect of various operating parameters on the extraction processes. For the subsequent 8 batches, the batches were operated at fairly constant operating conditions, to confirm the optimal process. Initially for the first 6 batches, the organic phase was selected as the continuous phase, however during extended operation of the column it was observed that this scenario was not stable due to coating of the Teflon plates and subsequent wetting of the plates by the dispersed aqueous phase. For subsequent tests the column was operated with aqueous phase continuous and stainless steel

plates, and this configuration proved stable. For the last 9 batches, the acid concentration was increased from 29 to 50 %m/m. This was implemented to ensure that the VPE used the same acid concentration as the mixer-settler, thus simplifying the acid dilution operation.

3.1.3 Extraction of TBHQ

An existing commercial process produces *tert*-butyl hydroquinone, an antioxidant that is added to edible oils. An investigation was conducted to recover TBHQ from an aqueous purge stream, and it was found that this was possible using liquid-liquid extraction. A Vibrating Plate Extraction column was used to reduce the concentration from approximately 0.5 %m/m in the feed to less than 100 ppm in the raffinate. This ensured that the valuable component could be recovered and recycled back to the process, as depicted in **Figure 3-3**.

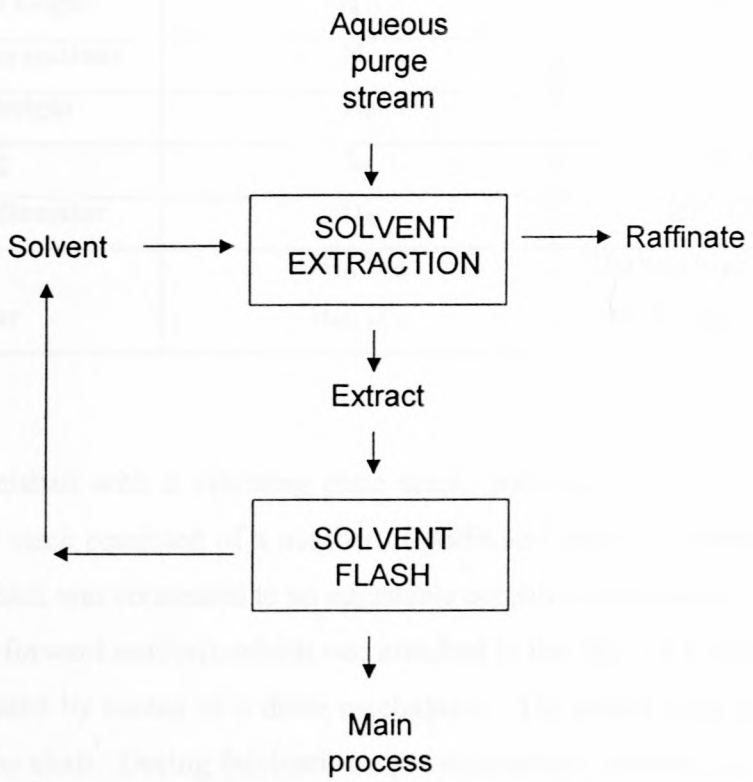

Figure 3-3: Extraction of TBHQ

Initially the process was operated at ambient temperature, however it was found that a temperature of 60°C was preferential for column hydrodynamics. A feed to solvent ratio of 2:1 (volume basis) was used. The extract was collected and a major portion of the solvent recovered

by flashing. The concentrated extract was recycled to the main process operation, while the recovered solvent was recycled to the extraction process.

3.2 Experimental Set-up

The VPE used to perform the pilot scale column extractions was 50 mm in diameter and consisted of a number of glass sections joined by stainless steel flanges. The column is depicted in **Figure 3-4**, while the dimensions of the unit are summarised in **Table 3-3**.

Table 3-3: Dimensions of pilot scale VPE

Dimension	Symbol	Size
Total Height	$H_T = H_{A1} \times N_A + H_{S1} + H_{S2}$	6,390mm
Glass section height	H_{A1}	595mm
Number glass sections	N_A	10
Active zone height	H_P	5,950mm
Plate spacing	S_P	110 mm
Active zone diameter	D_A	ID= 47.9mm
Top settler **Bottom settler**	H_{S2}, D_{S2} H_{S1}, D_{S1}	200 mm high, 120 mm ID 220 mm high, 126 mm ID

The VPE was furnished with a vibrating plate stack, positioned in the active section of the column. The plate stack consisted of a number of perforated plates mounted on a central shaft, the upper end of which was connected to an adjustable eccentric contrivance (for changing rotary into backward-and-forward motion), which was attached to the shaft of a drive motor. The plate stack was reciprocated by means of a drive mechanism. The plates were spaced either 100 or 110 mm apart on the shaft. During fabrication a pre-determined number of holes were drilled in each plate to enable both the continuous and dispersed phases to pass through the column. Two types of plate were available for the column, Teflon or stainless steel. A typical VPE column plate is depicted in **Figure 3-5**, and plate characteristics are summarised in **Table 3-4**.

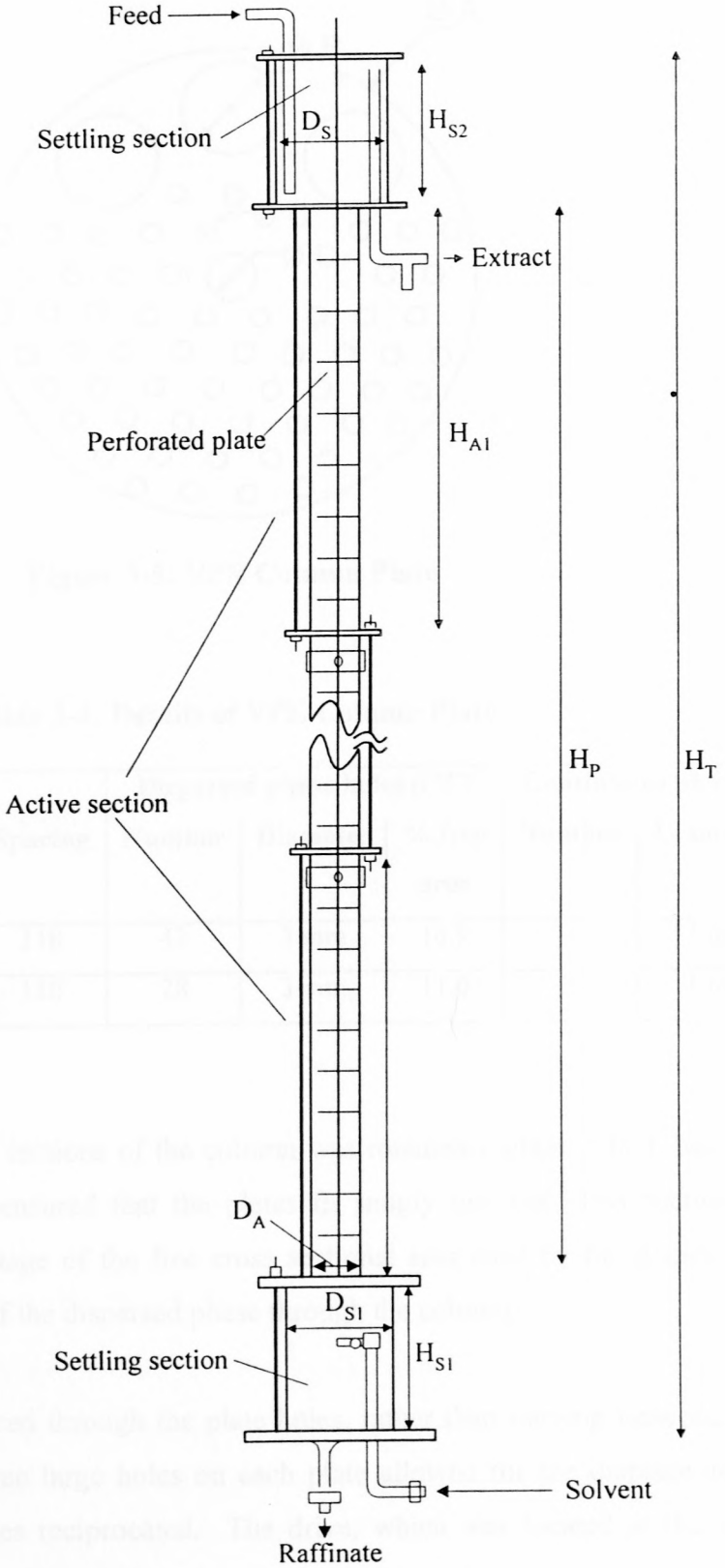

Figure 3-4: Pilot scale VPE

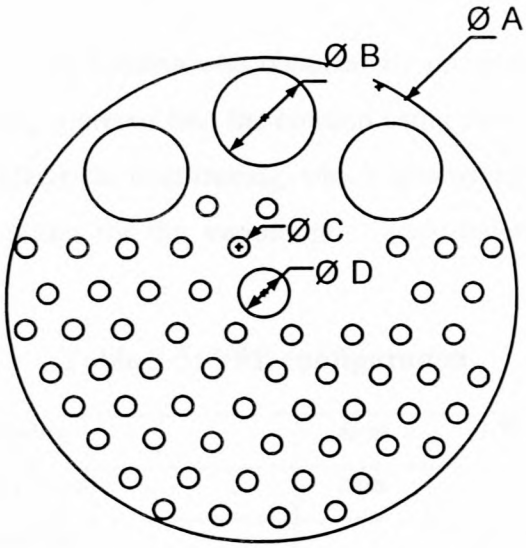

Figure 3-5: VPE Column Plate

Table 3-4: Details of VPE Column Plate

Set #	Plates			Dispersed phase holes (∅C)			Continuous phase holes (∅B)		
	Material	Number	Spacing	Number	Diameter	% free area	Number	Diameter	% free area
1	Stainless steel	54	110	43	3 mm	16.9	3	11 mm	15.8
2	Stainless steel	54	110	28	3 mm	11.0	3	11 mm	15.8

The glass used for the active sections of the column was rotametric glass, which had very low dimensional tolerances, and ensured that the plates fit snugly into the glass sections. This, together with the low percentage of the free cross sectional area used by the dispersed phase, resulted in a pumping effect of the dispersed phase through the column.

The dispersed phase was forced through the plate holes, rather than moving between the glass wall and the plates. The three large holes on each plate allowed for the displacement of the continuous phase as the plates reciprocated. The drive, which was located at the top of the column allowed for reciprocation of the plate stack, and was controlled using a frequency controller. Both the amplitude of reciprocation and the speed of reciprocation could be varied. The reciprocating speed was set such that on visual inspection, the average diameter of the dispersed phase in the vicinity of the reciprocating plates was 1 mm or less.

The operating temperature in the column was obtained by preheating the feed and solvent *via* heat exchangers, prior to being metered into the column using pumps. The column temperature was maintained by flexible electrical heat tracing, which was wrapped around the outside of the column. The VPE configuration for the various pilot scale batches is summarised below in **Table 3-5**.

Table 3-5: VPE configuration

Plate spacing	**mm**	100 - 110
Plate amplitude	**mm**	2 – 3
Plate material		Stainless steel
Continuous phase		Aqueous
Height of active length	**m**	5.95
Acid addition point position		
Acid 1	**m**	0.60
Acid 2	**m**	1.79
Sampler position[10]		
Flange a	**m**	0.595
Flange b	**m**	1.19
Flange c	**m**	1.79
Flange d	**m**	2.38
Flange e	**m**	2.975
Flange f	**m**	3.57
Flange g	**m**	4.165
Flange h	**m**	4.76
Flange i	**m**	5.355

Two stainless steel tanks were used to hold the feed and solvent. The feed tank, with a capacity of 1500ℓ, was insulated. The tank was equipped with a circulation pump to enable homogenisation of the feed and the circulation line was equipped with a steam heat exchanger, which was used to heat the feed to the desired temperature. The solvent tank, with a capacity of 200ℓ, was a closed vessel (with only a feed port and a vent port), to reduce exposure to solvent

[10] Distance from bottom of top setter, for extraction of *m*-cresol

fumes. The solvent tank was connected using Teflon (pfa) tubing to a pump and the solvent passed through a shell and tube heat exchanger (heated by hot water) prior to being fed to the bottom of the column. The solvent was heated online to minimise solvent fumes in the tank, and because it was preferential to pump cold solvent to ensure accurate pump rates. The heat exchanger was placed as close to the column as possible to minimise heat losses.

The extraction operations required pumps for the feed, solvent, acid and raffinate. The classification of the pilot plant meant that the pumps had to be explosion proof, and extraction operations require accurate and non-pulsating flow. The most suitable pumps to fulfil these criteria were Watson-Marlow peristaltic pumps. Each pump was equipped with an inverter and control box used to adjust the flowrates. Typically, prior to a run, the pumps were calibrated with water and the calibration curves generated were used to estimate pump settings during a run. Since accurate addition rates were essential for the extraction operations, each tank was fitted with a glass calibration vessel, which could be used to facilitate online pump calibration during operation.

3.3 Experimental Procedure

3.3.1 Equilibrium Determination

The first requirement for evaluating the performance or design of an extractor is reliable equilibrium data, which can be obtained by performing "shake tests", using a separating flask.

Measured quantities of feed and solvent (at a specific mass ratio) were poured into a flask and placed in a water bath to reach the required operating temperature. Once at temperature, the liquids were shaken to facilitate extraction of the solute into the solvent. For the *m*-cresol extractions, the pH of the aqueous phase was then measured and acid added to adjust the pH to a chosen level. The flask was then re-shaken and then left to settle in the water bath for at least ten minutes, during which time the phases separated. The pH of the raffinate was measured and if the pH was at the chosen level, the phases were separated and samples of the raffinate and extract were taken. If the pH of the aqueous phase was not correct, then the pH was again adjusted using acid, mixed and allowed to settle. This procedure was repeated until the correct pH was attained. After settling, the phases were separated, and samples of raffinate and extract

taken for analysis. The raffinate was returned to the flask and re-extracted with fresh solvent. This process was repeated a number of times, each time generating a point on the equilibrium curve.

3.3.2 *m*-cresol Extraction Feed Acid Titrations

Acid titrations were performed in order to determine the acid requirements for adjusting the pH of the feed to a predetermined level. The feed sample was pre-heated to the required temperature in a water bath and agitated using a stirrer bar. A sulphuric acid solution was added incrementally (0.1 mℓ to 0.5 mℓ) using a burette, to a known mass of feed, and the pH and temperature recorded after each incremental addition. Time was allowed between additions for the sample to equilibrate. In order to produce a satisfactory titration curve, each sample was acidified until an end pH of 7 was achieved. The incremental volume of acid added to reach the respective pH was normalised using the known sample mass. This allowed quantification of the amount of acid required for the continuous equipment to achieve a particular pH. Since the pH increased as the *m*-cresol was extracted into the solvent, it was found that acid titrations performed with toluene present in the feed sample gave a more accurate estimate of the amount of acid required, than those without toluene.

3.3.3 Typical VPE Column Extraction Operation

The feed material was loaded into the feed tank and then circulated through a steam heat exchanger to ensure that it was heated to the required process temperature. Fresh solvent was pumped into the solvent tank. Raffinate and extract drums were positioned next to the column, and the respective lines positioned in the drums. The column drive was switched on and the plate stack closely inspected to ensure that the plates were moving smoothly. The drive was set at the required agitation speed using the frequency controller (the required amplitude was set prior to commencing operation of the plate stack). The column heat tracing was switched on, and the set point temperatures adjusted to the required level to maintain the required temperature in the VPE column. The column was then filled with the continuous phase. It was essential that the drive was switched on to ensure that the plates were wetted by the continuous phase, and that any air bubbles were dislodged. Once the column was full, a pump was used to pump dispersed

phase into the column, until an interface was established. At this point the continuous phase pump was restarted. The feed and solvent were then pumped at the prescribed rates - at the chosen feed to solvent ratio.

For the *m*-cresol extraction, acid was pumped into the column at a rate calculated from the acid titration. 70% of the acid was added at the top addition point and 30% at the second addition point (the most acid being added at the position in the column of highest *m*-cresol concentration). Samples of raffinate were taken to monitor pH over time, and the raffinate pH was maintained at 9.0, by adjusting the total acid flowrate. The flowrate of feed, solvent and acid (for *m*-cresol extraction) was monitored online by performing volumetric calibrations. The position of the interface was manually controlled by altering the raffinate pump flowrate. A minimum of three to four mean residence times were allowed for the column to reach steady state, as recommended in the literature (Lo, et., al., 1983). Samples of the feed, solvent, raffinate and extract (and in some cases flange samples of the aqueous and organic phases) were then taken. The temperature throughout the length of the column was continuously monitored and recorded during the run. The operating time of the column was determined by the amount of available feed and was typically between 6 to 8 hours. Once the feed was finished, the column was drained and washed.

3.3.4 Unsteady State Column Measurements

After performing a laboratory investigation, it was found that the aqueous TBHQ extraction feed was conductive, and that conductivity could be used a means of measuring the dilution of the feed with water. This facilitated use of the feed as a type of "tracer" to determine and quantify the dynamic behaviour of the column. The column was operated in a manner similar to that described above, excepting that the column was initially filled with water, and then water and solvent were pumped into the column (as opposed to feed). Once the regime in the column had been established, the water feed was replaced by genuine feed. Samples of the raffinate were taken over time and the conductivity was measured. The relationship between conductivity and concentration was determined by measuring the conductivity of known concentrations of feed and generating a calibration curve. Since the feed displayed a significantly higher conductivity than water its was possible to measure the residence time distribution in the column (and hence determine the extent of axial mixing), using the raffinate conductivity measurements recorded over time.

CHAPTER 4. RESULTS AND DISCUSSIONS

4.1 Setting Up the Models

4.1.1 Steady State Model – *m*-cresol Extraction

A steady state Backflow model (as derived in **Section 2.7.5.1**) was used to predict the behaviour of the *m*-cresol extraction process. The model was set up in an excel spreadsheet. The results were then interpreted by "force fitting" the model to the experimentally determined concentration profiles (measured by taking steady state samples at the flanges of the column), using the solver function.[11] This allowed determination of the coefficients of backmixing and the overall mass transfer coefficient.

The characteristics of the process, which needed to be taken into account by the model, included:

- only the protonated species of *m*-cresol was extracted by the solvent, while the ionic species remained in the raffinate.
- acid was added at two points along the length of the column, resulting in re-protonation of *m*-cresol,
- the equilibrium relationship was non-linear,

In order to account for the fact that only the protonated species was extracted, the model could be structured by one of two approaches:

- either the model took into account the pH profile through the length of the column, thereby allowing calculation of the protonated *m*-cresol species,
- or, the addition of acid could be considered as addition of protonated *m*-cresol to the column.

The experimental concentration profile of protonated *m*-cresol (which the models would attempt to fit) was calculated using the pH profile and the analytically determined concentrations of total cresol. Since a small error in a pH reading could significantly influence the protonated species calculation (as is evident in **Figure 4-1** below) both methods were subject to direct error *via* the experimental concentration profiles. The first method was also prone to an indirect error from

[11] Appendix F.1

inaccurate pH readings, and consequently the decision was taken to use the second method for the *m*-cresol extraction.

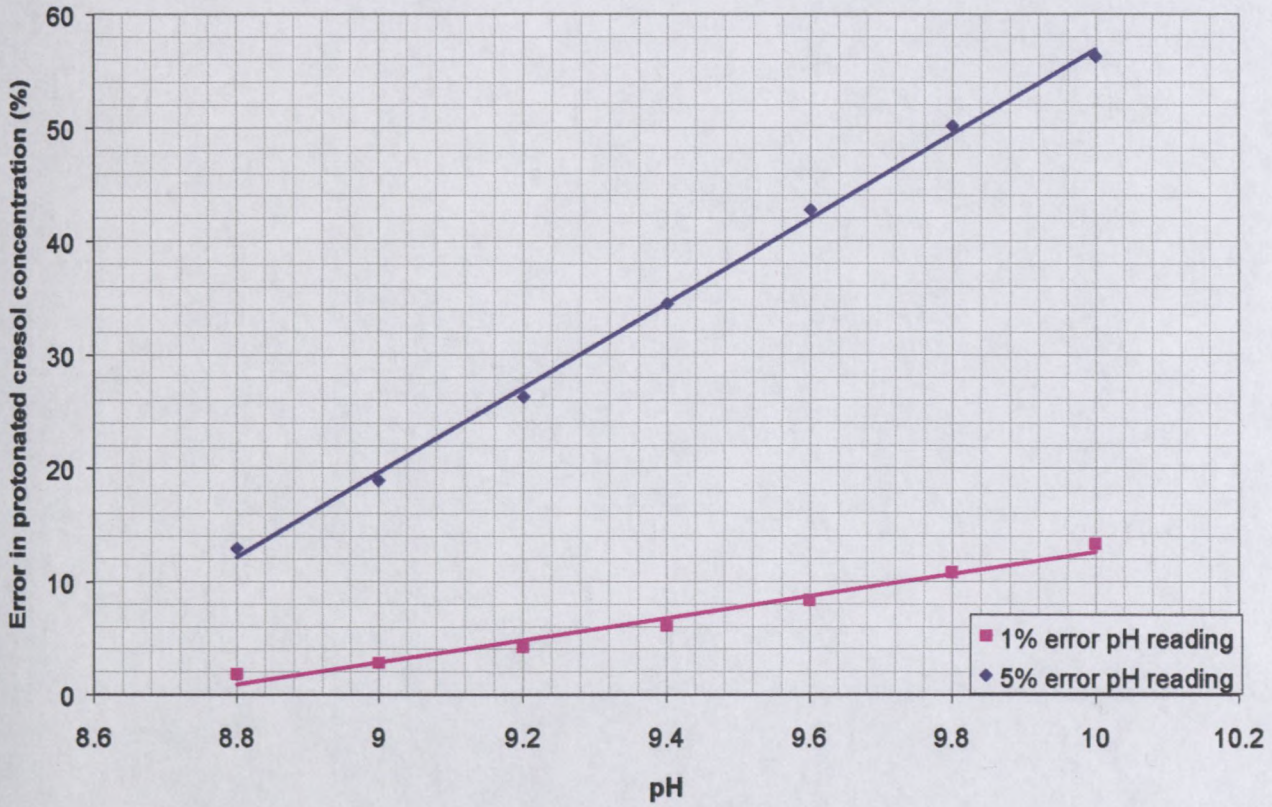

Figure 4-1: Effect of pH reading error on the calculated concentration of protonated *m*-cresol

The second method allowed a more simplified approach to this rather complex process. Some acid was consumed by organic impurities in the system, it was necessary to make an estimation as to the proportion of the added acid that was used to re-protonate the *m*-cresol. An estimation of this was made by considering the ratio of the moles of *m*-cresol re-protonated to the moles of acid (protons) added, as depicted in **Figure 4-2**. The assumption was made that all the de-protonated *m*-cresol available in the feed became re-protonated (i.e. either it was extracted or remained in the re-protonated form in the raffinate).

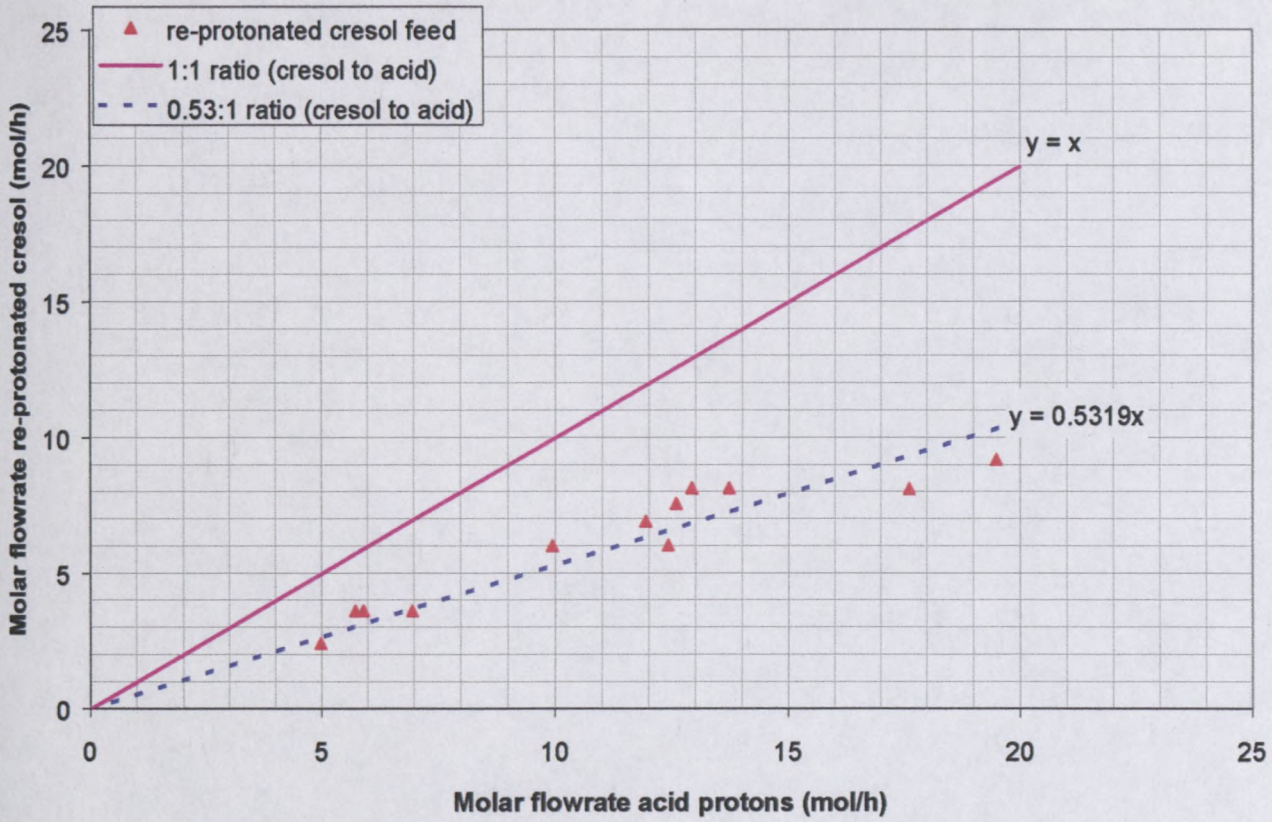

Figure 4-2: Molar ratios of acid added to *m*-cresol in the feed

It is evident that approximately 53% of the acid protons were used to re-protonate the de-protonated *m*-cresol species in the feed. The remaining acid was consumed by organic impurities.

By using this simplified scenario, the model was concerned only with the protonated species of *m*-cresol (since only the protonated form was extracted). The specific form of the Backflow model used was the Mass Transfer Coefficient model, where both forward and backmixing were taken into account. The backmixing coefficients of the continuous and dispersed phases were assumed constant through the length of the column. This assumption was adopted since it substantially simplified the mathematical description of the process. An attempt was made to extend the model, by allowing non-constant backmixing ratios along the column length, however the excel solver function was unable to manage the large number of variables (217 variables as opposed to 111 in the simplified case).

Experimental concentration profiles of *m*-cresol in both the dispersed and continuous phases were measured. Using the theory described above and the sample pH measurements, it was possible to convert the aqueous phase concentrations to protonated *m*-cresol values.

Two mass balances were calculated for each stage:

- the mass balance between the aqueous raffinate and organic extract phases (**Equation 4-1**),
- the mass balance between the aqueous raffinate phase and the mass transfer kinetics of the system (**Equation 4-2**),

The respective equations are shown below, with reference to **Figure 2.21** in **Section 2.7.5.1**. For both mass balances, modifications were made for the end sections.

$$F_x\left[(1+\alpha_x)c_{x,n-1}-(1+2\alpha_x)c_{x,n}+\alpha_x c_{x,n+1}\right]=F_y\left[\alpha_y c_{y,n-1}-(1+2\alpha_y)c_{y,n}+(1+\alpha_y)c_{y,n+1}\right] \quad \textbf{(4-1)}$$

$$(1+\alpha_x)c_{x,n-1}-(1+2\alpha_x)c_{x,n}+\alpha_x c_{x,n+1}=\frac{k_{ox}ash_c}{F_x}\left(c_{x,n}-c^*_{x,n}\right) \quad \textbf{(4-2)}$$

where:

a : superficial area of contact of the phases (/m),

c_j : concentration in phase j (kg/m^3),

F_j : volumetric flowrate of jth phase (m^3/s),

h_c : height of compartment (m),

k_{ox} : overall mass transfer coefficient based on X phase (m/s),

N : total number of actual stages required,

X : dimensionless concentration of X phase,

Y : dimensionless concentration of Y phase,

α_j : backmixing ratio for jth phase, that is, ratio of backflow to F_j

The excel solver function was used to minimise the sum of three errors:

- error 1 was equivalent to the squared difference between the two balances (**Equation 4-1** and **4-2**),
- error 2 was equivalent to the difference between the experimentally determined aqueous phase concentration profiles and those predicted by the model,

- error 3 was equivalent to the difference between the experimentally determined organic phase concentration profiles and those predicted by the model.

These three errors were added together and the resultant error minimised by adjusting and solving for the following variable parameters:

- overall mass transfer coefficient (k_{ox}),
- backmixing ratio of continuous phase (α_x),
- backmixing ratio of dispersed phase (α_y),
- 54 aqueous phase concentrations (one exiting each stage),
- 54 organic phase concentrations (one exiting each stage).

The data inputted into the spreadsheet included:

- feed and solvent total and solute-free mass rates,
- acid mass rates and concentrations at both acid addition points (the water in the acid solution becomes incorporated in the feed flowrate),
- the equivalent mass rate of *m*-cresol added at the acid addition points (calculated using the molar flowrate of protons and the molar ratio of acid protons to de-protonated *m*-cresol in the feed),
- *m*-cresol concentrations in feed, solvent, extract, raffinate and flange samples,
- partition coefficient at each stage (the y value in equilibrium with the calculated x at each stage is calculated using the equilibrium relationship determined from shake tests; the partition coefficient at each stage is calculated by dividing the equilibrium y concentration by the x concentration),
- column diameter and plate spacing.

Various constraints of the system included (as part of the solver function):

- concentration of extract and raffinate at each stage must be greater than or equal to 0,
- backmixing ratio of continuous and dispersed phase must be greater than or equal to 0,
- overall mass transfer coefficient k_{ox} must be greater than 0.

The following assumptions were made for the model:

- only protonated *m*-cresol was extracted into the organic solvent (negligible *p*HB was extracted), thus the feed solute-free mass rate could be calculated by considering only the extracted *m*-cresol,
- protonated *m*-cresol was "added" at the acid addition points, by using the ratio of de-protonated *m*-cresol in feed to acid (assuming all de-protonated *m*-cresol in the feed was re-protonated i.e. de-protonated species in the raffinate was negligible),
- a stage was considered to be in the middle of two plates, the concentrations being X_k and Y_{k+1} between the k^{th} and $k + 1^{st}$ plates. i.e. perfectly mixed stages.

The following were selected within the Excel solver function options:

- the ***Tangent*** approach was selected to obtain initial estimates of the basic variables in each one-dimensional search, whereby a linear extrapolation from a tangent vector is used (the other option is ***Quadratic*** whereby quadratic extrapolation is used, which can improve the results on highly non-linear problems).
- the ***Forward*** option was selected which *s*pecifies the differencing used to estimate partial derivatives of the objective and constraint functions; this option should be used for most problems, in which the constraint values change relatively slowly (the other option is ***Central*** which is used for problems in which the constraints change rapidly, especially near the limits; although this option requires more calculations, it might help when Solver returns a message that it could not improve the solution)
- a ***quasi-Newton method*** was selected to specify the algorithm used at each iteration to determine the direction to search; this method typically requires more memory but fewer iterations (the other option is the ***Conjugate*** method, which requires less memory than the Newton method but typically needs more iterations to reach a particular level of accuracy; this option is typically used when the problem is large and memory usage is a concern, or when stepping through iterations reveals slow progress)

Microsoft Excel Solver uses the Generalized Reduced Gradient non-linear optimisation code. Linear and integer problems use the simplex method with bounds on the variables, and the branch-and-bound method.

4.1.2 Unsteady State Model – TBHQ Extraction

Backmixing can be measured directly using a tracer. Typically the tracer is added near the outlet of the carrier phase and the concentration of tracer is measured above the point of addition (since this gives a measure of true backmixing). The actual method employed for TBHQ extraction yielded a residence time distribution profile (by observing the change in concentration in the raffinate), which was an indirect means of quantifying the backmixing in the column. In an extreme scenario, complete backmixing would result in a single stage, and the concentration profile would appear as a single, constant step change.

An unsteady state Backflow model (as derived and discussed in **Section 2.8.1.1**) was used to predict the behaviour of the TBHQ extraction process. The column was fitted with 54 plates, each of which was considered as a single stage, and consequently 54 ordinary differential equations (ODE's) needed to be solved stagewise. A fourth order Runge Kutta procedure was written using Visual Basic,[12] and was used in Excel together with a spreadsheet for inputting data.[13]

The characteristics of the extraction process include the following:

- non linear equilibrium relationship,
- the column extraction initially operated in the absence of mass transfer, and then as the water feed was replaced by real feed, mass transfer between the phases commenced.

It was assumed that the backmixing coefficient of the continuous phase was constant through the length of the column, since this substantially simplified the mathematical description of the process (however the excel spreadsheet was set-up in such a manner that the backmixing ratio could be altered for each individual stage). Typically the backmixing coefficient of the dispersed phase in the VPE is low, and as such it was assumed to be negligible and set to 0. The spreadsheet also allowed for the hold-up value at each stage to be entered individually.

---

[12] Appendix G.2

[13] Appendix G.1

Steady state operation was established in the column with a water-solvent system, by ensuring that three column volumes had been replaced. The water flowrate was then replaced by feed, which displayed a significantly higher conductivity than water. By measuring the conductivity of the raffinate and using the conductivity calibration curves previously generated, it was possible to determine profiles of the concentration of feed in the raffinate over time. The results were then interpreted by "force fitting" the model to the concentration profiles, thereby allowing determination of the backmixing coefficient. The method employed was similar to that employed by Karr et al., (1987), however in this case the equipment set-up was such that it was not possible to measure the conductivity at other positions along the length of the column. This would have required the positioning of conductivity probes in the column, since the time required to take samples at the flanges would be too long, as compared to the rate of change of the concentration profile in the column.

The data inputted into the spreadsheet included:

- total operating time and time increments,
- flowrates of feed and solvent,
- the respective volume of each stage (including the top and bottom settlers),
- the respective hold-up in each stage,
- the respective initial concentration in each stage,
- the feed concentration,
- the respective backflow ratio of the continuous phase in each stage (the dispersed phase backflow ratio was assumed to be negligible and set to 0).

By adjusting the continuous phase backflow ratio until the model fits the experimental data, it is thereby possible to determine the value of the continuous phase backflow ratios for each stage.

4.2 Results and Discussions

4.2.1 *m*-cresol Extraction

4.2.1.1. Acid Titrations

Acid titrations were performed on each batch of feed, and examples of some of the titration curves are plotted in **Figure 4-3**. 50 %m/m sulphuric acid was used for the titrations. The batches show reasonably consistent titration curves, with feed pH values ranging from 9.8 to

10.1. It appears that the titration curves shifted slightly to the right with each successive batch, which could be attributed to recycle implemented in the overall process, which would have resulted in the build-up of impurities in the system.

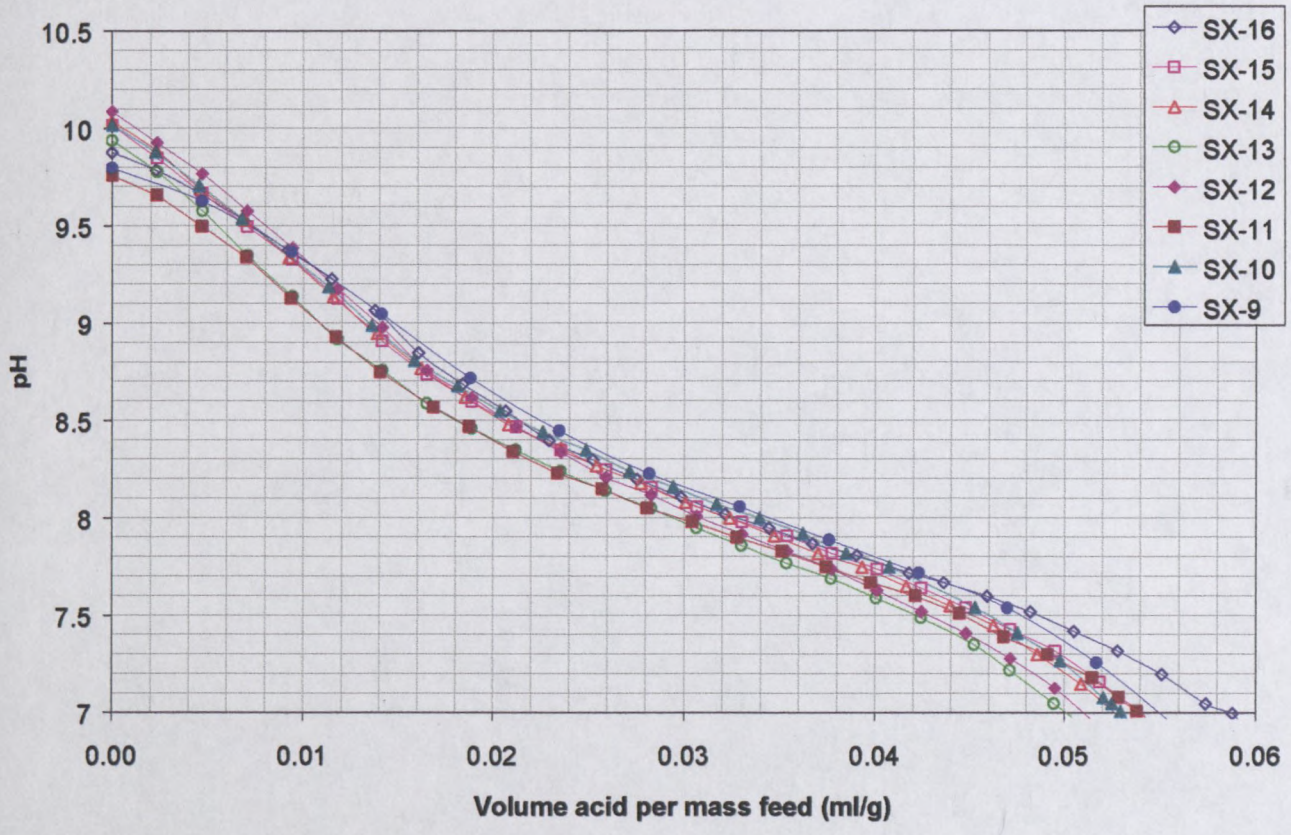

Figure 4-3 : Acid titration curves for batches SX-9 to SX-16

4.2.1.2. Equilibrium Data

The results of the shake tests performed to determine equilibrium data are depicted in **Figure 4-4**. The pH represented the pH of the aqueous phase in the shake flask after reaching equilibrium (i.e. the raffinate pH).

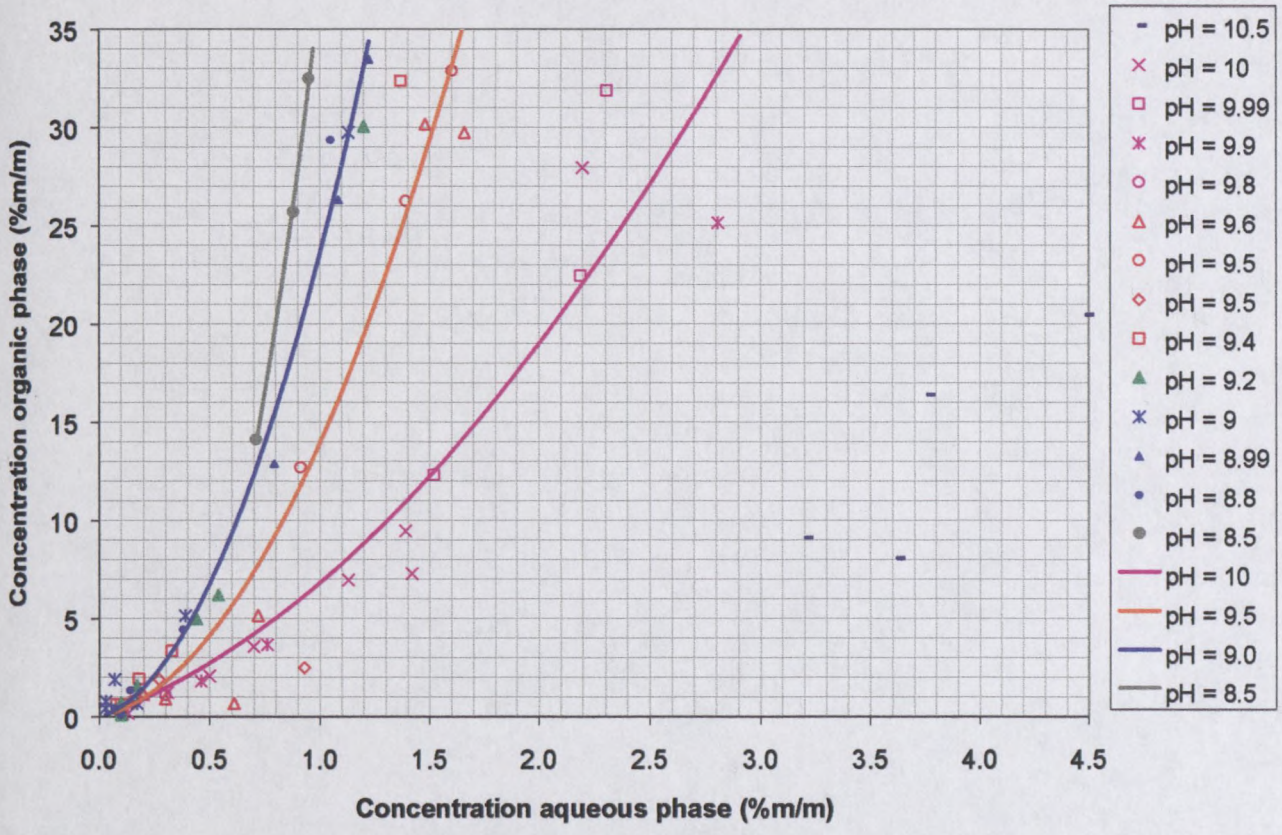

Figure 4-4: *m*-cresol analytical results equilibrium data

Since only the protonated species is extracted into the organic solvent, the overall partition coefficient of *m*-cresol (ionic and protonated) is dependent on pH (which is a measure of the relative amounts of protonated and de-protonated species). Each trend line in **Figure 4-4** represents a different pH. Using the total concentration of *m*-cresol (that has been determined analytically), and the measured pH, the concentration of de-protonated species in the aqueous phase was calculated by application of **Equation 2-7**. Hence the concentration of the protonated species in the aqueous phase was determined. The equilibrium data of the protonated species is depicted below in **Figure 4-5**.

Analytical control chart mean for **Figure 4-4** and **Figure 4-5** for total cresol is 6.64 (±0.34) at the 99.7 % confidence level.

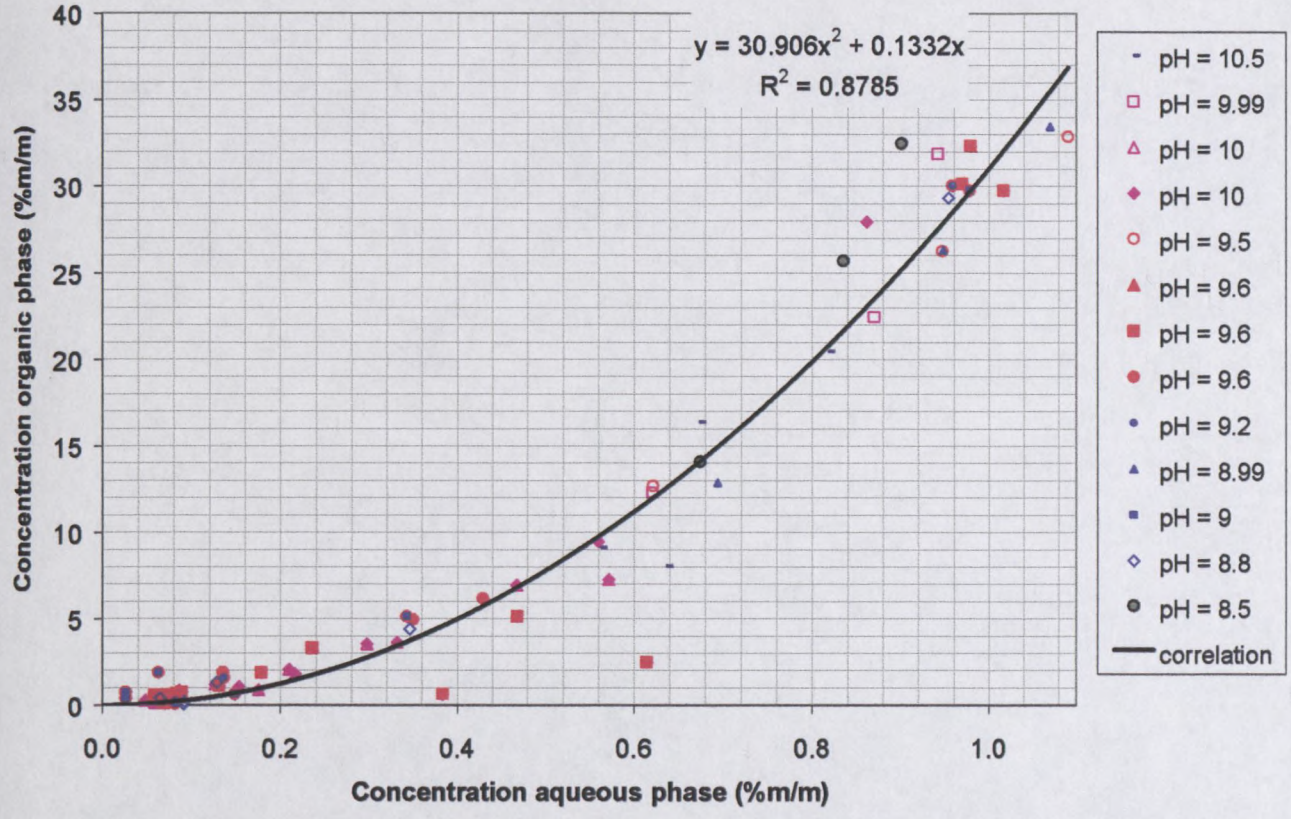

Figure 4-5: Protonated *m*-cresol equilibrium data

It is evident in **Figure 4-5** that the partition coefficient of protonated *m*-cresol is independent of pH. However the partition coefficient is not constant, but dependent on the concentration of protonated species in the organic phase. It is likely that this is the result of the association of simple molecules into complex molecules in the organic phase, as discussed previously.

Equation 2-5 was fitted to the data. The partition coefficient of the protonated species of *m*-cresol (excluding the dimer form) was calculated as 0.1332, while the equilibrium constant for association of *m*-cresol as a dimer form (k_{ass}) was determined to be 1,742.

It should be borne in mind that for the analysis done on the equilibrium data samples the two isomers of cresol (*meta* and *para*-cresol) were not distinguished, and that the *pKa* of only *m*-cresol was used. Consequently this result is the average of three different equilibrium constants for the dimerisation reactions (*m*-cresol – *m*-cresol, *p*-cresol – *p*-cresol, and *m*-cresol – *p*-cresol interactions)

4.2.1.3. Column Results and Concentration Profiles

The mixer-settler was used to reduce the concentration of *m*-cresol from 8.5 %m/m in the feed to less than 3 %m/m in the raffinate. The column reduced the concentration of *m*-cresol to less than 0.2 %m/m in the raffinate. It was preferable to minimise the concentration of *p*HB in the extract since this represented a loss of *p*HB to the overall process. The losses of *p*HB over the extraction process were less than 2% (0.4 %m/m concentration in the extract), which was acceptable for the process. The extract generated by the extraction column contained approximately 15 %m/m of *m*-cresol.

The average hold-up of the dispersed phase in the column for respective runs was measured and the results are given in **Table 4-1**.

Table 4-1: Hold-up measurements for various batches

Batch reference	**SX-15**	**SX-14**	**SX-13**	**SX-12**	**SX-11**	**SX-10A**	**SX-9C**	**SX-7**
Average hold-up (%)	6.6	6.6	8.4	8.5	9.7	5.8	6.4	8.14

The acid was added to the VPE at two positions - two thirds of the total acid required was added after 600 mm of active height and the remaining third, 1,790 mm from the top of the VPE. The acid addition was arranged in such a manner as to account for the decreasing concentration of *m*-cresol in the aqueous phase. In the VPE, the concentration of *m*-cresol was 0 %m/m in the solvent and 15 %m/m in the extract, while the pH of the feed and the raffinate were approximately 10 and 9 respectively. The lower pH (9) was required for sufficient removal of *m*-cresol from the raffinate, however it resulted in some extraction of *p*HB. Any *p*HB that was extracted in the region below the acid addition points (where the pH was low) was back extracted in the region above the first acid addition point, where the pH was high. This is evident in **Figure 4-6**, where the concentration of *p*HB in the extract is plotted versus column active height.

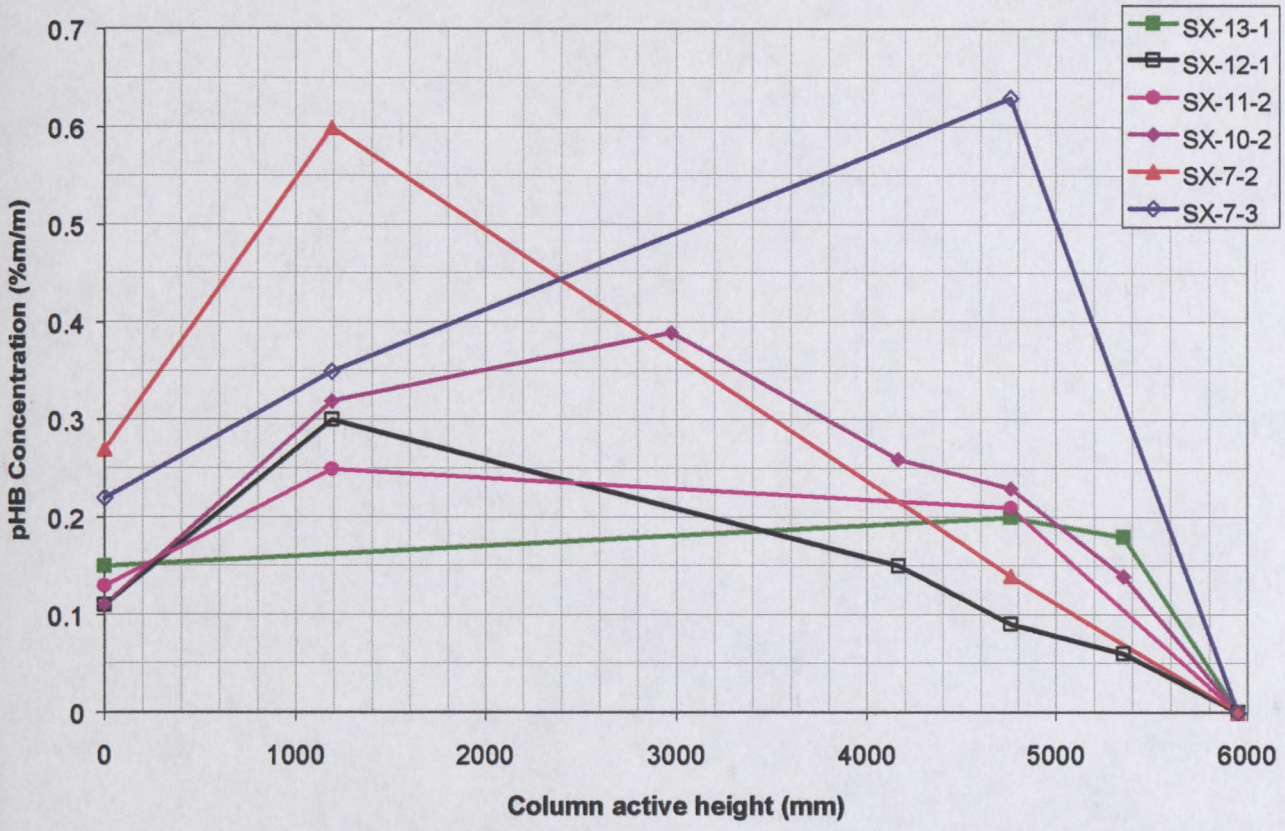

Figure 4-6: Concentration of *p*HB in the extract (for various tests) *versus* column active height.

The effect of temperature variations through the length of column was not accounted for. Since the re-protonation of the *m*-cresol is an exothermic reaction, it is likely that the temperature increased locally at the acid addition points, and combined with heat losses from the column, temperature gradients could have existed in the column. This would result in unstable density gradients and a potential increase in axial mixing. A typical temperature profile in the column, during a run is depicted in **Figure 4-7** below.

For the tests conducted, samples of the aqueous phase were taken along the length of the VPE, to allow measurement of pH (as shown in **Figure 4-8**) and determination of the concentrations of *m*-cresol. As previously mentioned, the acid was added at positions 600 mm and 1,790 mm from the top of the VPE respectively.

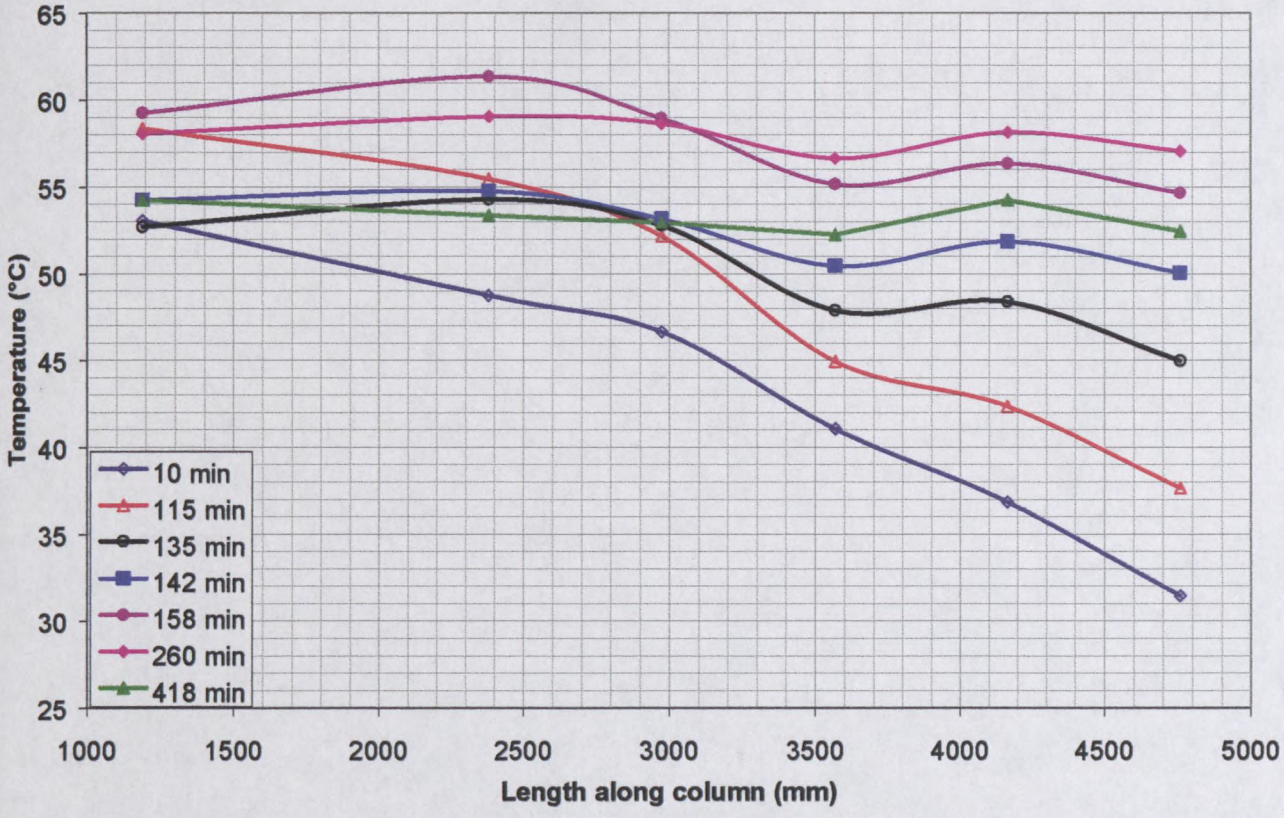

Figure 4-7: Typical temperature profile in the column

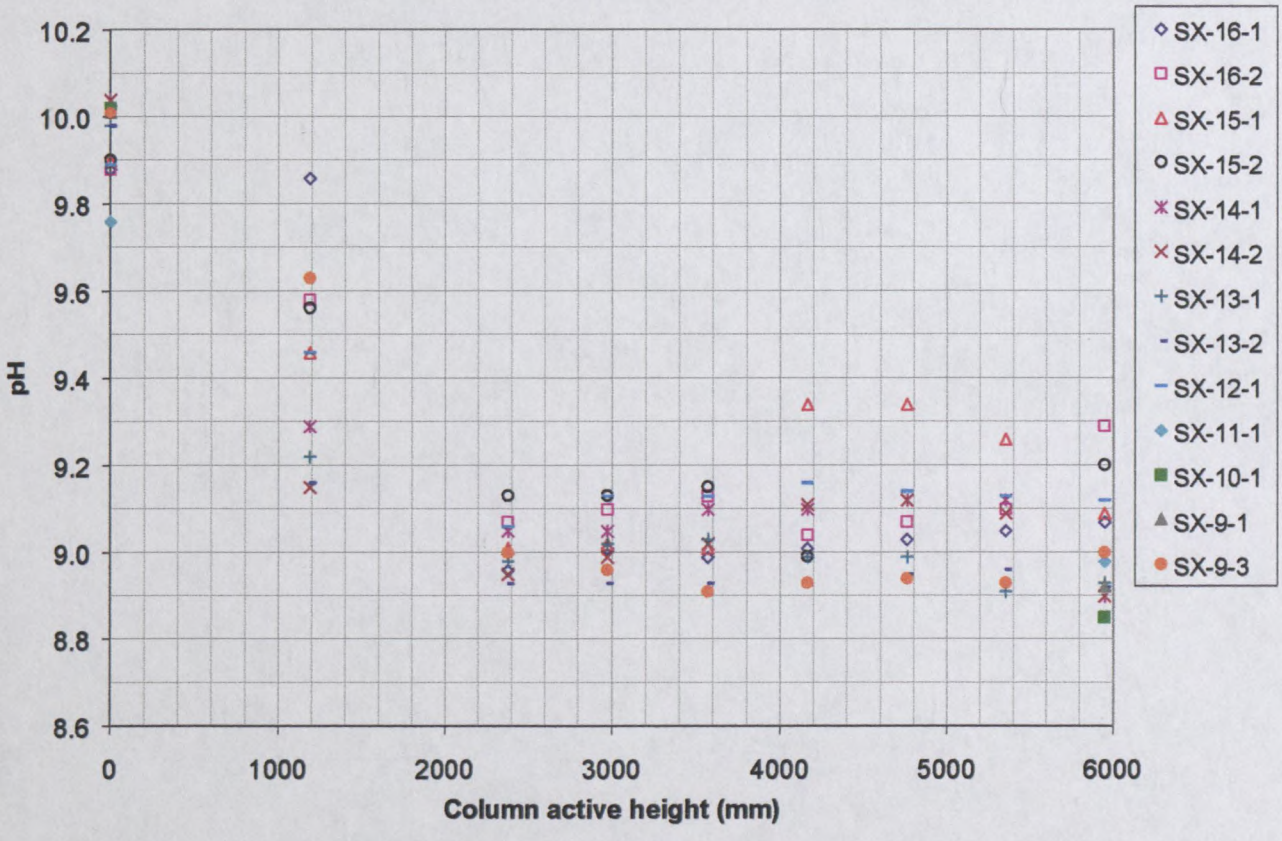

Figure 4-8: pH Profile along length of VPE for various tests

Combining the pH profile data and the *m*-cresol concentration profiles of the raffinate, with the theory discussed previously, it was possible to determine concentrations profiles of protonated *m*-cresol in the raffinate, versus column height, as depicted in **Figure 4-9**.

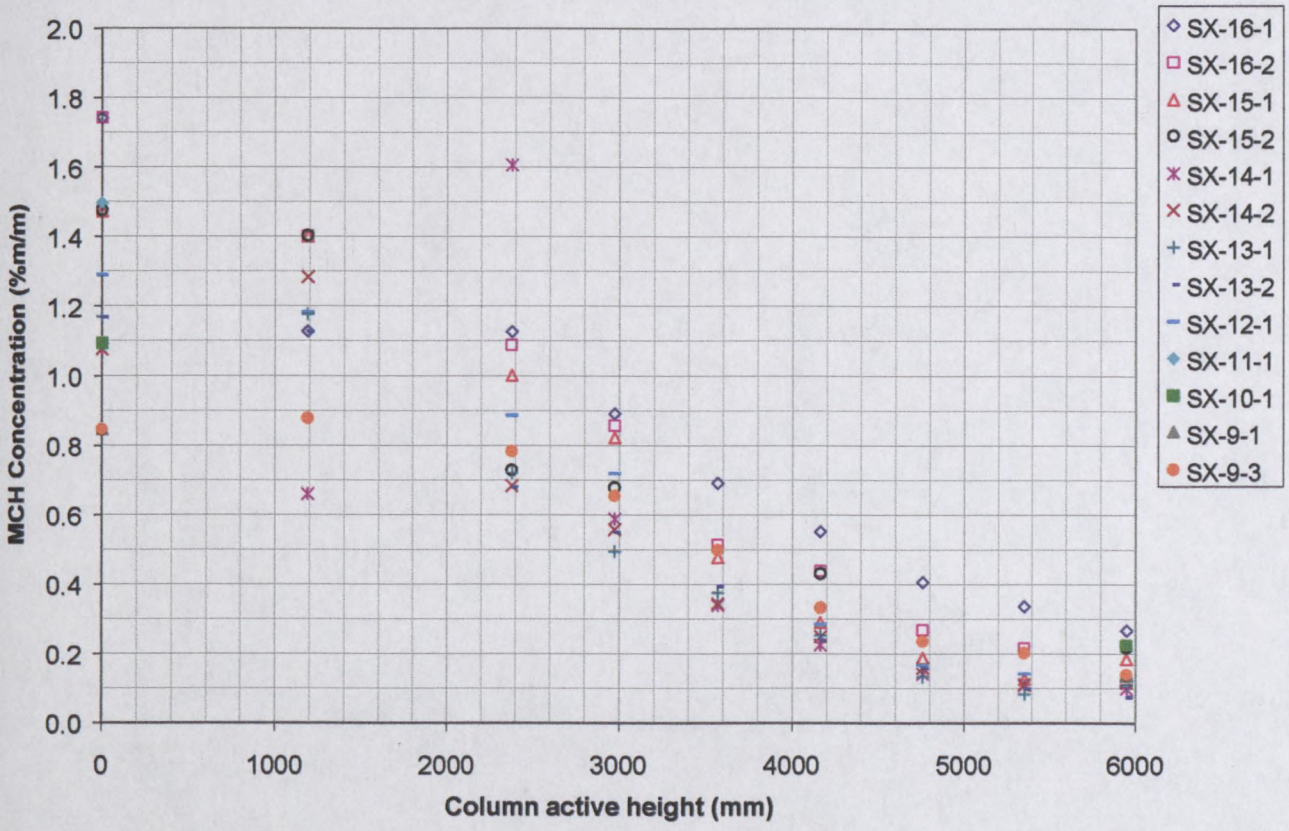

Figure 4-9: Protonated *m*-cresol concentration profile in the raffinate along length of VPE for various tests

4.2.1.4. Model Results

For each test, the protonated *m*-cresol concentration results were "force fitted" with the model in order to evaluate model parameters such as the backmixing ratios of each phase and the overall mass transfer coefficients. The model predictions of the aqueous raffinate and organic extract protonated *m*-cresol concentration profiles for all the tests are included in **Appendix D.1** and **D.2** respectively. A typical example of each is depicted below in **Figure 4-10** and **Figure 4-11** respectively (for Test SX-10-2)

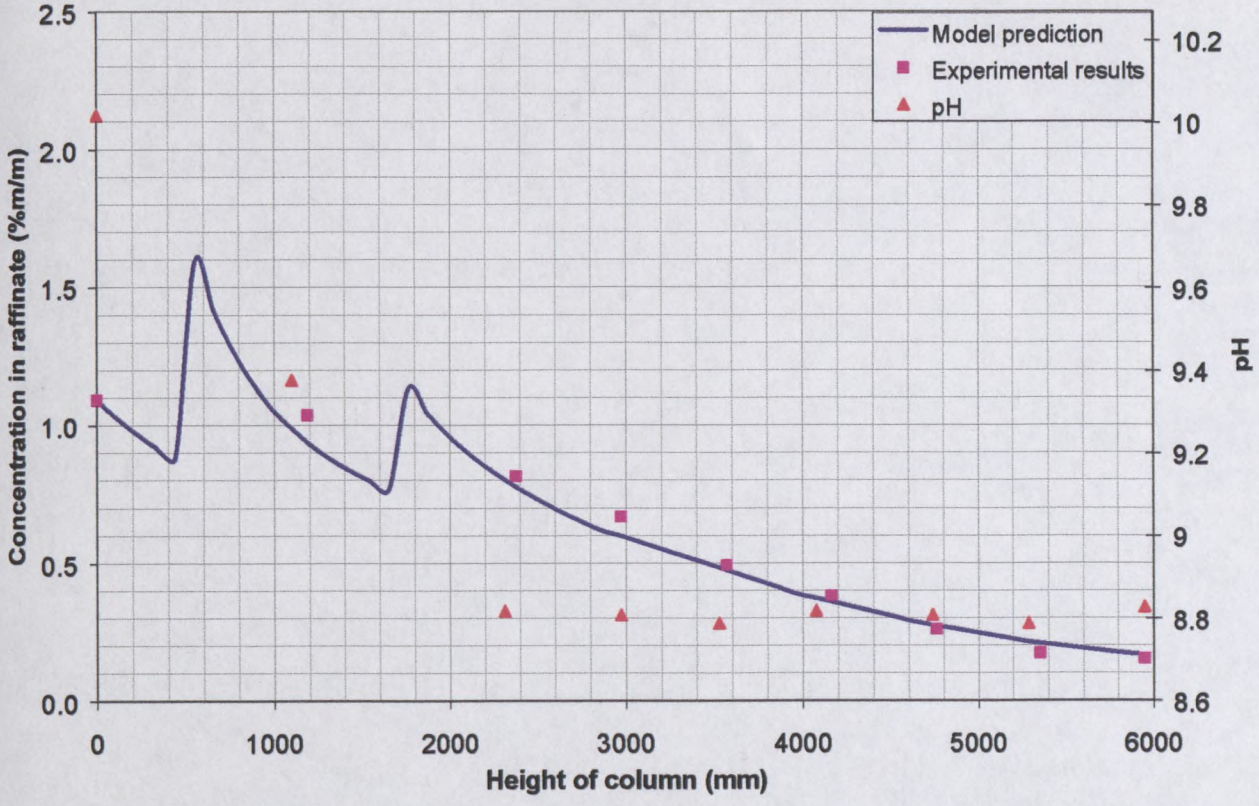

Figure 4-10: Typical raffinate concentration profile and model prediction (Test SX-10-2)

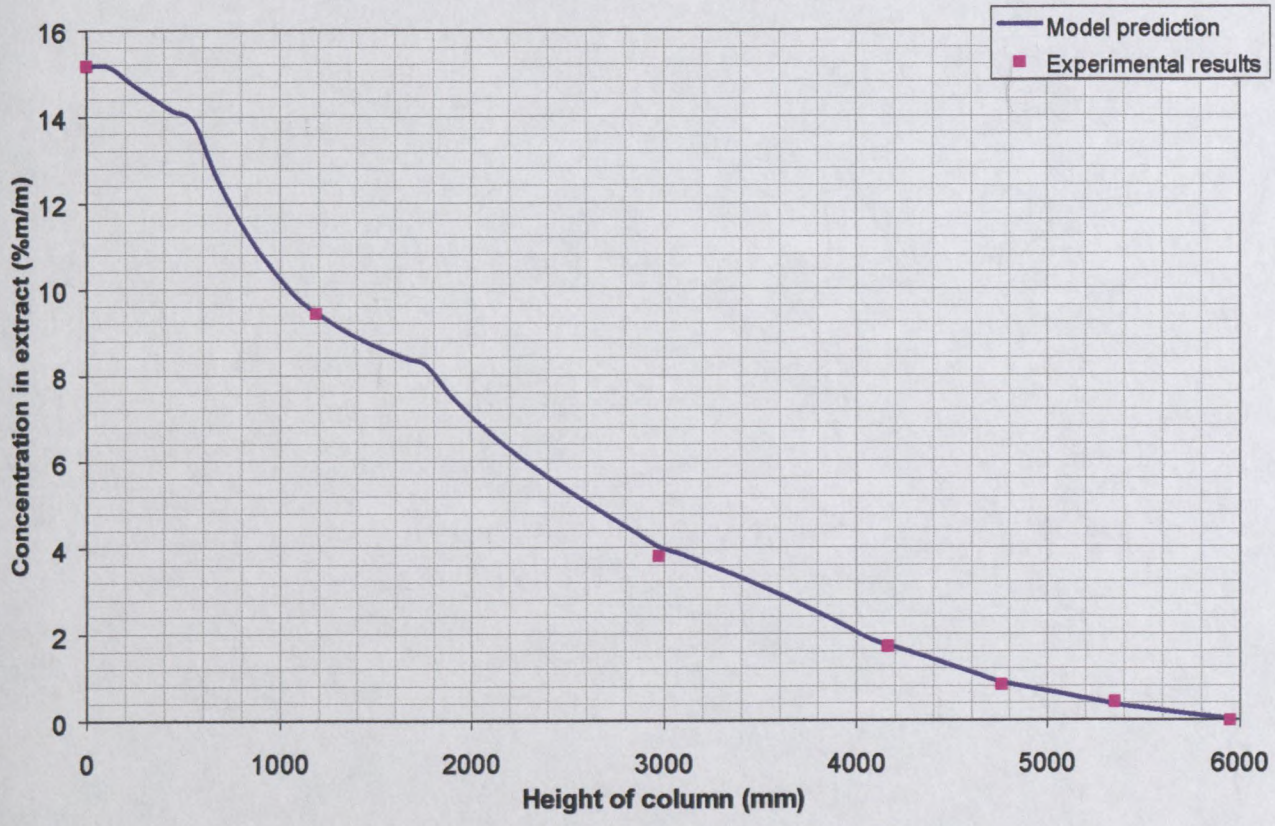

Figure 4-11: Typical extract concentration profile and model prediction (Test SX-10-2)

It is evident that the model fits the experimental data well. The discontinuities evident in **Figure 4-10** and **Figure 4-11** represent the points at which acid was added to the column. The addition of acid has the effect of releasing *m*-cresol, and since the acid addition points can essentially be thought of as protonated *m*-cresol addition points, by adding acid, the protonated *m*-cresol mass balance was changed.

The method of Height Equivalent to a Theoretical Stage (HETS) could be used to quantify the system. Typically the method assumes mass balance closure and no axial mixing (*i.e.* a single straight operating line). In this case however, the operating line is made up of a more than one line, as schematically depicted in **Figure 4-12** below.

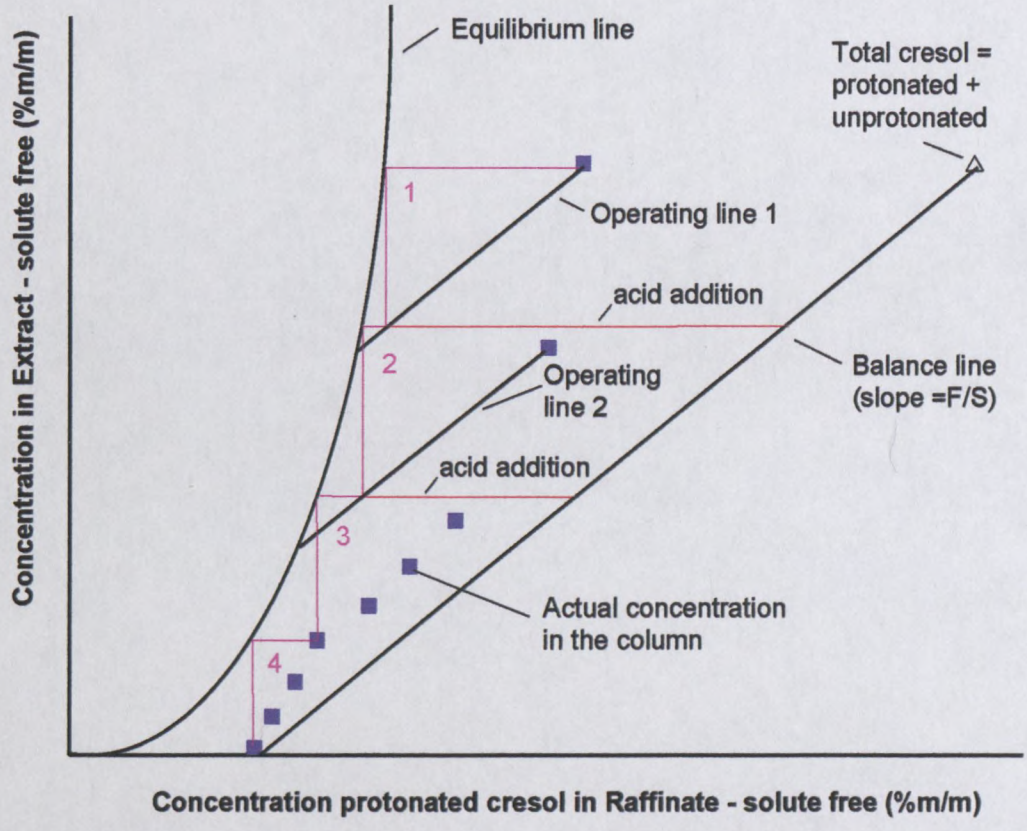

Figure 4-12: The method of HETS and the operating and equilibrium lines of *m*-cresol extraction

The balance line represents the overall mass balance of the column and is represented by a straight line (the start being the feed concentration of both protonated and de-protonated cresol). The actual concentration profile in the column is represented only by the protonated *m*-cresol species (since only the protonated species is extracted). Hence the actual column concentration

profiles do not lie on the balance line. In addition the actual concentration profile is non-linear, due to axial mixing in the column, which decreases the driving force for extraction by decreasing the distance between the column concentration profile and the equilibrium line.

If the method of Height Equivalent to a Theoretical Stage was to be employed for this system, the following procedure would give an approximate estimate of the HETS (with reference to **Figure 4-12**). The first stage is stepped off using the first operating line (the starting point is represented by the concentration of protonated cresol in the feed and extract). Acid is then added to the column (to flange a), which then results in a shift to the second operating line (the starting point of which is represented by the concentration of protonated cresol in the aqueous and organic phases as sampled at the second sampling point flange b in the column). The second stage is then stepped off, and the second acid addition (to flange c) results in a shift to the third operating line. For the remaining stages all the m-cresol is re-protonated. It is assumed that the two operating lines have the same slope as the balance line since the column operates at the same feed to solvent ratio through the length (the addition of acid has negligible effect on the ratio), however the effect of axial mixing on the shape of these operating lines has not been accounted for. By using the number of stages determined, it would be possible to calculate the HETS, and consequently the volumetric efficiency of the column.

A typical operating line, as predicted by the model (using the aqueous and organic phase concentration profiles) is depicted in **Figure 4-13** (for Test SX-10-2). The operating and equilibrium lines for each test are summarised in **Appendix D.3**.

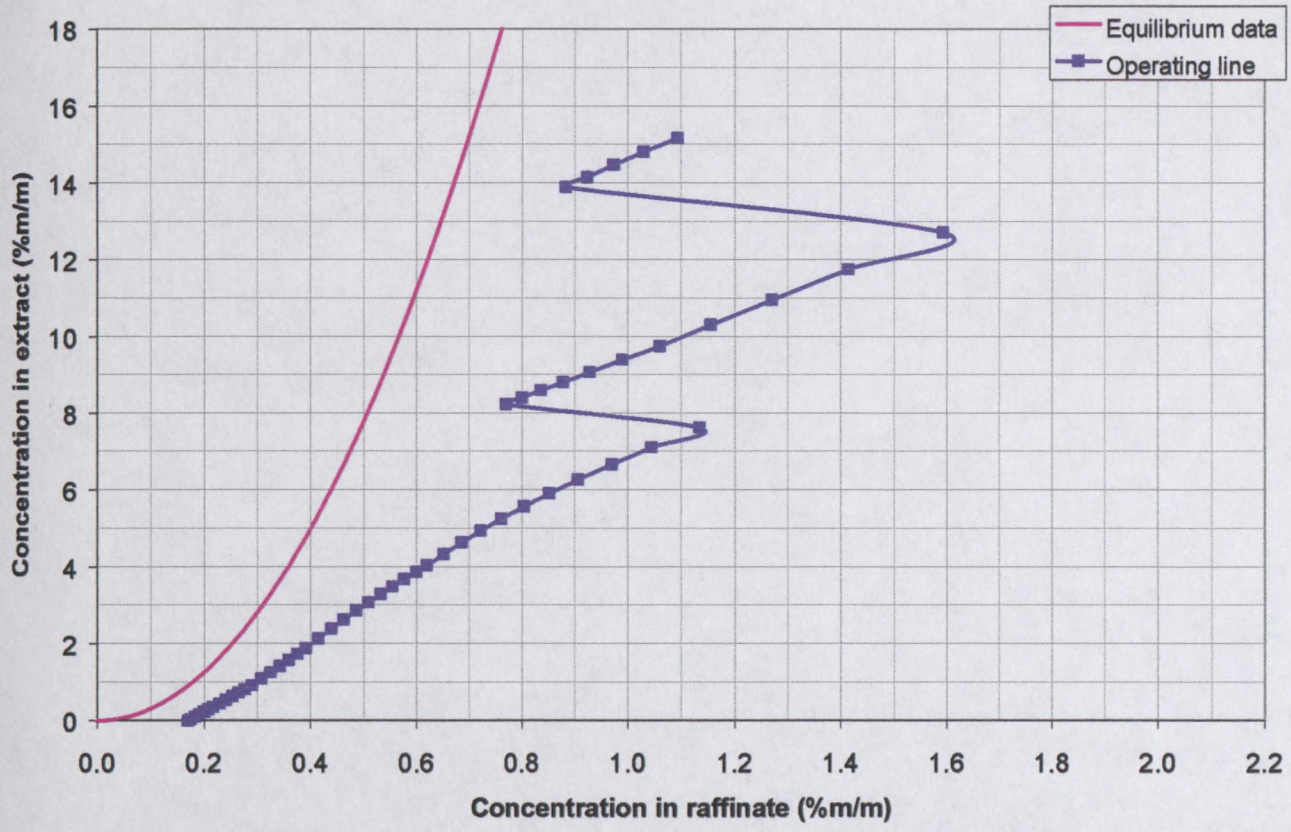

Figure 4-13: Typical equilibrium line and operating line, as predicted by the model (Test SX-10-2)

The effect of the addition of acid (effectively *m*-cresol addition) on the protonated *m*-cresol mass balance is evident as discontinuities in **Figure 4-13**. Axial mixing in the column resulted in the non-linearity of the operating line.

The model prediction of the experimental results allowed determination of the backmixing ratios of each phase and the overall mass transfer coefficients, as summarised in **Table 4-2**.

Table 4-2: Backmixing ratios and overall mass transfer coefficient results as predicted by the model

Test Name	overall mass transfer coefficient (/min)	backmixing ratio raffinate phase	backmixing ratio extract phase	raffinate concentration of protonated *m*-cresol (%m/m	raffinate pH	Total error	*m*-cresol mass closure %
SX-16-1	0.0112	0.130	0.086	0.27	9.07	0.89	94
SX-16-2	0.0118	1.51×10^{-4}	0.000	0.12	9.29	1.01	99
SX-15-1	0.0120	7.3×10^{-5}	0.000	0.19	9.09	1.67	115
SX-15-2	0.0130	0.000	0.000	0.22	9.20	1.05	110
SX-14-1	0.0136	1.56×10^{-6}	0.000	0.10	8.90	4.95	130
SX-14-2	0.0167	3.08×10^{-5}	0.000	0.12	8.90	1.53	118
SX-13-1	0.0189	8.8×10^{-5}	7.19×10^{-5}	0.11	8.93	1.23	113
SX-13-2	0.0162	3.56×10^{-5}	0.271	0.08	8.92	0.98	99
SX-12-1	0.0098	0.1191	8.42×10^{-4}	0.13	9.12	6.18	120
SX-11-2	0.0131	0.2958	3.42×10^{-5}	0.16	9.01	1.16	106
SX-10-2	0.0189	1.22×10^{-5}	0.00	0.16	8.83	1.13	111
SX-9-2	0.0147	0.5396	0.00	0.14	9.00	0.83	107
SX-9-3	0.0159	8.52×10^{-5}	5.03×10^{-2}	0.14	9.00	1.38	124

It is evident that the overall mass transfer coefficient ranges between 0.0098 and 0.0189 /min. Backmixing of the dispersed and continuous phases in the VPE is low, a typical property of the VPE.

A number of factors make it almost impossible to eliminate all variations under steady state operation, and can result in variations in the outlet concentrations and the column concentration profiles, such as:

- fluctuations in flow rates (the pumps were frequently calibrated on line during each run to ensure that a constant flowrate was achieved),
- temperature profiles along the length of the column,
- control of the position of the interface (a 10 mm change of height in the settler resulted in a 60 mm change in the active part of the column)

The greatest sources of inaccuracy are as a result of analytical errors (analytical results had an accuracy of +/- 10%) and pH reading errors (where a small error can have a significant effect on the calculated protonated *m*-cresol concentration).

4.2.2 Extraction of TBHQ

4.2.2.1. Calibration of the Conductivity Probe

The relationship between the conductivity measured and concentration was calibrated using solutions of known concentration prepared from water and feed. The conductivity of the samples was then measured, and as is evident from **Figure 4-14**, the conductivity showed a linear relationship with concentration.

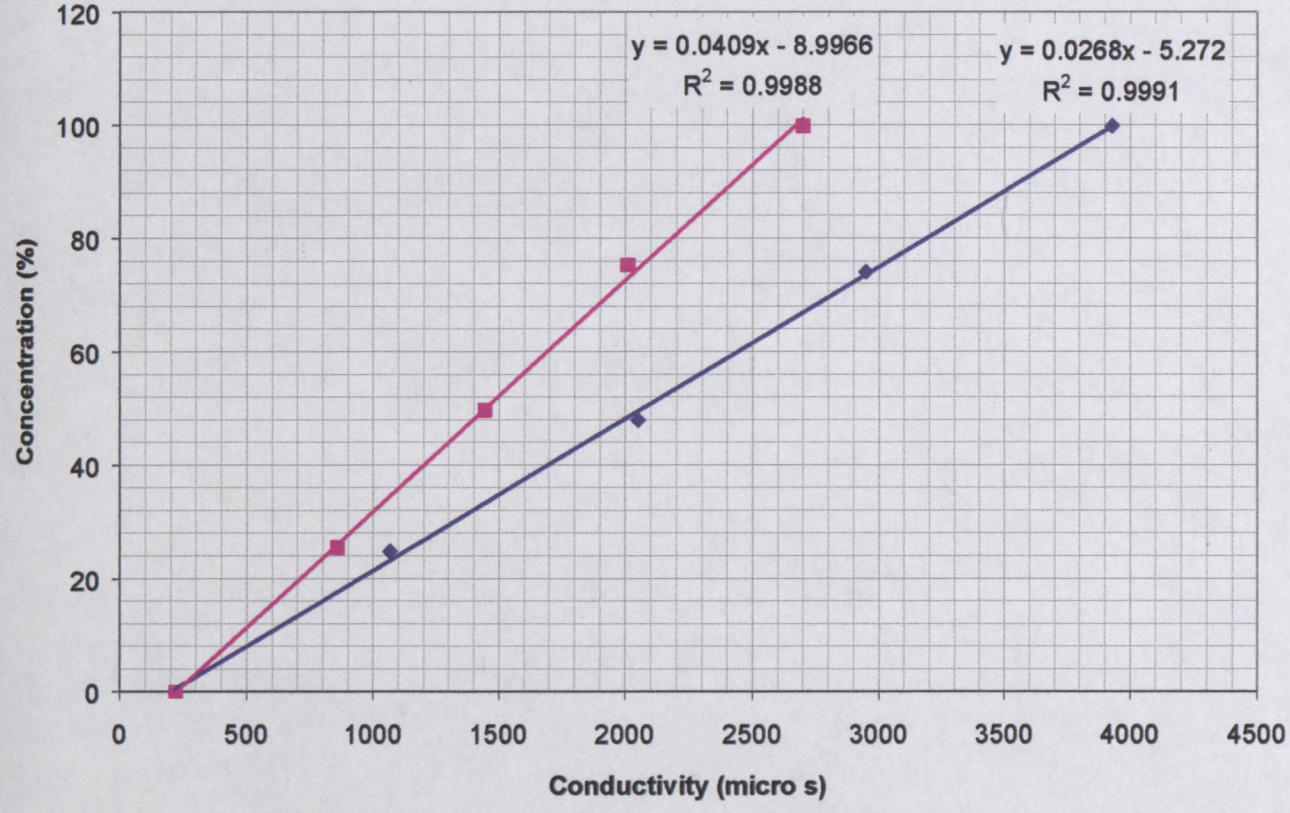

Figure 4-14: Typical conductivity calibration curves

4.2.2.2. Unsteady State Model Results

The unsteady state experiments were set up in such a manner that residence time profiles in the column were measured. Typical residence time distributions obtained experimentally are depicted below in **Figure 4-15**. The y axis concentration represents the concentration of the raffinate as a percentage of the feed concentration.

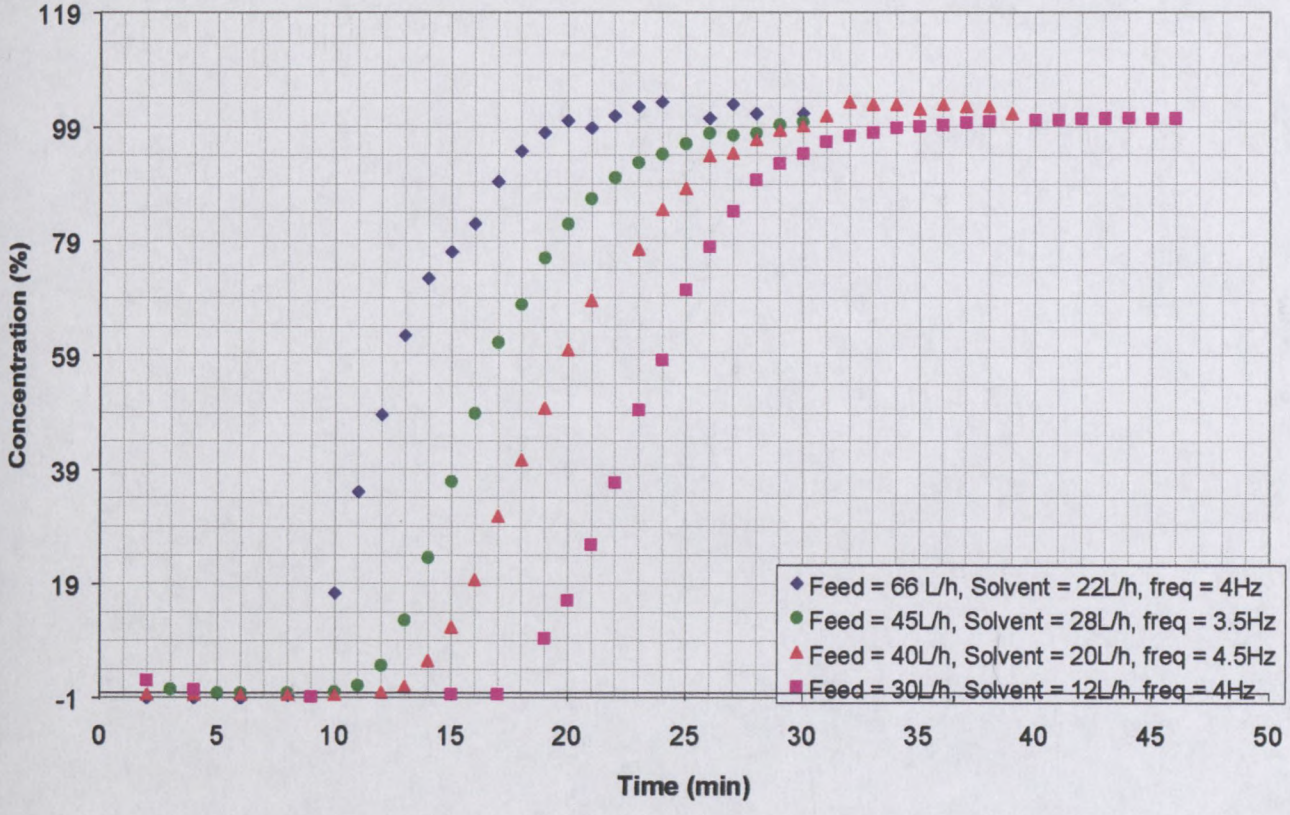

Figure 4-15: Residence time distribution profiles

The experimental data can be converted such that the concentration profile is plotted versus the number of column volumes replaced, as depicted in **Figure 4-16**.

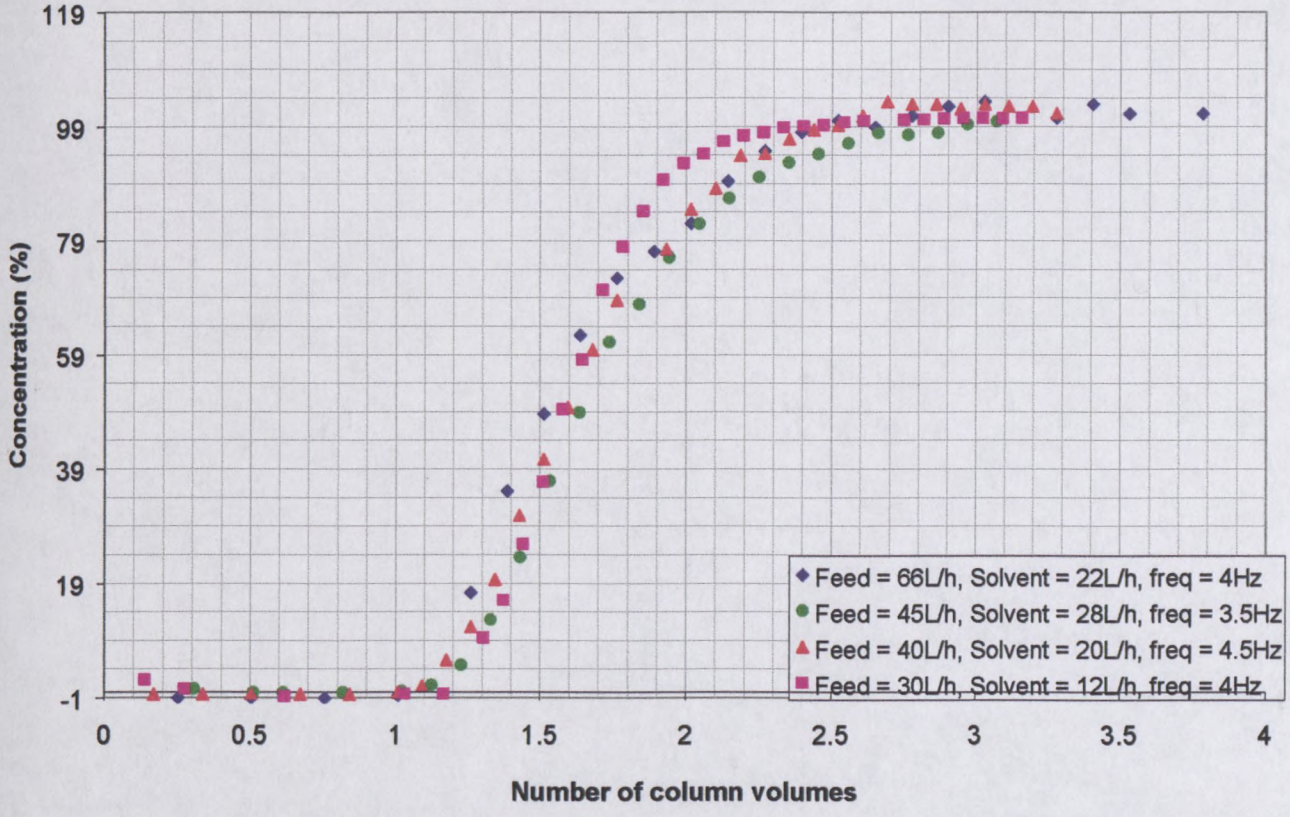

Figure 4-16: Number of column volumes replaced versus raffinate concentration

Differences between the curves of the first three runs is due to varying degrees of backmixing of the phases in the column. It is evident that the assumption that steady state is achieved within three column volume changes is conservative.

The extraction column set-up was such that a significant proportion of the column volume was occupied by the bottom and top settlers (volumes 2.26 *l* and 2,74*l* respectively). The effect of the settlers was to act as buffer tanks, which flatten the concentration curve. This was tested by using the model to quantify the effect of the settlers, as depicted in **Figure 4-17**, below:

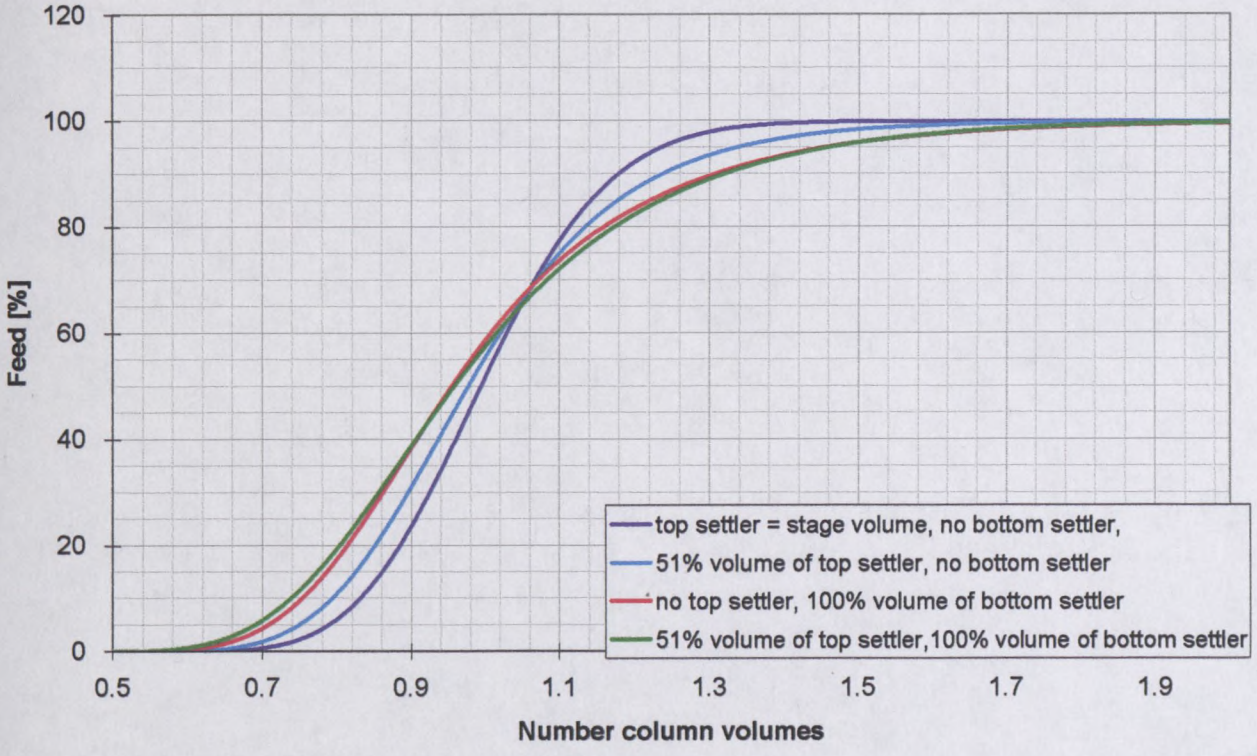

Figure 4-17:Effect of bottom and top settlers on residence time distribution (backflow ratios of continuous phase = 0)

The third case (100% volume of the bottom settler) represented the scenario whereby the raffinate was removed at an outlet at the bottom of the settler. The second case (50% volume of the top settler) represented the typical position used to control the interface (midway of the top settler height). It is evident that the volume of the bottom settler had a significant effect in terms of flattening the curve, and was more pronounced than the effect of the top settler. The column was initially set-up as depicted by the fourth case (51% of top settler and 100% of bottom settler). Flattening of the residence time distribution curve due to settler volumes masked changes due to backmixing in the system.

The sensitivity of the curves to axial mixing measurements, in the case of the top settler volume being taken as equal to a stage volume and no bottom settler, is depicted in **Figure 4-18** below (i.e. negligible settler volumes). The sensitivity of the curves to axial mixing measurements in the case of normal operation of the column (i.e. 51% of top settler volume and 100% of bottom settler volume) is depicted in **Figure 4-19** below.

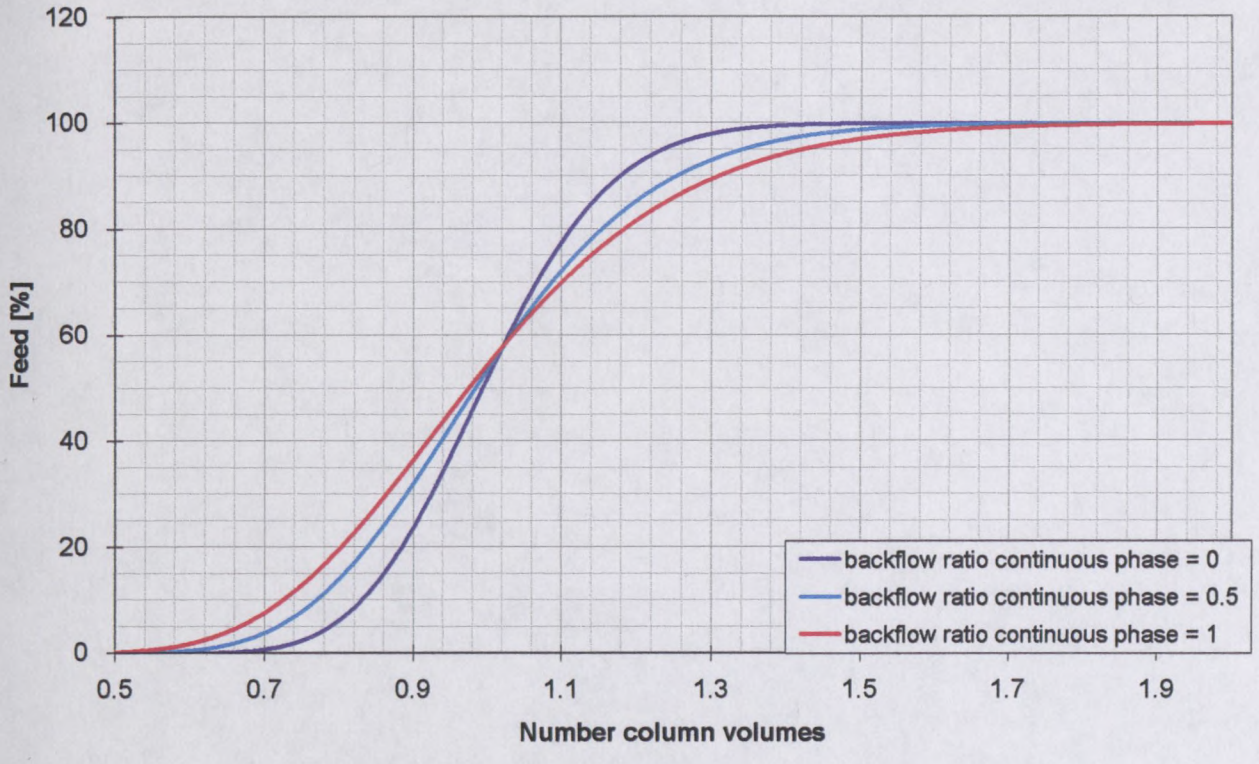

Figure 4-18: Effect backmixing on residence time distribution for column with no settlers

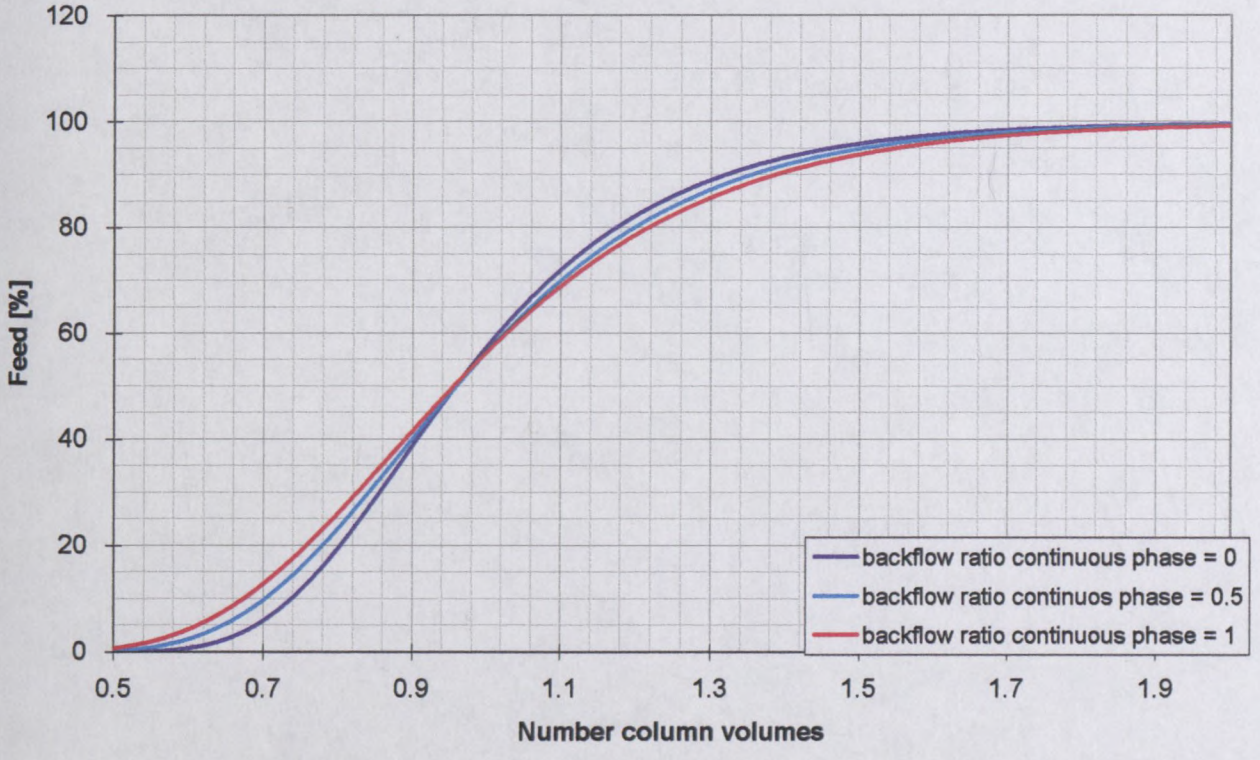

Figure 4-19: Effect of backmixing on residence time distribution for column under normal operation (i.e. with settlers)

It is evident by comparing **Figure 4-18** and **Figure 4-19** that for determining backmixing, it is preferable to operate the column with minimal hold-up in the settlers. To this end, the interface in the top settler was maintained 4 cm above the bottom of the top settler, and a pipe was installed into the bottom settler to remove raffinate from the upper portion of the bottom settler. Four tests were completed. The first three tests were performed by operating the column under normal conditions, and the last (SSX-16-1) with reduced settler volumes. Due to time and project constraints, no further work was possible. The experimental results and model predictions are included in **Appendix E**. It is evident that simultaneous measurement of the conductivity in other parts of the column would be required to quantify the extent of backmixing more precisely.

Possible deviations between the model and the experimental results could be caused by the following:

- non-uniformity in hold-up and drop size distribution through the length of the column,
- the effect of temperature variations through the length of column,
- change in column hydrodynamics (hold-up, etc.) as the system changed to a system where mass transfer between the phases occurred.

The effect of the choice of number of constantly-stirred-tank-reactors (CSTR's) on the model prediction is depicted in **Figure 4-20**, for the experimental results of Test 21-1. In each case the total volume of the CSTR's is assumed to be equivalent to that of the total column volume. For the model predictions, 54 CSTR's in series were used, together with 2 settlers. It is evident that the column represents at least 15 CSTR's in series. As the number of CSTR's increases, the flow approaches that of pure plug flow.

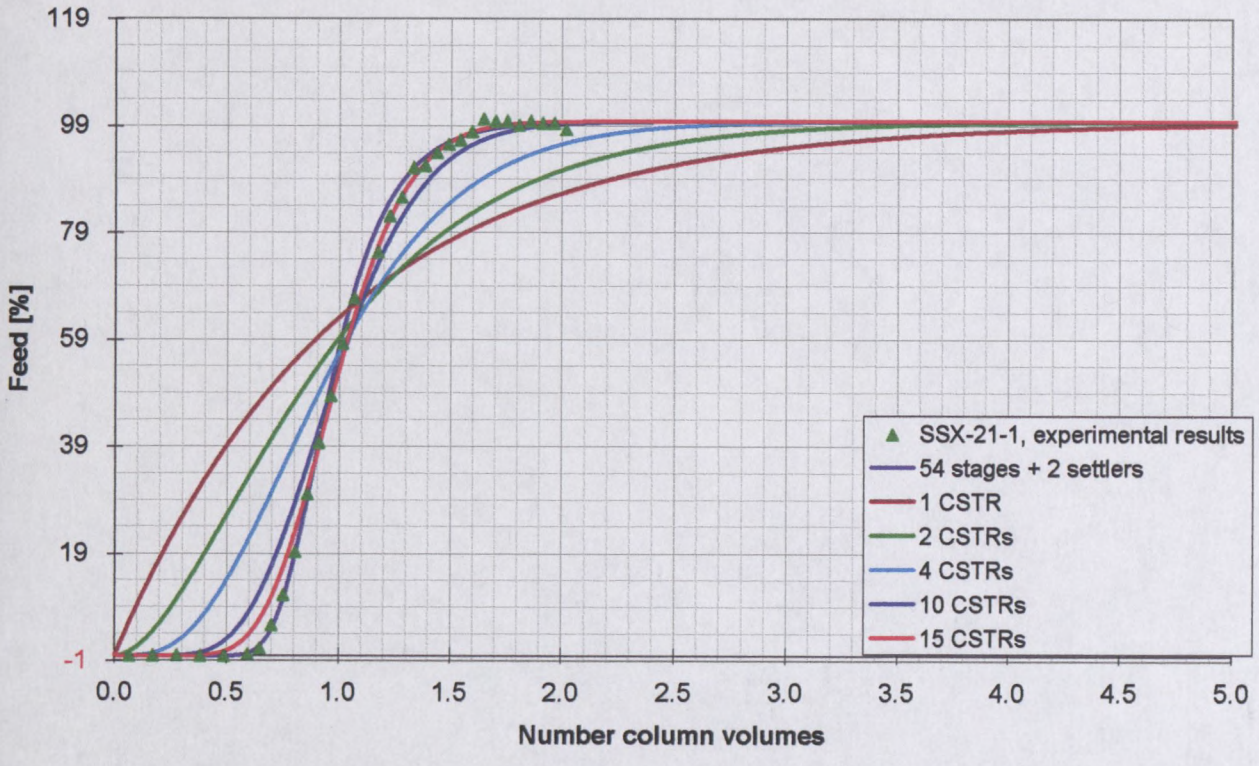

Figure 4-20: Results of Tests 21-1 and effect of the number of CSTR's

CHAPTER 5. CONCLUSIONS

The following conclusions can be made:

- The novel use of a VPE to perform a dissociation extraction has been proven. The acid added to the column was sufficiently mixed, and the manner of adding the acid was feasible.

- The theoretical methods of predicting the extent of association and protonation of *m*-cresol allowed quantification of the equilibrium data. The partition coefficient of the protonated species was determined to be 0.1332, while the equilibrium constant for association of *m*-cresol as a dimer form was calculated as 1,742. The equation describing the equilibrium data was used in the steady state backmixing model.

- For *m*-cresol extraction, eight consecutive batches were piloted and repeatable results were achieved. The mixer settler – VPE configuration was successfully used to reduce the concentration of *m*-cresol from 8.5 %m/m in the feed to less than 0.2 %m/m in the VPE raffinate, while losing only 2 % of component *p*HB (0.4 %m/m concentration in the mixer-settler extract).

- A steady state backflow model has been set-up, which allows quantification of backmixing in extraction column processes. The model can be used for modelling of liquid-liquid column extractions, in further process development work.

- The general form of the steady state backflow model was modified to allow prediction of a dissociation extraction in a VPE. The steady state backflow model fitted the *m*-cresol extraction experimental data well, allowing determination of the system parameters, and graphical depiction of the operating lines. Backmixing of the continuous phase in the VPE appeared to be low, (the backmixing ratio ranged from 0 to 0.3) while backmixing in the dispersed phase was negligible. This was in agreement with findings quoted in the literature. The overall mass transfer coefficients ranged from 0.0098 to 0.0189 /min.

- The dynamic response of a VPE can be modelled by using an unsteady state backflow model. The model developed can be used for modelling of liquid-liquid column extractions in further process development and prediction of dynamic column behaviour.

- For unsteady state experiments using conductivity (i.e. measurement of residence time distributions), it is preferable that the column be operated with minimum settler volumes, and that conductivity measurements be taken of the raffinate at the outlet and at a minimum of two other points in the column.

- In order to evaluate the dependence of the parameters (backflow ratios of each phase and mass transfer coefficients) on the operating parameters, sufficient data at varying operating conditions is required. This however was not possible due to the fact that the experimental work was completed with the aim to commercialise a process, and operated to produce consistent material for downstream processing.

CHAPTER 6. RECOMMENDATIONS AND FUTURE WORK

Recommendations for future work include the following:

- Setting up of a steady state backflow model and an unsteady state backflow model that account for non-constant mass transfer coefficients and backflow ratios along the length of the column.

- Validation of the models and evaluation of the dependence of the parameters (backflow ratios of each phase and mass transfer coefficients) on the operating parameters. This could be achieved by performing further experimental work a using simpler system, with generation of sufficient data at varying operating conditions. Simultaneous measurements of hold-up profiles, drop size distribution and mass transfer should be performed, and axial variations (such as unstable density gradients, temperature profiles) should be minimised.

- Comparison of the axial mixing characteristics of a 50 mm diameter Karr column and a 50 mm diameter VPE column, using experimentally determined data.

- Derivation of a combined Backflow-Diffusion model, and validation of the model using experimental results.

- The use of axial dispersion data in terms of scale-up to commercial columns requires further investigation by reviewing the literature. Validation of this would be beneficial by generating experimental data using a 150 mm diameter VPE, and comparing the performance to that of a 50 mm diameter VPE.

CHAPTER 7. REFERENCES

1. Aravamudan, K. and Baird, M. H. I., 1996, *Effect of Unstable Density Gradients on Back-Mixing in a Reciprocating Plate Column*, AIChE Journal, Vol. 42, No. 8, pages 2128 – 2140.
2. Atkins, P. W., 1978, *Physical Chemistry*, Oxford University Press, pages 363-369.
3. Baird, M. H. I., 1974, *Axial Dispersion in a Pulsed Plate Column*, Can. J. Chem. Engng, Vol. 52, pages 750 – 757.
4. Baird, M. H. I., Aravamudan, K., Rama Rao, N. V., Chadam, J. and Peirce, 1992, A. P., *Unsteady Axial Mixing by Natural Convection in a Vertical Column*, AIChE Journal, Vol. 38, No. 11, pages 1825 – 1834.
5. Baird, M. H. I. and Rama Rao, N. V., 1988, *Characteristics of a Countercurrent Reciprocating Plate Bubble Column II: Axial Mixing and Mass Transfer*, Can. J. chem. Engng, Vol. 66, pages 222 – 232.
6. Baird, M. H. I. and Rama Rao, N. V., 1991, *Axial Mixing in a Reciprocating Plate Column with Very Small Density Gradients*, AIChE Journal, Vol. 37, No. 7, pages 1019 – 1206.
7. Baird, M. H. I. and Rama Rao, N. V., and Prochazka, J. and Sovova, H., 1994, *Liquid-Liquid Extraction Equipment*, Chap. 11, John Wiley, pages 311 – 358.
8. Bell, R.L. and Babb, A.L., 1969, *Hold-up and Axial Distribution of Hold-up in a Pulsed Sieve-Plate Solvent Extraction Column*, Ind. Engng Chem. Proc. Des. Dev., Vol. 8, No. 3, pages 392- 400
9. Blass, E., Goettert, W., and Hampe, M.J., 1994, *Liquid-Liquid Extraction Equipment*, Chap. 18, John Wiley, pages 738 – 748.
10. Blass, E., 1994, *Liquid-Liquid Extraction Equipment*, Chap. 14, John Wiley, pages 533 – 568.
11. Cusack, R.W., Fremeaux, P. and Glatz, D., 1991, *A Fresh Look at Liquid-Liquid Extraction,*– Part 1, Chemical Engineering, February, pages 66 – 76
12. Cusack, R.W. and Fremeaux, P., 1991, *A Fresh Look at Liquid-Liquid Extraction,*– Part 2, Chemical Engineering, pages 132 – 138.
13. Cusack, R.W., Karr, A.E., 1991, *A Fresh Look at Liquid-Liquid Extraction,*– Part 3, Chemical Engineering, pages 112 – 119.
14. Defives, D. and Schneider, G., 1961, *Retention of Dispersed Phase in a Pulse Column*, Genie Chmique, Vol. 85, pages 246 – 251.

15. Glasstone, S., 1955, *Textbook of Physical Chemistry*; Macmillan and Co. Limited, pages 738-739

16. Godfrey, J.C., 1994, *Liquid-Liquid Extraction Equipment*, (Godfrey, J.C. and Slater, M.J. Eds.), Chapter 12, John Wiley, pages 366-409.

17. Gourdon, C., Casamatta, G. and Muratet, G., 1994, *Liquid-Liquid Extraction Equipment*, (Godfrey, J.C. and Slater, M.J. Eds.), Chapter 7, John Wiley, pages 141-176.

18. Hafez, M. M., Baird, M. H. I. and Nirdosh, I., 1979, *Flooding and Axial Dispersion in Reciprocating Plate Extraction Columns*, The Canadian Journal of Chemical Engineering, Vol. 57, pages 150 – 158.

19. Haverland, H. and Slater, M. J., 1994, *Liquid-Liquid Extraction Equipment*, Chap. 10, John Wiley, pages 279 – 303

20. Heyberger, A., Kratky, M. and Prochazka, J., 1982, *Parameter Evaluation of an Extractor with Back Mixing*, Chemical Engineering Science, Vol. 38, No. 8, pages 1303-1307

21. Holmes, T.L., Karr, A. E. and Baird, M. H. I., 1991, *Effect of Unfavourable Continuous Phase Density Gradient on Axial Mixing*, AIChE Journal, Vol. 37, No. 3, pages 360 – 366.

22. Ingham, J., 1971, *Recent Advances in Liquid-Liquid Extraction*; Chapter 8, Pergamon Press, pages 237-256

23. Jiricny, V. and Prochazka, J., 1980, *Counter-current Flow of Dispersed and Continuous Phase, III, Measurements of Hold-up Profiles and Particle Size Distributions in a Vibrating Plate Contactor*, Chem. Eng. Sci. Vol. 35, No. 11, pages 2237-2245

24. Karr, A. E., Ramanujam, S., Lo, T. C. and Baird, M. H. I., 1987, *Axial Mixing and Scale-up of Reciprocating Plate Columns*, The Canadian Journal of Chemical Engineering, Vol. 65, pages 373 – 381.

25. Kim, S. D. and Baird, M. H. I., 1976a, *Axial Dispersion in a Reciprocating Plate Extraction Column*, The Canadian Journal of Chemical Engineering, Vol. 54, pages 81 – 89.

26. Kim, S. D. and Baird, M. H. I., 1976b, *Effect of Hole Size on the Hydrodynamics of a Reciprocating Perforated Plate Extraction Column*, Can., J. chem. Engng, Vol. 54, pages 235-237.

27. Kolmogoroff, A. N., 1941, *The Local Structure of Turbulence in Incompressible Viscous Fluid for Very Large Reynolds Numbers*, Akad. Nauk U.S.S.R., Vol. 30, pages 301 -

28. Korchinsky, W. J., 1994, *Liquid-Liquid Extraction Equipment*, Chap. 9, John Wiley, pages 248 – 273

29. Kostanyan, A. E., Pebalk, V. L. and Pelevina, T. K., September/October 1979, *A Physical Model of Lengthwise Mixing in Columns with Vibrating Plates*, translated from Teor. Osn. Khim. Tekhnol., Vol. 13, No. 5, pages 749 – 755.
30. Kumar, A. and Hartland, S.; 1994, *Liquid-Liquid Extraction Equipment*, (Godfrey, J.C. and Slater, M.J. Eds.), Chapter 17, John Wiley, pages 628-735.
31. Lide, D. R., 1992/3, *CRC Handbook of Chemistry and Physics*, 76th Edition, CRC Press, page 8-51
32. Lo. T.C., 1979, *Handbook of Separation Techniques for Chemical Engineers*, (Schweitzer, P.A., Ed.) Chap. 1.10, McGraw-Hill, pages 1-285 to 1-342.
33. Lo, T.C. and Prochazka, J.,1983, *Handbook of Solvent Extraction*, Chap. 12, John Wiley, pages 373-387.
34. Marqardt, D. W., 1963, J. Soc. Appl. Math., Vol. 11, pages 431
35. Miyauchi, T. and Vermeulen, T., 1963a, *Longitudinal Dispersion in Two-Phase Continuous-Flow Operations*, Ind. Eng. Chem. Fund. Vol. 2, page 305.
36. Miyauchi, T. and Vermeulen, T., 1963b, *Diffusion and Back-flow Models for Two Phase Axial Dispersion*, Ind. Eng. Chem. Fund. Vol. 2, pages 304 - 310.
37. Nemecek, M., and Prochazka, J., 1974, *Longitudinal Mixing in Vibrating-Sieve-Plate Column Two Phase Flow*, The Canadian Journal of Chemical Engineering, Vol. 52, pages 739 - 748.
38. Novotny, P., Prochazka, J. and Landau, J., 1970, *Longitudinal Mixing in Reciprocating and Pulsed Sieve-Plate Column - Single Stage Flow*, The Canadian Journal of Chemical Engineering, Vol. 48, pages 405 - 410.
39. Parthasarathy, P., Sriniketan, N., Srinivas. N. S. and Varma, Y. B. G., 1984, *Axial Mixing of Continuous Phase in Reciprocating Plate Columns*, Chem. Engng Sci., Vol. 39, pages 987 – 995.
40. Pollock, G. G. and Johnson, A. I., 1969, *The Dynamics of Extraction Processes – Part 1: Introduction and Critical Review of Previous Work*, The Canadian Journal of Chemical Engineering, Vol. 47, pages 469 – 476.
41. Pratt, H. R. C., 1983a, *Handbook of Solvent Extraction*, Chap. 3, John Wiley, pages 91-124.
42. Pratt, H. R. C., 1983b, *Handbook of Solvent Extraction*, Chap. 5, John Wiley, pages 152-198.
43. Pratt, H. R. C. and Baird, M. H. I., 1983, *Handbook of Solvent Extraction*, Chap. 6, John Wiley, pages 199 - 247.

44. Prochazka, J. and Landau, J., 1963, *Studies on Extraction I – Back-mixing and Efficiency of Continuous Stagewise Countercurrent Extractors*, Coll. Czech. Chem. Commun., Vol. 28, pages 1927 – 1945.

45. Prochazka, J. and Landau, J., 1966, *Studies on Extraction IV – Relationship Between the Efficiency and Mass Transfer Coefficient for Extraction with Back-mixing*, Coll. Czech. Chem. Commun., Vol. 31, pages 1685 – 1694.

46. Rama Rao, N. V., Srinivas. N. S. and Varma, Y. B. G., 1983, *Axial Dispersion Studies in a Reciprocating Column*, Proceedings of ISEC '83, pages 102 – 103.

47. Rama Rao, N. V., Baird, M. H. I., 1998, *Backmixing in a Reciprocating Plate Column with Stable Density Gradients*, AIChE Journal, Vol. 44, No. 4, pages 859 – 863.

48. Robbins, L. A., 1984, *Perry's Chemical Engineer's Handbook - 7th Edition*, (Perry, R. H., Ed.), Chap. 15, McGraw-Hill, pages 15-1 to 15-20.

49. Rod, V., 1965, *The Calculation of Mass Transfer Coefficients and of Axial Dispersion Coefficients from Concentration Profiles*, Coll. Czech. Chem. Commun., Vol. 30, pages 3822 – 3833.

50. Slater, M.J., 1994, *Liquid-Liquid Extraction Equipment*, (Godfrey, J.C. and Slater, M.J. Eds.), Chapter 4 John Wiley, pages 48-82.

51. Slavickova, A., Angelov, G., Heyberger, A. and Prochazka, J., 1978, *Countercurrent Extraction with Backmixing – Evaluation of Parameters*, Coll. Czech. Chem. Commun., Vol. 43, pages 2682 – 2706.

52. Sleicher, C.A., Jr., 1959, *Axial Mixing and Extraction Efficiency*, AIChE Journal, Vol. 5, No. 2, pages 145 – 149.

53. Souhrada, F., Prochazka, J., and Landau, J., 1966a, *Studies on Extraction V – Determination of Back-mixing and Efficiency of Stagewise Extractors*, Coll. Czech. Chem. Commun., Vol. 31, pages 1695 – 1711.

54. Souhrada, F., Prochazka, J., and Landau, J., 1966b, *Studies on Extraction VI – Back-mixing in Single-Phase Flow in a Stagewise Process*, Coll. Czech. Chem. Commun., Vol. 31, pages 1877 – 1881.

55. Souhrada, F., Landau, J. and Prochazka, J., 1970, *Dynamic Simulation of a Stagewise Mass Transfer Process with Backmixing*, The Canadian Journal of Chemical Engineering, Vol. 48, pages 322 – 327.

56. Steiner, L., and Hartland, S., 1983, *Handbook of Solvent Extraction*, Chap. 7, John Wiley, pages 249-264.

57. Stemerding, S., Lumb, E.C. and Lips, J., 1963, *Axial Mixing in a Rotating-disc Extraction Column*, Chem. Ingr. Tech., Vol. 35, pages 844 – 850

58. Stevens, G. W., 1994, *Liquid-Liquid Extraction Equipment*, Chap. 8, John Wiley, pages 228–244.

59. Stevens, G. W. and Baird, M. H. I., 1990, *A Model for Axial Mixing in Reciprocating Plate Columns*, Chemical Engineering Science, Vol. 45, No. 2, pages 457 – 465.

60. Strand, C.F., Olney, R. B. and Ackerman, G. H., 1962, *Fundamental Aspects of Rotating Disk Contactor Performance*, AIChE J., Vol. 8, pages 252–261

61. Treybal, R. E., 1951, *Liquid Extraction*; Chap 8,9, McGraw-Hill, pages 241-256, 274-275

62. Vermeulen, T., Moon, J. S., Hennico, A. and Miyauchi, T., September 1966, *Axial Dispersion in Extraction Columns*, Chemical Engineering Progress, Vol. 62, No. 9, pages 95 – 102

63. Westerterp, K.R. and Meyberg, W.H., 1962, *Axial Mixing in a Rotating Disc Contactor – II, Backmixing*, Chem. Eng. Science, Vol. 17, pages 373-377

APPENDICES

APPENDIX A: NOTATION

a : specific interfacial or superficial area of contact of the phases (m^2/m^3),

A^- : de-protonated species of component A,

a_A^* : activity of component A,

am : amplitude (m),

A : interfacial surface area (m^2),

A_ξ : non-associated form of A in extract phase,

A_δ : associated (dimer) form of A in extract phase,

B = L/d_c (m), ratio of column length to the local characteristic dimension,

c : concentration (kg/m^3),

c_j : concentration in phase j (kg/m^3),

c_j^* : solute concentration in phase j, in equilibrium with the other phase in the system (kg/m^3) or (mol/l),

c_{ji} : interfacial concentration of phase j (kg/m^3) or (mol/l),

C : solute concentration in the bulk of a phase (mol/l),

C_{A-} : concentration of de-protonated form of component A (%m/m),

$C_{A,E}$: concentration of component A in extract phase (%m/m),

$C_{A,F}$: concentration of component A in feed phase (%m/m),

$C_{A,R}$: concentration of component A in raffinate phase (%m/m),

$C_{A,S}$: concentration of component A in solvent phase (%m/m),

$C_{A,\delta}$: concentration of associated (dimer) form of A in extract phase (%m/m),

$C_{A,\zeta}$: concentration of non-associated form of component A in extract phase (%m/m),

C_f : concentration of tracer (kg/m^3),

C_{H+} : concentration of protons (%m/m),

$C_{HA,E}$: concentration of protonated component A in extract phase (%m/m),

$C_{HA,R}$: concentration of protonated component A in raffinate phase (%m/m),

CSA : cross sectional area of column (m^2),

d_h : diameter of holes in plate (m),

d_i : diameter of droplet of size group i (m),

d_c : characteristic dimension (m),

d_t : thickness of plate (m),

D_c : diameter of column (m),

D_A : extent of de-protonation,

E : extraction factor, mU_x / U_y,

E : axial dispersion coefficient (m^2/s),

E_i : extract mass rate on solute-free basis (kg/s),

E_j : effective longitudinal diffusion coefficient in the jth phase (m^2/s),

E_l : axial dispersion coefficient in the poorly mixed region (m^2/s),

f : backflow coefficient in continuous phase,

f_c : frequency of reciprocating motion (Hz),

$f()$: mathematical function of,

F_j : volumetric flowrate of jth phase (m^3/s),

g : backflow coefficient in dispersed phase,

g_c : gravitational constant,

h : height of hypothetical stage (m),

h_c : height of compartment/stage (m),

h_{im} : height of imperfectly mixed region,

h^* = $h_1 + h_2$, overall height of ideal mixers,

H : stage height,

H : height of stage (m),

H' : flowrate of the continuous phase (kg/s),

H^+ : protons,

H_A : column active height (m),

HA : protonated species of component A,

$HETS$: Height Equivalent to a Theoretical Stage (m),

HTU : Height Transfer Unit (m),

H_{Tj} : height of a transfer unit for phase j (m),

H_{Toj} : height of an overall transfer unit based on phase j (m),

I_a : agitation intensity (/min),

k_{ass} : association equilibrium constant,

k_j : mass transfer coefficient of phase j (m/s),

k_{oj} : overall mass transfer coefficient based on phase j (m/s),

K : mass transfer coefficient of phase j (kg/m^2s),

K' : empirical parameter,

Ka : de-protonation equilibrium constant,

K_l $= \frac{E_l}{v.l}$, constant,

l : mixing length,

l_v : characteristic size of vortices in the poorly mixed region (m),

L' : flowrate of the dispersed phase (kg/s),

L : length or height of differential extractor (m),

m : reciprocal slope of equilibrium line, dc_x^*/dc_y,

m_A : partition (or distribution) coefficient of component A,

m_A' : overall partition (or distribution) coefficient of component A,

m_{HA} : partition (or distribution) coefficient of protonated species of component A,

$m^\bullet$: reciprocal slope of equilibrium line,

m^* : slope of equilibrium line,

M : mass rate (kg/hr),

n : stage number counted from feed inlet,

N_F : flux (kg/s),

N : total number of actual stages required,

N_A : flux of solute A (kg/m^2s),

N_f : flux of mass transfer (mol/h),

N_{ox} $= k_{ox}\, a\, L / U_x$, number of "true" overall transfer units based on X phase,

N'_{ox} : number of perfectly mixed transfer units per stage,

N_S : number of stages

N_{Tj} : Number of transfer units based on stage j,

N_{Toj} : Number of overall transfer units based on stage j,

pH $= -log\ (C_{H+})$

Pe : local Peclet number,

PeB $= U_jL/E_j$: column Peclet number,

P : Peclet number,

P_j $= U_j d_c/E_j$, turbulent Peclet number of jth phase,

pKa $= -log\ (Ka)$,

Ps : plate spacing (m),

q : intercept of equilibrium line,

r : radius of the drops (m),

r_n : mass transfer rate (kg/m^3s),

rpm : rotational speed (rpm),

R : raffinate mass rate on solute free basis (kg/h),

R_{ed} = $d_i v_i / v_d$, droplet Reynold's number,

R_f : rate of flow of tracer to the extractor (m^3/h),

R_i : raffinate solvent rate on solute-free basis (kg/s),

R_r : rate of flow of back-mixed stream (m^3/h),

s : number of stages to which the tracer is fed,

S : fractional open area of plates (m),

S = U_y / mU_x, stripping factor, ,

SSV : number of volume replacements

$Sel_{A/B}$: selectivity of the solvent for component A relative to component B,

t : time (s),

u : mean flow velocity referred to cross sectional area of extractor,

u_c : continuous phase velocity (m/s),

u_d : dispersed phase velocity (m/s),

U_j : superficial velocity of phase j in extractor (m/s),

U_∞ : terminal settling velocity of a single droplet in viscous flow (m/h),

v : characteristic velocities of vortices in the poorly mixed region (m/s),

v_i : velocity in column of droplet(s) of diameter d_i (m/s),

V : volume (m^3),

W : apparent weight of the drop allowing for buoyancy (kg),

x : weight or mole fraction of component in x phase,

x' : weight or mole ratio of solute to solvent in x phase,

X : dimensionless concentration of solute in X phase,

y : weight or mole fraction of component in y phase,

y' : weight or mole ratio of solute to solvent in y phase,

Y : dimensionless concentration of solute in Y phase,

z : length measured from X (feed) = phase inlet (m),

z_a : axial distance (m),

Z = z/L, fractional length within contactor

Greek Symbols

α : coefficient of backmixing,

α_e : overall effective coefficient of backmixing,

α_j : backmixing ratio for jth phase, that is, ratio of backflow to F_j,

Δ : difference,

ε : fractional free area of plate,

ε_t : total specific energy dissipation rate (W/kg),

ϕ $= arcsin\left(\dfrac{u_c}{2.\pi.am.f_c}\right)$, phase angle,

γ_{Aj}^{*} : activity coefficient of component A in phase j,

γ $\equiv Y_1 - \kappa X_0 = Y_{N+1} - \kappa X_N$

γ_1 $= \dfrac{\gamma}{\left(1+\alpha_y+\alpha_x \kappa/m\right)}$,

η_e : extraction efficiency

η_v : volumetric efficiency (/h),

η_j : stage efficiency of phase j,

η_{Mj} : Murphree efficiency based on phase j

η_o : overall efficiency

φ : volumetric ratio of the dispersed phase (hold-up),

κ $\equiv F_x/F_y = \dfrac{(Y_1 - Y_{N+1})}{(X_0 - X_N)}$,

λ_A : extent of association of component A,

μ : viscosity (Pa.s)

θ $= t\,F/\varphi$, dimensionless time,

ρ : density (kg/m^3),

σ : interfacial tension (N),

ϖ $= \dfrac{\left[\alpha_y m + (1+\alpha_x)\kappa\right]}{\left(1+\alpha_y+\alpha_x \kappa/m\right)}$, slope of the inner operating line,

ψ : specific throughput (m^3/m^{2}h),

Subscripts

A : component A, the solute to be removed from the feedstream

B : component B, the solute that is to remain in the raffinate

c : continuous phase

d : dispersed phase

E : extract

F : feed

I : Y-phase inlet end, within contactor

n : typical stage

N : last stage (i.e. adjacent to feed)

o : feed inlet/extract outlet end of extractor

O : X-phase inlet end, within contactor

R : raffinate

S : solvent

Superscripts

I : Y-phase inlet end, external to contactor

O : Y-phase inlet end, external to contactor

* : equilibrium value

' : solute free basis

APPENDIX B: THEORY

Appendix B.1: General Theory

Partition coefficient

$$m_A = \frac{C_{A,E}^{*}}{C_{A,R}^{*}} \qquad \textbf{(B-1)}$$

Selectivity

$$sel_{A/B} = \frac{m_A}{m_B} \qquad \textbf{(B-2)}$$

Activity

$$a_A^{*} = \gamma_{A,R}^{*}.C_{A,R}^{*} = \gamma_{A,E}^{*}.C_{A,E}^{*} \qquad \textbf{(B-3)}$$

Extraction efficiency of A (extract)

$$\eta_{e,A,E} = \left(\frac{M_E.C_{A,E}}{M_F.C_{A,F}}\right).100 \qquad \textbf{(B-4)}$$

Extraction efficiency of A (raffinate)

$$\eta_{e,A,R} = \left(\frac{M_F C_{A,F} - M_R.C_{A,R}}{M_F.C_{A,F}}\right).100 \qquad \textbf{(B-5)}$$

Extraction efficiency of $\eta_{e,HA,E} = \left(1 - \frac{M_R.C_{HA,R}}{M_E.C_{HA,E} - M_S.C_{HA,S} + M_R.C_{HA,R}}\right).100$ **(B-6)**

protonated species

Association equilibrium constant

$$k_{ass} = \frac{C_{A,\delta}}{(C_{A,\xi})^2} \qquad \textbf{(B-7)}$$

Extent of association

$$C_{A,\xi} = C_{A,E}(1 - \lambda_A) \qquad \textbf{(B-8)}$$

$$C_{A,\delta} = \tfrac{1}{2} C_{A,E}(\lambda_A) \qquad \textbf{(B-9)}$$

Equilibrium data relationship

$$C_{A,E} = \tfrac{1}{2} k_{ass}\, m_A^{\,2}\, C_{A,R}^{\,2} + m_A\, C_{A,R} \qquad \textbf{(B-10)}$$

Overall partition coefficient

$$m_A' = \frac{C_{HA,E} + C_{A-,E}}{C_{HA,R} + C_{A-,R}} \qquad \textbf{(B-11)}$$

Partition coefficient protonated species

$$m_{HA} = \frac{C_{HA,E}}{C_{HA,R}} \qquad \textbf{(B-12)}$$

Terminal settling velocity

$$U_{\infty} = \left(\frac{2\Delta\rho\, g_c\, r}{9\mu_C} \right) f\left(\frac{\mu_D}{\mu_C}, \frac{r\sigma}{W} \right) \qquad \textbf{(B-13)}$$

Appendix B.2: Acid - Base Theory

De-protontion equilibrium constant

$$Ka_A = \frac{C_{A^-}.C_{H^+}}{C_A} \qquad \textbf{(B-14)}$$

Extent of de-protonation

$$D_A = \frac{C_{A^-}}{C_A} = \frac{C_{A^-}}{C_{HA} + C_{A^-}} \qquad \textbf{(B-15)}$$

pH

$$pH = -log(C_{H^+}) \qquad \textbf{(B-16)}$$

pKa

$$pKa = -log(Ka) \qquad \textbf{(B-17)}$$

Extent of de-protonation

$$D_A = \frac{1}{10^{pKa_A - pH} + 1} \qquad \textbf{(B-18)}$$

Appendixx B.3: Column Theory

Agitation intensity

$$I_a = \frac{am.rpm}{Ps} \qquad \textbf{(B-19)}$$

Specific throughput

$$\psi = \frac{F}{CSA} \qquad \textbf{(B-20)}$$

Volumetric efficiency

$$\eta_v = \frac{\psi}{HETS} \qquad \textbf{(B-21)}$$

Steady state volume replacements

$$SSV = \frac{F_{TOT}}{V_{TOT}} \qquad \textbf{(B-22)}$$

APPENDIX C: DERIVATIONS

Appendix C.1 Expression for Extent of De-protonation as a Function of pKa and pH

Consider the de-protonation of an acid in an aqueous solution:

$$A \xleftrightarrow{Ka_A} A^- + H^+ \qquad \textbf{(C-1)}$$

The de-protonation of any particular acid will have an equilibrium constant, (*Ka*), which is a measure of the extent of de-protonation at equilibrium:

$$Ka_A = \frac{C_{A^-}.C_{H^+}}{C_A} \qquad \textbf{(C-2)}$$

The extent of de-protonation is defined as follows:

$$D_A = \frac{C_{A^-}}{C_{A_{TOT}}} = \frac{C_{A^-}}{C_A + C_{A^-}} \qquad \textbf{(C-3)}$$

By incorporating **Equations C-2** and **C-3**, and the definitions of *pH* and *pKa*, it is possible to derive the following equation, which relates the extent of de-protonation to the pKa of the component and the pH of the system:

$$D_A = \frac{1}{10^{pKa_A - pH} + 1} \qquad \textbf{(C-4)}$$

Appendix C.2: Expression to Describe Equilibrium Data

Derivation of expression for concentration of protonated species in organic phase as a function of concentration of protonated species in organic phase, the partition coefficient of protonated, undimerised A and the association equilibrium constant:

Consider that component A forms a dimer in the organic phase:

$$2A_\xi \xleftrightarrow{k_{ass}} A_\delta \qquad \textbf{(C-5)}$$

The association of the component has an equilibrium constant, (k_A):

$$k_{ass} = \frac{C_{A_\delta}}{(C_{A_\xi})^2} \qquad \textbf{(C-6)}$$

By definition, the *partition coefficient* of A (excluding associated molecules) is:

$$m_A = \frac{C_{A_{\xi,E}}}{C_{A_R}} \qquad \textbf{(C-7)}$$

By defining λ_A as the extent of association in the organic phase:

$$\begin{aligned} C_A &= C_{A_E}(1-\lambda_A) \\ C_A &= \tfrac{1}{2} C_{A_E}(\lambda_A) \end{aligned} \qquad \textbf{(C-8 (a) and (b))}$$

By substituting **Equations C-8 (a)** and **(b)** into **Equation C-6** it is possible to solve for λ_A. This is substituted into **Equation C-8 (a)** and combined with **Equation C-7** to yield the following relationship:

$$C_{A_E} = \tfrac{1}{2} k_{ass} m_A^{\,2} C_{A_R}^{\,2} + m_A C_{A_R} \qquad \textbf{(C-9)}$$

APPENDIX D: STEADY STATE MODEL RESULTS

Appendix D1: Aqueous Phase Profiles

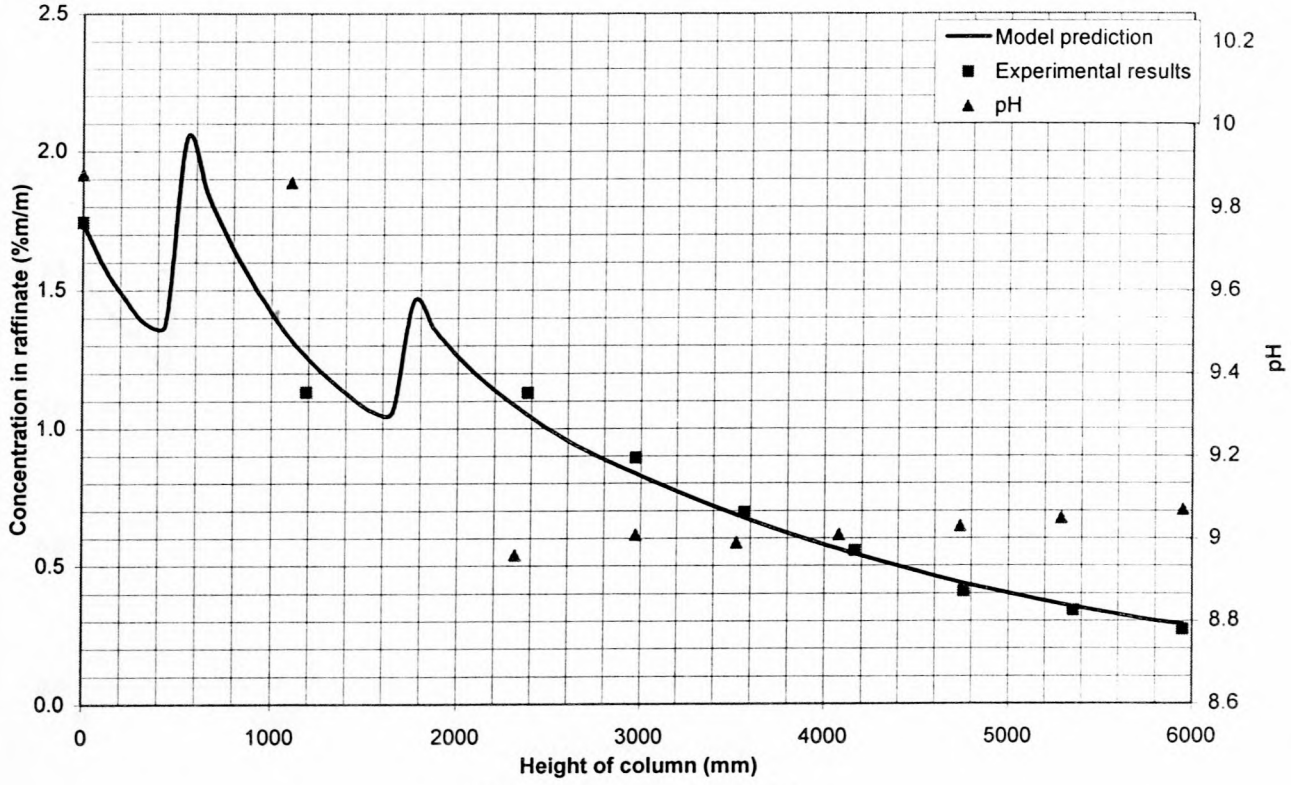

Figure D.1: Test SX-16-1

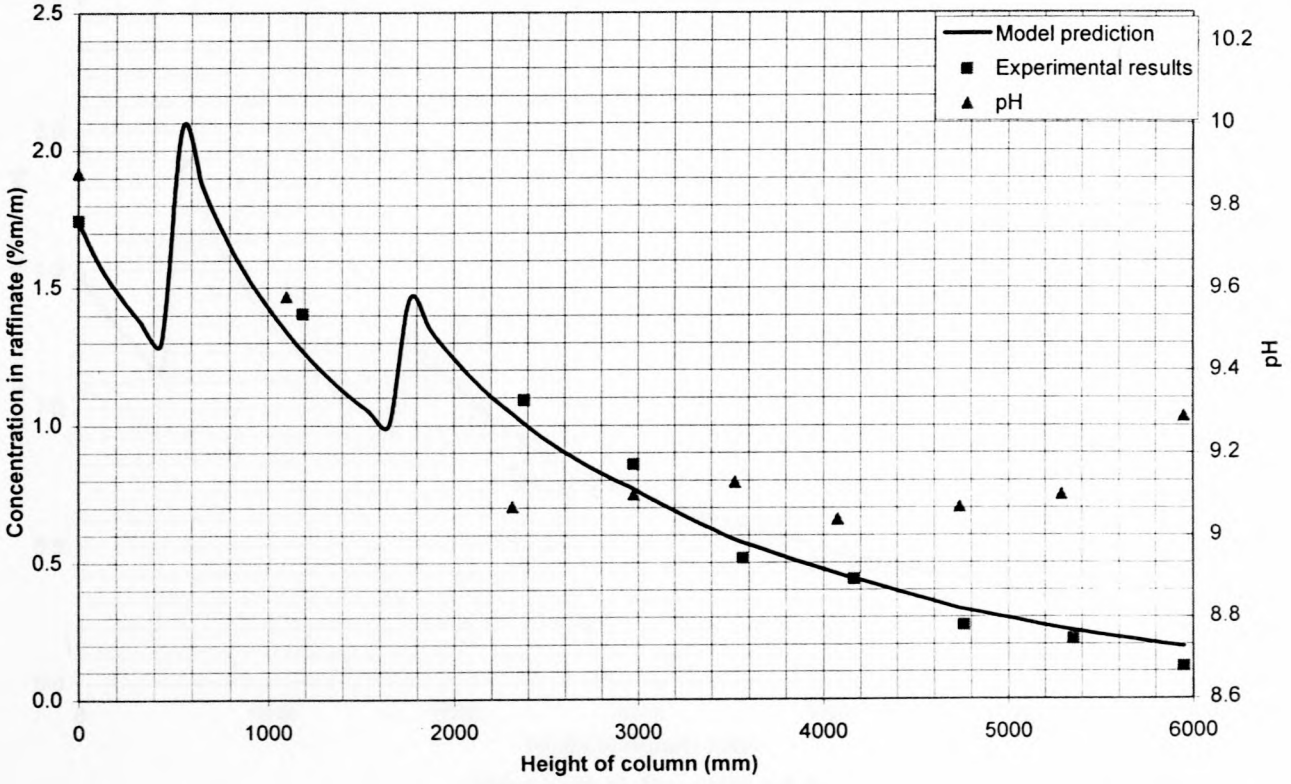

Figure D.2: Test SX-16-2

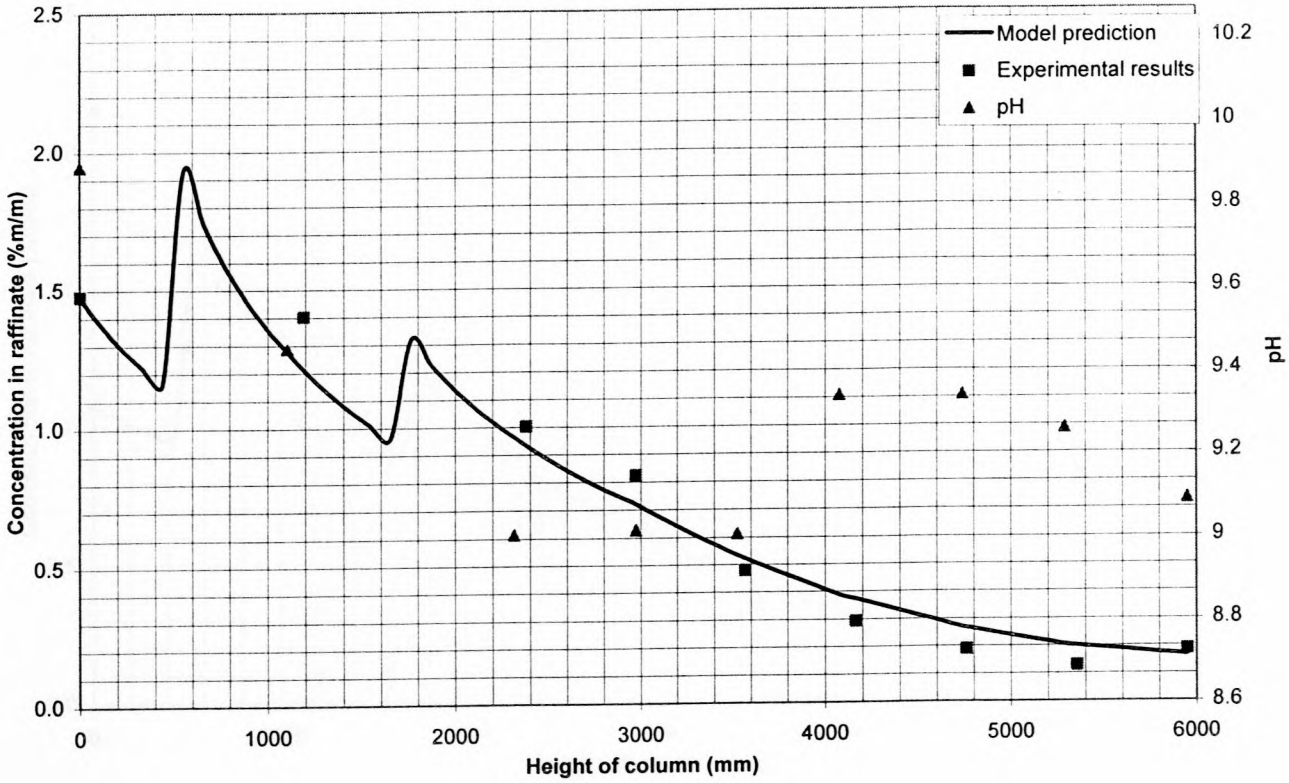

Figure D.3: Test SX-15-1

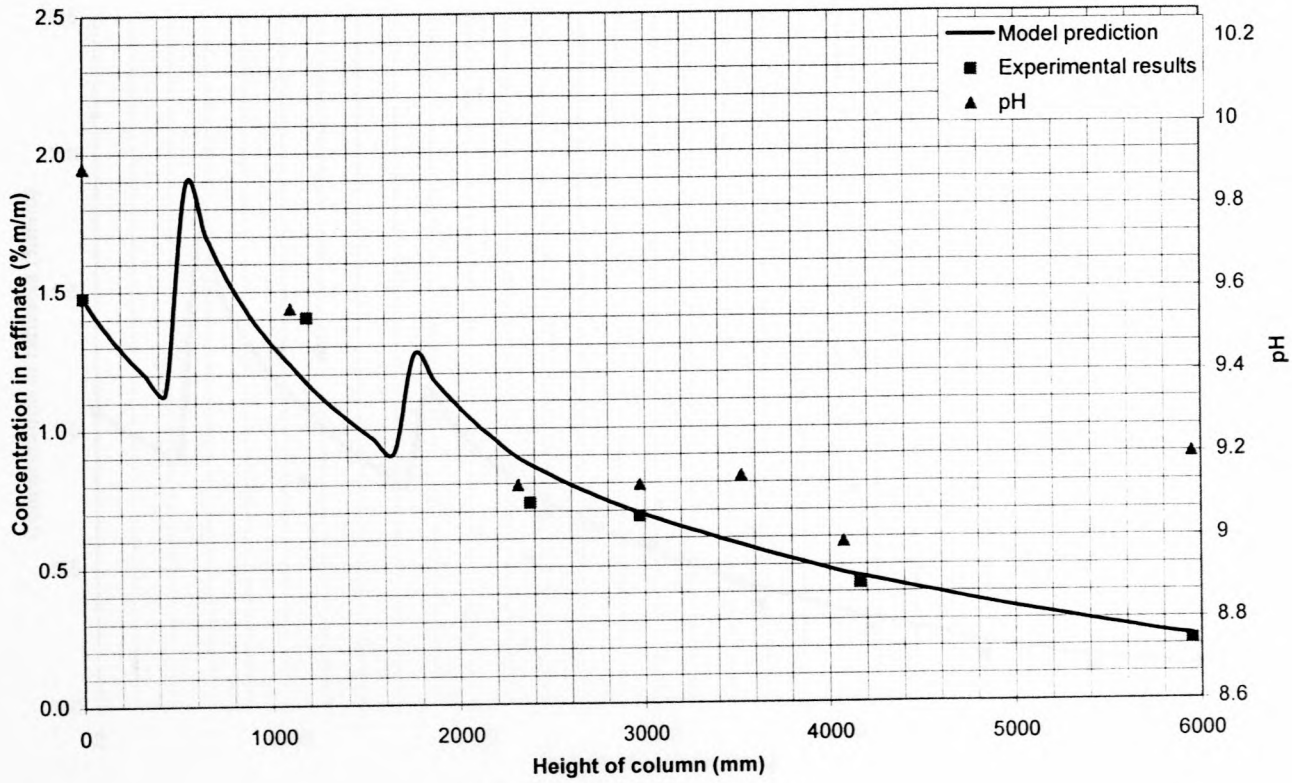

Figure D.4: Test SX-15-2

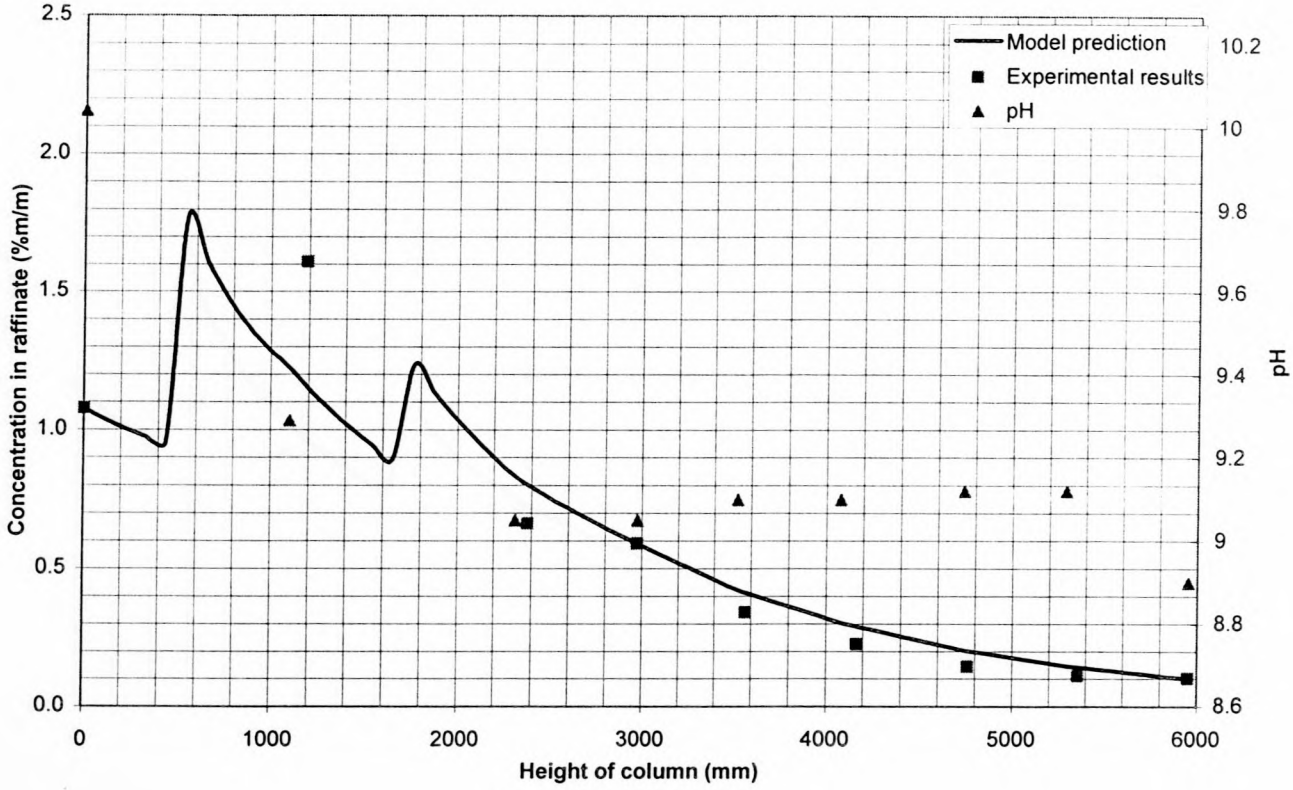

Figure D.5: Test SX-14-1

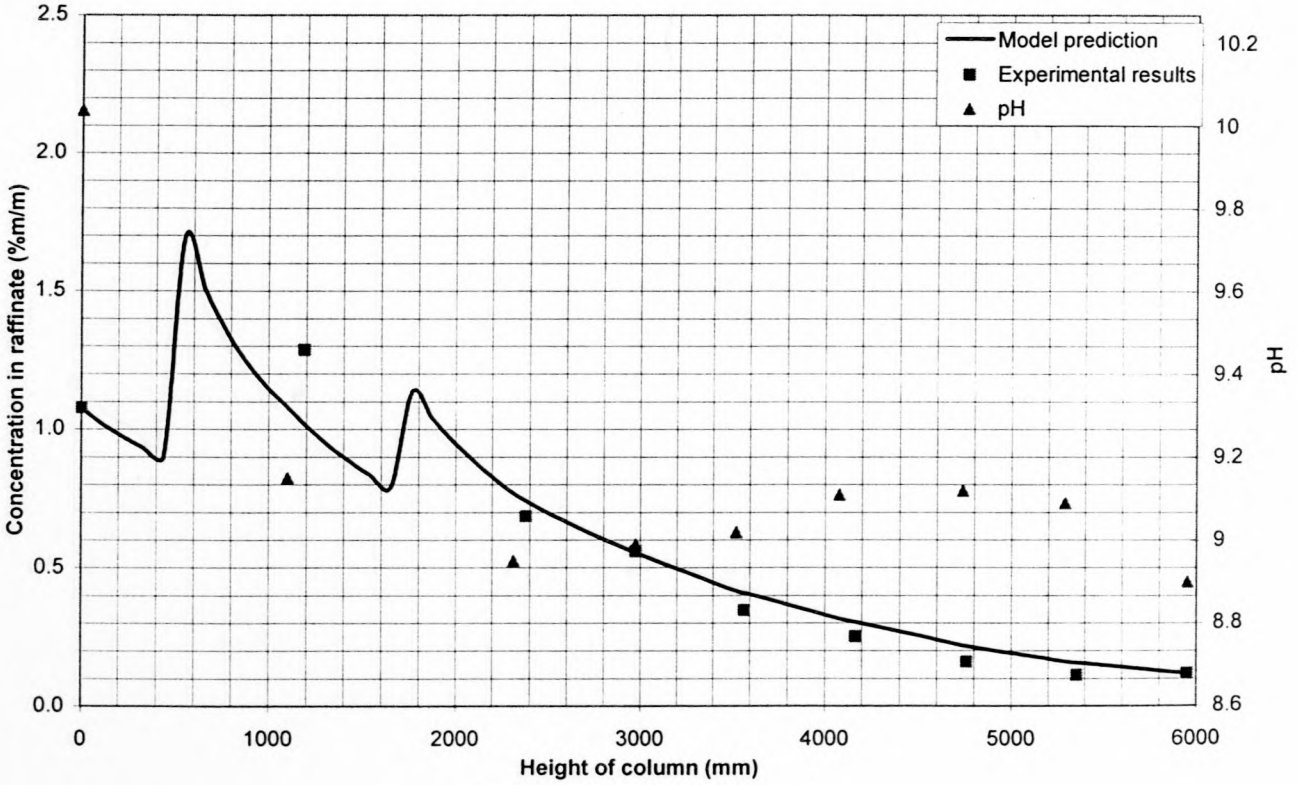

Figure D.6: Test SX-14-2

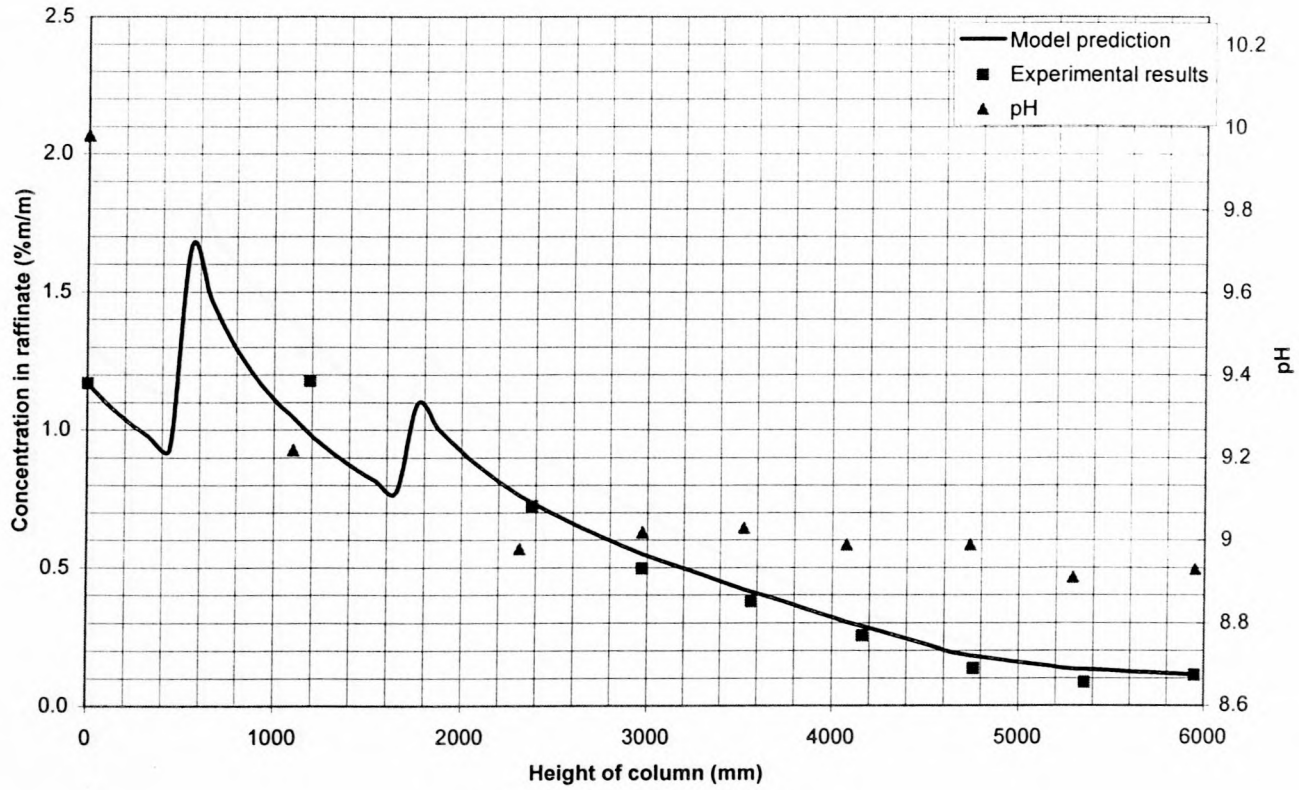

Figure D.7: Test SX-13-1

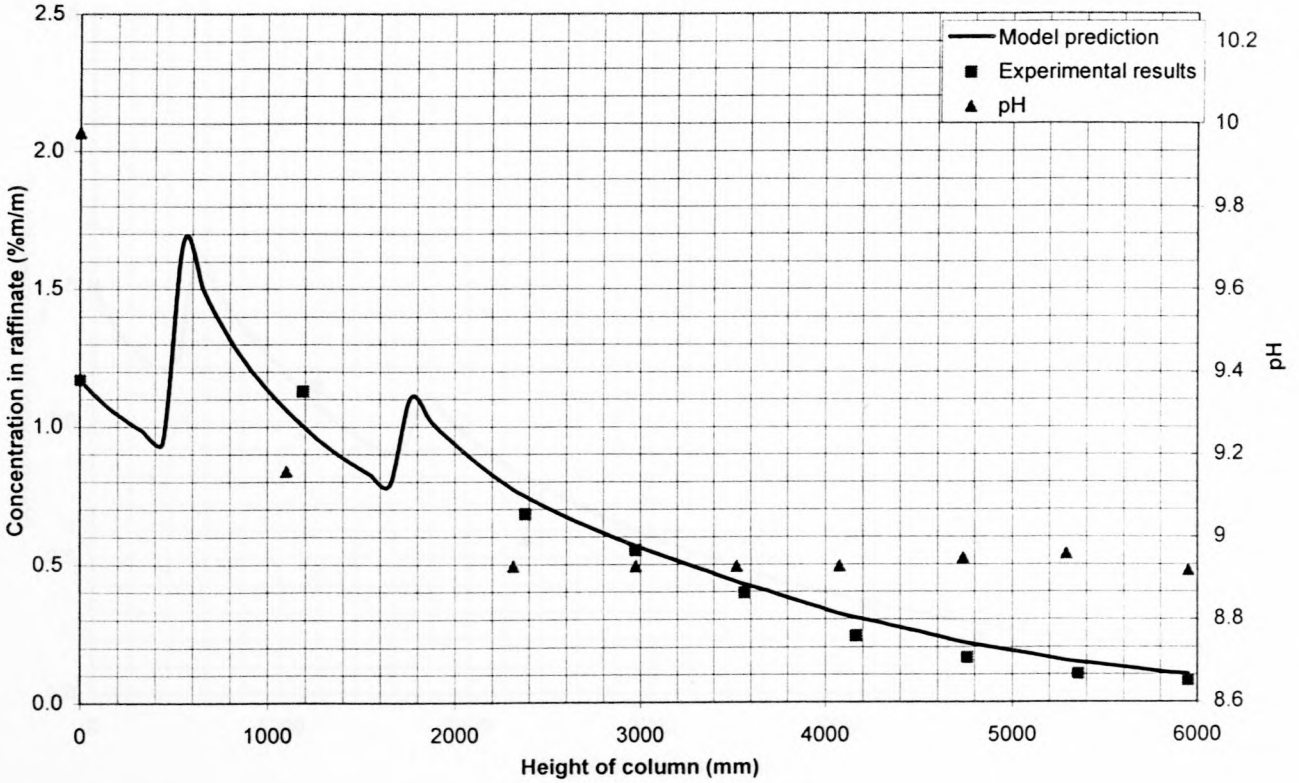

Figure D.8:Test SX-13-2

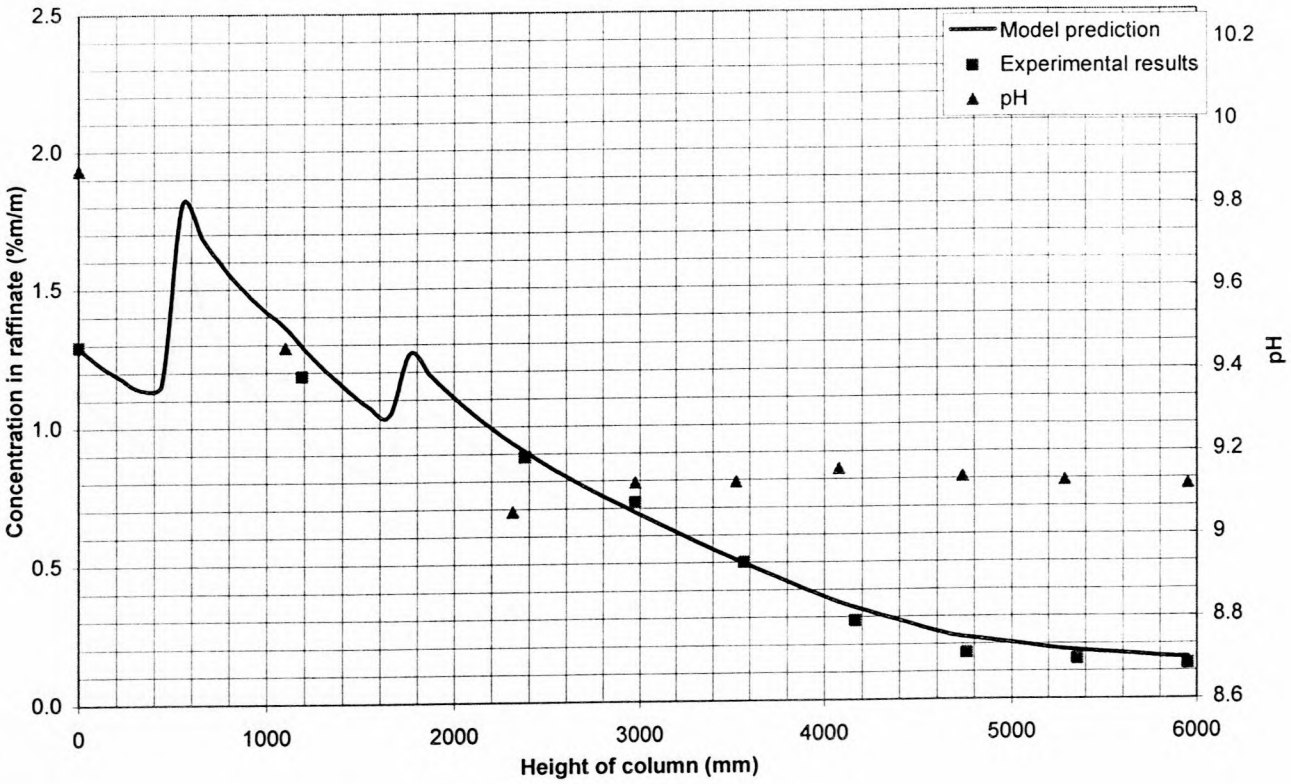

Figure D.9:Test SX-12-1

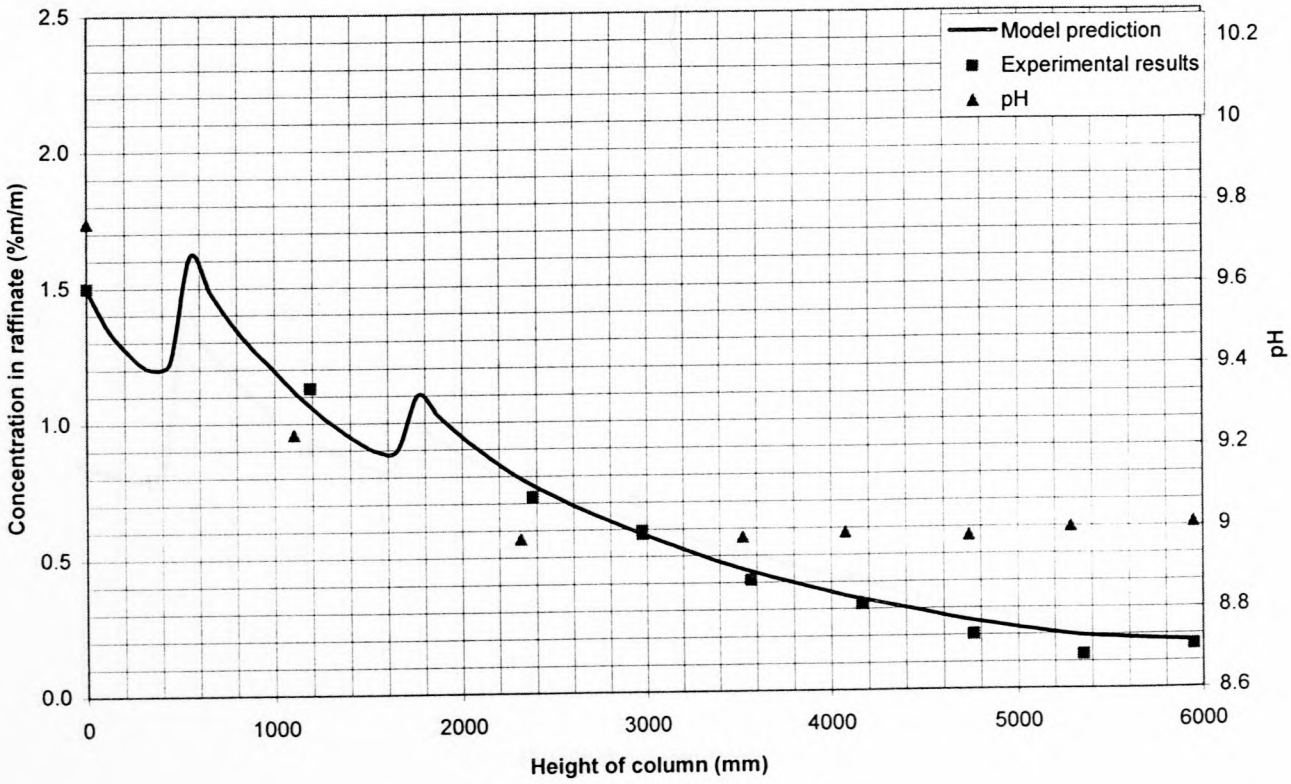

Figure D.10:Test SX-11-2

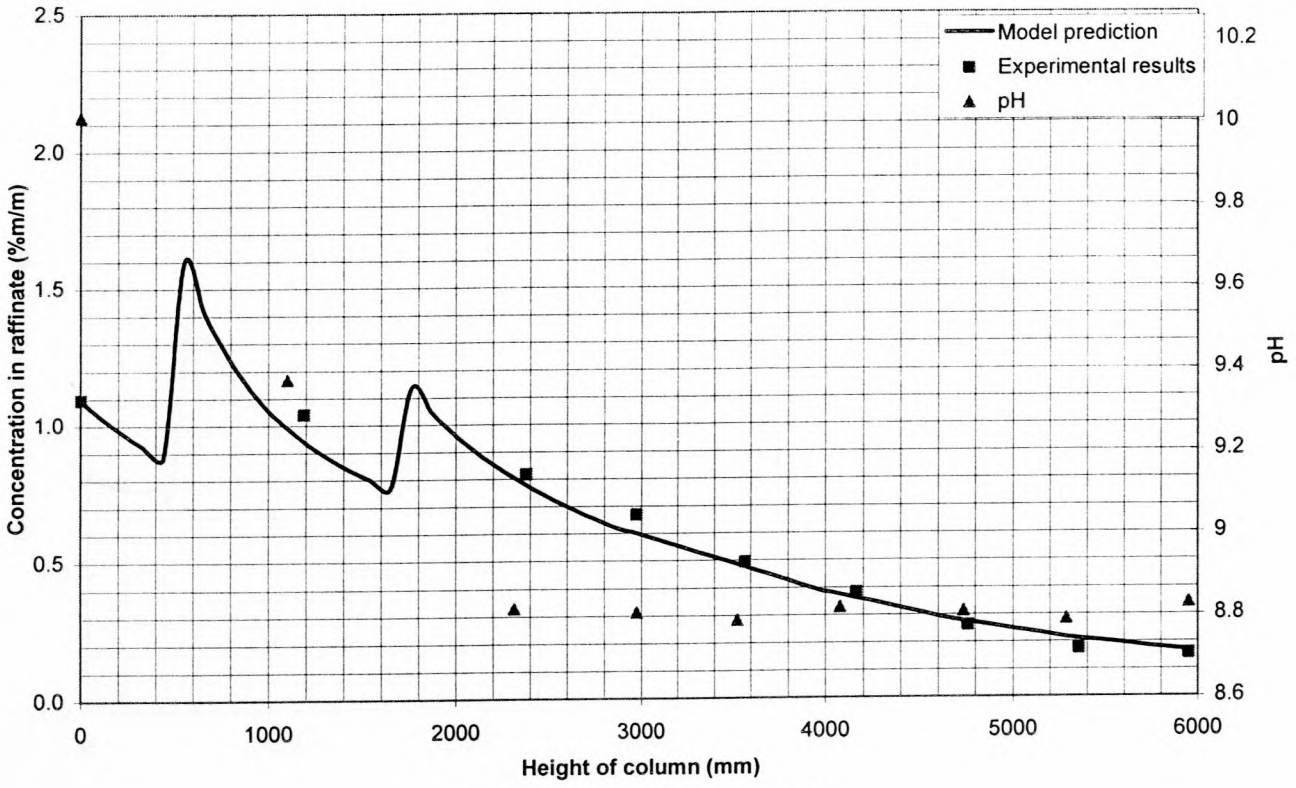

Figure D.11: Test SX-10-2

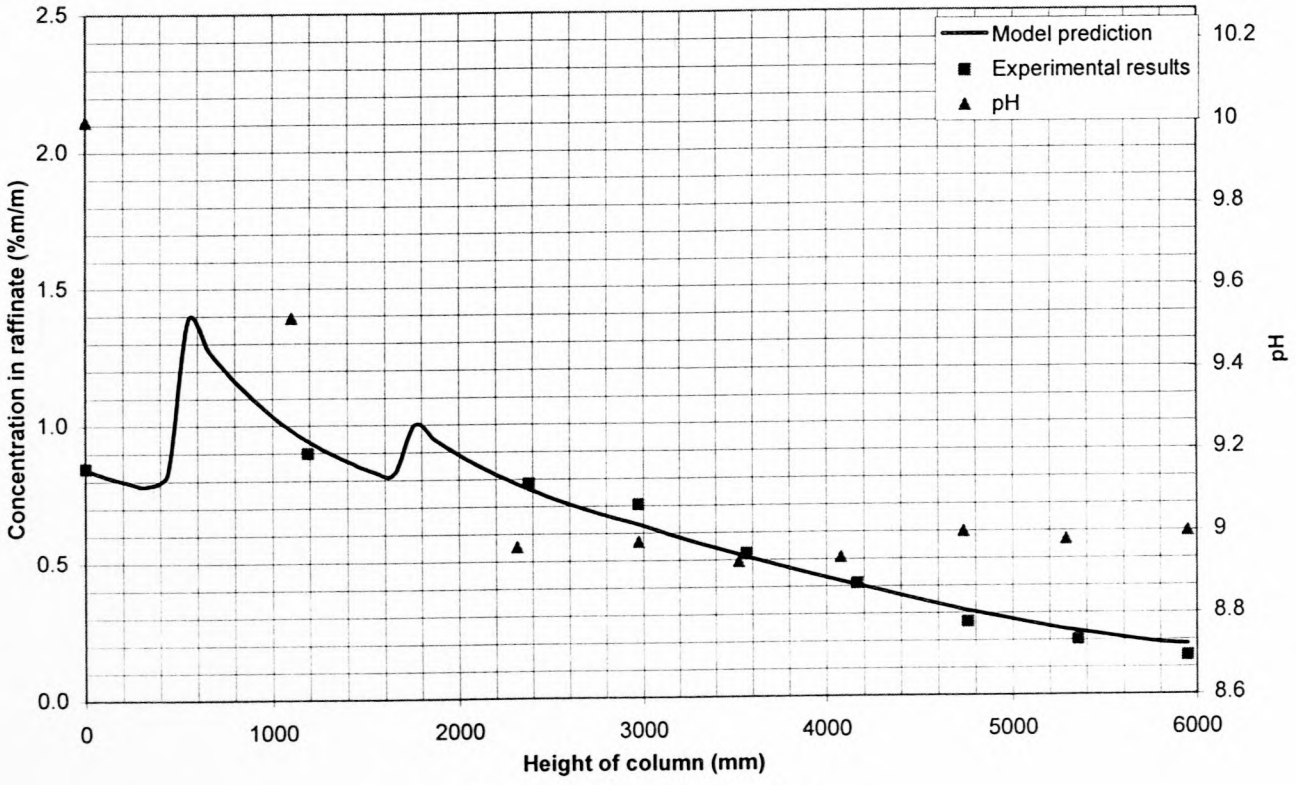

Figure D.12: Test SX-9-2

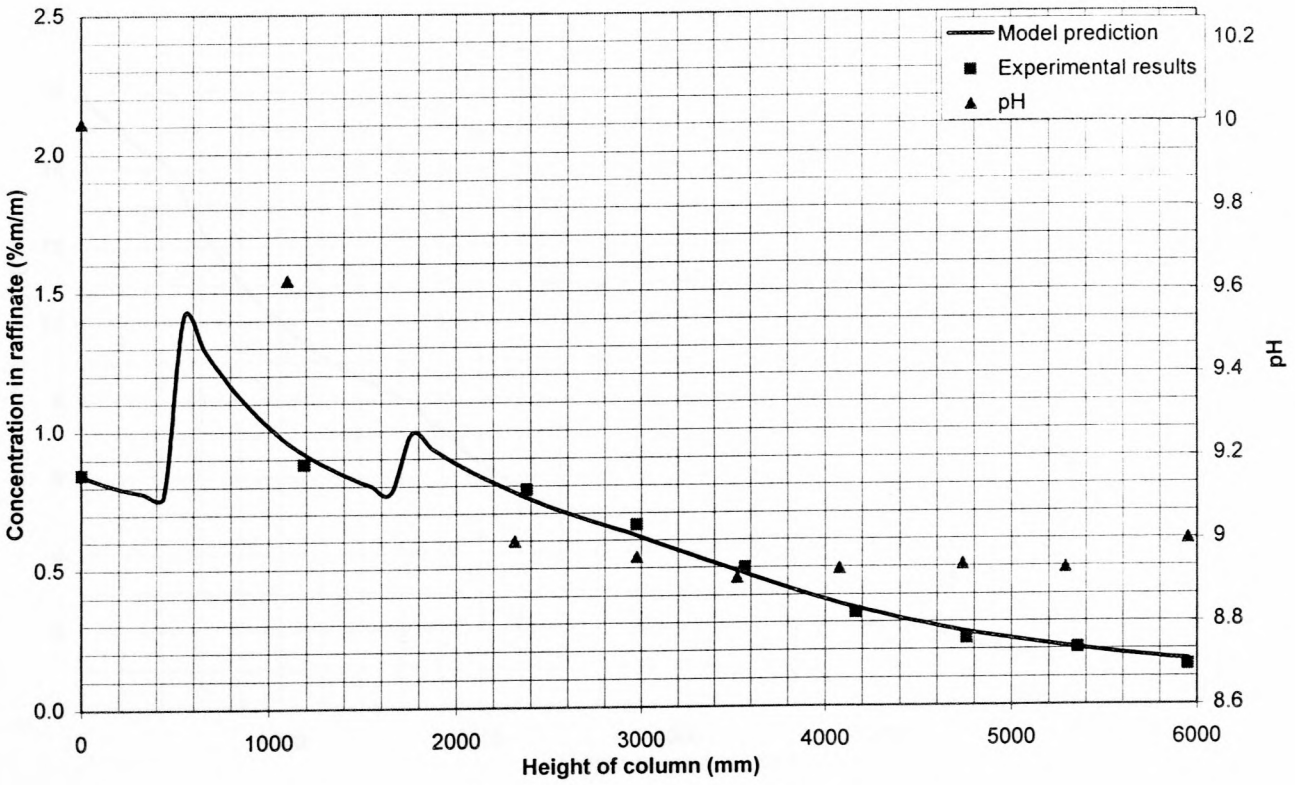

Figure D.13: Test SX-9-3

Appendix D2: Organic Phase Profiles

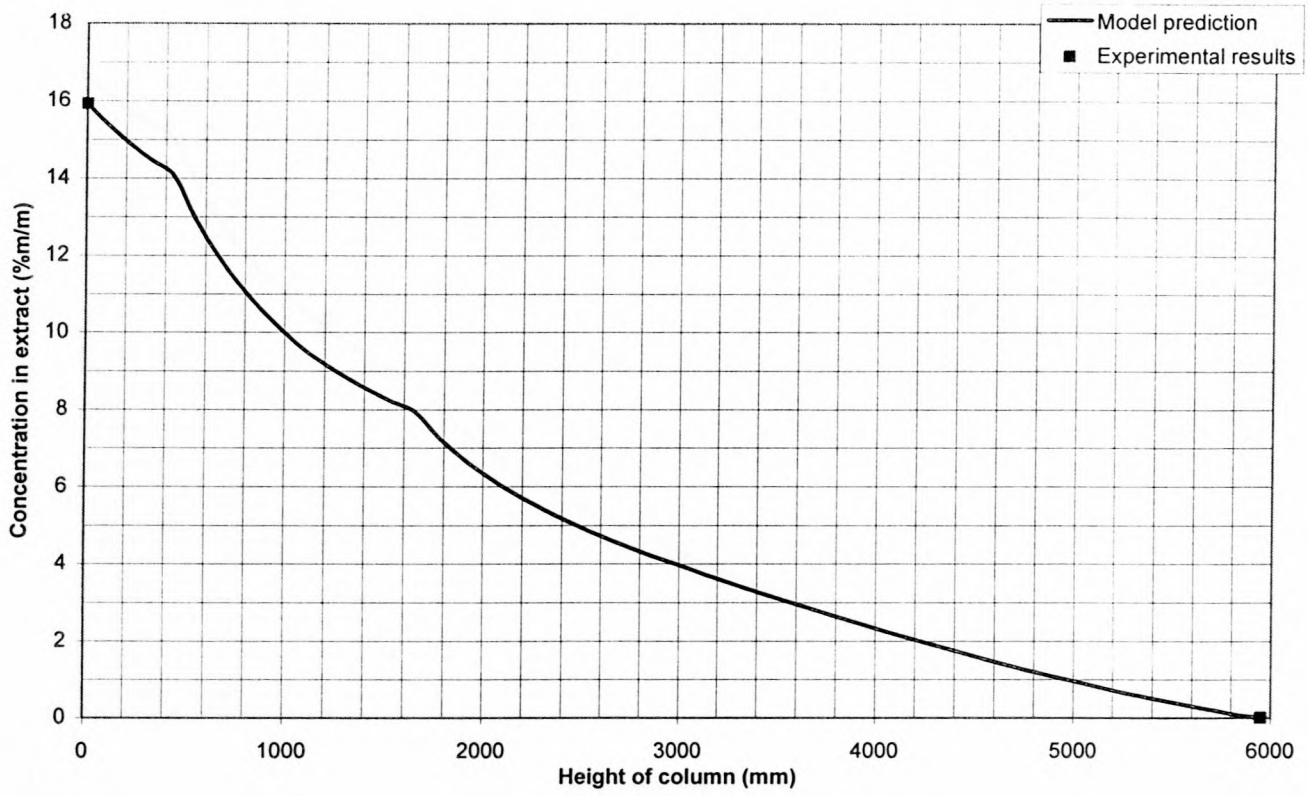

Figure D.16: Test SX-16-1

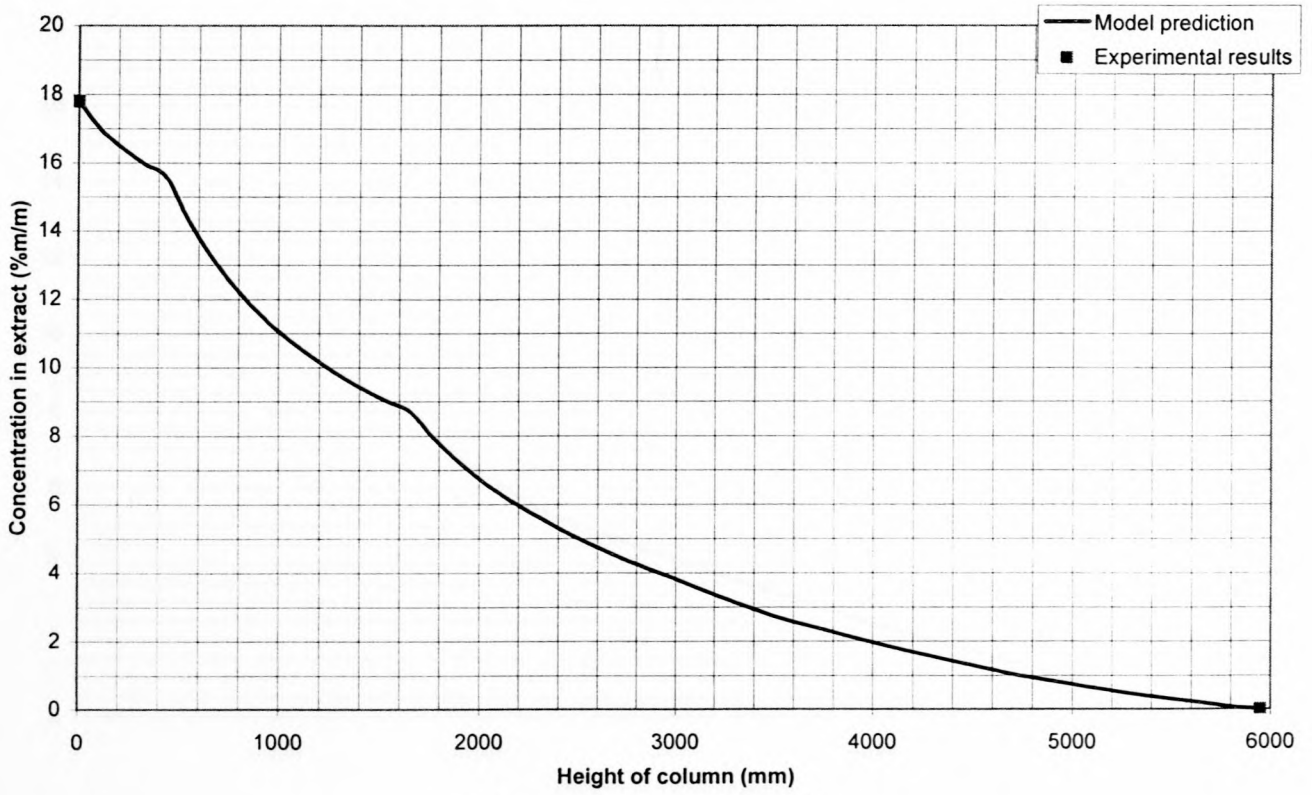

Figure D.17: Test SX-16-2

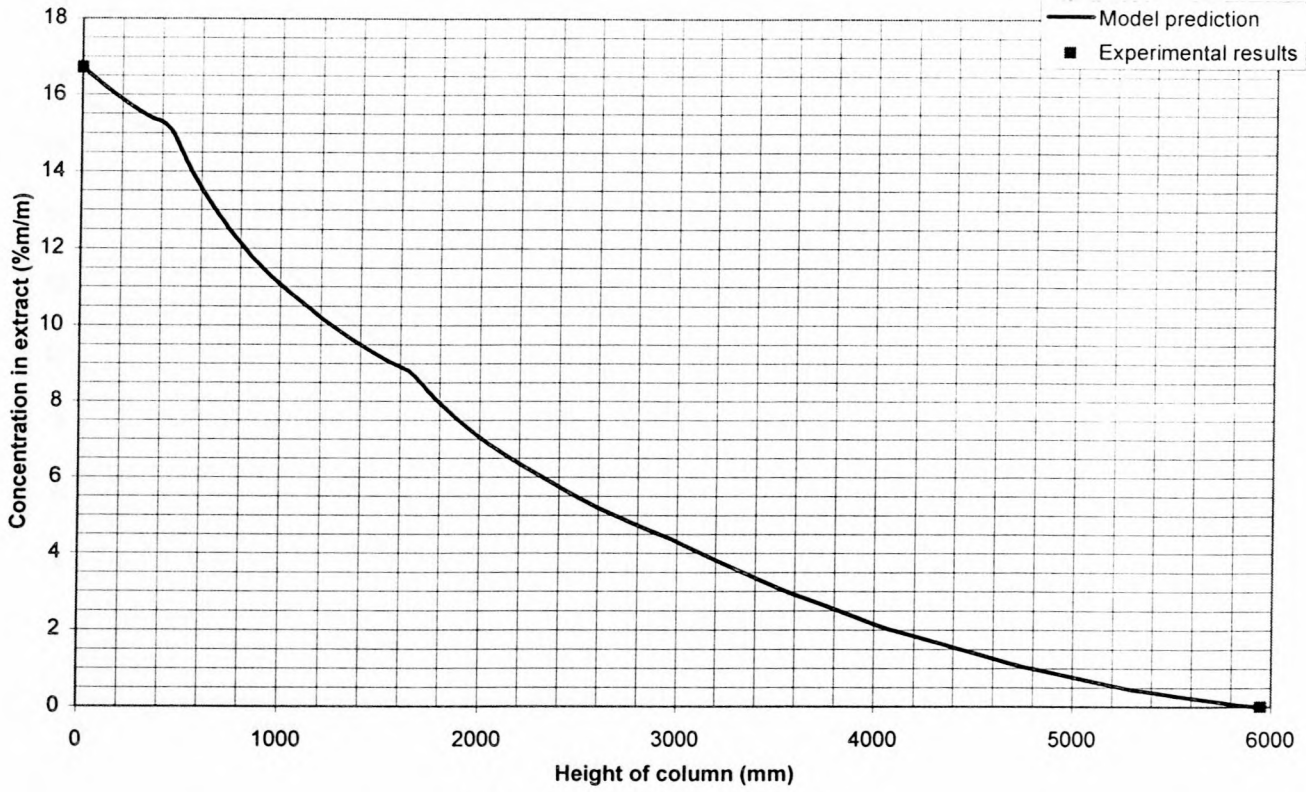

Figure D.18: Test SX-15-1

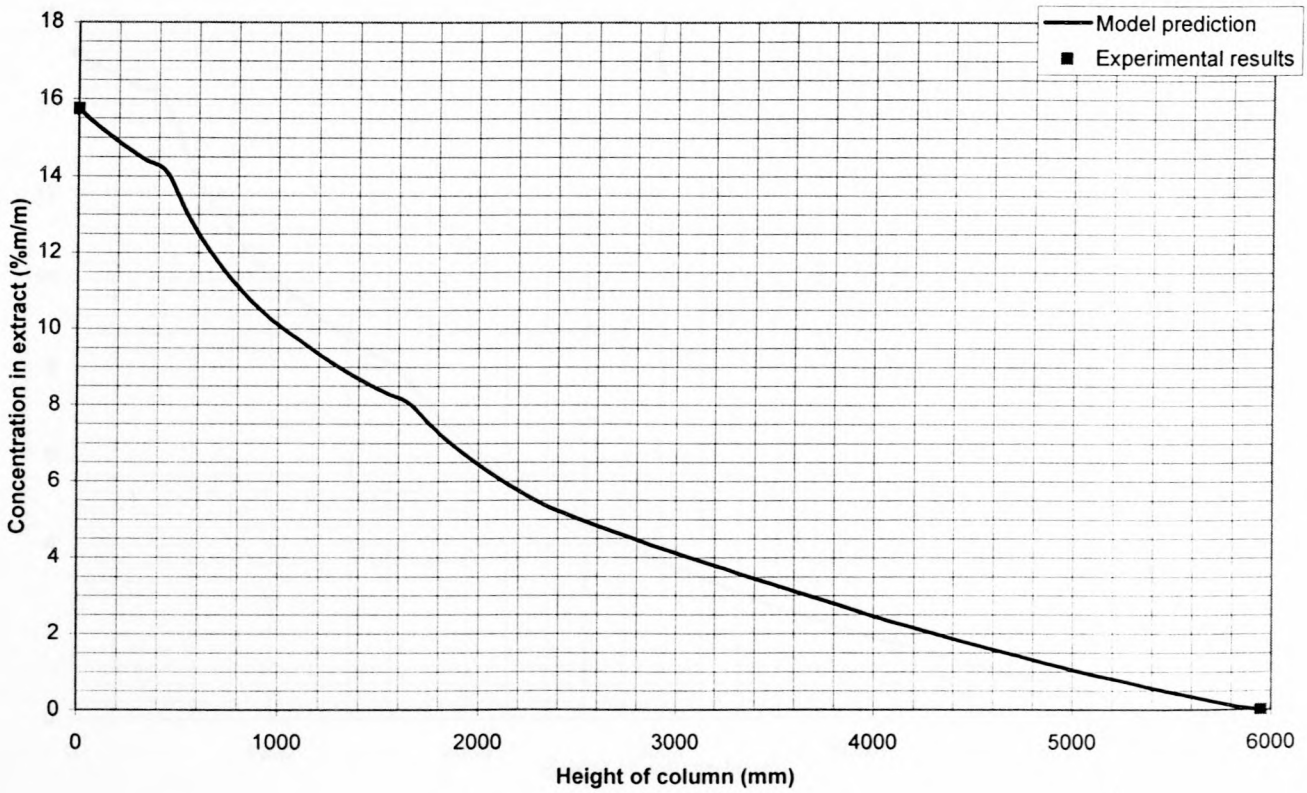

Figure D.19: Test SX-15-2

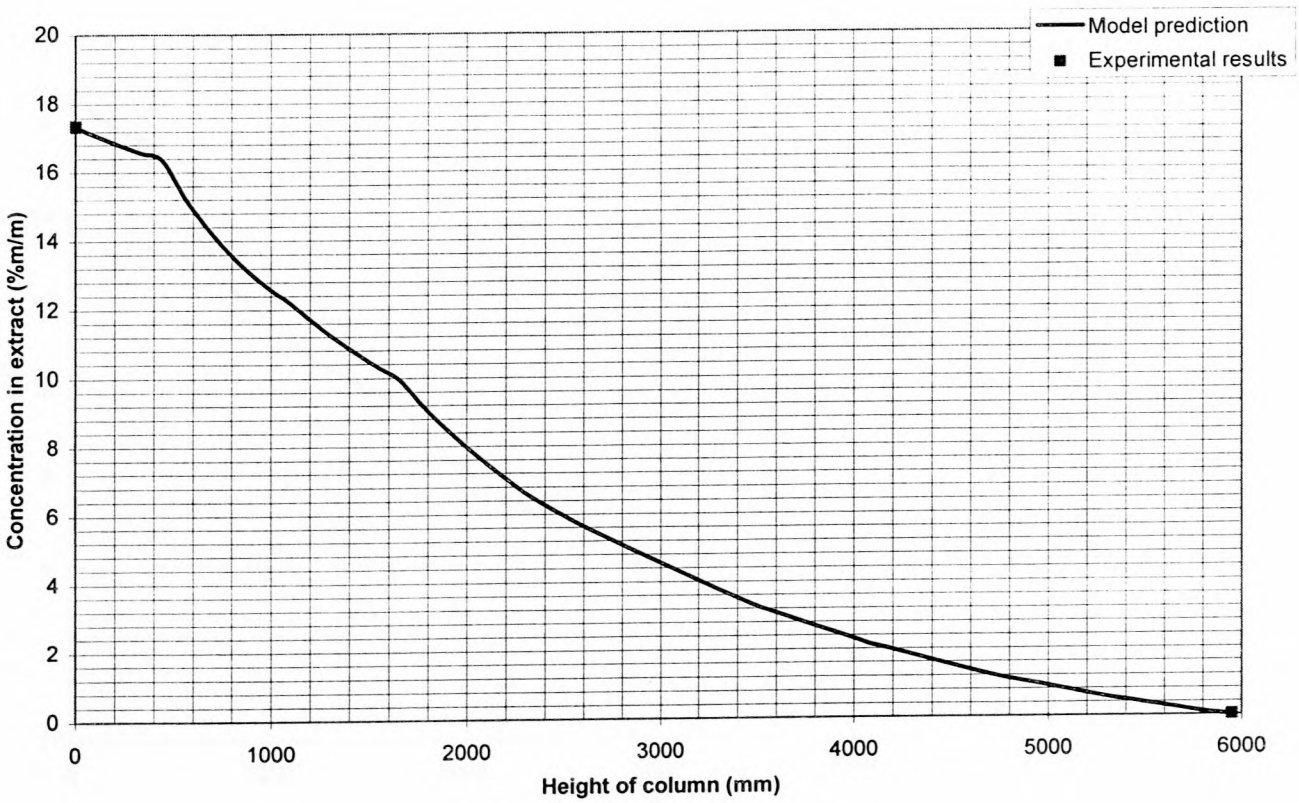

Figure D.20: Test SX-14-1

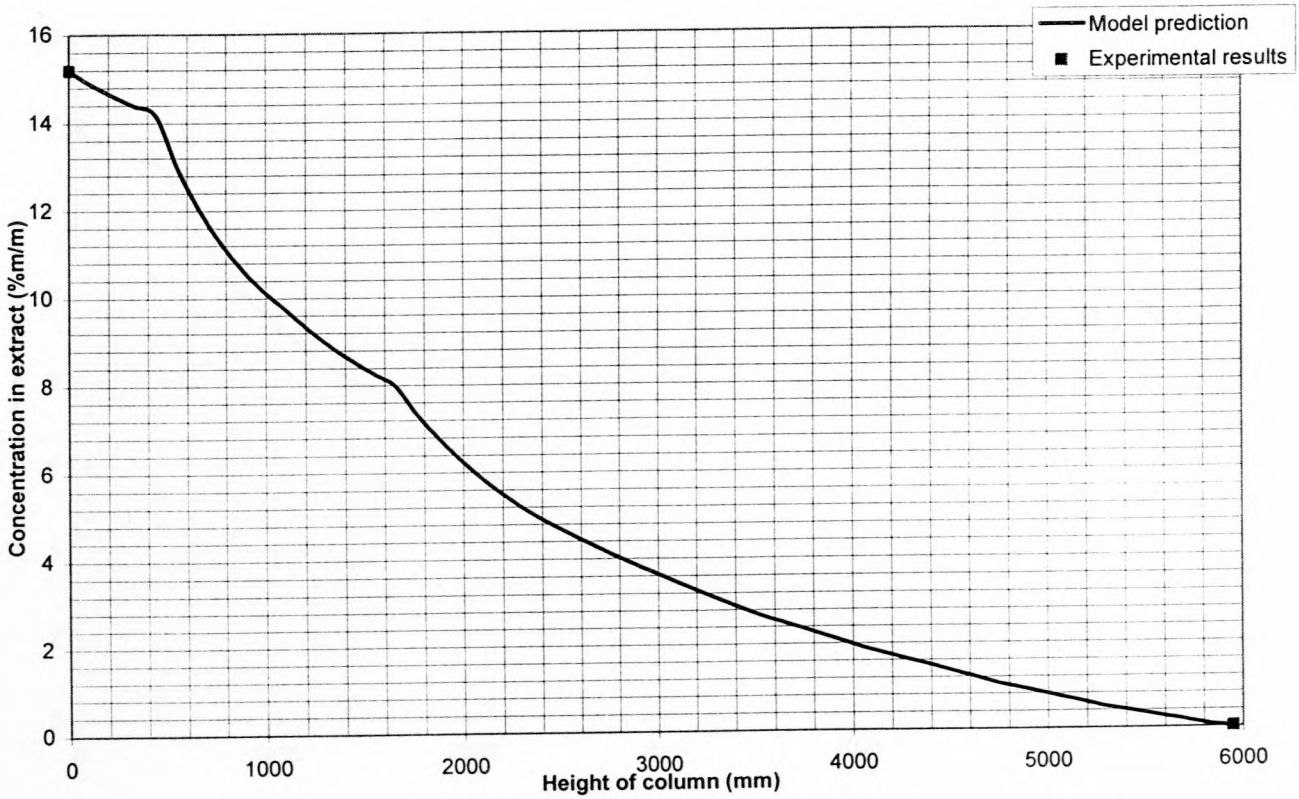

Figure D.21: Test SX-14-2

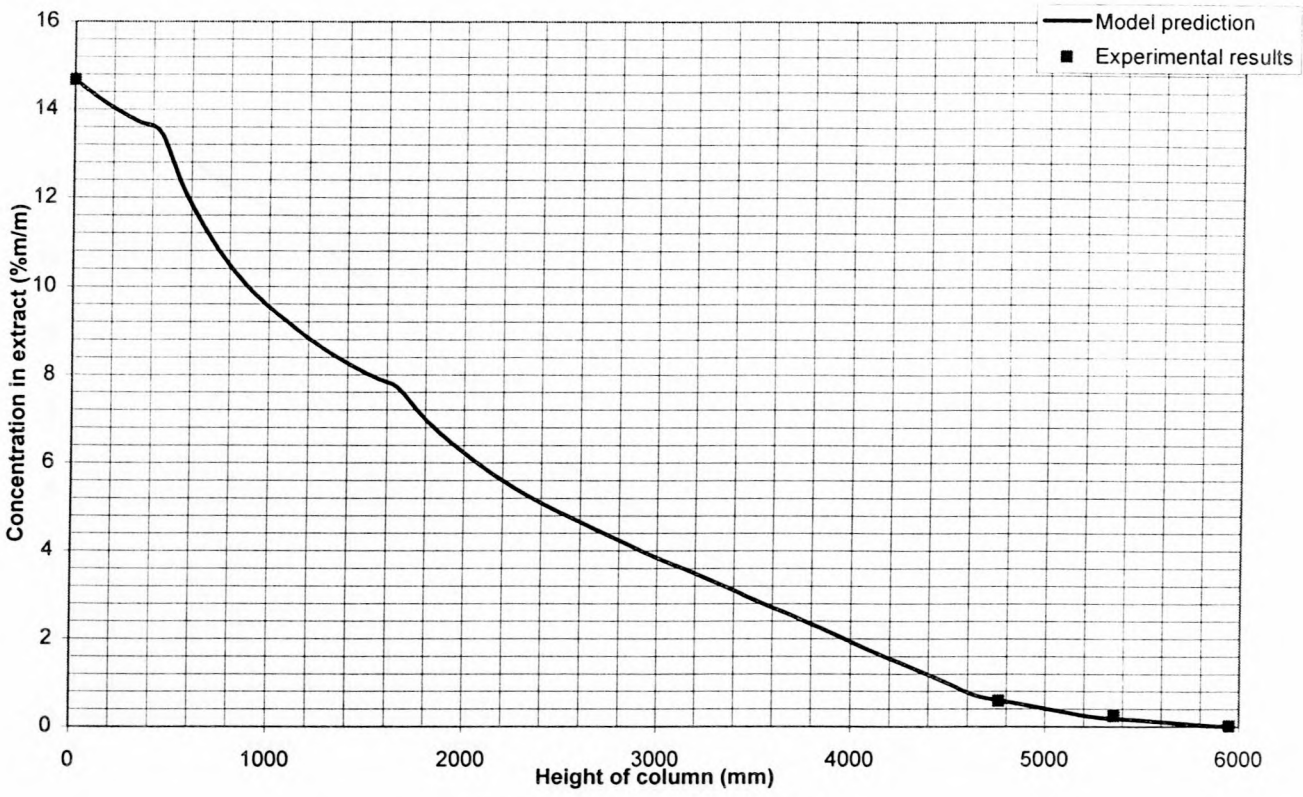

Figure D.22: Test SX-13-1

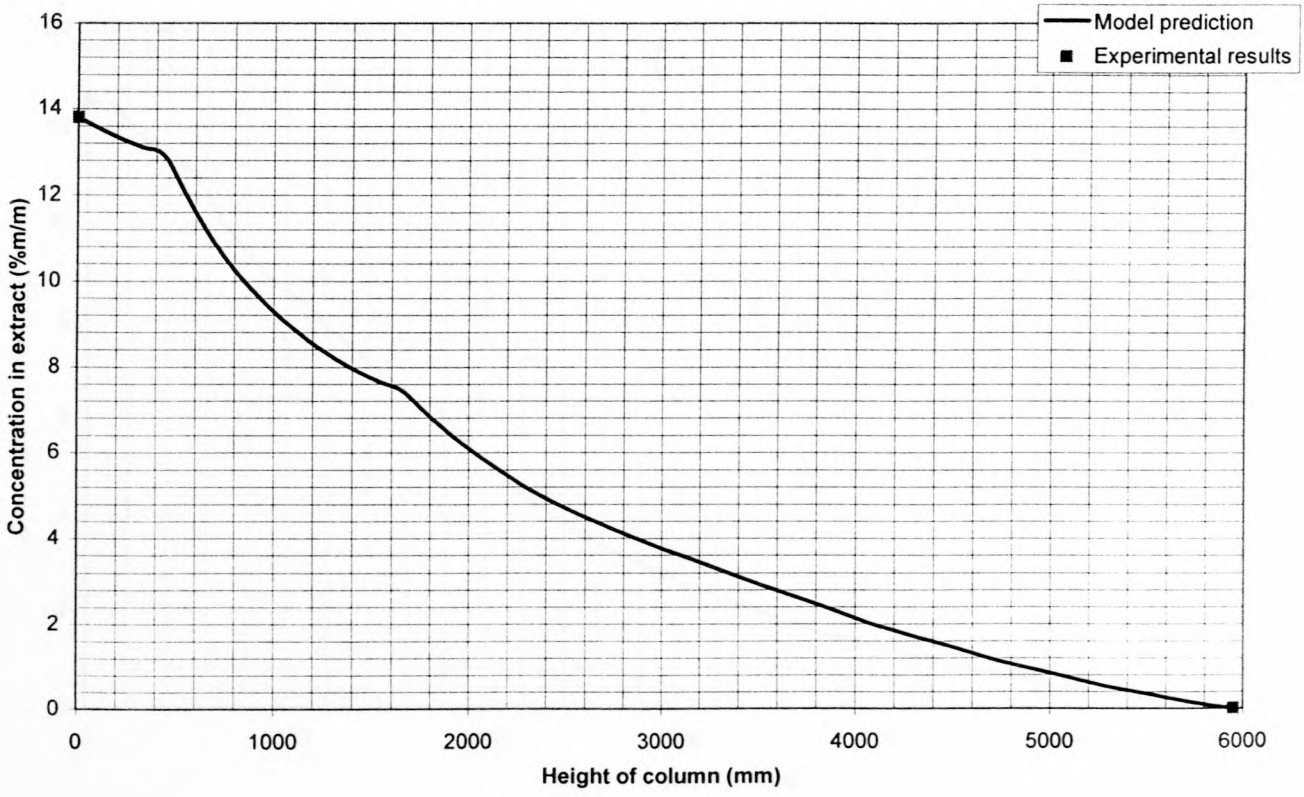

Figure D.23:Test SX-13-2

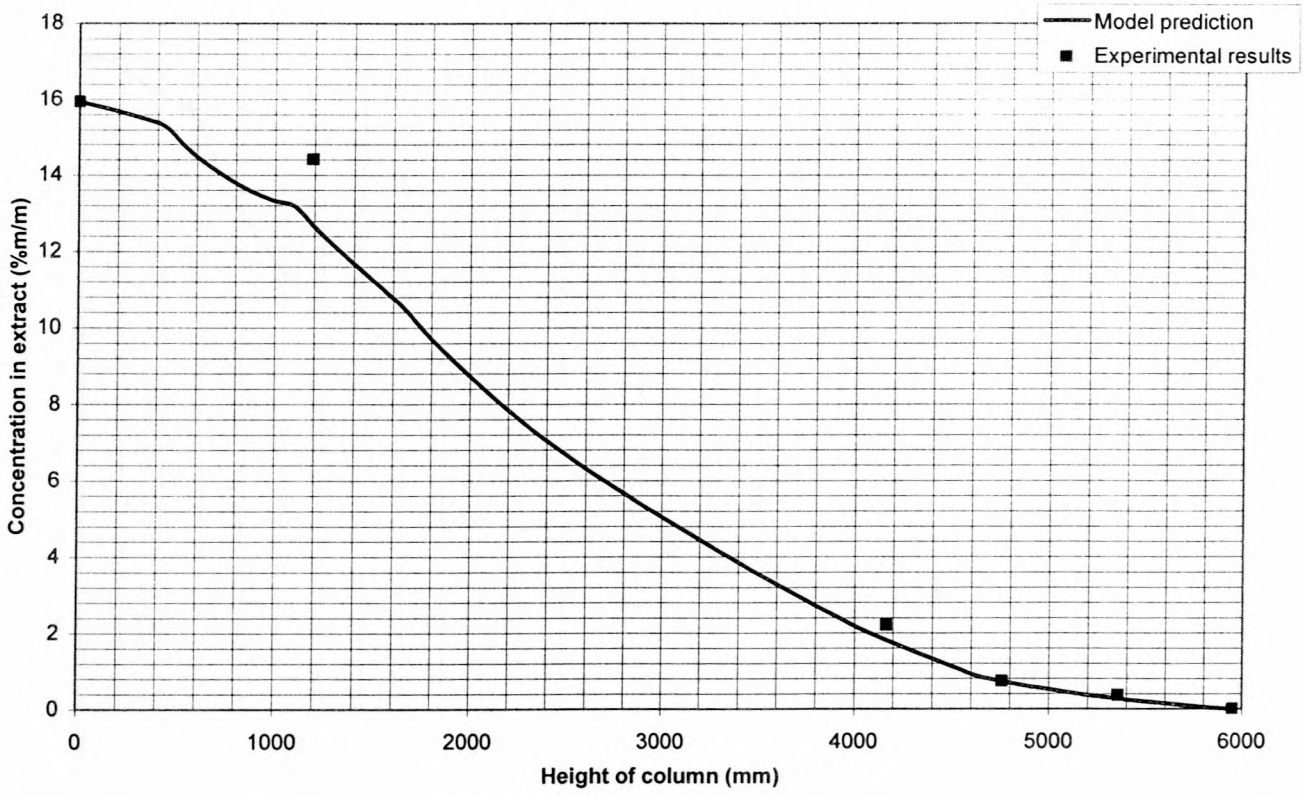

Figure D.24:Test SX-12-1

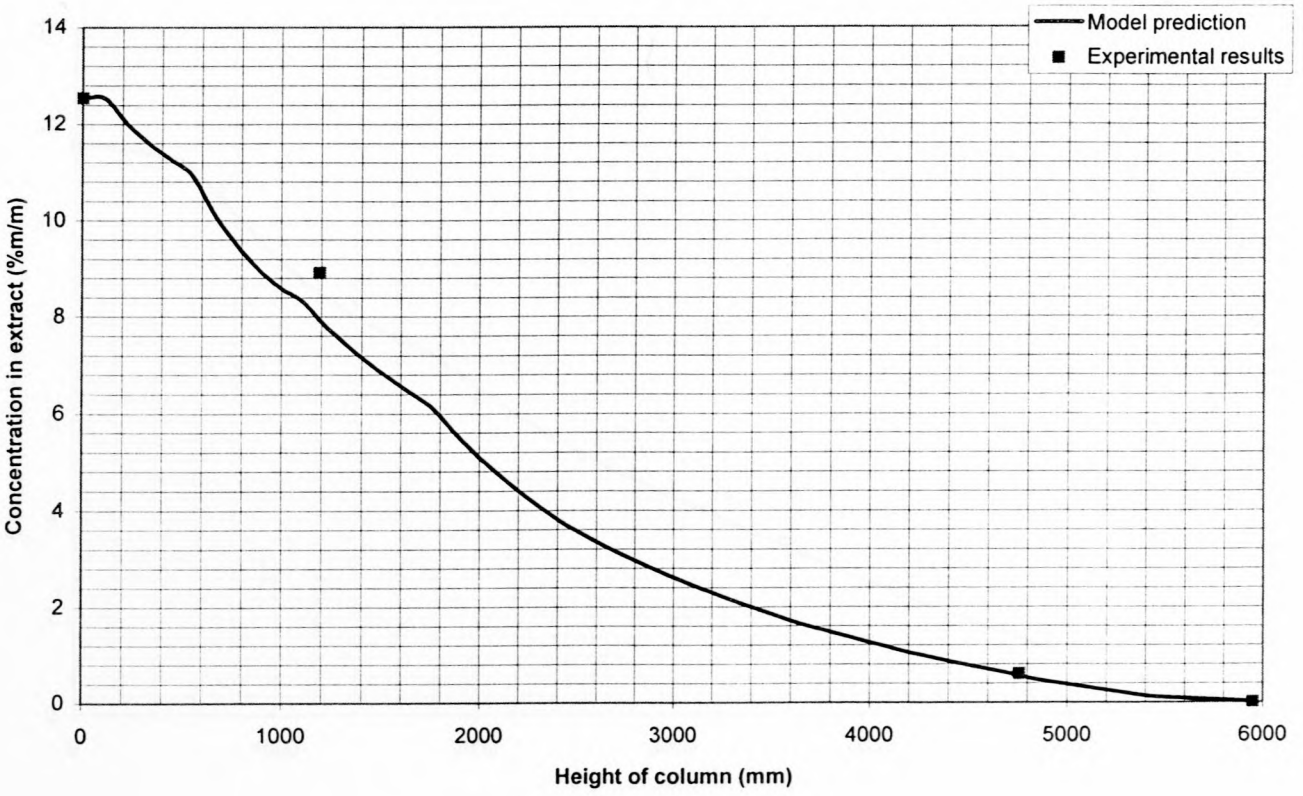

Figure D.25:Test SX-11-2

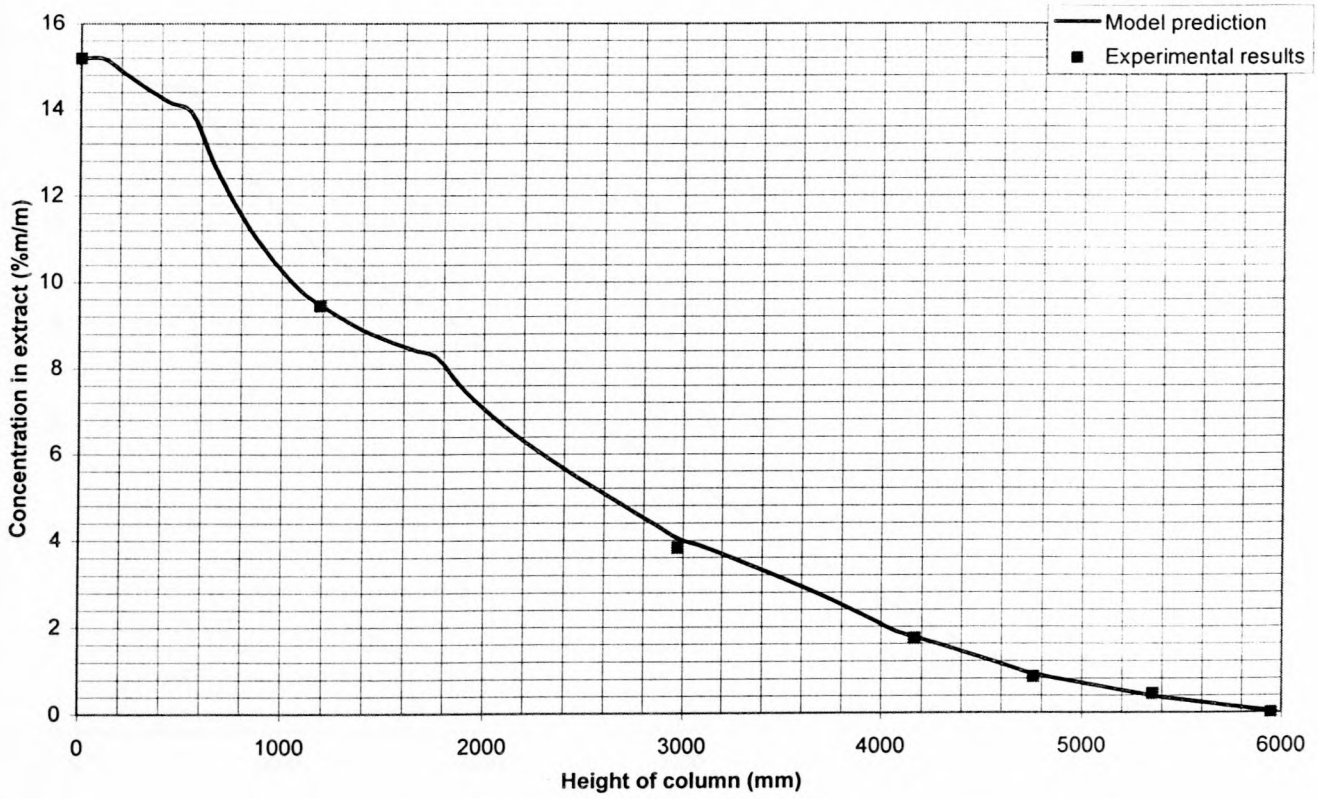

Figure D.26: Test SX-10-2

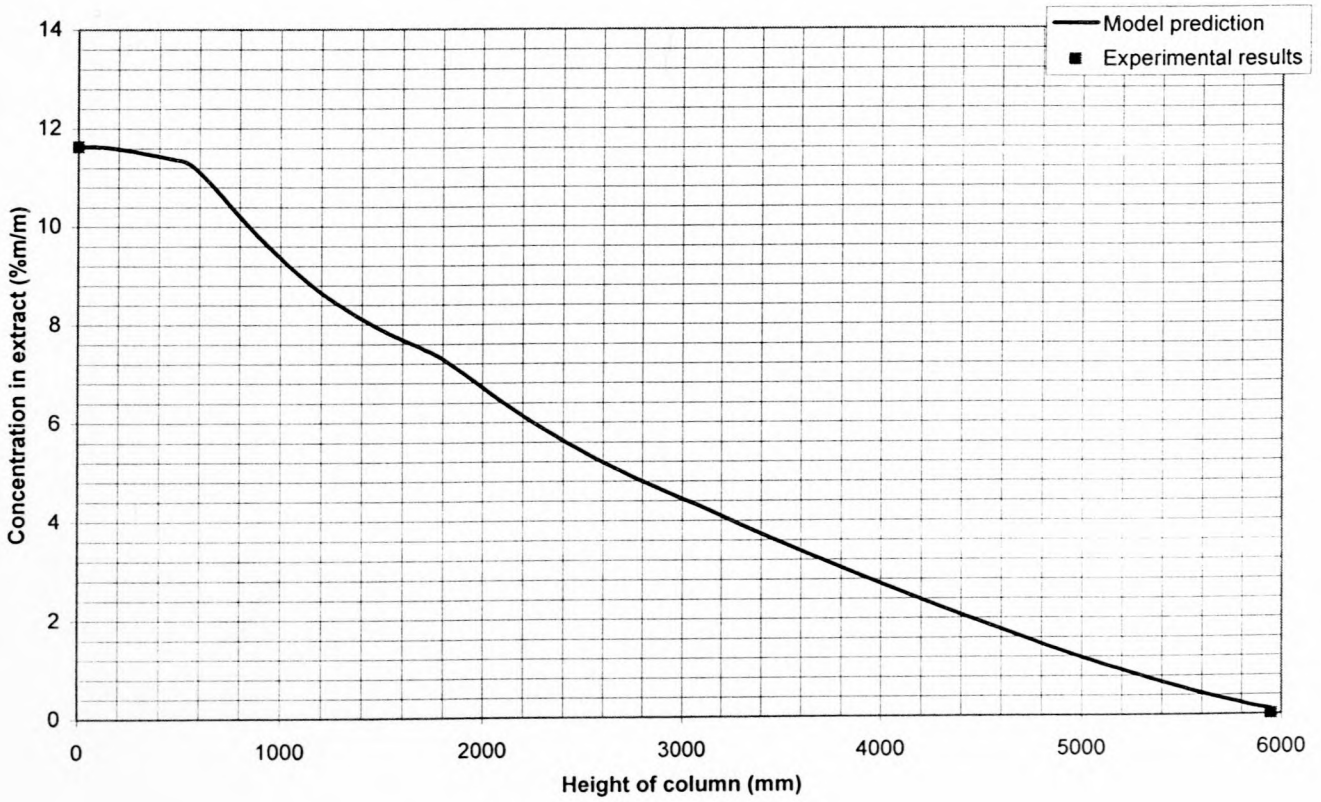

Figure D.27: Test SX-9-2

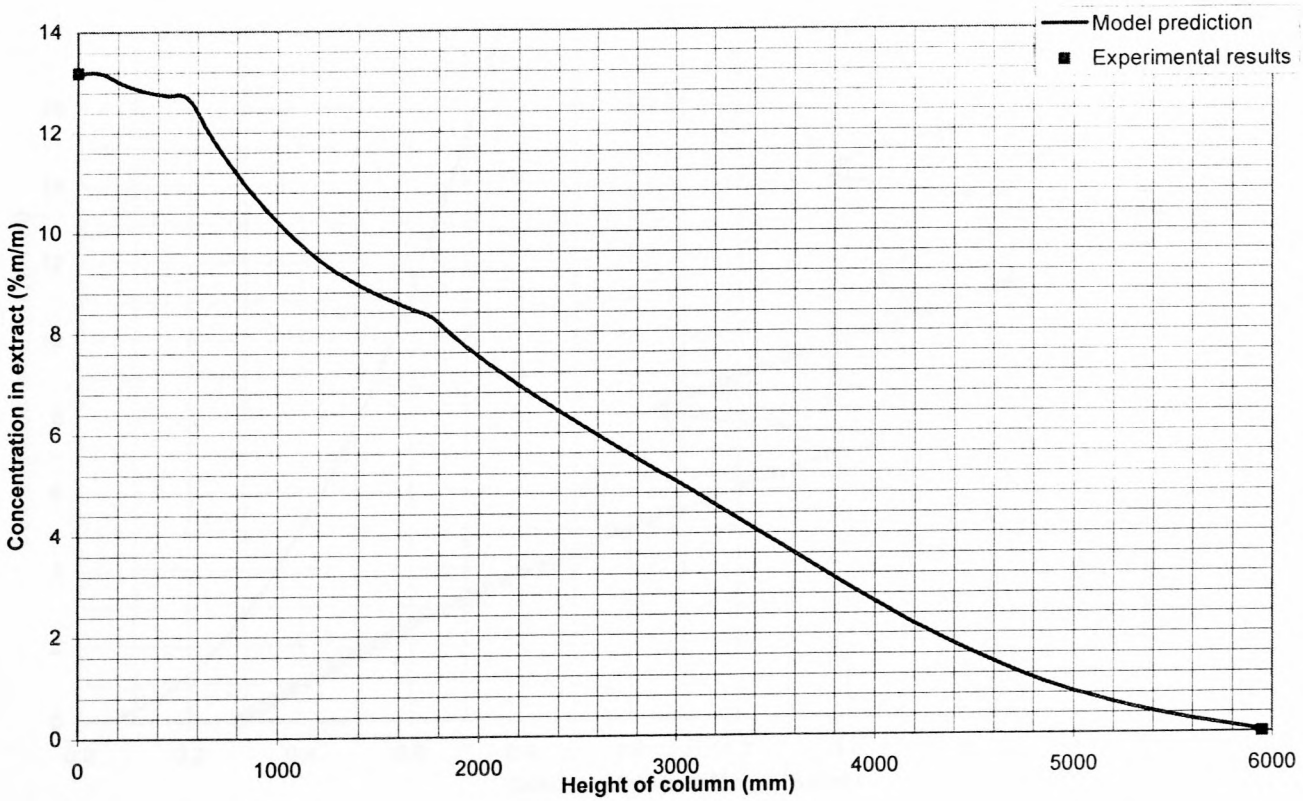

Figure D.28: Test SX-9-3

Appendix D3: Operating Lines

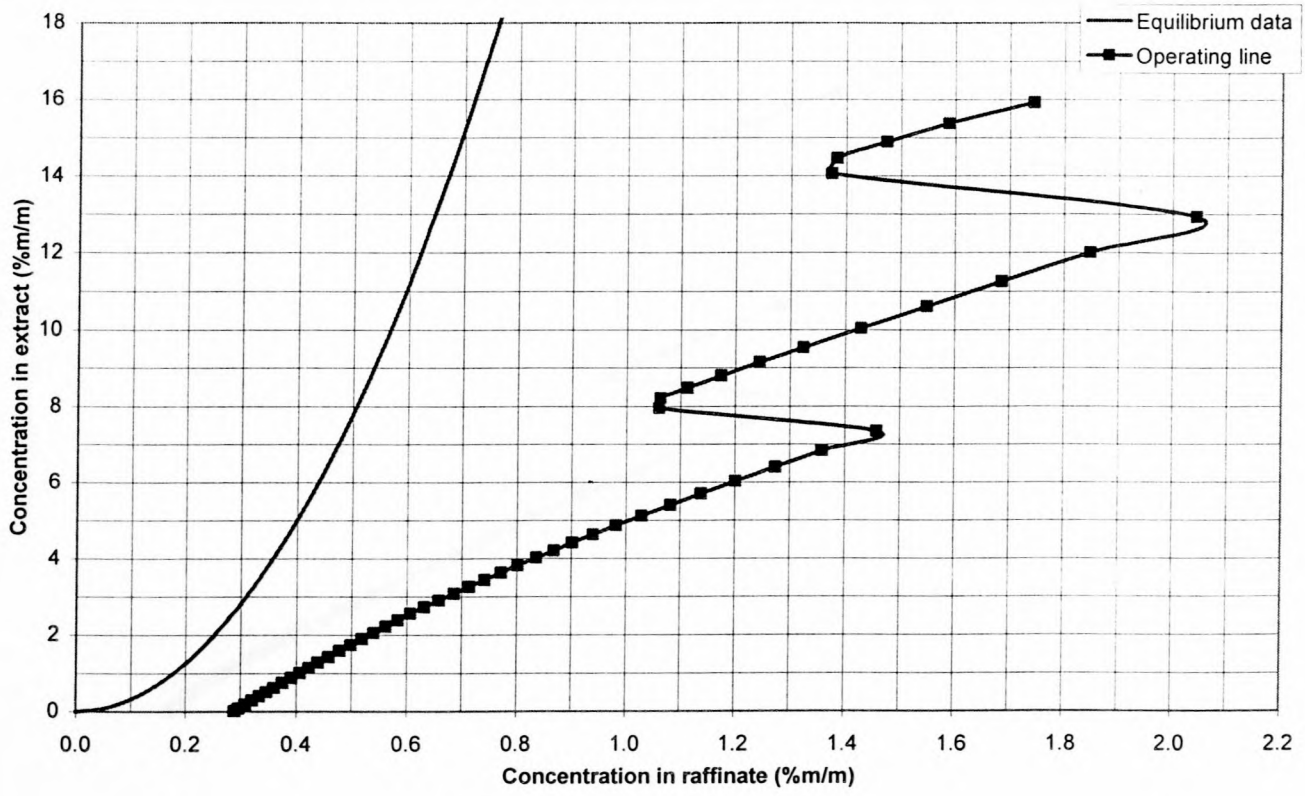

Figure D.31: Test SX-16-1

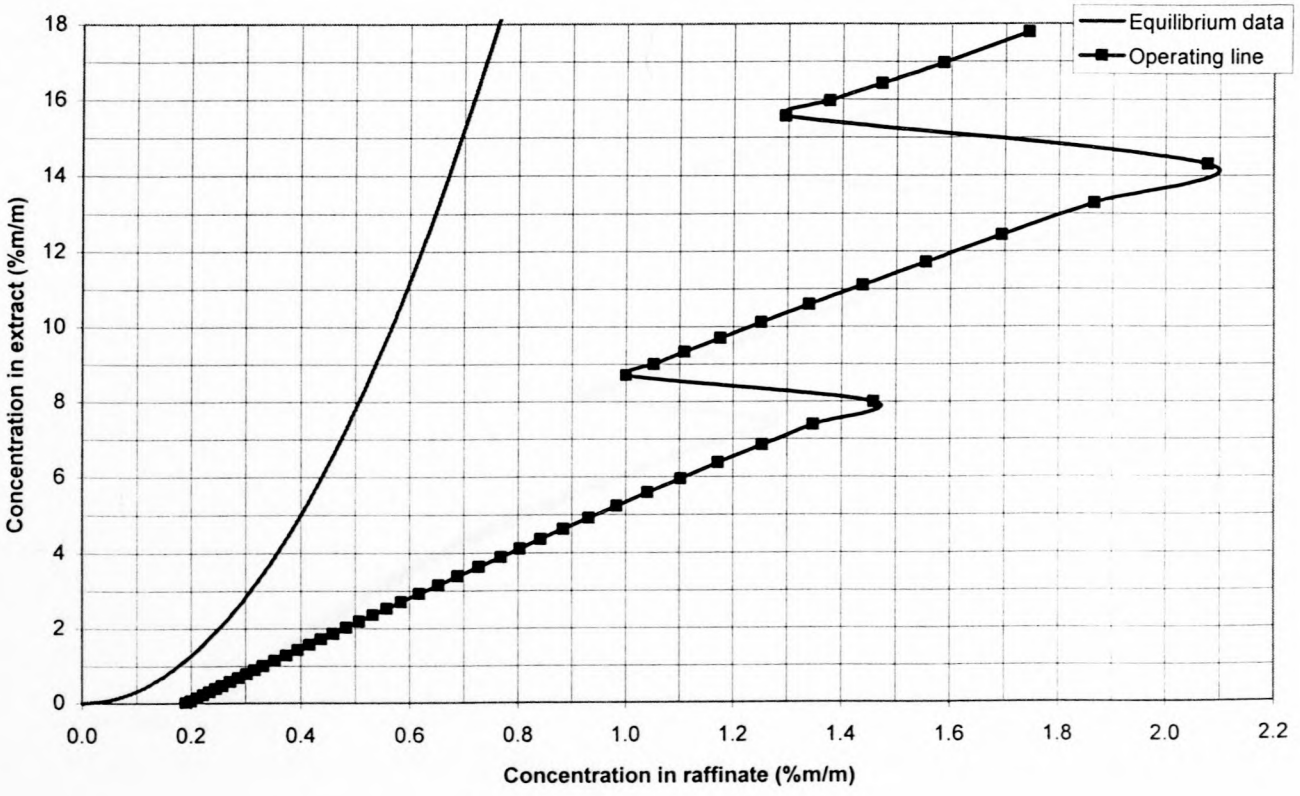

Figure D.32: Test SX-16-2

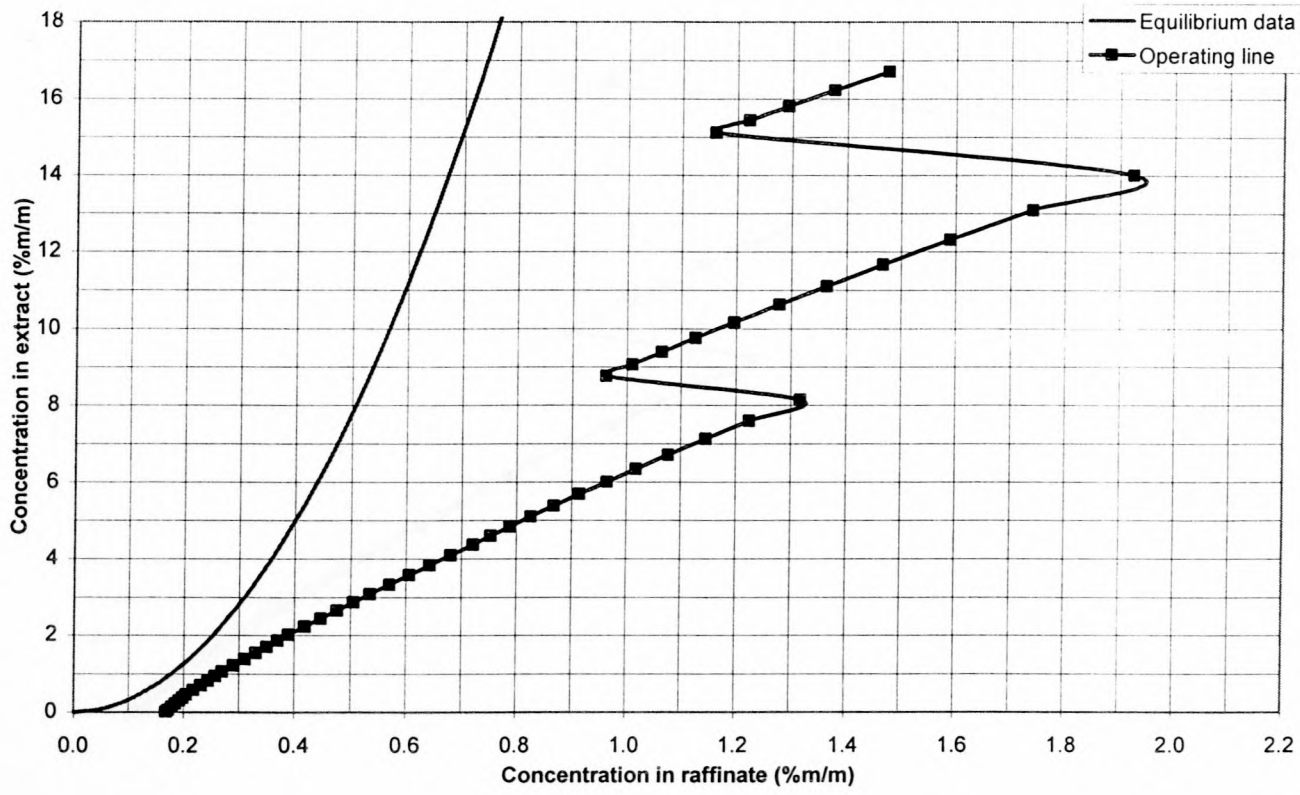

Figure D.33: Test SX-15-1

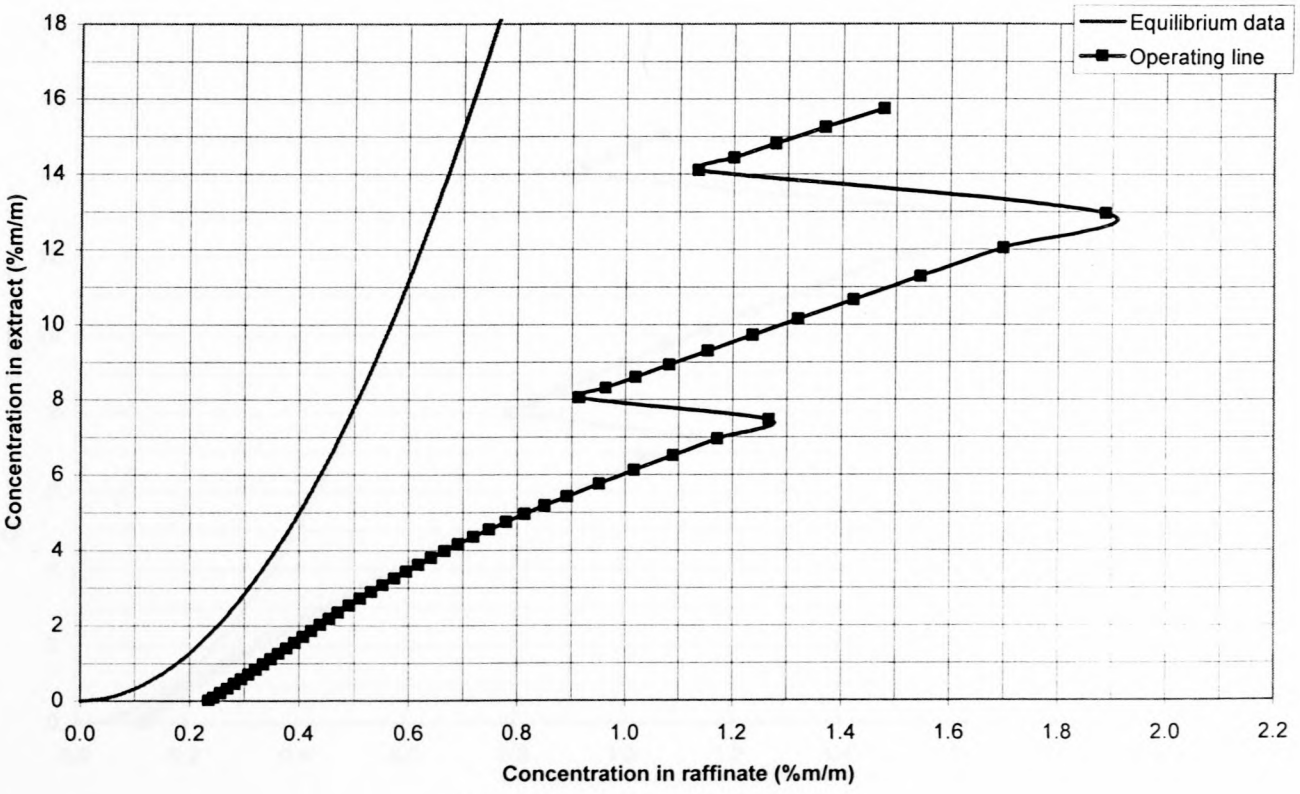

Figure D.34: Test SX-15-2

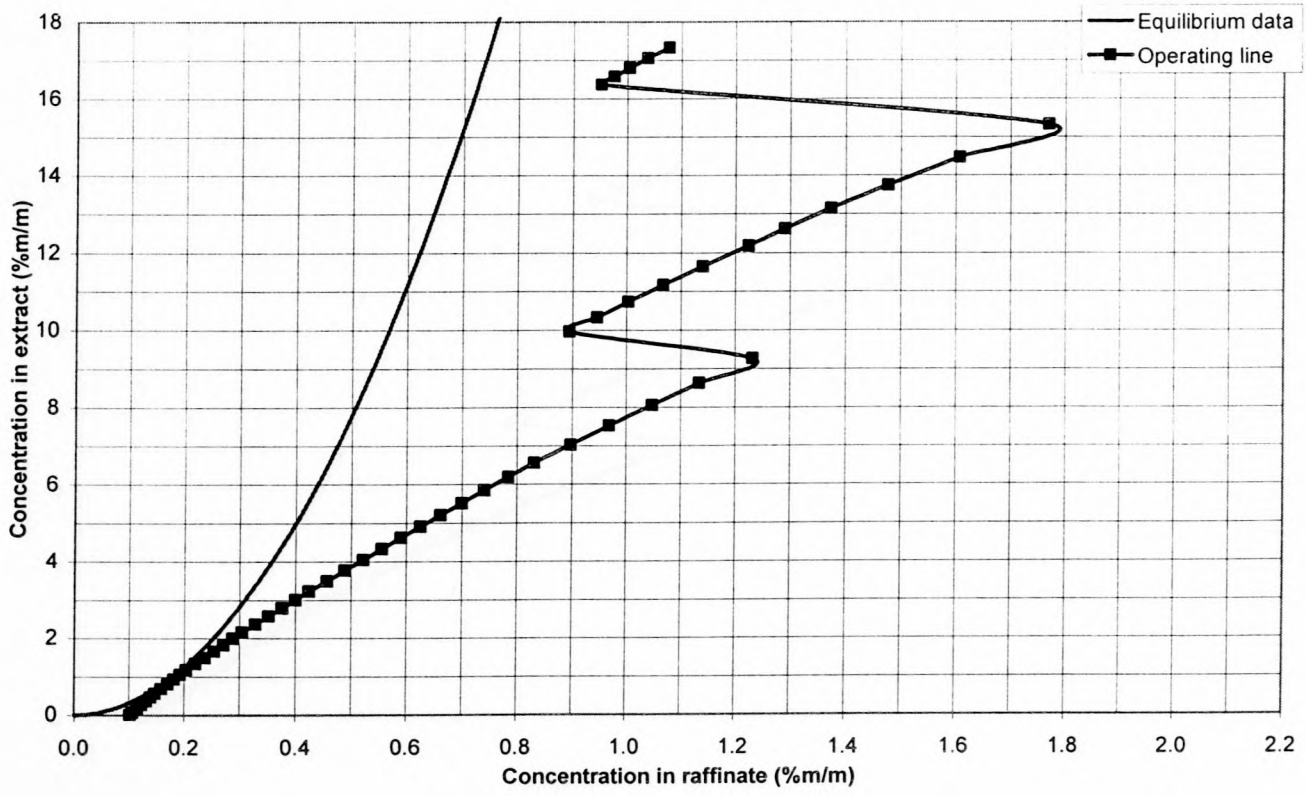

Figure D.35: Test SX-14-1

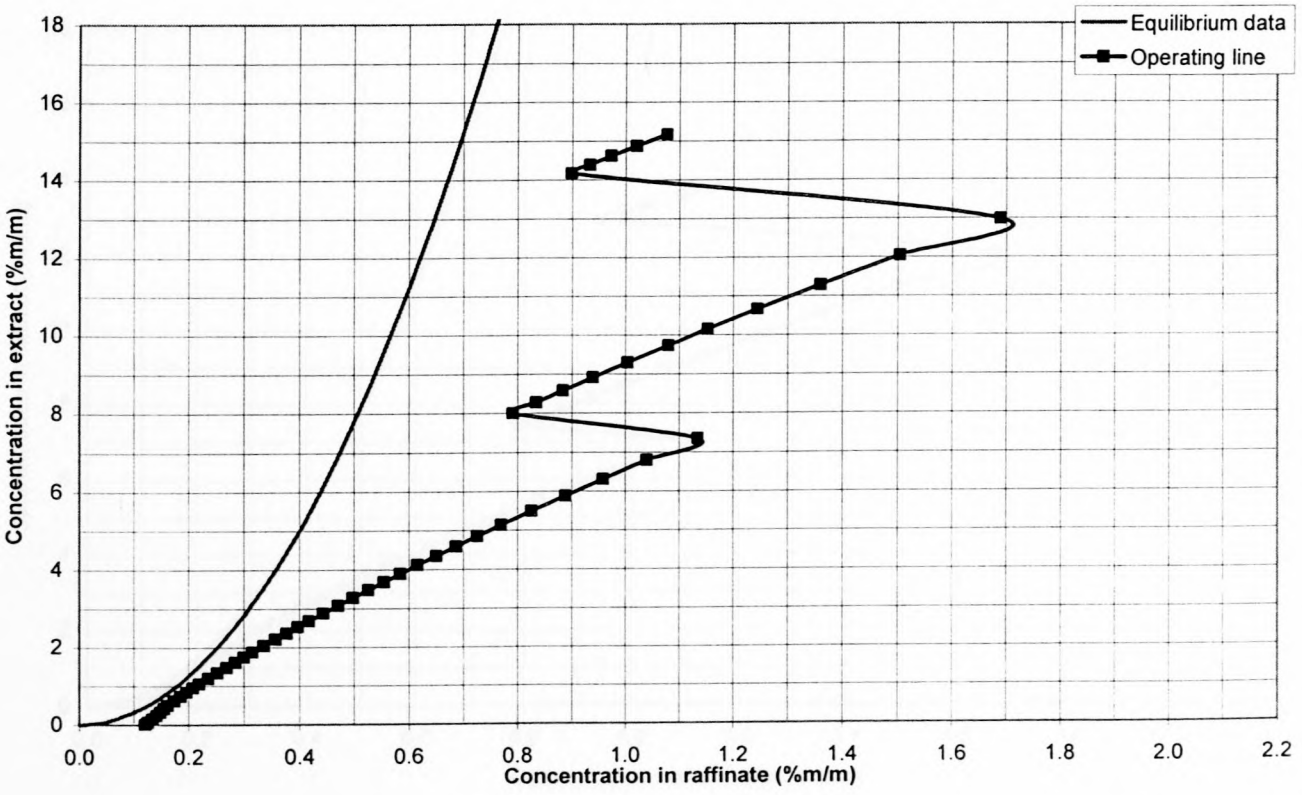

Figure D.36: Test SX-14-2

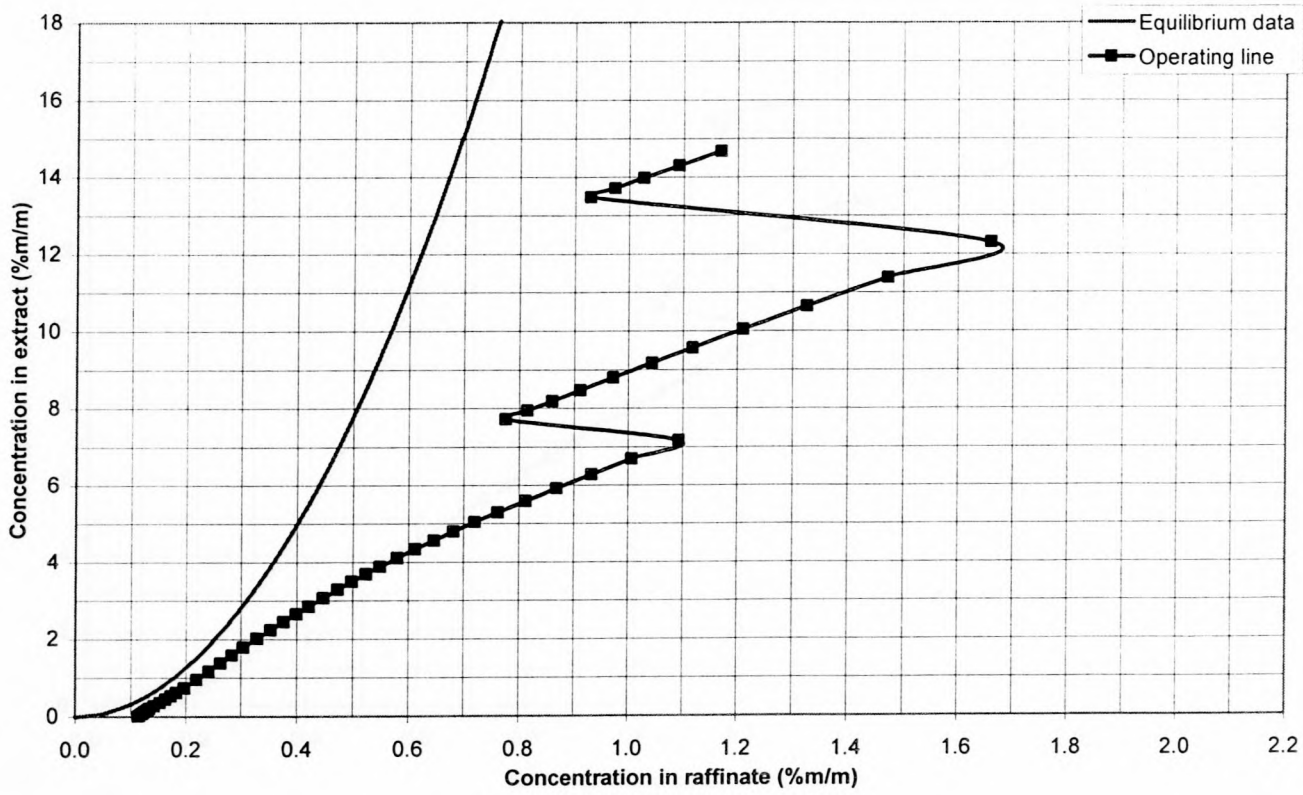

Figure D.37: Test SX-13-1

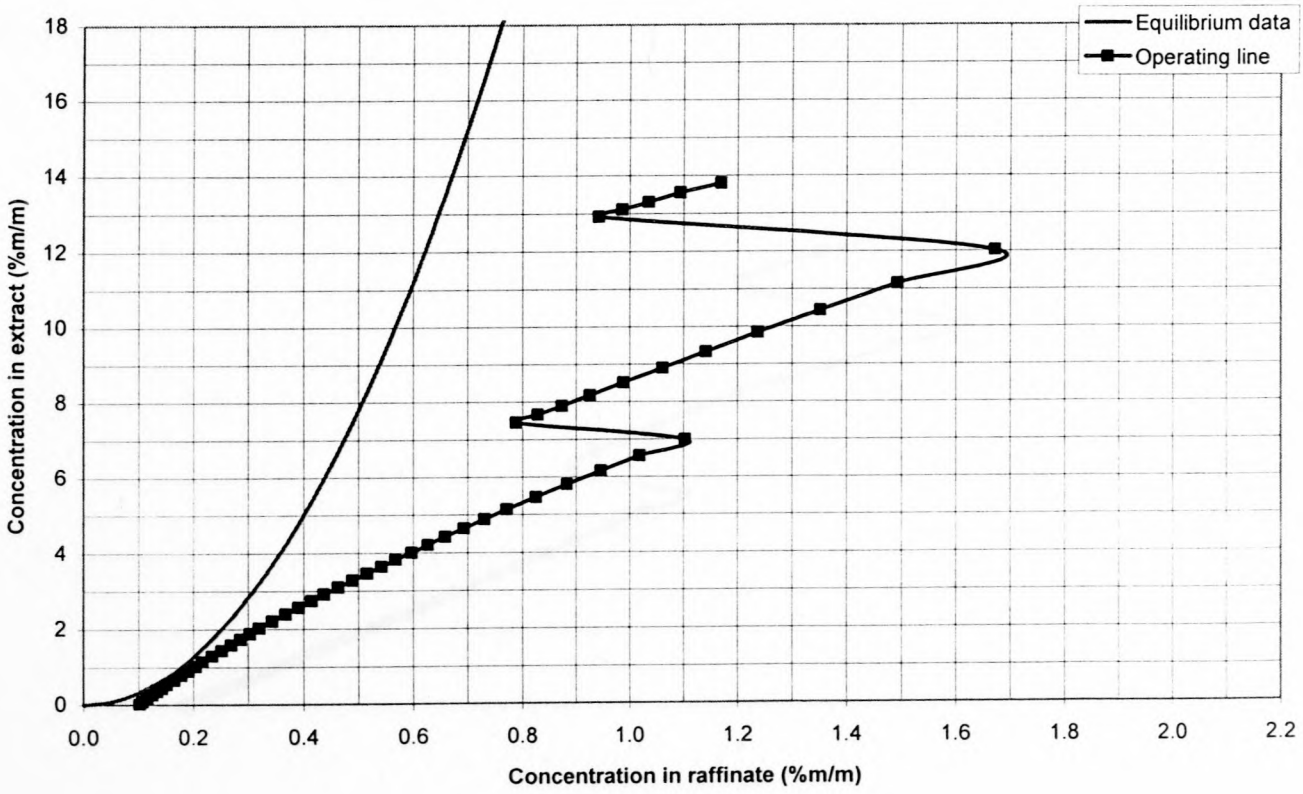

Figure D.38:Test SX-13-2

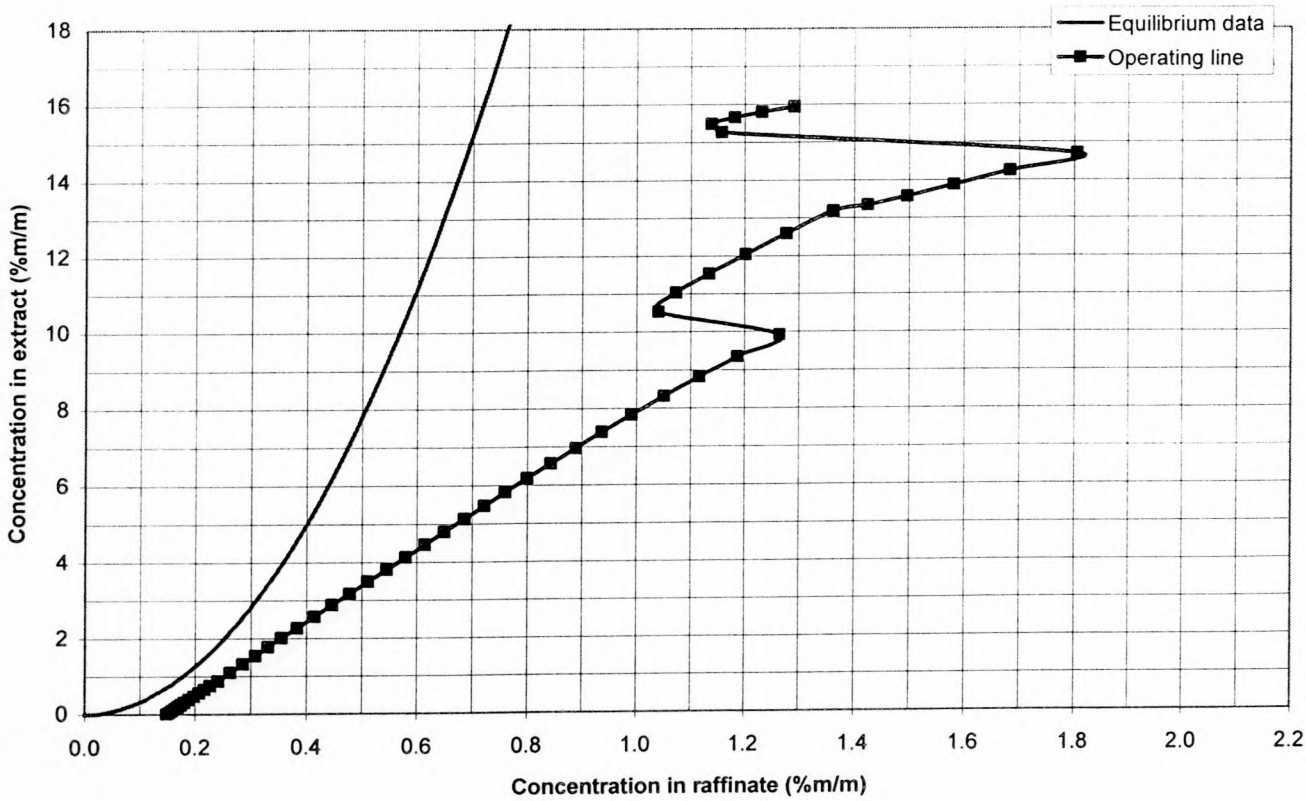

Figure D.39:Test SX-12-1

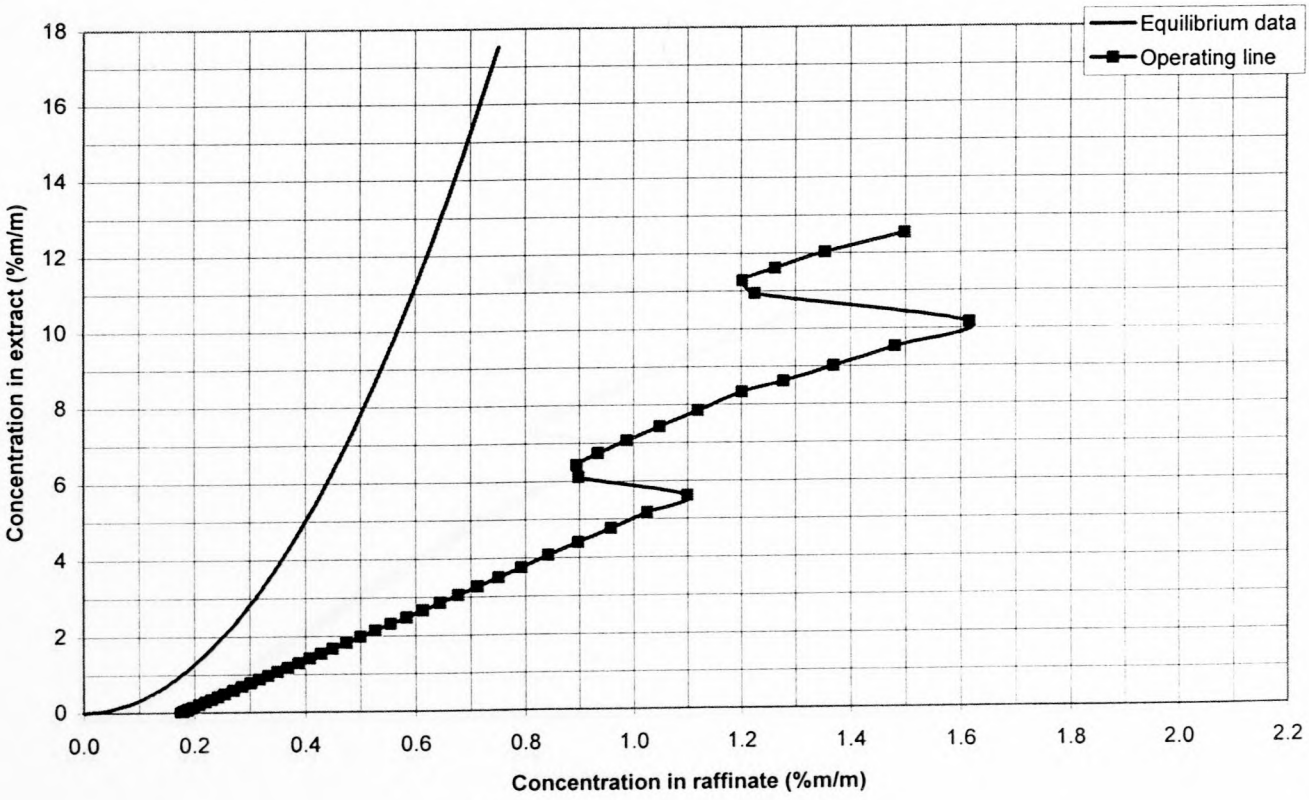

Figure D.40:Test SX-11-2

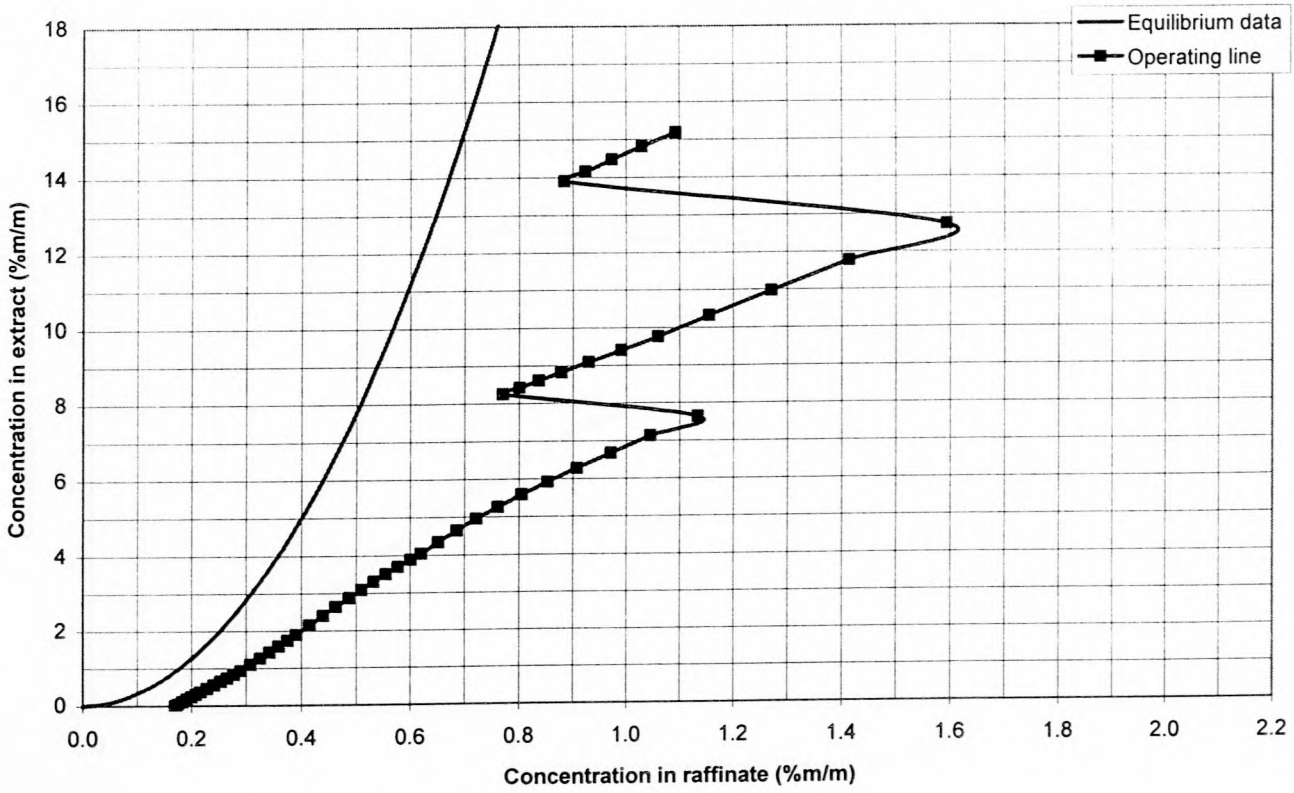

Figure D.41: Test SX-10-2

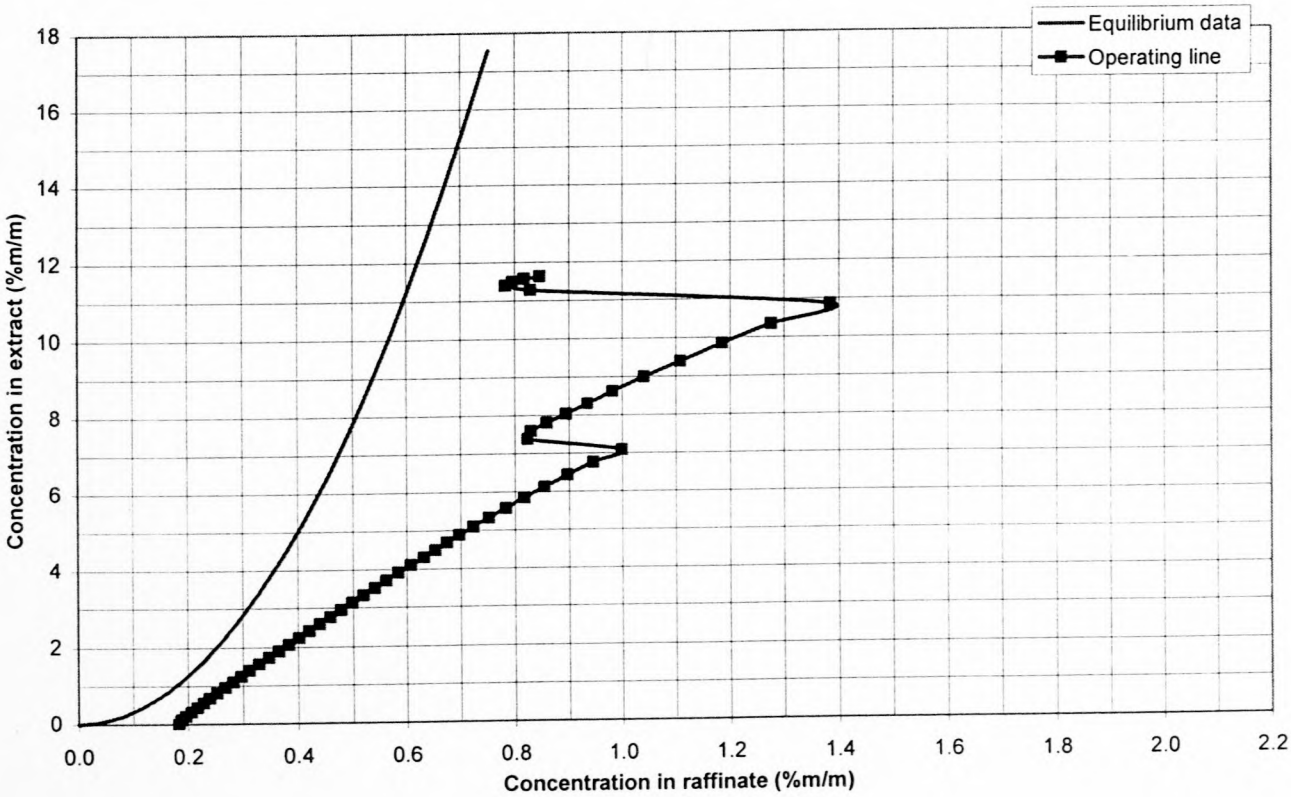

Figure D.42: Test SX-9-2

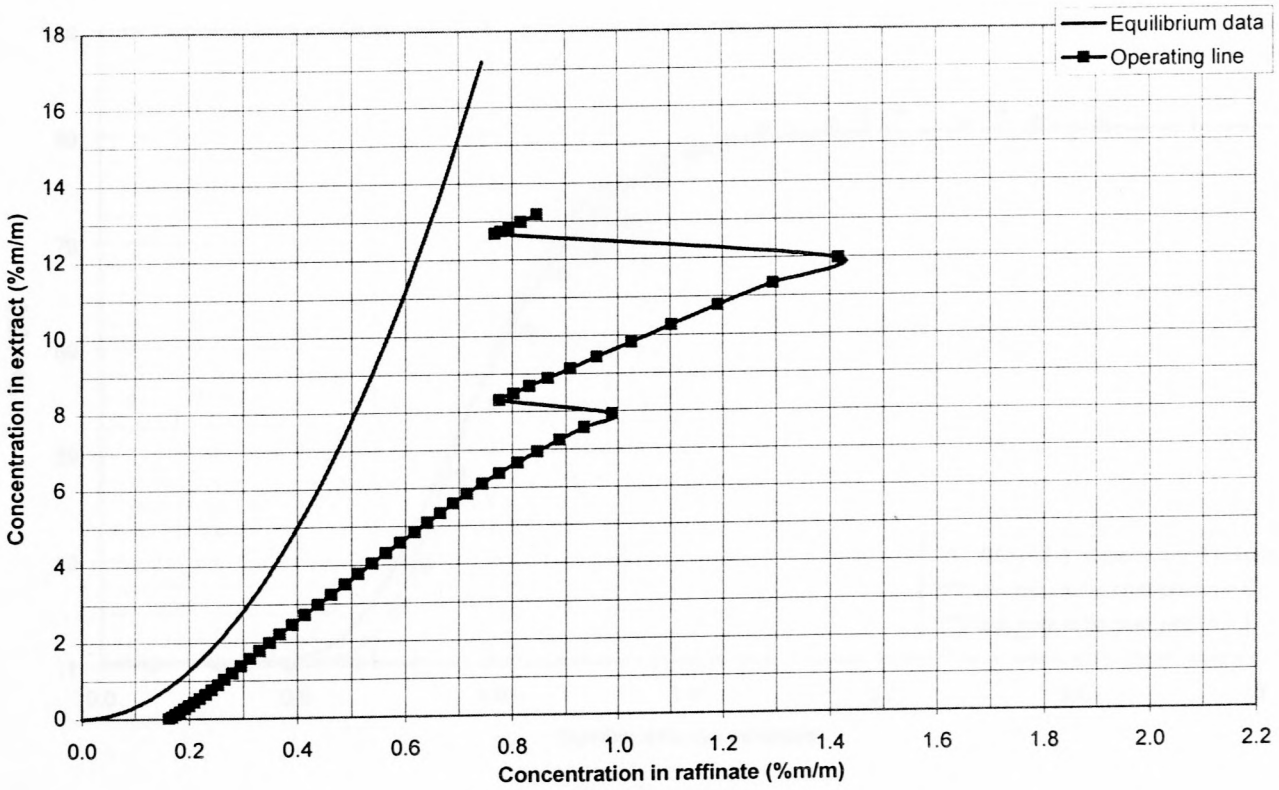

Figure D.43: Test SX-9-3

APPENDIX E: UNSTEADY STATE MODEL RESULTS

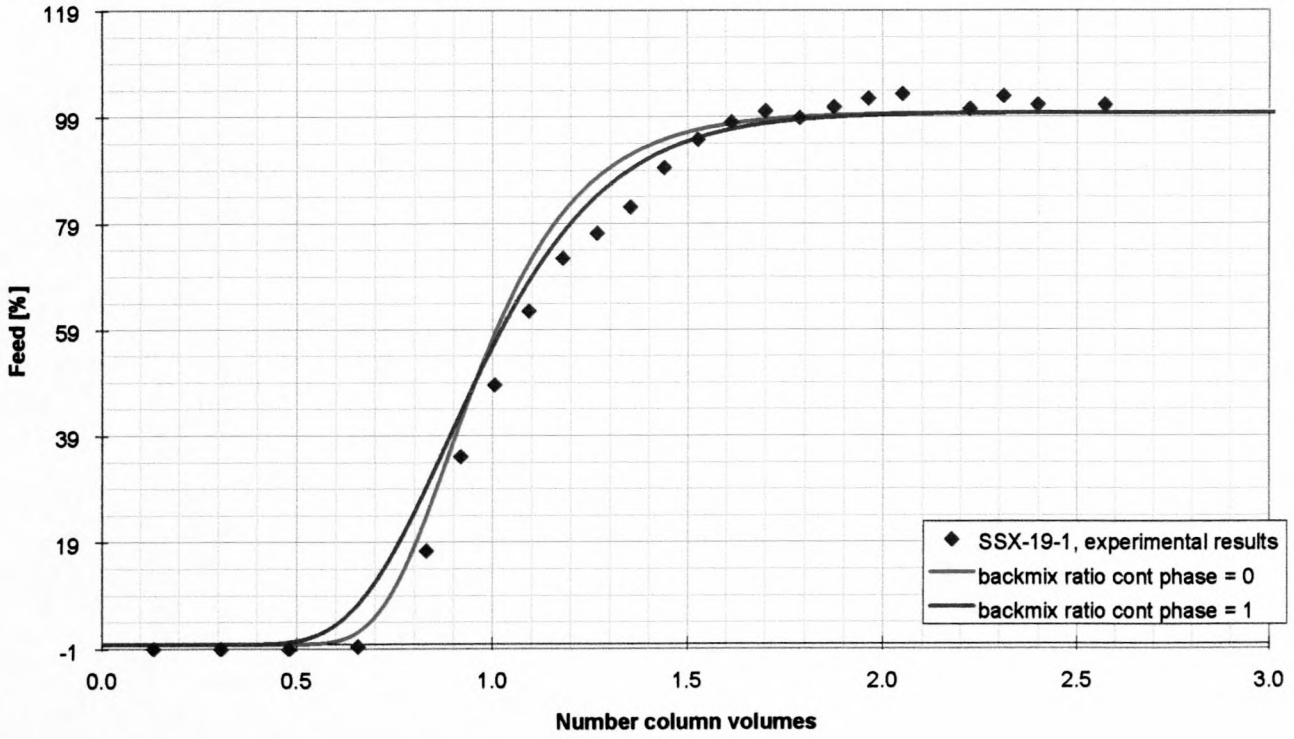

Figure E.1: Test SSX-19-1

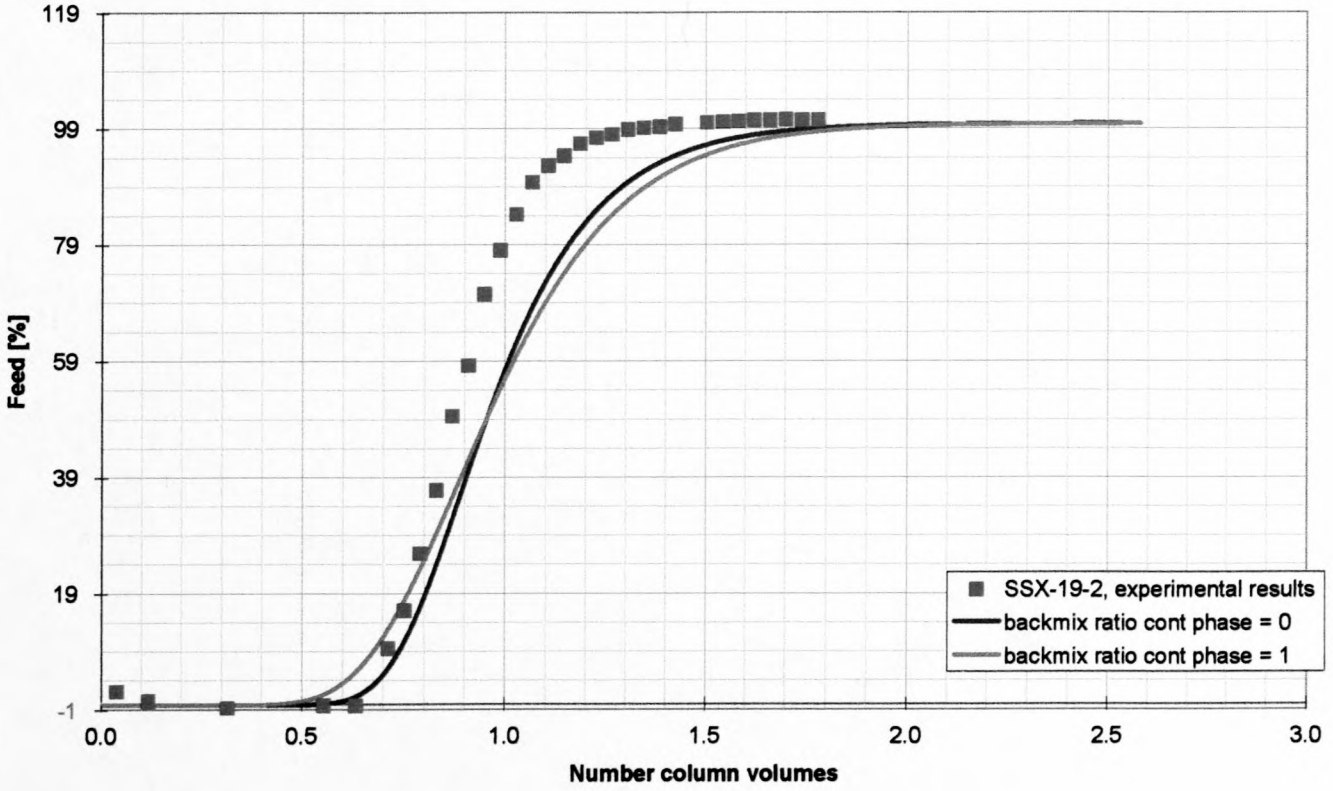

Figure E.2: Test SSX-19-2

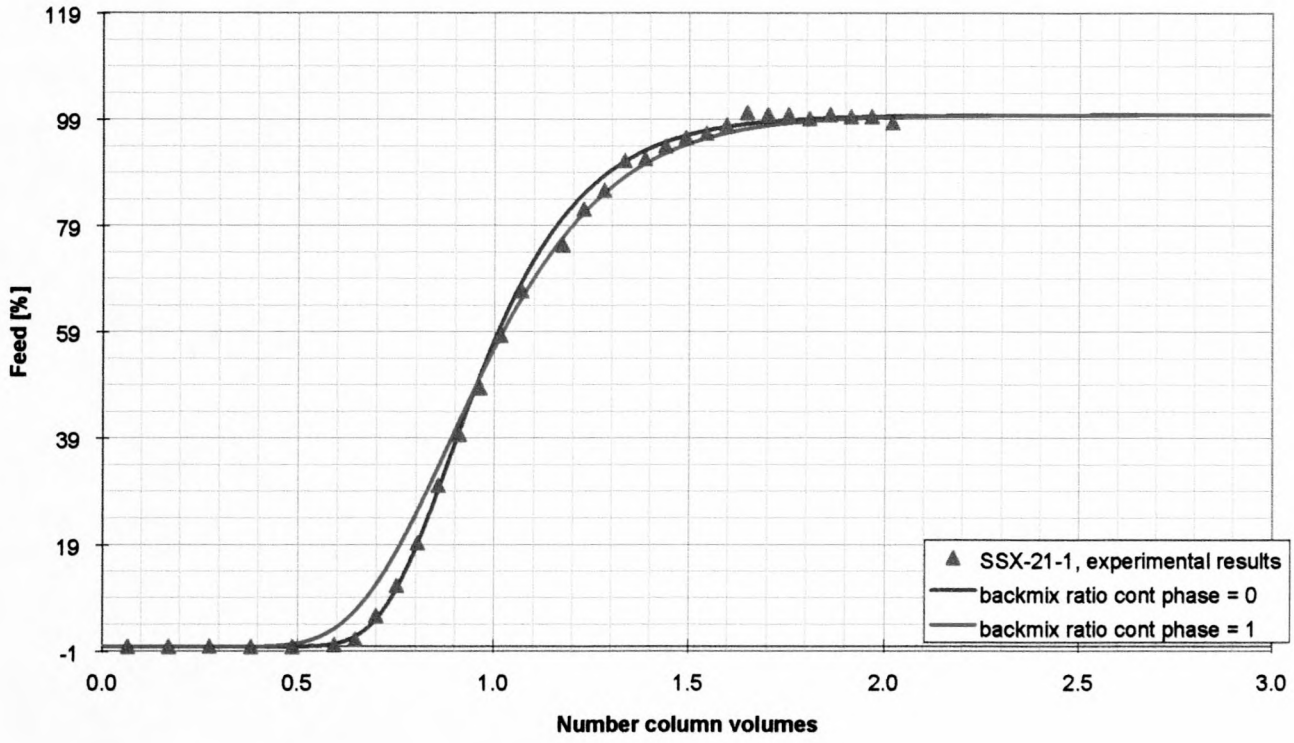

Figure E.3: Test SSX-21-1

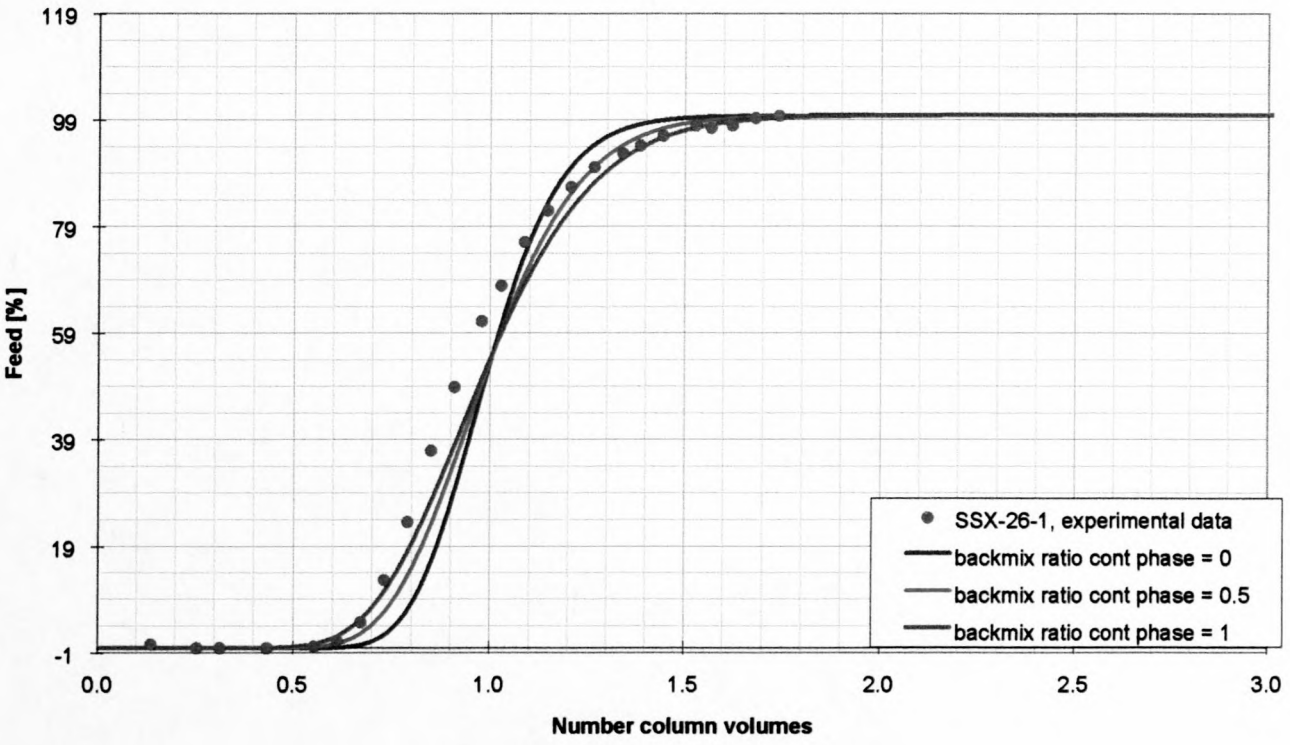

Figure E.4: Test SSX-26-1

F.1 Excel Spreadsheet

SX-16-1

SS MODEL :

Raffinate Phase

backmixing ratio	brx		*0.130*	ratio of backflow to F_x
feed total massrate	F_x	kg/min	1.02	
feed solute free conc	X_f	%	1.775	
solute free feed massrate	F	kg/min	0.98	
backflow raffinate phase	brx.F	kg/min	0.13	

Extract Phase

backmixing ratio	bry		*0.086*	ratio of backflow to F_y
solvent total massrate	S_y	kg/min	0.16	
solvent solute free conc	Y_s	%	0.01	
solute free solvent massrate	S	kg/min	0.162	
backflow extract phase	bry.S	kg/min	0.01	

General

overall mass transfer coefficient	kla	/min	*0.0112*	**ERROR**	**0.44**	**MB**
volume	V	L	0.20	**ERROR**	**0.45**	**Exp x**
pKa m-cresol at 50°C			9.83	**ERROR**	**0.00**	**Exp y**
				ERROR	**0.89**	**TOTAL**

	F	b	d	e	f	g	h	i	R/S
% MCH	**0**	**1190**	**2380**	**2975**	**3570**	**4165**	**4760**	**5355**	**5950**
aqueous	1.74	1.13	1.13	0.89	0.69	0.55	0.41	0.34	0.27
organic	15.92								0.01
calculated	15.9								0.01

Input Data				**Acid Point 1 (600mm)**	**2 (1790mm)**
feed massrate		kg/h	61.1		
feed massrate, solute free		kg/h	58.6		
feed concentration	$c_{x,f}$	%m/m	1.74		
solvent massrate		kg/h	9.7		
solvent concentration	$c_{y,s}$	%m/m	0.01		
extract concentration		%m/m	15.9		
m-cresol massrate		kg/h		0.64	0.36
m-cresol massrate		kg/min		0.011	0.006
water added		kg/h		0.61	0.34
water added		kg/min		0.010	0.006

Column Dimensions		
Height compartment	mm	110
Diameter column	mm	47.9
CSA column	m^2	0.0018
Compartment volume	m^3	0.0002
Compartment volume	L	0.1982

CALCULATION											Protonated species								ERRORS						
	concentration			Mass Balance		Error	solute free op line		Equilibrium		Column	Equilibrium		partition		pH	Extent	Extent	Column	calc	actual	error	calc	actual	error
Stage	c_x	c_y	F_	MB	MT		X	Y	X	Y	height	x	y	coeffic	y calc		Dissoc	Proton	height	c_x	c_x		c_y	c_y	
no.	%m/m	%m/m					%m/m	%m/m	%m/m	%m/m	mm	%m/m	%m/m	m	%m/m				mm	%m/m	%m/m		%m/m		
0	1.74	15.92					1.775	18.941			0	1.74	94.24	54.0	94.24	9.9	0.53	0.47	0	1.74	1.74	0.0E+00	15.92	15.92	6.1E-05
1	1.59	15.92	0.977	7E-05	4.4E-05	6.9E-09	*1.614*	*18.941*	1.614	358.22	110	1.59	78.18	49.2	78.18		0.52	0.48							
2	1.47	15.38	0.977	9.5E-05	2.9E-05	9.8E-09	*1.496*	*18.173*	1.496	206.46	220	1.47	67.37	45.7	67.37		0.12	0.88							
3	1.38	14.89	0.977	8.8E-05	3.6E-05	9.0E-09	*1.403*	*17.496*	1.403	145.87	331	1.38	59.33	42.9	59.33		0.13	0.87							
4	1.37	14.47	0.977	1.0E-04	1.8E-05	1.1E-08	*1.393*	*16.913*	1.393	140.98	441	1.37	58.50	42.6	58.50		0.13	0.87							
5	2.04	14.06	0.987	6.1E-05	8.4E-05	1.1E-08	*2.087*	*16.361*	2.087	-440.00	551	2.04	129.41	63.3	129.41		0.13	0.87							
6	1.85	12.93	0.987	1.5E-04	5.7E-06	2.1E-08	*1.883*	*14.852*	1.883	-1835.27	661	1.85	105.76	57.2	105.76		0.00	1.00							
7	1.69	12.01	0.987	1.6E-04	-5.2E-07	2.5E-08	*1.715*	*13.644*	1.715	739.42	771	1.69	88.09	52.2	88.09		0.00	1.00							
8	1.55	11.25	0.987	1.4E-04	3.0E-05	2.0E-08	*1.573*	*12.680*	1.573	289.29	881	1.55	74.31	48.0	74.31		0.00	1.00							
9	1.43	10.61	0.987	1.1E-04	7.0E-05	1.7E-08	*1.450*	*11.872*	1.450	172.38	992	1.43	63.29	44.3	63.29		0.00	1.00							
10	1.32	10.05	0.987	8.9E-05	1.1E-04	2.0E-08	*1.342*	*11.167*	1.342	119.23	1102	1.32	54.38	41.1	54.38	9.9	0.52	0.48	1102	1.32	1.13	3.754E-02			
11	1.24	9.54	0.987	6.9E-05	-3.4E-05	5.9E-09	*1.260*	*10.541*	1.260	92.49	1212	1.24	48.05	38.6	48.05		0.00	1.00							
12	1.17	9.14	0.987	4.5E-05	-2.5E-05	2.7E-09	*1.189*	*10.065*	1.189	74.81	1322	1.17	42.79	36.4	42.79		0.00	1.00							
13	1.11	8.80	0.987	3.2E-05	-1.7E-05	1.3E-09	*1.125*	*9.644*	1.125	62.38	1432	1.11	38.42	34.5	38.42		0.00	1.00							
14	1.06	8.48	0.987	4.3E-05	-2.1E-05	2.3E-09	*1.074*	*9.265*	1.074	53.96	1543	1.06	35.05	33.0	35.05		0.00	1.00							
15	1.06	8.20	0.987	6.5E-05	-4.2E-05	6.1E-09	*1.072*	*8.938*	1.072	53.62	1653	1.06	34.90	32.9	34.90		0.00	1.00							
16	1.46	7.95	0.993	4.5E-05	-3.3E-05	3.1E-09	*1.479*	*8.637*	1.479	193.10	1763	1.46	65.88	45.2	65.88		0.00	1.00							
17	1.36	7.35	0.993	8.1E-05	-7.9E-05	1.3E-08	*1.378*	*7.928*	1.378	134.03	1873	1.36	57.27	42.1	57.27		0.00	1.00							
18	1.27	6.83	0.993	9.1E-05	-8.6E-05	1.6E-08	*1.291*	*7.334*	1.291	101.48	1983	1.27	50.37	39.5	50.37		0.00	1.00							
19	1.20	6.40	0.993	7.1E-05	-9.9E-05	1.5E-08	*1.216*	*6.840*	1.216	81.15	2094	1.20	44.80	37.3	44.80		0.00	1.00							
20	1.14	6.03	0.993	6.0E-05	-9.9E-05	1.3E-08	*1.151*	*6.414*	1.151	67.17	2204	1.14	40.18	35.3	40.18		0.00	1.00							
21	1.08	5.70	0.993	4.5E-05	-1.1E-04	1.3E-08	*1.094*	*6.041*	1.094	57.05	2314	1.08	36.33	33.6	36.33	9	0.12	0.88	2314	1.08	1.13	2.213E-03			
22	1.03	5.40	0.993	3.8E-05	-6.4E-05	5.6E-09	*1.040*	*5.712*	1.040	48.96	2424	1.03	32.87	31.9	32.87		0.00	1.00							
23	0.98	5.12	0.993	2.5E-05	-6.6E-05	4.9E-09	*0.992*	*5.398*	0.992	42.71	2534	0.98	29.93	30.5	29.93		0.00	1.00							
24	0.94	4.86	0.993	2.1E-05	-5.9E-05	4.0E-09	*0.948*	*5.113*	0.948	37.71	2644	0.94	27.38	29.2	27.38		0.00	1.00							
25	0.90	4.63	0.993	-2.0E-06	-7.4E-05	5.5E-09	*0.910*	*4.852*	0.910	33.78	2755	0.90	25.25	28.0	25.25		0.00	1.00							
26	0.87	4.41	0.993	-8.1E-06	-7.5E-05	5.8E-09	*0.875*	*4.613*	0.875	30.53	2865	0.87	23.39	27.0	23.39		0.00	1.00							
27	0.84	4.21	0.993	-2.6E-06	-6.4E-05	4.1E-09	*0.843*	*4.393*	0.843	27.69	2975	0.84	21.69	26.0	21.69	9	0.13	0.87	2975	0.84	0.89	3.273E-03			
28	0.80	4.02	0.993	-1.2E-05	-1.2E-05	3.1E-10	*0.809*	*4.191*	0.809	24.98	3085	0.80	19.99	24.9	19.99		0.00	1.00							
29	0.77	3.82	0.993	-2.5E-05	-1.3E-05	7.8E-10	*0.777*	*3.973*	0.777	22.68	3195	0.77	18.49	24.0	18.49		0.00	1.00							
30	0.74	3.63	0.993	-2.7E-05	-2.7E-06	7.4E-10	*0.748*	*3.765*	0.748	20.65	3306	0.74	17.12	23.1	17.12		0.00	1.00							
31	0.71	3.44	0.993	-2.8E-05	9.5E-06	8.9E-10	*0.719*	*3.565*	0.719	18.83	3416	0.71	15.85	22.2	15.85		0.00	1.00							
32	0.69	3.26	0.993	-2.6E-05	2.6E-05	1.4E-09	*0.691*	*3.371*	0.691	17.16	3526	0.69	14.65	21.3	14.65	9	0.13	0.87	3526	0.69	0.69	5.0E-05			
33	0.66	3.08	0.993	-2.8E-05	4.8E-05	3.0E-09	*0.663*	*3.183*	0.663	15.60	3636	0.66	13.50	20.5	13.50		0.00	1.00							
34	0.63	2.91	0.993	-3.1E-05	5.7E-05	4.3E-09	*0.636*	*2.994*	0.636	14.20	3746	0.63	12.43	19.7	12.43		0.00	1.00							

35	0.61	2.73	0.993	-3.5E-05	6.5E-05	5.4E-09	*0.610*	*2.809*	0.610	12.94	3856	0.61	11.46	18.9	11.46		0.00	1.00												
36	0.58	2.56	0.993	-5.5E-05	5.5E-05	6.1E-09	*0.587*	*2.628*	0.587	11.86	3967	0.58	10.60	18.2	10.60		0.00	1.00												
37	0.56	2.39	0.993	-6.0E-05	6.0E-05	7.2E-09	*0.565*	*2.450*	0.565	10.88	4077	0.56	9.81	17.5	9.81	9	0.13	0.87	4077	0.56	0.55	5.2E-05							
38	0.54	2.22	0.993	-5.6E-05	6.6E-05	7.6E-09	*0.543*	*2.274*	0.543	9.98	4187	0.54	9.07	16.8	9.07		0.00	1.00												
39	0.52	2.06	0.993	-5.9E-05	7.1E-05	8.5E-09	*0.521*	*2.105*	0.521	9.15	4297	0.52	8.39	16.2	8.39		0.00	1.00												
40	0.50	1.90	0.993	-6.0E-05	7.5E-05	9.3E-09	*0.501*	*1.938*	0.501	8.39	4407	0.50	7.74	15.5	7.74		0.00	1.00												
41	0.48	1.74	0.993	-6.0E-05	8.1E-05	1.0E-08	*0.481*	*1.774*	0.481	7.68	4518	0.48	7.14	14.9	7.14		0.00	1.00												
42	0.46	1.59	0.993	-6.0E-05	8.7E-05	1.1E-08	*0.461*	*1.613*	0.461	7.03	4628	0.46	6.57	14.3	6.57		0.00	1.00												
43	0.44	1.43	0.993	-6.0E-05	9.3E-05	1.2E-08	*0.442*	*1.454*	0.442	6.42	4738	0.44	6.03	13.7	6.03	9	0.14	0.86	4738	0.44	0.41	1.0E-03							
44	0.42	1.28	0.993	-6.0E-05	7.0E-05	8.5E-09	*0.425*	*1.296*	0.425	5.92	4848	0.42	5.59	13.2	5.59		0.00	1.00												
45	0.41	1.14	0.993	-6.0E-05	7.2E-05	8.7E-09	*0.409*	*1.156*	0.409	5.46	4958	0.41	5.18	12.7	5.18		0.00	1.00												
46	0.39	1.01	0.993	-5.8E-05	7.5E-05	8.9E-09	*0.393*	*1.019*	0.393	5.03	5069	0.39	4.78	12.2	4.78		0.00	1.00												
47	0.38	0.88	0.993	-5.6E-05	7.8E-05	9.1E-09	*0.377*	*0.886*	0.377	4.62	5179	0.38	4.41	11.7	4.41		0.00	1.00												
48	0.36	0.75	0.993	-5.4E-05	8.0E-05	9.3E-09	*0.362*	*0.755*	0.362	4.24	5289	0.36	4.07	11.3	4.07	9.1	0.14	0.86	5289	0.36	0.34	5.0E-04							
49	0.35	0.62	0.993	-5.2E-05	6.4E-05	6.7E-09	*0.348*	*0.627*	0.348	3.92	5399	0.35	3.77	10.9	3.77		0.00	1.00												
50	0.33	0.51	0.993	-5.0E-05	6.4E-05	6.6E-09	*0.335*	*0.511*	0.335	3.62	5509	0.33	3.50	10.5	3.50		0.00	1.00												
51	0.32	0.40	0.993	-4.8E-05	6.6E-05	6.7E-09	*0.322*	*0.400*	0.322	3.34	5619	0.32	3.24	10.1	3.24		0.00	1.00												
52	0.31	0.29	0.993	-4.9E-05	6.8E-05	7.0E-09	*0.310*	*0.290*	0.310	3.08	5730	0.31	2.99	9.7	2.99		0.00	1.00												
53	0.30	0.18	0.993	-4.8E-05	6.9E-05	7.1E-09	*0.298*	*0.181*	0.298	2.84	5840	0.30	2.76	9.3	2.76		0.00	1.00												
54	0.29	0.07	0.993	-5.4E-06	2.7E-05	7.4E-10	*0.290*	*0.074*	0.290	2.70	5950	0.29	2.62	9.1	2.62	9.1	0.15	0.85	5950	0.29	0.27	3.9E-04	0.074	0.01	0.0041				
					Total	**4.4E-07**			0.251	2.00		0.25	1.96								**sum**	0.045		**sum**	0.0041				
									0.251	2.00		0.25	1.96																
									0.200	1.28		0.20	1.26																
									0.150	0.72		0.15	0.72																
									0.100	0.32		0.10	0.32																
									0.05	0.08		0.05	0.08																
									0.00	0.00		0.00	0.00																

APPENDIX G: UNSTEADY STATE BACKFLOW MODEL

G.1 Excel Spreadsheet

Initial Conditions

t0		0		
t_{max}	[hr]	3.33	[min]	200
h	[hr]	0.001	[min]	0.05
Q	[L/hr]	41.6		
Qf	[L/hr]	41.6		
Qs	[L/hr]	20.2		
F:S ratio		2.1		
# stages		54.1		
Vstage	[L]	0.20	[mL]	198.2
Vtop set	[L]	1.43	[mL]	1434
Vbot set	[L]	2.62	[mL]	2618
V_{total}	[L]	14.8		
$t_{residence}$	[hr]	0.4	[min]	21.3
Cf	[%]	100		

Initial concentrations		Holdup (%) disp phase	cont phase	Volumes (L)		Backflow ratio cont phase	
c0_1	0	8	92	V_1	3.700	B_1	0
c0_2	0	8	92	V_2	3.700	B_2	0
c0_3	0	8	92	V_3	3.700	B_3	0
c0_4	0	8	92	V_4	3.700	B_4	0
c0_5	0	8	92	V_5	0.030	B_5	0
c0_6	0	8	92	V_6	0.030	B_6	0
c0_7	0	8	92	V_7	0.030	B_7	0
c0_8	0	8	92	V_8	0.030	B_8	0
c0_9	0	8	92	V_9	0.030	B_9	0
c0_10	0	8	92	V_10	0.030	B_10	0
c0_11	0	8	92	V_11	0.030	B_11	0
c0_12	0	8	92	V_12	0.030	B_12	0
c0_13	0	8	92	V_13	0.030	B_13	0
c0_14	0	8	92	V_14	0.030	B_14	0
c0_15	0	8	92	V_15	0.030	B_15	0
c0_16	0	8	92	V_16	0.030	B_16	0
c0_17	0	8	92	V_17	0.030	B_17	0
c0_18	0	8	92	V_18	0.030	B_18	0
c0_19	0	8	92	V_19	0.030	B_19	0
c0_20	0	8	92	V_20	0.030	B_20	0
c0_21	0	8	92	V_21	0.030	B_21	0
c0_22	0	8	92	V_22	0.030	B_22	0
c0_23	0	8	92	V_23	0.030	B_23	0
c0_24	0	8	92	V_24	0.030	B_24	0
c0_25	0	8	92	V_25	0.030	B_25	0
c0_26	0	8	92	V_26	0.030	B_26	0

c0_27	0	8	92	V_27	0.030	B_27	0
c0_28	0	8	92	V_28	0.030	B_28	0
c0_29	0	8	92	V_29	0.030	B_29	0
c0_30	0	8	92	V_30	0.030	B_30	0
c0_31	0	8	92	V_31	0.030	B_31	0
c0_32	0	8	92	V_32	0.030	B_32	0
c0_33	0	8	92	V_33	0.030	B_33	0
c0_34	0	8	92	V_34	0.030	B_34	0
c0_35	0	8	92	V_35	0.030	B_35	0
c0_36	0	8	92	V_36	0.030	B_36	0
c0_37	0	8	92	V_37	0.030	B_37	0
c0_38	0	8	92	V_38	0.030	B_38	0
c0_39	0	8	92	V_39	0.030	B_39	0
c0_40	0	8	92	V_40	0.030	B_40	0
c0_41	0	8	92	V_41	0.030	B_41	0
c0_42	0	8	92	V_42	0.030	B_42	0
c0_43	0	8	92	V_43	0.030	B_43	0
c0_44	0	8	92	V_44	0.030	B_44	0
c0_45	0	8	92	V_45	0.030	B_45	0
c0_46	0	8	92	V_46	0.030	B_46	0
c0_47	0	8	92	V_47	0.030	B_47	0
c0_48	0	8	92	V_48	0.030	B_48	0
c0_49	0	8	92	V_49	0.030	B_49	0
c0_50	0	8	92	V_50	0.030	B_50	0
c0_51	0	8	92	V_51	0.030	B_51	0
c0_52	0	8	92	V_52	0.030	B_52	0
c0_53	0	8	92	V_53	0.030	B_53	0
c0_54	0	8	92	V_54	0.030	B_54	0
c0_55	0	8	92	V_55	0.030	B_55	0
c0_56	0	8	92	V_56	0.030		

G.2 Runge Kutta Visual Basic Code

```
Sub RK()
'Sets up data output
   'Clears "data" sheet of old data
      Worksheets("data").Select
      Columns("A:E").Select
      Selection.ClearContents
   'Puts in time & reactor concentration data headings
      With Worksheets("data")
         .Cells(3, 2).Value = "t (hr)"
         .Cells(3, 3).Value = "c1"
         .Cells(3, 4).Value = "c2"
         .Cells(3, 5).Value = "c3"
         .Cells(3, 6).Value = "c4"
         .Cells(3, 7).Value = "c5"
         .Cells(3, 8).Value = "c6"
         .Cells(3, 9).Value = "c7"
         .Cells(3, 10).Value = "c8"
         .Cells(3, 11).Value = "c9"
         .Cells(3, 12).Value = "c10"
         .Cells(3, 13).Value = "c15"
         .Cells(3, 14).Value = "c30"
         .Cells(3, 15).Value = "c56"
      End With
' Initial Conditions
t = Range("t0").Value
Q = Range("Q").Value   'Feed flowrate
Cf = Range("Cf").Value 'Feed concentration
' Reactor concentrations
c1 = Range("c0_1").Value
c2 = Range("c0_2").Value
c3 = Range("c0_3").Value
c4 = Range("c0_4").Value
c5 = Range("c0_5").Value
c6 = Range("c0_6").Value
c7 = Range("c0_7").Value
c8 = Range("c0_8").Value
c9 = Range("c0_9").Value
```

```
c10 = Range("c0_10").Value
c11 = Range("c0_11").Value
c12 = Range("c0_12").Value
c13 = Range("c0_13").Value
c14 = Range("c0_14").Value
c15 = Range("c0_15").Value
c16 = Range("c0_16").Value
c17 = Range("c0_17").Value
c18 = Range("c0_18").Value
c19 = Range("c0_19").Value
c20 = Range("c0_20").Value
c21 = Range("c0_21").Value
c22 = Range("c0_22").Value
c23 = Range("c0_23").Value
c24 = Range("c0_24").Value
c25 = Range("c0_25").Value
c26 = Range("c0_26").Value
c27 = Range("c0_27").Value
c28 = Range("c0_28").Value
c29 = Range("c0_29").Value
c30 = Range("c0_30").Value
c31 = Range("c0_31").Value
c32 = Range("c0_32").Value
c33 = Range("c0_33").Value
c34 = Range("c0_34").Value
c35 = Range("c0_35").Value
c36 = Range("c0_36").Value
c37 = Range("c0_37").Value
c38 = Range("c0_38").Value
c39 = Range("c0_39").Value
c40 = Range("c0_40").Value
c41 = Range("c0_41").Value
c42 = Range("c0_42").Value
c43 = Range("c0_43").Value
c44 = Range("c0_44").Value
c45 = Range("c0_45").Value
c46 = Range("c0_46").Value
c47 = Range("c0_47").Value
c48 = Range("c0_48").Value
```

```
c49 = Range("c0_49").Value
c50 = Range("c0_50").Value
c51 = Range("c0_51").Value
c52 = Range("c0_52").Value
c53 = Range("c0_53").Value
c54 = Range("c0_54").Value
c55 = Range("c0_55").Value
c56 = Range("c0_56").Value

' Reactor volumes
V1 = Range("V_1").Value
V2 = Range("V_2").Value
V3 = Range("V_3").Value
V4 = Range("V_4").Value
V5 = Range("V_5").Value
V6 = Range("V_6").Value
V7 = Range("V_7").Value
V8 = Range("V_8").Value
V9 = Range("V_9").Value
V10 = Range("V_10").Value
V11 = Range("V_11").Value
V12 = Range("V_12").Value
V13 = Range("V_13").Value
V14 = Range("V_14").Value
V15 = Range("V_15").Value
V16 = Range("V_16").Value
V17 = Range("V_17").Value
V18 = Range("V_18").Value
V19 = Range("V_19").Value
V20 = Range("V_20").Value
V21 = Range("V_21").Value
V22 = Range("V_22").Value
V23 = Range("V_23").Value
V24 = Range("V_24").Value
V25 = Range("V_25").Value
V26 = Range("V_26").Value
V27 = Range("V_27").Value
V28 = Range("V_28").Value
V29 = Range("V_29").Value
```

```
V30 = Range("V_30").Value
V31 = Range("V_31").Value
V32 = Range("V_32").Value
V33 = Range("V_33").Value
V34 = Range("V_34").Value
V35 = Range("V_35").Value
V36 = Range("V_36").Value
V37 = Range("V_37").Value
V38 = Range("V_38").Value
V39 = Range("V_39").Value
V40 = Range("V_40").Value
V41 = Range("V_41").Value
V42 = Range("V_42").Value
V43 = Range("V_43").Value
V44 = Range("V_44").Value
V45 = Range("V_45").Value
V46 = Range("V_46").Value
V47 = Range("V_47").Value
V48 = Range("V_48").Value
V49 = Range("V_49").Value
V50 = Range("V_50").Value
V51 = Range("V_51").Value
V52 = Range("V_52").Value
V53 = Range("V_53").Value
V54 = Range("V_54").Value
V55 = Range("V_55").Value
V56 = Range("V_56").Value

' Backmixing
B1 = Range("B_1").Value
B2 = Range("B_2").Value
B3 = Range("B_3").Value
B4 = Range("B_4").Value
B5 = Range("B_5").Value
B6 = Range("B_6").Value
B7 = Range("B_7").Value
B8 = Range("B_8").Value
B9 = Range("B_9").Value
B10 = Range("B_10").Value
```

```
B11 = Range("B_11").Value
B12 = Range("B_12").Value
B13 = Range("B_13").Value
B14 = Range("B_14").Value
B15 = Range("B_15").Value
B16 = Range("B_16").Value
B17 = Range("B_17").Value
B18 = Range("B_18").Value
B19 = Range("B_19").Value
B20 = Range("B_20").Value
B21 = Range("B_21").Value
B22 = Range("B_22").Value
B23 = Range("B_23").Value
B24 = Range("B_24").Value
B25 = Range("B_25").Value
B26 = Range("B_26").Value
B27 = Range("B_27").Value
B28 = Range("B_28").Value
B29 = Range("B_29").Value
B30 = Range("B_30").Value
B31 = Range("B_31").Value
B32 = Range("B_32").Value
B33 = Range("B_33").Value
B34 = Range("B_34").Value
B35 = Range("B_35").Value
B36 = Range("B_36").Value
B37 = Range("B_37").Value
B38 = Range("B_38").Value
B39 = Range("B_39").Value
B40 = Range("B_40").Value
B41 = Range("B_41").Value
B42 = Range("B_42").Value
B43 = Range("B_43").Value
B44 = Range("B_44").Value
B45 = Range("B_45").Value
B46 = Range("B_46").Value
B47 = Range("B_47").Value
B48 = Range("B_48").Value
B49 = Range("B_49").Value
```

```
B50 = Range("B_50").Value
B51 = Range("B_51").Value
B52 = Range("B_52").Value
B53 = Range("B_53").Value
B54 = Range("B_54").Value
B55 = Range("B_55").Value

'  Time increments for Runge Kutta
h = Range("h").Value
tmax = Range("tmax").Value
i = 0   'i acts as a counter - to keep track of loops

'  Note: tf,c1f,etc are floating variables

Do     'Runs Runge-Kutta Loops

   'Setting K0,L0,...,Z0
      tf = t
      c1f = c1
      c2f = c2
      c3f = c3
      c4f = c4
      c5f = c5
      c6f = c6
      c7f = c7
      c8f = c8
      c9f = c9
      c10f = c10
      c11f = c11
      c12f = c12
      c13f = c13
      c14f = c14
      c15f = c15
      c16f = c16
      c17f = c17
      c18f = c18
      c19f = c19
      c20f = c20
      c21f = c21
```

```
c22f = c22
c23f = c23
c24f = c24
c25f = c25
c26f = c26
c27f = c27
c28f = c28
c29f = c29
c30f = c30
c31f = c31
c32f = c32
c33f = c33
c34f = c34
c35f = c35
c36f = c36
c37f = c37
c38f = c38
c39f = c39
c40f = c40
c41f = c41
c42f = c42
c43f = c43
c44f = c44
c45f = c45
c46f = c46
c47f = c47
c48f = c48
c49f = c49
c50f = c50
c51f = c51
c52f = c52
c53f = c53
c54f = c54
c55f = c55
c56f = c56

  K0 = h * ODE1(tf, Q, B1, Cf, V1, c1f, c2f)
  L0 = h * ODE2(tf, Q, B1, B2, V2, c1f, c2f, c3f)
  M0 = h * ODE3(tf, Q, B2, B3, V3, c2f, c3f, c4f)
```

```
N0 = h * ODE4(tf, Q, B3, B4, V4, c3f, c4f, c5f)
P0 = h * ODE5(tf, Q, B4, B5, V5, c4f, c5f, c6f)
Q0 = h * ODE6(tf, Q, B5, B6, V6, c5f, c6f, c7f)
R0 = h * ODE7(tf, Q, B6, B7, V7, c6f, c7f, c8f)
S0 = h * ODE8(tf, Q, B7, B8, V8, c7f, c8f, c9f)
T0 = h * ODE9(tf, Q, B8, B9, V9, c8f, c9f, c10f)
U0 = h * ODE10(tf, Q, B9, B10, V10, c9f, c10f, c11f)
W0 = h * ODE11(tf, Q, B10, B11, V11, c10f, c11f, c12f)
X0 = h * ODE12(tf, Q, B11, B12, V12, c11f, c12f, c13f)
Y0 = h * ODE13(tf, Q, B12, B13, V13, c12f, c13f, c14f)
Z0 = h * ODE14(tf, Q, B13, B14, V14, c13f, c14f, c15f)
AA0 = h * ODE15(tf, Q, B14, B15, V15, c14f, c15f, c16f)
AB0 = h * ODE16(tf, Q, B15, B16, V16, c15f, c16f, c17f)
AC0 = h * ODE17(tf, Q, B16, B17, V17, c16f, c17f, c18f)
AD0 = h * ODE18(tf, Q, B17, B18, V18, c17f, c18f, c19f)
AE0 = h * ODE19(tf, Q, B18, B19, V19, c18f, c19f, c20f)
AF0 = h * ODE20(tf, Q, B19, B20, V20, c19f, c20f, c21f)
AG0 = h * ODE21(tf, Q, B20, B21, V21, c20f, c21f, c22f)
AH0 = h * ODE22(tf, Q, B21, B22, V22, c21f, c22f, c23f)
AI0 = h * ODE23(tf, Q, B22, B23, V23, c22f, c23f, c24f)
AJ0 = h * ODE24(tf, Q, B23, B24, V24, c23f, c24f, c25f)
AK0 = h * ODE25(tf, Q, B24, B25, V25, c24f, c25f, c26f)
AL0 = h * ODE26(tf, Q, B25, B26, V26, c25f, c26f, c27f)
AM0 = h * ODE27(tf, Q, B26, B27, V27, c26f, c27f, c28f)
AN0 = h * ODE28(tf, Q, B27, B28, V28, c27f, c28f, c29f)
AO0 = h * ODE29(tf, Q, B28, B29, V29, c28f, c29f, c30f)
AP0 = h * ODE30(tf, Q, B29, B30, V30, c29f, c30f, c31f)
AQ0 = h * ODE31(tf, Q, B30, B31, V31, c30f, c31f, c32f)
AR0 = h * ODE32(tf, Q, B31, B32, V32, c31f, c32f, c33f)
AS0 = h * ODE33(tf, Q, B32, B33, V33, c32f, c33f, c34f)
AT0 = h * ODE34(tf, Q, B33, B34, V34, c33f, c34f, c35f)
AU0 = h * ODE35(tf, Q, B34, B35, V35, c34f, c35f, c36f)
AV0 = h * ODE36(tf, Q, B35, B36, V36, c35f, c36f, c37f)
AW0 = h * ODE37(tf, Q, B36, B37, V37, c36f, c37f, c38f)
AX0 = h * ODE38(tf, Q, B37, B38, V38, c37f, c38f, c39f)
AY0 = h * ODE39(tf, Q, B38, B39, V39, c38f, c39f, c40f)
AZ0 = h * ODE40(tf, Q, B39, B40, V40, c39f, c40f, c41f)
BA0 = h * ODE41(tf, Q, B40, B41, V41, c40f, c41f, c42f)
BB0 = h * ODE42(tf, Q, B41, B42, V42, c41f, c42f, c43f)
```

```
    BC0 = h * ODE43(tf, Q, B42, B43, V43, c42f, c43f, c44f)
    BD0 = h * ODE44(tf, Q, B43, B44, V44, c43f, c44f, c45f)
    BE0 = h * ODE45(tf, Q, B44, B45, V45, c44f, c45f, c46f)
    BF0 = h * ODE46(tf, Q, B45, B46, V46, c45f, c46f, c47f)
    BG0 = h * ODE47(tf, Q, B46, B47, V47, c46f, c47f, c48f)
    BH0 = h * ODE48(tf, Q, B47, B48, V48, c47f, c48f, c49f)
    BI0 = h * ODE49(tf, Q, B48, B49, V49, c48f, c49f, c50f)
    BJ0 = h * ODE50(tf, Q, B49, B50, V50, c49f, c50f, c51f)
    BK0 = h * ODE51(tf, Q, B50, B51, V51, c50f, c51f, c52f)
    BL0 = h * ODE52(tf, Q, B51, B52, V52, c51f, c52f, c53f)
    BM0 = h * ODE53(tf, Q, B52, B53, V53, c52f, c53f, c54f)
    BN0 = h * ODE54(tf, Q, B53, B54, V54, c53f, c54f, c55f)
    BP0 = h * ODE55(tf, Q, B54, B55, V55, c54f, c55f, c56f)
    BQ0 = h * ODE56(tf, Q, B55, V56, c55f, c56f)

'Setting K1,L1,...,Z1
    tf = t + h / 2
    c1f = c1 + K0 / 2
    c2f = c2 + L0 / 2
    c3f = c3 + M0 / 2
    c4f = c4 + N0 / 2
    c5f = c5 + P0 / 2
    c6f = c6 + Q0 / 2
    c7f = c7 + R0 / 2
    c8f = c8 + S0 / 2
    c9f = c9 + T0 / 2
    c10f = c10 + U0 / 2
    c11f = c11 + W0 / 2
    c12f = c12 + X0 / 2
    c13f = c13 + Y0 / 2
    c14f = c14 + Z0 / 2
    c15f = c15 + AA0 / 2
    c16f = c16 + AB0 / 2
    c17f = c17 + AC0 / 2
    c18f = c18 + AD0 / 2
    c19f = c19 + AE0 / 2
    c20f = c20 + AF0 / 2
    c21f = c21 + AG0 / 2
    c22f = c22 + AH0 / 2
```

```
c23f = c23 + AI0 / 2
c24f = c24 + AJ0 / 2
c25f = c25 + AK0 / 2
c26f = c26 + AL0 / 2
c27f = c27 + AM0 / 2
c28f = c28 + AN0 / 2
c29f = c29 + AO0 / 2
c30f = c30 + AP0 / 2
c31f = c31 + AQ0 / 2
c32f = c32 + AR0 / 2
c33f = c33 + AS0 / 2
c34f = c34 + AT0 / 2
c35f = c35 + AU0 / 2
c36f = c36 + AV0 / 2
c37f = c37 + AW0 / 2
c38f = c38 + AX0 / 2
c39f = c39 + AY0 / 2
c40f = c40 + AZ0 / 2
c41f = c41 + BA0 / 2
c42f = c42 + BB0 / 2
c43f = c43 + BC0 / 2
c44f = c44 + BD0 / 2
c45f = c45 + BE0 / 2
c46f = c46 + BF0 / 2
c47f = c47 + BG0 / 2
c48f = c48 + BH0 / 2
c49f = c49 + BI0 / 2
c50f = c50 + BJ0 / 2
c51f = c51 + BK0 / 2
c52f = c52 + BL0 / 2
c53f = c53 + BM0 / 2
c54f = c54 + BN0 / 2
c55f = c55 + BP0 / 2
c56f = c56 + BQ0 / 2

  K1 = h * ODE1(tf, Q, B1, Cf, V1, c1f, c2f)
  L1 = h * ODE2(tf, Q, B1, B2, V2, c1f, c2f, c3f)
  M1 = h * ODE3(tf, Q, B2, B3, V3, c2f, c3f, c4f)
  N1 = h * ODE4(tf, Q, B3, B4, V4, c3f, c4f, c5f)
```

```
P1 = h * ODE5(tf, Q, B4, B5, V5, c4f, c5f, c6f)
Q1 = h * ODE6(tf, Q, B5, B6, V6, c5f, c6f, c7f)
R1 = h * ODE7(tf, Q, B6, B7, V7, c6f, c7f, c8f)
S1 = h * ODE8(tf, Q, B7, B8, V8, c7f, c8f, c9f)
T1 = h * ODE9(tf, Q, B8, B9, V9, c8f, c9f, c10f)
U1 = h * ODE10(tf, Q, B9, B10, V10, c9f, c10f, c11f)
W1 = h * ODE11(tf, Q, B10, B11, V11, c10f, c11f, c12f)
X1 = h * ODE12(tf, Q, B11, B12, V12, c11f, c12f, c13f)
Y1 = h * ODE13(tf, Q, B12, B13, V13, c12f, c13f, c14f)
Z1 = h * ODE14(tf, Q, B13, B14, V14, c13f, c14f, c15f)
AA1 = h * ODE15(tf, Q, B14, B15, V15, c14f, c15f, c16f)
AB1 = h * ODE16(tf, Q, B15, B16, V16, c15f, c16f, c17f)
AC1 = h * ODE17(tf, Q, B16, B17, V17, c16f, c17f, c18f)
AD1 = h * ODE18(tf, Q, B17, B18, V18, c17f, c18f, c19f)
AE1 = h * ODE19(tf, Q, B18, B19, V19, c18f, c19f, c20f)
AF1 = h * ODE20(tf, Q, B19, B20, V20, c19f, c20f, c21f)
AG1 = h * ODE21(tf, Q, B20, B21, V21, c20f, c21f, c22f)
AH1 = h * ODE22(tf, Q, B21, B22, V22, c21f, c22f, c23f)
AI1 = h * ODE23(tf, Q, B22, B23, V23, c22f, c23f, c24f)
AJ1 = h * ODE24(tf, Q, B23, B24, V24, c23f, c24f, c25f)
AK1 = h * ODE25(tf, Q, B24, B25, V25, c24f, c25f, c26f)
AL1 = h * ODE26(tf, Q, B25, B26, V26, c25f, c26f, c27f)
AM1 = h * ODE27(tf, Q, B26, B27, V27, c26f, c27f, c28f)
AN1 = h * ODE28(tf, Q, B27, B28, V28, c27f, c28f, c29f)
AO1 = h * ODE29(tf, Q, B28, B29, V29, c28f, c29f, c30f)
AP1 = h * ODE30(tf, Q, B29, B30, V30, c29f, c30f, c31f)
AQ1 = h * ODE31(tf, Q, B30, B31, V31, c30f, c31f, c32f)
AR1 = h * ODE32(tf, Q, B31, B32, V32, c31f, c32f, c33f)
AS1 = h * ODE33(tf, Q, B32, B33, V33, c32f, c33f, c34f)
AT1 = h * ODE34(tf, Q, B33, B34, V34, c33f, c34f, c35f)
AU1 = h * ODE35(tf, Q, B34, B35, V35, c34f, c35f, c36f)
AV1 = h * ODE36(tf, Q, B35, B36, V36, c35f, c36f, c37f)
AW1 = h * ODE37(tf, Q, B36, B37, V37, c36f, c37f, c38f)
AX1 = h * ODE38(tf, Q, B37, B38, V38, c37f, c38f, c39f)
AY1 = h * ODE39(tf, Q, B38, B39, V39, c38f, c39f, c40f)
AZ1 = h * ODE40(tf, Q, B39, B40, V40, c39f, c40f, c41f)
BA1 = h * ODE41(tf, Q, B40, B41, V41, c40f, c41f, c42f)
BB1 = h * ODE42(tf, Q, B41, B42, V42, c41f, c42f, c43f)
BC1 = h * ODE43(tf, Q, B42, B43, V43, c42f, c43f, c44f)
```

```
    BD1 = h * ODE44(tf, Q, B43, B44, V44, c43f, c44f, c45f)
    BE1 = h * ODE45(tf, Q, B44, B45, V45, c44f, c45f, c46f)
    BF1 = h * ODE46(tf, Q, B45, B46, V46, c45f, c46f, c47f)
    BG1 = h * ODE47(tf, Q, B46, B47, V47, c46f, c47f, c48f)
    BH1 = h * ODE48(tf, Q, B47, B48, V48, c47f, c48f, c49f)
    BI1 = h * ODE49(tf, Q, B48, B49, V49, c48f, c49f, c50f)
    BJ1 = h * ODE50(tf, Q, B49, B50, V50, c49f, c50f, c51f)
    BK1 = h * ODE51(tf, Q, B50, B51, V51, c50f, c51f, c52f)
    BL1 = h * ODE52(tf, Q, B51, B52, V52, c51f, c52f, c53f)
    BM1 = h * ODE53(tf, Q, B52, B53, V53, c52f, c53f, c54f)
    BN1 = h * ODE54(tf, Q, B53, B54, V54, c53f, c54f, c55f)
    BP1 = h * ODE55(tf, Q, B54, B55, V55, c54f, c55f, c56f)
    BQ1 = h * ODE56(tf, Q, B55, V56, c55f, c56f)

'Setting K2,L2,...,Z2
  tf = t + h / 2
  c1f = c1 + K1 / 2
  c2f = c2 + L1 / 2
  c3f = c3 + M1 / 2
  c4f = c4 + N1 / 2
  c5f = c5 + P1 / 2
  c6f = c6 + Q1 / 2
  c7f = c7 + R1 / 2
  c8f = c8 + S1 / 2
  c9f = c9 + T1 / 2
  c10f = c10 + U1 / 2
  c11f = c11 + W1 / 2
  c12f = c12 + X1 / 2
  c13f = c13 + Y1 / 2
  c14f = c14 + Z1 / 2
  c15f = c15 + AA1 / 2
  c16f = c16 + AB1 / 2
  c17f = c17 + AC1 / 2
  c18f = c18 + AD1 / 2
  c19f = c19 + AE1 / 2
  c20f = c20 + AF1 / 2
  c21f = c21 + AG1 / 2
  c22f = c22 + AH1 / 2
  c23f = c23 + AI1 / 2
```

```
c24f = c24 + AJ1 / 2
c25f = c25 + AK1 / 2
c26f = c26 + AL1 / 2
c27f = c27 + AM1 / 2
c28f = c28 + AN1 / 2
c29f = c29 + AO1 / 2
c30f = c30 + AP1 / 2
c31f = c31 + AQ1 / 2
c32f = c32 + AR1 / 2
c33f = c33 + AS1 / 2
c34f = c34 + AT1 / 2
c35f = c35 + AU1 / 2
c36f = c36 + AV1 / 2
c37f = c37 + AW1 / 2
c38f = c38 + AX1 / 2
c39f = c39 + AY1 / 2
c40f = c40 + AZ1 / 2
c41f = c41 + BA1 / 2
c42f = c42 + BB1 / 2
c43f = c43 + BC1 / 2
c44f = c44 + BD1 / 2
c45f = c45 + BE1 / 2
c46f = c46 + BF1 / 2
c47f = c47 + BG1 / 2
c48f = c48 + BH1 / 2
c49f = c49 + BI1 / 2
c50f = c50 + BJ1 / 2
c51f = c51 + BK1 / 2
c52f = c52 + BL1 / 2
c53f = c53 + BM1 / 2
c54f = c54 + BN1 / 2
c55f = c55 + BP1 / 2
c56f = c56 + BQ1 / 2

    K2 = h * ODE1(tf, Q, B1, Cf, V1, c1f, c2f)
    L2 = h * ODE2(tf, Q, B1, B2, V2, c1f, c2f, c3f)
    M2 = h * ODE3(tf, Q, B2, B3, V3, c2f, c3f, c4f)
    N2 = h * ODE4(tf, Q, B3, B4, V4, c3f, c4f, c5f)
    P2 = h * ODE5(tf, Q, B4, B5, V5, c4f, c5f, c6f)
```

```
Q2 = h * ODE6(tf, Q, B5, B6, V6, c5f, c6f, c7f)
R2 = h * ODE7(tf, Q, B6, B7, V7, c6f, c7f, c8f)
S2 = h * ODE8(tf, Q, B7, B8, V8, c7f, c8f, c9f)
T2 = h * ODE9(tf, Q, B8, B9, V9, c8f, c9f, c10f)
U2 = h * ODE10(tf, Q, B9, B10, V10, c9f, c10f, c11f)
W2 = h * ODE11(tf, Q, B10, B11, V11, c10f, c11f, c12f)
X2 = h * ODE12(tf, Q, B11, B12, V12, c11f, c12f, c13f)
Y2 = h * ODE13(tf, Q, B12, B13, V13, c12f, c13f, c14f)
Z2 = h * ODE14(tf, Q, B13, B14, V14, c13f, c14f, c15f)
AA2 = h * ODE15(tf, Q, B14, B15, V15, c14f, c15f, c16f)
AB2 = h * ODE16(tf, Q, B15, B16, V16, c15f, c16f, c17f)
AC2 = h * ODE17(tf, Q, B16, B17, V17, c16f, c17f, c18f)
AD2 = h * ODE18(tf, Q, B17, B18, V18, c17f, c18f, c19f)
AE2 = h * ODE19(tf, Q, B18, B19, V19, c18f, c19f, c20f)
AF2 = h * ODE20(tf, Q, B19, B20, V20, c19f, c20f, c21f)
AG2 = h * ODE21(tf, Q, B20, B21, V21, c20f, c21f, c22f)
AH2 = h * ODE22(tf, Q, B21, B22, V22, c21f, c22f, c23f)
AI2 = h * ODE23(tf, Q, B22, B23, V23, c22f, c23f, c24f)
AJ2 = h * ODE24(tf, Q, B23, B24, V24, c23f, c24f, c25f)
AK2 = h * ODE25(tf, Q, B24, B25, V25, c24f, c25f, c26f)
AL2 = h * ODE26(tf, Q, B25, B26, V26, c25f, c26f, c27f)
AM2 = h * ODE27(tf, Q, B26, B27, V27, c26f, c27f, c28f)
AN2 = h * ODE28(tf, Q, B27, B28, V28, c27f, c28f, c29f)
AO2 = h * ODE29(tf, Q, B28, B29, V29, c28f, c29f, c30f)
AP2 = h * ODE30(tf, Q, B29, B30, V30, c29f, c30f, c31f)
AQ2 = h * ODE31(tf, Q, B30, B31, V31, c30f, c31f, c32f)
AR2 = h * ODE32(tf, Q, B31, B32, V32, c31f, c32f, c33f)
AS2 = h * ODE33(tf, Q, B32, B33, V33, c32f, c33f, c34f)
AT2 = h * ODE34(tf, Q, B33, B34, V34, c33f, c34f, c35f)
AU2 = h * ODE35(tf, Q, B34, B35, V35, c34f, c35f, c36f)
AV2 = h * ODE36(tf, Q, B35, B36, V36, c35f, c36f, c37f)
AW2 = h * ODE37(tf, Q, B36, B37, V37, c36f, c37f, c38f)
AX2 = h * ODE38(tf, Q, B37, B38, V38, c37f, c38f, c39f)
AY2 = h * ODE39(tf, Q, B38, B39, V39, c38f, c39f, c40f)
AZ2 = h * ODE40(tf, Q, B39, B40, V40, c39f, c40f, c41f)
BA2 = h * ODE41(tf, Q, B40, B41, V41, c40f, c41f, c42f)
BB2 = h * ODE42(tf, Q, B41, B42, V42, c41f, c42f, c43f)
BC2 = h * ODE43(tf, Q, B42, B43, V43, c42f, c43f, c44f)
BD2 = h * ODE44(tf, Q, B43, B44, V44, c43f, c44f, c45f)
```

```
    BE2 = h * ODE45(tf, Q, B44, B45, V45, c44f, c45f, c46f)
    BF2 = h * ODE46(tf, Q, B45, B46, V46, c45f, c46f, c47f)
    BG2 = h * ODE47(tf, Q, B46, B47, V47, c46f, c47f, c48f)
    BH2 = h * ODE48(tf, Q, B47, B48, V48, c47f, c48f, c49f)
    BI2 = h * ODE49(tf, Q, B48, B49, V49, c48f, c49f, c50f)
    BJ2 = h * ODE50(tf, Q, B49, B50, V50, c49f, c50f, c51f)
    BK2 = h * ODE51(tf, Q, B50, B51, V51, c50f, c51f, c52f)
    BL2 = h * ODE52(tf, Q, B51, B52, V52, c51f, c52f, c53f)
    BM2 = h * ODE53(tf, Q, B52, B53, V53, c52f, c53f, c54f)
    BN2 = h * ODE54(tf, Q, B53, B54, V54, c53f, c54f, c55f)
    BP2 = h * ODE55(tf, Q, B54, B55, V55, c54f, c55f, c56f)
    BQ2 = h * ODE56(tf, Q, B55, V56, c55f, c56f)

'Setting K3,L3,...,Z3
    tf = t + h
    c1f = c1 + K2
    c2f = c2 + L2
    c3f = c3 + M2
    c4f = c4 + N2
    c5f = c5 + P2
    c6f = c6 + Q2
    c7f = c7 + R2
    c8f = c8 + S2
    c9f = c9 + T2
    c10f = c10 + U2
    c11f = c11 + W2
    c12f = c12 + X2
    c13f = c13 + Y2
    c14f = c14 + Z2
    c15f = c15 + AA2
    c16f = c16 + AB2
    c17f = c17 + AC2
    c18f = c18 + AD2
    c19f = c19 + AE2
    c20f = c20 + AF2
    c21f = c21 + AG2
    c22f = c22 + AH2
    c23f = c23 + AI2
    c24f = c24 + AJ2
```

```
c25f = c25 + AK2
c26f = c26 + AL2
c27f = c27 + AM2
c28f = c28 + AN2
c29f = c29 + AO2
c30f = c30 + AP2
c31f = c31 + AQ2
c32f = c32 + AR2
c33f = c33 + AS2
c34f = c34 + AT2
c35f = c35 + AU2
c36f = c36 + AV2
c37f = c37 + AW2
c38f = c38 + AX2
c39f = c39 + AY2
c40f = c40 + AZ2
c41f = c41 + BA2
c42f = c42 + BB2
c43f = c43 + BC2
c44f = c44 + BD2
c45f = c45 + BE2
c46f = c46 + BF2
c47f = c47 + BG2
c48f = c48 + BH2
c49f = c49 + BI2
c50f = c50 + BJ2
c51f = c51 + BK2
c52f = c52 + BL2
c53f = c53 + BM2
c54f = c54 + BN2
c55f = c55 + BP2
c56f = c56 + BQ2

  K3 = h * ODE1(tf, Q, B1, Cf, V1, c1f, c2f)
  L3 = h * ODE2(tf, Q, B1, B2, V2, c1f, c2f, c3f)
  M3 = h * ODE3(tf, Q, B2, B3, V3, c2f, c3f, c4f)
  N3 = h * ODE4(tf, Q, B3, B4, V4, c3f, c4f, c5f)
  P3 = h * ODE5(tf, Q, B4, B5, V5, c4f, c5f, c6f)
  Q3 = h * ODE6(tf, Q, B5, B6, V6, c5f, c6f, c7f)
```

```
R3 = h * ODE7(tf, Q, B6, B7, V7, c6f, c7f, c8f)
S3 = h * ODE8(tf, Q, B7, B8, V8, c7f, c8f, c9f)
T3 = h * ODE9(tf, Q, B8, B9, V9, c8f, c9f, c10f)
U3 = h * ODE10(tf, Q, B9, B10, V10, c9f, c10f, c11f)
W3 = h * ODE11(tf, Q, B10, B11, V11, c10f, c11f, c12f)
X3 = h * ODE12(tf, Q, B11, B12, V12, c11f, c12f, c13f)
Y3 = h * ODE13(tf, Q, B12, B13, V13, c12f, c13f, c14f)
Z3 = h * ODE14(tf, Q, B13, B14, V14, c13f, c14f, c15f)
AA3 = h * ODE15(tf, Q, B14, B15, V15, c14f, c15f, c16f)
AB3 = h * ODE16(tf, Q, B15, B16, V16, c15f, c16f, c17f)
AC3 = h * ODE17(tf, Q, B16, B17, V17, c16f, c17f, c18f)
AD3 = h * ODE18(tf, Q, B17, B18, V18, c17f, c18f, c19f)
AE3 = h * ODE19(tf, Q, B18, B19, V19, c18f, c19f, c20f)
AF3 = h * ODE20(tf, Q, B19, B20, V20, c19f, c20f, c21f)
AG3 = h * ODE21(tf, Q, B20, B21, V21, c20f, c21f, c22f)
AH3 = h * ODE22(tf, Q, B21, B22, V22, c21f, c22f, c23f)
AI3 = h * ODE23(tf, Q, B22, B23, V23, c22f, c23f, c24f)
AJ3 = h * ODE24(tf, Q, B23, B24, V24, c23f, c24f, c25f)
AK3 = h * ODE25(tf, Q, B24, B25, V25, c24f, c25f, c26f)
AL3 = h * ODE26(tf, Q, B25, B26, V26, c25f, c26f, c27f)
AM3 = h * ODE27(tf, Q, B26, B27, V27, c26f, c27f, c28f)
AN3 = h * ODE28(tf, Q, B27, B28, V28, c27f, c28f, c29f)
AO3 = h * ODE29(tf, Q, B28, B29, V29, c28f, c29f, c30f)
AP3 = h * ODE30(tf, Q, B29, B30, V30, c29f, c30f, c31f)
AQ3 = h * ODE31(tf, Q, B30, B31, V31, c30f, c31f, c32f)
AR3 = h * ODE32(tf, Q, B31, B32, V32, c31f, c32f, c33f)
AS3 = h * ODE33(tf, Q, B32, B33, V33, c32f, c33f, c34f)
AT3 = h * ODE34(tf, Q, B33, B34, V34, c33f, c34f, c35f)
AU3 = h * ODE35(tf, Q, B34, B35, V35, c34f, c35f, c36f)
AV3 = h * ODE36(tf, Q, B35, B36, V36, c35f, c36f, c37f)
AW3 = h * ODE37(tf, Q, B36, B37, V37, c36f, c37f, c38f)
AX3 = h * ODE38(tf, Q, B37, B38, V38, c37f, c38f, c39f)
AY3 = h * ODE39(tf, Q, B38, B39, V39, c38f, c39f, c40f)
AZ3 = h * ODE40(tf, Q, B39, B40, V40, c39f, c40f, c41f)
BA3 = h * ODE41(tf, Q, B40, B41, V41, c40f, c41f, c42f)
BB3 = h * ODE42(tf, Q, B41, B42, V42, c41f, c42f, c43f)
BC3 = h * ODE43(tf, Q, B42, B43, V43, c42f, c43f, c44f)
BD3 = h * ODE44(tf, Q, B43, B44, V44, c43f, c44f, c45f)
BE3 = h * ODE45(tf, Q, B44, B45, V45, c44f, c45f, c46f)
```

```
    BF3 = h * ODE46(tf, Q, B45, B46, V46, c45f, c46f, c47f)
    BG3 = h * ODE47(tf, Q, B46, B47, V47, c46f, c47f, c48f)
    BH3 = h * ODE48(tf, Q, B47, B48, V48, c47f, c48f, c49f)
    BI3 = h * ODE49(tf, Q, B48, B49, V49, c48f, c49f, c50f)
    BJ3 = h * ODE50(tf, Q, B49, B50, V50, c49f, c50f, c51f)
    BK3 = h * ODE51(tf, Q, B50, B51, V51, c50f, c51f, c52f)
    BL3 = h * ODE52(tf, Q, B51, B52, V52, c51f, c52f, c53f)
    BM3 = h * ODE53(tf, Q, B52, B53, V53, c52f, c53f, c54f)
    BN3 = h * ODE54(tf, Q, B53, B54, V54, c53f, c54f, c55f)
    BP3 = h * ODE55(tf, Q, B54, B55, V55, c54f, c55f, c56f)
    BQ3 = h * ODE56(tf, Q, B55, V56, c55f, c56f)

'Advancing
    c1 = c1 + (K0 + 2 * (K1 + K2) + K3) / 6
    c2 = c2 + (L0 + 2 * (L1 + L2) + L3) / 6
    c3 = c3 + (M0 + 2 * (M1 + M2) + M3) / 6
    c4 = c4 + (N0 + 2 * (N1 + N2) + N3) / 6
    c5 = c5 + (P0 + 2 * (P1 + P2) + P3) / 6
    c6 = c6 + (Q0 + 2 * (Q1 + Q2) + Q3) / 6
    c7 = c7 + (R0 + 2 * (R1 + R2) + R3) / 6
    c8 = c8 + (S0 + 2 * (S1 + S2) + S3) / 6
    c9 = c9 + (T0 + 2 * (T1 + T2) + T3) / 6
    c10 = c10 + (U0 + 2 * (U1 + U2) + U3) / 6
    c11 = c11 + (W0 + 2 * (W1 + W2) + W3) / 6
    c12 = c12 + (X0 + 2 * (X1 + X2) + X3) / 6
    c13 = c13 + (Y0 + 2 * (Y1 + Y2) + Y3) / 6
    c14 = c14 + (Z0 + 2 * (Z1 + Z2) + Z3) / 6
    c15 = c15 + (AA0 + 2 * (AA1 + AA2) + AA3) / 6
    c16 = c16 + (AB0 + 2 * (AB1 + AB2) + AB3) / 6
    c17 = c17 + (AC0 + 2 * (AC1 + AC2) + AC3) / 6
    c18 = c18 + (AD0 + 2 * (AD1 + AD2) + AD3) / 6
    c19 = c19 + (AE0 + 2 * (AE1 + AE2) + AE3) / 6
    c20 = c20 + (AF0 + 2 * (AF1 + AF2) + AF3) / 6
    c21 = c21 + (AG0 + 2 * (AG1 + AG2) + AG3) / 6
    c22 = c22 + (AH0 + 2 * (AH1 + AH2) + AH3) / 6
    c23 = c23 + (AI0 + 2 * (AI1 + AI2) + AI3) / 6
    c24 = c24 + (AJ0 + 2 * (AJ1 + AJ2) + AJ3) / 6
    c25 = c25 + (AK0 + 2 * (AK1 + AK2) + AK3) / 6
    c26 = c26 + (AL0 + 2 * (AL1 + AL2) + AL3) / 6
```

```
    c27 = c27 + (AM0 + 2 * (AM1 + AM2) + AM3) / 6
    c28 = c28 + (AN0 + 2 * (AN1 + AN2) + AN3) / 6
    c29 = c29 + (AO0 + 2 * (AO1 + AO2) + AO3) / 6
    c30 = c30 + (AP0 + 2 * (AP1 + AP2) + AP3) / 6
    c31 = c31 + (AQ0 + 2 * (AQ1 + AQ2) + AQ3) / 6
    c32 = c32 + (AR0 + 2 * (AR1 + AR2) + AR3) / 6
    c33 = c33 + (AS0 + 2 * (AS1 + AS2) + AS3) / 6
    c34 = c34 + (AT0 + 2 * (AT1 + AT2) + AT3) / 6
    c35 = c35 + (AU0 + 2 * (AU1 + AU2) + AU3) / 6
    c36 = c36 + (AV0 + 2 * (AV1 + AV2) + AV3) / 6
    c37 = c37 + (AW0 + 2 * (AW1 + AW2) + AW3) / 6
    c38 = c38 + (AX0 + 2 * (AX1 + AX2) + AX3) / 6
    c39 = c39 + (AY0 + 2 * (AY1 + AY2) + AY3) / 6
    c40 = c40 + (AZ0 + 2 * (AZ1 + AZ2) + AZ3) / 6
    c41 = c41 + (BA0 + 2 * (BA1 + BA2) + BA3) / 6
    c42 = c42 + (BB0 + 2 * (BB1 + BB2) + BB3) / 6
    c43 = c43 + (BC0 + 2 * (BC1 + BC2) + BC3) / 6
    c44 = c44 + (BD0 + 2 * (BD1 + BD2) + BD3) / 6
    c45 = c45 + (BE0 + 2 * (BE1 + BE2) + BE3) / 6
    c46 = c46 + (BF0 + 2 * (BF1 + BF2) + BF3) / 6
    c47 = c47 + (BG0 + 2 * (BG1 + BG2) + BG3) / 6
    c48 = c48 + (BH0 + 2 * (BH1 + BH2) + BH3) / 6
    c49 = c49 + (BI0 + 2 * (BI1 + BI2) + BI3) / 6
    c50 = c50 + (BJ0 + 2 * (BJ1 + BJ2) + BJ3) / 6
    c51 = c51 + (BK0 + 2 * (BK1 + BK2) + BK3) / 6
    c52 = c52 + (BL0 + 2 * (BL1 + BL2) + BL3) / 6
    c53 = c53 + (BM0 + 2 * (BM1 + BM2) + BM3) / 6
    c54 = c54 + (BN0 + 2 * (BN1 + BN2) + BN3) / 6
    c55 = c55 + (BP0 + 2 * (BP1 + BP2) + BP3) / 6
    c56 = c56 + (BQ0 + 2 * (BQ1 + BQ2) + BQ3) / 6


    t = t + h
    i = i + 1 'Advancing the counter

'Data output to "Data" worksheet
    With Worksheets("data")
        .Cells(4 + i, 2).Value = t
        .Cells(4 + i, 3).Value = c1
        .Cells(4 + i, 4).Value = c2
```

```
        .Cells(4 + i, 5).Value = c3
        .Cells(4 + i, 6).Value = c4
        .Cells(4 + i, 7).Value = c5
        .Cells(4 + i, 8).Value = c6
        .Cells(4 + i, 9).Value = c7
        .Cells(4 + i, 10).Value = c8
        .Cells(4 + i, 11).Value = c9
        .Cells(4 + i, 12).Value = c10
        .Cells(4 + i, 13).Value = c15
        .Cells(4 + i, 14).Value = c30
        .Cells(4 + i, 15).Value = c56
    End With

Loop While t < tmax

End Sub

'ODE EQUATIONS FOR CSTR MASS BALANCES - no reaction

Function ODE1(tf, Q, B1, Cf, V1, c1, c2)
ODE1 = Q * (Cf + B1 * c2 - c1 - B1 * c1) / V1
End Function

Function ODE2(tf, Q, B1, B2, V2, c1, c2, c3)
ODE2 = Q * (c1 + B1 * c1 + B2 * c3 - c2 - B1 * c2 - B2 * c2) / V2
End Function

Function ODE3(tf, Q, B2, B3, V3, c2, c3, c4)
ODE3 = Q * (c2 + B2 * c2 + B3 * c4 - c3 - B2 * c3 - B3 * c3) / V3
End Function

Function ODE4(tf, Q, B3, B4, V4, c3, c4, c5)
ODE4 = Q * (c3 + B3 * c3 + B4 * c5 - c4 - B3 * c4 - B4 * c4) / V4
End Function

Function ODE5(tf, Q, B4, B5, V5, c4, c5, c6)
ODE5 = Q * (c4 + B4 * c4 + B5 * c6 - c5 - B4 * c5 - B5 * c5) / V5
End Function
```

```
Function ODE6(tf, Q, B5, B6, V6, c5, c6, c7)
ODE6 = Q * (c5 + B5 * c5 + B6 * c7 - c6 - B5 * c6 - B6 * c6) / V6
End Function

Function ODE7(tf, Q, B6, B7, V7, c6, c7, c8)
ODE7 = Q * (c6 + B6 * c6 + B7 * c8 - c7 - B6 * c7 - B7 * c7) / V7
End Function

Function ODE8(tf, Q, B7, B8, V8, c7, c8, c9)
ODE8 = Q * (c7 + B7 * c7 + B8 * c9 - c8 - B7 * c8 - B8 * c8) / V8
End Function

Function ODE9(tf, Q, B8, B9, V9, c8, c9, c10)
ODE9 = Q * (c8 + B8 * c8 + B9 * c10 - c9 - B8 * c9 - B9 * c9) / V9
End Function

Function ODE10(tf, Q, B9, B10, V10, c9, c10, c11)
ODE10 = Q * (c9 + B9 * c9 + B10 * c11 - c10 - B9 * c10 - B10 * c10) / V10
End Function

Function ODE11(tf, Q, B10, B11, V11, c10, c11, c12)
ODE11 = Q * (c10 + B10 * c10 + B11 * c12 - c11 - B10 * c11 - B11 * c11) / V11
End Function

Function ODE12(tf, Q, B11, B12, V12, c11, c12, c13)
ODE12 = Q * (c11 + B11 * c11 + B12 * c13 - c12 - B11 * c12 - B12 * c12) / V12
End Function

Function ODE13(tf, Q, B12, B13, V13, c12, c13, c14)
ODE13 = Q * (c12 + B12 * c12 + B13 * c14 - c13 - B12 * c13 - B13 * c13) / V13
End Function

Function ODE14(tf, Q, B13, B14, V14, c13, c14, c15)
ODE14 = Q * (c13 + B13 * c13 + B14 * c15 - c14 - B13 * c14 - B14 * c14) / V14
End Function

Function ODE15(tf, Q, B14, B15, V15, c14, c15, c16)
ODE15 = Q * (c14 + B14 * c14 + B15 * c16 - c15 - B14 * c15 - B15 * c15) / V15
End Function
```

```
Function ODE16(tf, Q, B15, B16, V16, c15, c16, c17)
ODE16 = Q * (c15 + B15 * c15 + B16 * c17 - c16 - B15 * c16 - B16 * c16) / V16
End Function

Function ODE17(tf, Q, B16, B17, V17, c16, c17, c18)
ODE17 = Q * (c16 + B16 * c16 + B17 * c18 - c17 - B16 * c17 - B17 * c17) / V17
End Function

Function ODE18(tf, Q, B17, B18, V18, c17, c18, c19)
ODE18 = Q * (c17 + B17 * c17 + B18 * c19 - c18 - B17 * c18 - B18 * c18) / V18
End Function

Function ODE19(tf, Q, B18, B19, V19, c18, c19, c20)
ODE19 = Q * (c18 + B18 * c18 + B19 * c20 - c19 - B18 * c19 - B19 * c19) / V19
End Function

Function ODE20(tf, Q, B19, B20, V20, c19, c20, c21)
ODE20 = Q * (c19 + B19 * c19 + B20 * c21 - c20 - B19 * c20 - B20 * c20) / V20
End Function

Function ODE21(tf, Q, B20, B21, V21, c20, c21, c22)
ODE21 = Q * (c20 + B20 * c20 + B21 * c22 - c21 - B20 * c21 - B21 * c21) / V21
End Function

Function ODE22(tf, Q, B21, B22, V22, c21, c22, c23)
ODE22 = Q * (c21 + B21 * c21 + B22 * c23 - c22 - B21 * c22 - B22 * c22) / V22
End Function

Function ODE23(tf, Q, B22, B23, V23, c22, c23, c24)
ODE23 = Q * (c22 + B22 * c22 + B23 * c24 - c23 - B22 * c23 - B23 * c23) / V23
End Function

Function ODE24(tf, Q, B23, B24, V24, c23, c24, c25)
ODE24 = Q * (c23 + B23 * c23 + B24 * c25 - c24 - B23 * c24 - B24 * c24) / V24
End Function

Function ODE25(tf, Q, B24, B25, V25, c24, c25, c26)
ODE25 = Q * (c24 + B24 * c24 + B25 * c26 - c25 - B24 * c25 - B25 * c25) / V25
```

```
End Function

Function ODE26(tf, Q, B25, B26, V26, c25, c26, c27)
ODE26 = Q * (c25 + B25 * c25 + B26 * c27 - c26 - B25 * c26 - B26 * c26) / V26
End Function

Function ODE27(tf, Q, B26, B27, V27, c26, c27, c28)
ODE27 = Q * (c26 + B26 * c26 + B27 * c28 - c27 - B26 * c27 - B27 * c27) / V27
End Function

Function ODE28(tf, Q, B27, B28, V28, c27, c28, c29)
ODE28 = Q * (c27 + B27 * c27 + B28 * c29 - c28 - B27 * c28 - B28 * c28) / V28
End Function

Function ODE29(tf, Q, B28, B29, V29, c28, c29, c30)
ODE29 = Q * (c28 + B28 * c28 + B29 * c30 - c29 - B28 * c29 - B29 * c29) / V29
End Function

Function ODE30(tf, Q, B29, B30, V30, c29, c30, c31)
ODE30 = Q * (c29 + B29 * c29 + B30 * c31 - c30 - B29 * c30 - B30 * c30) / V30
End Function

Function ODE31(tf, Q, B30, B31, V31, c30, c31, c32)
ODE31 = Q * (c30 + B30 * c30 + B31 * c32 - c31 - B30 * c31 - B31 * c31) / V31
End Function

Function ODE32(tf, Q, B31, B32, V32, c31, c32, c33)
ODE32 = Q * (c31 + B31 * c31 + B32 * c33 - c32 - B31 * c32 - B32 * c32) / V32
End Function

Function ODE33(tf, Q, B32, B33, V33, c32, c33, c34)
ODE33 = Q * (c32 + B32 * c32 + B33 * c34 - c33 - B32 * c33 - B33 * c33) / V33
End Function

Function ODE34(tf, Q, B33, B34, V34, c33, c34, c35)
ODE34 = Q * (c33 + B33 * c33 + B34 * c35 - c34 - B33 * c34 - B34 * c34) / V34
End Function

Function ODE35(tf, Q, B34, B35, V35, c34, c35, c36)
```

```
ODE35 = Q * (c34 + B34 * c34 + B35 * c36 - c35 - B34 * c35 - B35 * c35) / V35
End Function

Function ODE36(tf, Q, B35, B36, V36, c35, c36, c37)
ODE36 = Q * (c35 + B35 * c35 + B36 * c37 - c36 - B35 * c36 - B36 * c36) / V36
End Function

Function ODE37(tf, Q, B36, B37, V37, c36, c37, c38)
ODE37 = Q * (c36 + B36 * c36 + B37 * c38 - c37 - B36 * c37 - B37 * c37) / V37
End Function

Function ODE38(tf, Q, B37, B38, V38, c37, c38, c39)
ODE38 = Q * (c37 + B37 * c37 + B38 * c39 - c38 - B37 * c38 - B38 * c38) / V38
End Function

Function ODE39(tf, Q, B38, B39, V39, c38, c39, c40)
ODE39 = Q * (c38 + B38 * c38 + B39 * c40 - c39 - B38 * c39 - B39 * c39) / V39
End Function

Function ODE40(tf, Q, B39, B40, V40, c39, c40, c41)
ODE40 = Q * (c39 + B39 * c39 + B40 * c41 - c40 - B39 * c40 - B40 * c40) / V40
End Function

Function ODE41(tf, Q, B40, B41, V41, c40, c41, c42)
ODE41 = Q * (c40 + B40 * c40 + B41 * c42 - c41 - B40 * c41 - B41 * c41) / V41
End Function

Function ODE42(tf, Q, B41, B42, V42, c41, c42, c43)
ODE42 = Q * (c41 + B41 * c41 + B42 * c43 - c42 - B41 * c42 - B42 * c42) / V42
End Function

Function ODE43(tf, Q, B42, B43, V43, c42, c43, c44)
ODE43 = Q * (c42 + B42 * c42 + B43 * c44 - c43 - B42 * c43 - B43 * c43) / V43
End Function

Function ODE44(tf, Q, B43, B44, V44, c43, c44, c45)
ODE44 = Q * (c43 + B43 * c43 + B44 * c45 - c44 - B43 * c44 - B44 * c44) / V44
End Function
```

```
Function ODE45(tf, Q, B44, B45, V45, c44, c45, c46)
ODE45 = Q * (c44 + B44 * c44 + B45 * c46 - c45 - B44 * c45 - B45 * c45) / V45
End Function

Function ODE46(tf, Q, B45, B46, V46, c45, c46, c47)
ODE46 = Q * (c45 + B45 * c45 + B46 * c47 - c46 - B45 * c46 - B46 * c46) / V46
End Function

Function ODE47(tf, Q, B46, B47, V47, c46, c47, c48)
ODE47 = Q * (c46 + B46 * c46 + B47 * c48 - c47 - B46 * c47 - B47 * c47) / V47
End Function

Function ODE48(tf, Q, B47, B48, V48, c47, c48, c49)
ODE48 = Q * (c47 + B47 * c47 + B48 * c49 - c48 - B47 * c48 - B48 * c48) / V48
End Function

Function ODE49(tf, Q, B48, B49, V49, c48, c49, c50)
ODE49 = Q * (c48 + B48 * c48 + B49 * c50 - c49 - B48 * c49 - B49 * c49) / V49
End Function

Function ODE50(tf, Q, B49, B50, V50, c49, c50, c51)
ODE50 = Q * (c49 + B49 * c49 + B50 * c51 - c50 - B49 * c50 - B50 * c50) / V50
End Function

Function ODE51(tf, Q, B50, B51, V51, c50, c51, c52)
ODE51 = Q * (c50 + B50 * c50 + B51 * c52 - c51 - B50 * c51 - B51 * c51) / V51
End Function

Function ODE52(tf, Q, B51, B52, V52, c51, c52, c53)
ODE52 = Q * (c51 + B51 * c51 + B52 * c53 - c52 - B51 * c52 - B52 * c52) / V52
End Function

Function ODE53(tf, Q, B52, B53, V53, c52, c53, c54)
ODE53 = Q * (c52 + B52 * c52 + B53 * c54 - c53 - B52 * c53 - B53 * c53) / V53
End Function

Function ODE54(tf, Q, B53, B54, V54, c53, c54, c55)
ODE54 = Q * (c53 + B53 * c53 + B54 * c55 - c54 - B53 * c54 - B54 * c54) / V54
End Function
```

```
Function ODE55(tf, Q, B54, B55, V55, c54, c55, c56)
ODE55 = Q * (c54 + B54 * c54 + B55 * c56 - c55 - B54 * c55 - B55 * c55) / V55
End Function

Function ODE56(tf, Q, B55, V56, c55, c56)
ODE56 = Q * (c55 + B55 * c55 - c56 - B55 * c56) / V56
End Function
```